FACULTAD DE INGENIERÍA Y CIENCIAS APLICADAS

INGENIO

VOL. 8 N . 2,2025 - ISSN 2697-3243 / ISSN 2588-0829

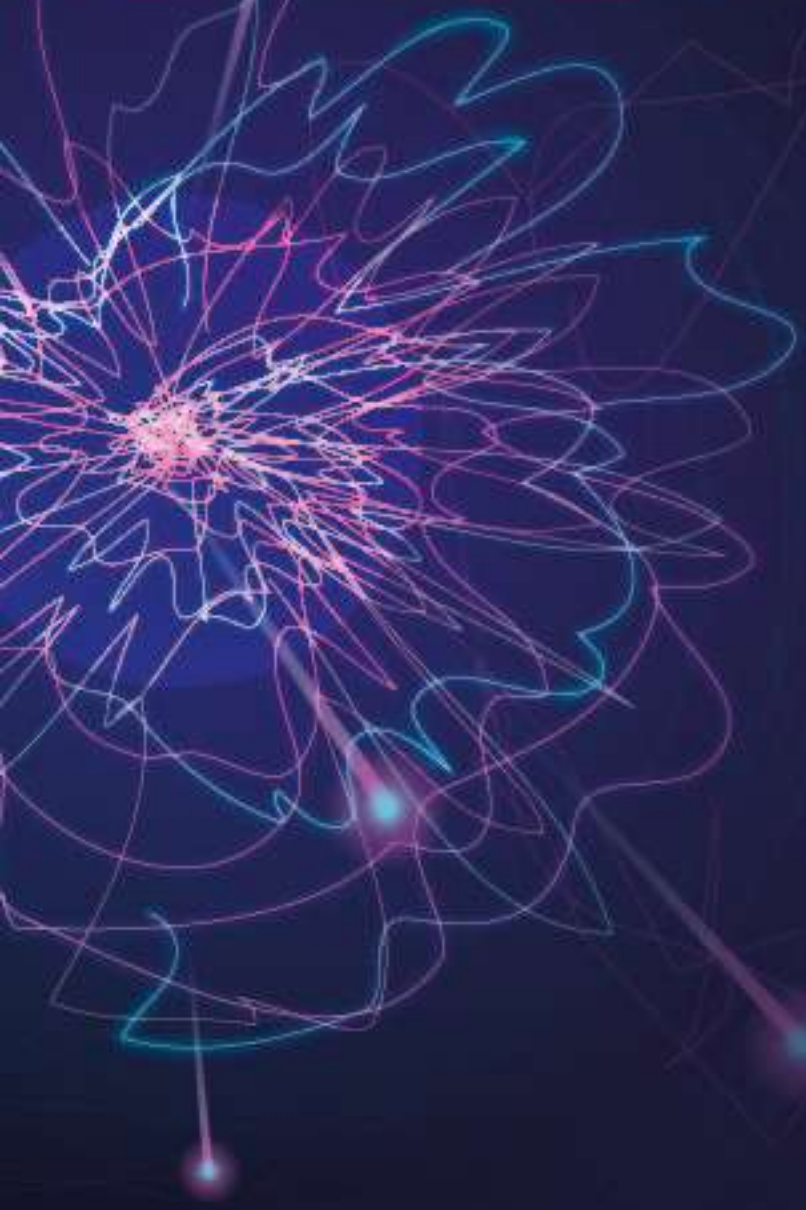

INGENIERÍA, INNOVACIÓN E INVESTIGACIÓN

Revista INGENIO es una revista semestral de la Facultad de Ingeniería y Ciencias Aplicadas de la Universidad Central del Ecua- dor fundada en el año 2017 | Vol. 8, núm. 2 | julio - diciembre 2025 | p-ISSN 2588-0829 e-ISSN 2697-3243 |

Este número estuvo bajo la coordinación editorial de: Mgs.Tatiana Freire, Dipl.

Revista Ingenio
fing.revista.ingenio@uce.edu.ec
vicedecanat.fing@uce.edu.ec

Sitio web:
http://revistadigital.uce.edu.ec/index.php/INGENIO/index
Correo electrónico:
fing.revista.ingenio@uce.edu.ec

ISSN impresa 2588-0829
ISSN electrónica 2697-3243

Director | MSc. Edison Benavides
Diagramación | Ing. Christian Echeverría
Corrección de textos | MSc. Jhonatan Salazar Achig
Portada | Ing. Katherine Cervantes, Ingeniería en Diseño Industrial, Universidad Central del Ecuador

Editorial Universitaria, 2025
Ciudadela Universitaria, av. América, s. n.
Quito, Ecuador
+593 (02) 2524 033
editorial@uce.edu.ec

ÍNDICE

Artículo Original

Estudio de Caso

FACULTAD DE INGENIERÍA Y CIENCIAS APLICADAS
UNIVERSIDAD CENTRAL DEL ECUADOR

INGENIO
2025, VOL 8(2), JULIO - DICIEMBRE, PP. 5-52

REVISTA INGENIO

Demographic Trends: Forecast of the Child Population From 0 to 3 years Old for the Year 2030

Tendencias Demográficas: Pronóstico de la Población Infantil de 0 a 3 años para el Año 2030

Gandy Rene López Fuertes | Ministerio de Inclusión Económica y Social, MIES -Ecuador
Guillermo Alexis Albuja Proaño | Universidad Central del Ecuador, UCE - Ecuador
Iván Cristian Naula Reina | Universidad Central del Ecuador, UCE - Ecuador
Jeimy Sugey Hernández Martínez | Universidad de Pueblos y Nacionalidades del Ecuador Amawtay Wasi, UAW -Ecuador
Gustavo Napoleón López Fuertes | Instituto Superior Universitario Central Técnico, ISUCT - Ecuador

Recibido: 18/11/2024
Recibido tras revisión: 27/12/2024
Aceptado: 24/3/2025
Publicado: 10/07/2025

KEY WORDS
Child poverty, child welfare, multiple regression, Fay-Herriot model, demographic projections

ABSTRACT
This paper estimates the number of children aged 0-3 living in poverty in Ecuador, using combined data from the 2014 Living Conditions Survey (LCS) and the 2010 Population and Housing Census (CPV), as the current data do not provide sufficient detail by region. To do so, we employ the Small Area Estimation (SAE) method, based on the Fay-Herriot model, which uses multiple linear regression to integrate survey and census data. This approach allows the analysis of specific sub-populations, such as cantons or districts, where surveys alone do not provide reliable results due to small samples. In addition, consumption-based poverty is simulated and the child population is projected up to 2030, comparing these projections with estimates from the Economic Commission for Latin America and the Caribbean (ECLAC) to verify their accuracy. The main purpose of this research is to provide accurate and detailed information on children in poverty, thus supporting the creation of effective public policies in Ecuador [1].

PALABRAS CLAVE
Pobreza infantil, bienestar infantil, regresión múltiple, modelo Fay-Herriot, proyecciones demográficas.

RESUMEN
Este trabajo calcula la cantidad de niños y niñas de 0 a 3 años en Ecuador que viven en condiciones de pobreza, utilizando información combinada de la Encuesta de Condiciones de Vida (ECV) 2014 y el Censo de Población y Vivienda (CPV) 2010, ya que los datos actuales no ofrecen suficiente detalle por regiones. Para ello, se emplea el método de Estimación para Áreas Pequeñas (SAE), basado en el modelo Fay-Herriot, que utiliza regresión lineal múltiple para integrar datos de encuestas y censos. Este enfoque permite analizar subpoblaciones específicas, como cantones o distritos, donde las encuestas por sí solas no brindan resultados confiables debido a muestras pequeñas. Además, se simula la pobreza basada en el consumo y se proyecta la población infantil hasta el año 2030, comparando estas proyecciones con estimaciones de la Comisión Económica para América Latina y el Caribe (CEPAL) para verificar su exactitud. El propósito principal de esta investigación es ofrecer información precisa y detallada sobre la infancia en pobreza, apoyando así la creación de políticas públicas efectivas en Ecuador.

1. Introduction

The absence of specific data on child poverty at the local level in Ecuador is a critical barrier to designing and implementing social policies that actually work. Without knowing how many children aged 0-3 face poverty in each canton or district, decision-makers are unable to distribute resources effectively or create programs that respond to the realities of the most neglected communities [1], [2]. This lack of detailed information not only hinders the fight against child poverty, but could also aggravate existing social and economic gaps in the country.

The lack of geographically disaggregated information for certain population groups, such as the child population, is a critical problem that directly affects decision-making in economic and social policies. In Ecuador, this limitation prevents the effective targeting of resources to areas of greatest need, which can exacerbate regional inequalities [2]. At the international level, similar

https://doi.org/10.29166/ingenio.v8i2.7545

pISSN 2588-0829
eISSN 2697-3243
fing.revista.ingenio@uce.edu.ec

countries such as Perú and Colombia face similar challenges, where the lack of disaggregated data has hindered the implementation of child poverty reduction programs [3]. This study is relevant because it offers an innovative methodological solution to overcome these limitations, allowing for better planning and resource allocation. The central research question is: How can the child population in Ecuador be estimated according to poverty levels using the Small Area Estimation methodology? This research is novel in combining survey and census data to generate accurate district-level estimates, which is crucial for the design of effective public policies in similar contexts [4].

The problem of the scarcity of disaggregated data is not unique to Ecuador. In several Latin American countries, this limitation has slowed progress in reducing poverty and inequality. For example, in Colombia, the lack of accurate information on rural areas has caused rural support programs to lose impact [5]. In México, the lack of detailed statistics at the municipal level has made it difficult for health policies to effectively reach indigenous communities [6]. These cases show how the absence of reliable data can hinder policy decisions in diverse contexts, highlighting the need for solutions such as the one this study proposes.

What makes this study special is its innovative approach in employing the Small Subpopulation Estimation (SAE) methodology, based on the Fay-Herriot model and multiple regression, to accurately estimate child poverty in specific regions of Ecuador. Unlike conventional methods, which typically rely on small sample surveys, this technique combines information from sources such as the 2014 Living Conditions Survey (LCS) and the 2010 Population and Housing Census (CPV), achieving robust results even in places where direct data are scarce [1]. This advance not only raises the quality of estimates, but also provides a practical tool for policy to reach where it is most needed.

The main objective of this work is to determine how many children aged 0-3 will be living in poverty in Ecuador by 2030, with a detailed breakdown by canton and district. The question guiding this research is: How many children aged 0-3 will be living in consumption poverty in 2030 in Ecuador, and how will this reality be distributed among the different regions of the country? Answering this question is key to guiding child development policies and ensuring that efforts are concentrated in the most critical areas.

The study of poverty and social injustice represents a complex challenge due to the interaction of multiple factors, elements and intrinsic variables that converge in the same objective. This problem has been the subject of much research and debate, which has proposed various concepts and realities that demonstrate that an individual cannot disassociate himself from a just environment that will keep him out of poverty and allow him to overcome the inequalities of his environment. The analysis of poverty encompasses various aspects. Some of these aspects are under the control of the individual, but most are influenced by social forces and economic and political power. The differences between theories and conceptualizations are based on how the problem of poverty and vulnerability is addressed. However, they all share the common goal of achieving a more equitable and just society to combat social inequality [7]. Approximately 700 million people live on less than $2.15 a day, which is considered the extreme poverty line. This situation remains prevalent in parts of sub-Saharan Africa, fragile and conflict-affected regions, and rural areas. After decades of progress, the rate of global poverty reduction began to slow in 2015, coinciding with moderate economic growth. The Sustainable Development Goal of eradicating extreme poverty by 2030 still seems unattainable.

The COVID-19 pandemic and a series of major shocks between 2020 and 2022 dealt a severe blow to efforts to reduce global poverty, setting back three years of progress. Low-income countries were hardest hit and have yet to recover. In 2022, a total of 712 million people were living in extreme poverty worldwide, an increase of 23 million compared to 2019. Poverty and inequality cannot be reduced without also addressing interrelated global challenges, such as slow economic growth, fragility and conflict, and climate change.

Climate change is hampering poverty reduction and poses a major threat to the future. The lives and livelihoods of the poor are most exposed to climate-related risks. Every year, millions of households fall into poverty or become trapped in poverty due to natural disasters. Higher temperatures are already causing declining productivity in Africa and Latin America, and will further reduce economic growth, especially in the poorest regions of the world. Eradicating poverty requires addressing its multiple dimensions. Countries cannot adequately address this problem without also improving people's well-being in a comprehensive manner, including more equitable access to health, education, and basic infrastructure and services, including digital services. Policymakers must intensify their efforts to grow their countries economies in ways that create high-quality jobs and employment and protect the most vulnerable. Employment is the surest way to reduce poverty and inequality. Its impact is further multiplied in communities and across generations by empowering women, girls and youth [8].

To further contextualize the relevance of our study, it is important to recognize that the small area estimation (SAE) methodology has been successfully applied in a variety of geographical and socio-economic contexts to address similar challenges related to measuring poverty and inequality at the local level [4]. For example, research in Latin American countries has used SAE to generate accurate poverty estimates in rural and marginalized areas

where census data are limited or outdated [9]. These studies have shown that the SAE can be a valuable tool for evidence-based decision-making and targeting of public policies aimed at the most vulnerable population. By delving deeper into this previous research, we can better understand the strengths and limitations of the SAE and adapt its application to the specific case of Ecuador, in order to obtain more accurate and relevant results.

The Small Area Estimation (SAE) method is a powerful tool that has been successfully used in different countries to measure poverty and inequality at the local level. For example, in Latin America, recent studies have applied this approach to obtain accurate poverty data in rural and marginalized areas where census information is scarce or old [10]. Similarly, in the European Union, SAE is used to produce detailed regional statistics on income and living conditions, helping governments to target their policies more effectively [11]. In Canada, this method has been used to estimate the incidence of chronic diseases in indigenous communities, improving the allocation of resources for health programs [12]. These cases demonstrate how SAE can be adapted to different contexts, providing a solid basis for our analysis in Ecuador [1].

The identification of individuals in situations of vulnerability and poverty is the first essential step for the implementation, execution and monitoring of inclusion programs. This is fundamental to advance in the creation of opportunities that facilitate equality and social cohesion, also considering the gender approach as a cross-cutting element in any social policy [13]. Data from the VII population and VI housing census, conducted in 2010, are a key source for obtaining population information down to the lowest level of territorial disaggregation, i.e. at the district level. The variables that measure poverty through Unsatisfied Basic Needs (UBN) and consumption allow us to get closer to the social reality of individuals. However, the use of the UBN poverty indicator has certain limitations. Firstly, this type of poverty is based on a multidimensional logic that emphasizes services such as drinking water and sanitation, as well as housing conditions. Given the current national coverage of these services, which is low by international standards, lack of access may affect households that are not necessarily in vulnerable conditions. This can lead to an overestimation of the population in need of care [14].

According to the 2010 Population and Housing Census, the incidence of poverty measured by UBN was 60.1%, which represents the percentage of people in households that do not satisfy one or more basic needs. In contrast, poverty measured by consumption was 25.8% in 2014, indicating a percentage of people whose per capita consumption is below the poverty line. This suggests that regardless of the method used to estimate poverty, the Living Conditions Survey provides a more accurate estimate. According to [15], poverty measured through consumption is more aligned with the notion of vulnerability, as it depends mainly on the labor market and available resources [13]. The dependence of consumption poverty on factors such as labor demand and available resources implies that any macroeconomic shock can affect overall consumption levels among inhabitants, which has a significant impact on those in extreme poverty. Unlike poverty measured by UBN, the latter is more related to structural issues linked to the country's infrastructure and basic services. In the specific case of Ecuador, the components related to sanitation and overcrowding have the greatest influence on the indicator [14].

The current government is implementing a programmed to improve access to drinking water and sanitation, complementing housing initiatives. When a household has these basic services, it is automatically no longer considered poor; furthermore, the chances of falling back into this condition are minimal because UBN poverty is closely related to structural aspects [13]. This situation limits the design of projects aimed at creating conditions that foster both economic and social inclusion, which is crucial for achieving greater equity among members of society. Therefore, it is necessary to measure poverty from a perspective more focused on socio-economic components such as consumption poverty [14].

However, the initial sources to obtain these indicators present a maximum territorial disaggregation at the provincial and regional levels, which hinders effective planning at the cantonal and district levels. In this context, it is proposed to implement methodologies such as Small Area Estimation (SAE), which allows estimating population parameters based on census data applied to population subsets obtained through surveys [13]. SAE facilitates obtaining parameters measured in surveys and translating them to census data with high population disaggregation. This makes it possible to identify populations in small areas using variables not available in the 2010 Census but present in surveys such as the 2014 Living Conditions Survey [14].

This methodological proposal makes it possible to put into practice the fundamental concepts of the estimation of small areas, which responds to an estimation of population parameters. Consequently, we know that at present our country in particular, does not have geographically disaggregated information of the entire population in general, and specifically of a certain population group, which is used for planning and decision making for economic and social policy, as indicated by [4]. The identification of people in vulnerability and poverty is the first step for the implementation, execution and monitoring of inclusion programs, with the aim of making progress in the generation of opportunities that allow equality and social cohesion to be achieved, in addition to the intrinsic consideration of gender and ethnicity as a cross-cutting core of any social policy, as mentioned by [16].

The data from the VII population census and VI housing census of 2010, as a source from which population data is obtained up to the lowest territorial disaggregation level, i.e. district. According to [17], the variables poverty by Unsatisfied Basic Needs and poverty by consumption allow an approximation to be made of the social reality of individuals. The Small Area Estimation (SAE) methodology is a mathematical and statistical method that models information from one or more data sources to produce estimates of a variable of interest, for example poverty at the local level, as indicated by [18]. SAE is most useful when domain (sub-population) sample sizes are too small to provide adequate precision for estimators. Consequently, the methodology (SAE) will allow estimating at a disaggregated level the population of children aged 0-3 years from 2014 to 2030, based on the Living Conditions Survey of 2014 and the VII Population Census and VI Housing Census of 2010.

To fully understand the applicability and relevance of Small Area Estimation (SAE) in our context, it is essential to recognize its use and evolution in other countries and regions. Globally, SAE has been successfully implemented in a number of nations to address similar challenges related to measuring poverty and inequality at the local level. For example, in the European Union, the EAS is used to generate detailed regional statistics on income and living conditions, enabling member states to design more effective and targeted policies [19]. In Latin America, countries such as Brazil and México have used SAE to improve the accuracy of poverty estimates in rural and marginalized areas, where census data are limited or outdated [20].

The adoption of SAE is not only limited to poverty measurement, but also extends to other areas such as public health, education and agricultural development. In Canadá, for example, SAE is used to estimate the prevalence of chronic diseases in indigenous communities, facilitating the allocation of resources and the implementation of prevention programs [12]. In the African context, SAE has proven valuable for monitoring sustainable development indicators at the local level, allowing governments and non-governmental organizations to assess the impact of their interventions and adjust their strategies accordingly [21].

These examples illustrate the versatility and potential of SAE as a tool for evidence-based decision-making at the local level. By adapting and applying SAE in our specific context, we can benefit from lessons learned and best practices identified in other countries and regions, while addressing our own unique needs and challenges. The originality of our research lies in the combination of census data and household surveys to estimate child poverty at the small area level, which will allow us to generate valuable information for planning and policy design for the most vulnerable population.

Poverty and social inequality are complex issues that involve a variety of factors and require comprehensive approaches to their analysis. This study seeks to estimate how many children aged 0-3 live in poverty in Ecuador, using the Small Area Estimation (SAE) method to integrate data from the 2014 Living Conditions Survey (LCS) and the 2010 Population and Housing Census (CPV). This is intended to generate detailed estimates at the canton and district levels, providing valuable information for designing public policies that address the country's most vulnerable groups [8].

In order to enrich the theoretical and methodological framework of this study, a comprehensive review of recent scientific literature on the application of Small Area Estimation (SAE) in similar contexts has been conducted. This review has identified relevant studies that address specific methodological challenges, such as the selection of appropriate regression models, the validation of assumptions and the assessment of the sensitivity of estimates to different scenarios [22]. Research exploring the use of machine learning and big data techniques to improve the precision of small area estimates and overcome the limitations of traditional methods has also been included [23]. The incorporation of these recent studies helps to strengthen the evidence base of our research and place it in the context of more current debates on the measurement and analysis of child poverty.

Recent studies support the value of the SAE methodology in similar situations. For example, an analysis by [8], applied this technique to measure poverty in rural areas of Latin America, confirming its accuracy when compared to census data. At the national level, the National Institute of Statistics and Census of Ecuador [23] has started to use SAE to refine its official statistics, showing promising results. These experiences, both local and global, reinforce the strength and importance of the approach this study adopts.

This research has been based on an extensive review of the scientific literature, both in the field of Small Area Estimation (SAE) methodology and in the analysis of child poverty and demographic projections. Throughout the study, references are presented to support both the methodology and the data used in this study.

For studies that have used SAE in other geographical contexts, we recommend consulting the work of [24] in the field of public health, as well as the studies of [25] in the context of agriculture. These works provide concrete examples of how SEM can be applied in different areas and with different data sources.

In terms of updated data sources, the most recent World Bank and ECLAC reports on poverty and inequality in Latin America have been reviewed, as well as the most recent population and housing censuses of the countries in the region. These reports provide updated data on

the socio-economic situation of the population and can be used to validate and complement the results of this study.

Finally, for recent studies on population projections and poverty, we have consulted the work of [26] on demographic trends at the global level, as well as the studies of [27] on poverty and inequality in the world. These works provide a global perspective on demographic trends and poverty, which can help contextualize the results of this study.

2. Methodology

2.1 SMALL AREA ESTIMATION

Small Area Estimation (SAE) techniques are a set of statistical methods for estimating parameters for small subpopulations. These techniques are especially useful when the subpopulation of interest is contained within a larger study. In this context, the term "small area" generally refers to a small geographical boundary, such as a province, canton, parish or district. It may also encompass a "small domain", which refers to a specific demographic group within a larger region [28].

When a survey is conducted at the national or state level, the sample size in small areas may be insufficient to generate accurate estimates. To address this challenge, additional data, such as census records, can be used, which are available for these small areas and help to obtain more reliable estimates [29]. The SAE methodology allows information to be obtained at levels of territorial disaggregation that cannot be achieved by standard methods. This is valuable as it provides reliable estimates on one or several relevant variables in areas where existing information is insufficient to provide valid estimates [30]. All SAE methods rely on auxiliary data available for sub-populations. However, in many cases, the information may be limited and only allow estimates to be made for larger geographic areas or certain population subgroups [31].

Since not all poverty-related variables are collected in a census that covers the entire population, it is essential to resort to tools that provide more detailed information on specific localities, such as surveys or administrative records [32]. The availability of accurate data on living conditions is essential for targeting policies and programs to reduce poverty. Having adequate poverty estimates is crucial for managing programs and allocating resources to local jurisdictions [28]. Identifying vulnerable and poor populations is essential for the design and implementation of programs that promote economic and social inclusion. This aims to generate opportunities that facilitate equality and social cohesion [30]. The SAE methodology is based on modelling information from various sources to produce estimates on variables of interest at the local level. It is particularly useful when sample sizes in the domains are too small to provide acceptable precision in the estimators [29].

According to [4], the Small Area Estimation (SAE) methodology is a valuable technique for obtaining reliable estimates for small areas, which are subpopulations with little or no sample information. This methodology uses mixed models, which combine information from the sample and from auxiliary sources, such as censuses or administrative records. This makes it possible to obtain more accurate and efficient estimators than direct estimators. In addition, the SAE methodology offers several methods to calculate the mean square error and confidence intervals, which are fundamental to measure the uncertainty of small area estimators. In recent years, the SAE methodology has incorporated advanced techniques, such as machine learning, to improve the performance and flexibility of small area estimators. These techniques allow adapting to changing conditions, and provide more accurate estimates for small areas. However, it is important to remember that these are only estimates and may be subject to errors and variations due to the uncertainty inherent in any estimation process.

The SAE methodology has a number of advantages over traditional estimation methods. Firstly, SAE allows more precise estimates to be obtained in small areas. Secondly, SAE allows information from different sources to be incorporated, which can improve the precision of the estimates. Third, SAE is a flexible technique that can be adapted to different types of data. All small area estimation (SAE) methods rely on auxiliary data available at the sub-population level, such as administrative records, specific surveys or data from the latest census. This information is essential to construct predictor variables that are integrated into a statistical model, which is then used to predict the values of the variable of interest in various small areas [29].

In order to generate estimates using SAE, it is essential to take into account several factors. It is necessary to assess whether there is a demand for such statistics, whether there is the commitment and willingness of an entity to provide methodological support and expert staff, whether the available information is sufficient, and whether the auxiliary data and variables of interest are correlated [32].

The relevance of these aspects lies in the fact that, over time, policy makers have increasingly started to use quantitative and qualitative information to design, implement and monitor projects and programs of public interest. National or regional information is no longer sufficient, especially in a context where decentralized public management is sought. There is a growing demand for data that provide more detailed and specific territorial disaggregation; for example, it is not uncommon to request information on specific population groups within certain parishes or districts [33]. Currently, various sources of information are used to adequately define target populations in

order to direct concrete actions for the benefit of these communities. More detailed data therefore facilitates decision-making and is essential for the design of targeted public policies and realistic financial planning [34].

The main source of information used remains the census, as it provides a wide range of household data and covers the entire population, allowing for well-disaggregated information. However, since the census is conducted every ten years, many variables may lose relevance over time [31]. On the other hand, there are surveys that collect specific information more frequently; however, these only allow estimates to be made for large geographic areas or larger population groups.

Mechanisms need to be sought to generate more specific and disaggregated statistics. One option would be to modify the design of surveys to meet information needs or to increase the sample size of existing surveys, although this may involve high costs. Another alternative would be to collect information in smaller localities; however, this would require each local government to finance the process, which is not always feasible [10]. In this context, estimation techniques such as SAE are gaining popularity by providing statistical information at smaller territorial levels. SAE produces estimates on variables of interest using census data and other sources that provide more detailed information on specific localities [29].

The effectiveness of SAE methods depends to a large extent on the availability of suitable predictor variables that are measured uniformly across the population. It is crucial to analyses each variable used in the estimation and select the most appropriate predictive model. In addition, the effective use of SAE methods requires a thorough assessment of model quality. Finally, when estimating in smaller domains, it is important to validate their accuracy. Fortunately, there have been significant advances in the development of SAE models that minimize the mean square error and provide more accurate estimates [29].

To ensure the transparency and reproducibility of our study, it is important to provide additional details on the statistical models used and the data sources selected. In particular, the model for estimating consumption poverty is based on multiple linear regression [35]. The selection of the independent variables was made based on previous scientific literature and the availability of data in the selected sources, such as the 2010 Population and Housing Census and the 2014 Living Conditions Survey [14]. These data were carefully processed and validated to ensure their quality and reliability.

The Small Area Estimation (SAE) methodology was chosen because of its ability to overcome the limitations of traditional estimation methods, which often require large samples to generate accurate estimates [4]. In contrast, SAE allows combining survey data with census information to obtain reliable estimates at the local level, even in areas with small samples [35]. This methodology is particularly useful when seeking to analyze variables such as consumption poverty, which are not available in censuses but are available in surveys such as the Living Conditions Survey (LCS 2014) [14].

Econometric models, specifically multiple linear regression and generalized linear regression (GLS), were selected to integrate data from the 2014 LCS and the 2010 Census of Population and Housing (CPV). These models allow for predicting variables such as per capita consumption in small areas by relating them to demographic and socioeconomic factors [9]. The choice of these techniques is justified by their ability to handle multiple variables and correct for possible correlations between them, which is essential for obtaining accurate estimates of child poverty [36].

The sample used was based on a probability sampling design, ensuring representativeness of the population studied. Small areas were selected based on geographic relevance and data availability, allowing for adequate coverage of the most vulnerable regions [84]. For data analysis, Stata software was used, which offers advanced tools for implementing complex statistical models [37].

Independent variables were selected based on their relevance in explaining consumption poverty. Demographic variables such as age and gender were included, as well as socio-economic variables such as household income and parental education level [38]. Dummy variables, such as membership in a specific ethnic group, were included to capture significant differences in poverty among different population groups [39].

2.2 METHODOLOGICAL ASPECTS OF SAE

Domains can be defined on the basis of characteristics that segment the population into a set of sub-populations that are mutually exclusive. Generally, these domains are established according to geographical areas, such as states, provinces, municipalities, regions, districts or metropolitan areas, as well as by socio-demographic groups, which may include categories such as age, gender or ethnicity within a broader region [40]. Small area estimation (SAE) is classified into two types of estimators: direct and indirect. A direct estimator is based exclusively on sample information from a specific domain. This type of estimator can incorporate known auxiliary information, such as the values of an auxiliary variable X, X that is related to the variable of interest Y, Y. However, a disadvantage of direct estimators is that they can have large standard errors, especially if the sample size in the domain is small or non-existent [19], [41].

On the other hand, an indirect estimator uses values of the variable of interest Y, Y from a related domain or from a specific time period. This approach increases the "effective" sample size and reduces the standard error. The information used for these estimators is obtained from

recent censuses or current administrative records. There are three main types of indirect estimators: the indirect domain estimator, which uses values from another domain; the indirect time estimator, which uses values from another period; and the estimator that combines both aspects, using values from another domain and another period simultaneously [28].

2.3 GENERAL MATHEMATICAL MODEL FOR INDIRECT ESTIMATION AT THE AREA LEVEL

In Small Area Estimation (SAE) [42], an area-level model is used when the data from a survey, such as the Living Conditions Survey (LCS 2014), is available for specific areas but lacks sufficient sample size to make reliable estimates at a smaller geographic level (e.g., cantons, districts). The area-level model combines these direct survey estimates with auxiliary information available for the entire population from sources like the Census of Population and Housing (CPV 2010).

In [42], indicates the general mathematical model for area-level SAE is based on the Fay-Herriot model, which assumes the following structure:

$$\widehat{Y}_i = X_i^T\beta + u_i + e_i \qquad i=1,\ldots,m \tag{1}$$

Where:

$\widehat{Y}_i$ is the direct estimate of the parameter of interest (e.g., poverty rate or consumption poverty) for area obtained from the survey (LCS 2014).

X_i^T is a vector of auxiliary variables for area (e.g., socio-economic variables from CPV 2010).

β is a vector of unknown regression coefficients that relate the auxiliary variables to the area-level estimates.

u_i is the random area effect, capturing the variation specific to area that is not explained by the auxiliary variables. It follows a normal distribution $u_i \sim N(0,\sigma_u^2)$.

e_i is the sampling error associated with the direct estimate $\widehat{Y}_i$, assumed to follow a normal distribution $e_i \sim N(0,\sigma_{e_i}^2)$.

2.3.1 Steps in the Model

1. Model specification: The Fay-Herriot model combines direct estimates from a survey with auxiliary data, assuming a linear relationship between the two.
2. Error structure:

e_i: The survey sampling error, which depends on the sample size in each area.

u_i: The area-level random effect, which accounts for unexplained variability between areas.

The goal is to estimate the population parameter for each area using both the survey data and the auxiliary data. The empirical best linear unbiased predictor (EBLUP) is often used for this purpose.

2.4. ESTIMATION PROCESS FOR THE FAY-HERRIOT MODEL

Step 1: Linear model setup

The model assumes that for each area i, the estimate $\widehat{Y}_i$ from the survey can be modeled as (1). The vector X_i contains the auxiliary variables (e.g., census data from CPV 2010), and the regression coefficients β describe the relationship between these variables and the survey estimate $\widehat{Y}_i$.

Step 2: Estimation of β using Generalized Least Squares (GLS)

The regression coefficients β are estimated using Generalized Least Squares (GLS), accounting for the heteroscedastic errors e_i across areas:

$$\widehat{\beta} = \left(\sum_{i=1}^{m} X_i^T V_i^{-1} X_i\right)^{-1}\left(\sum_{i=1}^{m} X_i^T V_i^{-1}\widehat{Y}_i\right) \tag{2}$$

Where is the variance-covariance matrix for area , defined as:

$$V_i = \sigma_u^2 + \sigma_{e_i}^2 \tag{3}$$

The term σ_u^2 is the variance of the area-specific effect u_i, and $\sigma_{e_i}^2$ is the sampling error variance of the direct survey estimate $\widehat{Y}_i$.

Step 3: Empirical Best Linear Unbiased Prediction (EBLUP)

Once the regression coefficients are estimated, the EBLUP for the parameter of interest (e.g., poverty rate) in area is given by:

$$\widehat{Y_i^{EBLUP}} = X_i^T\hat{\beta} + \hat{u}_i \tag{4}$$

Where:

$$u_i = \frac{\sigma_u^2}{\sigma_u^2 + \sigma_{e_i}^2}\left(\hat{Y}_i - X_i^T\hat{\beta}\right) \tag{5}$$

This formula adjusts the direct estimate by incorporating the auxiliary data from , effectively combining the direct survey data with census information to produce a more reliable estimate at the area level.

2.4.1 Particular Model for LCS 2014 and CPV 2010

In your case, you have two data sources: Living Conditions Survey (LCS 2014): This provides direct estimates of consumption poverty but lacks sufficient sample size to give reliable estimates for smaller geographic areas (e.g., cantons or districts).

Census of Population and Housing (CPV 2010): This provides detailed auxiliary information at a highly disaggregated geographic level but does not contain direct measures of consumption poverty.

Given this, the indirect method should be applied at the area level because: LCS 2014 provides area-level estimates of poverty for larger areas (e.g., provinces), but these estimates are subject to high variability due to small sample sizes in some areas. CPV 2010 provides auxiliary data at smaller geographic levels (e.g., cantons or districts), which can be used to improve the estimates from LCS 2014. The particular model for your case would look like this (1). Where:

$\hat{Y}_i$ is the direct estimate of consumption poverty for area from LCS 2014.

X_i^T is the vector of auxiliary variables (e.g., income levels, housing characteristics) from CPV 2010.

β is the vector of regression coefficients to be estimated.

u_i is the random area effect specific to area .

e_i is the sampling error from the LCS 2014 estimate.

2.4.2 Model interpretation: Auxiliary data from CPV 2010 helps predict the consumption poverty rate for smaller areas. Random effects () account for area-specific deviations not explained by the census data. The EBLUP estimator combines direct survey estimates from LCS 2014 with predictions based on census data from CPV 2010 to produce more accurate small-area estimates.

Decision: For your case, you should work at the area level because the data from LCS 2014 provides estimates for areas, while CPV 2010 provides auxiliary variables at a more detailed geographic level. By applying the Fay-Herriot model, you can improve the reliability of the consumption poverty estimates for small areas by combining the survey and census data.

2.5 LOGARITHMIC FAY-HERRIOT MODEL FOR INDIRECT ESTIMATION

In [42], it is indicated that, in order to include the logarithmic consumption poverty model in the indirect small area estimation (SAE) model, the formulation is slightly changed. The (ln) transformation helps deal with skewed distributions of the dependent variable (poverty by consumption), making the model more robust and suitable for handling extreme values. In this case, we model the logarithm of the poverty by consumption variable from the Living Conditions Survey (LCS 2014). The indirect model at the area level is now written as follows:

$$ln(\hat{Y}_i) = X_i^T\beta + u_i + e_i \qquad i=1,\ldots,m \qquad (6)$$

$ln(\hat{Y}_i)$ is the log-transformed direct estimate of consumption poverty for area from LCS 2014.

X_i^T is the vector of auxiliary variables (e.g., socioeconomic indicators, housing conditions) from the Census of Population and Housing (CPV 2010).

β is the vector of regression coefficients to be estimated.

u_i is the random area effect, which accounts for unexplained variation specific to area . It follows a normal distribution $u_i \sim N(0,\sigma_u^2)$.

e_i is the sampling error associated with the direct estimate , assumed to follow a normal distribution $e_i \sim N(0,\sigma_{e_i}^2)$.

2.5.1 Estimation Steps with Logarithmic Model

Step 1: Linear Model in Log Space

The direct estimates from LCS 2014 are transformed by taking the logarithm of the poverty by consumption estimates (6). This model allows the log-transformed direct estimate to depend linearly on the auxiliary data from CPV 2010, with adjustments for random effects and sampling error.

Step 2: Estimation of using GLS (Generalized Least Squares)

As in the standard Fay-Herriot model, the regression coefficients are estimated using Generalized Least Squares (GLS). However, now we are working with the log-transformed estimates:

$$\hat{\beta} = \left(\sum_{i=1}^{m} X_i^T V_i^{-1} X_i\right)^{-1}\left(\sum_{i=1}^{m} X_i^T V_i^{-1} ln(\hat{Y}_i)\right) \qquad (7)$$

Where V_i is the variance-covariance matrix for area *i*, defined as:

$$V_i = \sigma_u^2 + \sigma_{e_i}^2 \qquad (8)$$

This accounts for both the variability between areas (through u_i) and the sampling error (through e_i).

Step 3: Empirical Best Linear Unbiased Prediction (EBLUP) in Log Space

The EBLUP for the log-transformed poverty by consumption in area is given by:

$$ln\left(\widehat{Y_i^{EBLUP}} = X_i^T\hat{\beta} + \hat{u}_i\right) \qquad (9)$$

Where:

$$\hat{u}_i = \frac{\sigma_u^2}{\sigma_u^2 + \sigma_{e_i}^2} \left(ln\ (\hat{Y}_i) - X_i^T \hat{\beta} \right) \quad (10)$$

This predictor combines the direct estimate of log-transformed poverty by consumption $ln\ (\hat{Y}_i)$ with predictions based on auxiliary data from CPV 2010, adjusted for area-specific random effects.

Step 4: Back-Transformation to Original Scale

To obtain the estimate of poverty by consumption on the original scale (non-logarithmic), the EBLUP estimates are back-transformed:

$$\widehat{Y_i^{EBLUP}} = exp\ (X_i^T \hat{\beta} + \hat{u}_i) \quad (11)$$

This back-transformation gives the final estimate of poverty by consumption for area .

Particular Model for Log-transformed Consumption Poverty in Ecuador

For your case with LCS 2014 and CPV 2010, the logarithmic Fay-Herriot model applied to poverty by consumption would look like this:

$$ln\ (\hat{Y}_i) = X_i^T \beta + u_i + e_i \qquad i=1,...,m$$

$ln\ (\hat{Y}_i)$ is the log-transformed estimate of consumption poverty for area from LCS 2014.

X_i^T represents a set of auxiliary variables from CPV 2010, such as income, education, employment, housing conditions, and other socio-economic factors.

β is the vector of coefficients to be estimated.

u_i captures random area effects for area i, reflecting variations not explained by the auxiliary data.

e_i is the sampling error of the direct estimate from LCS 2014.

By taking the logarithm of the poverty by consumption variable, you ensure the model handles skewness and extreme values more effectively. The auxiliary data from CPV 2010 allows the model to make reliable predictions at smaller geographic levels (cantons, districts) where LCS 2014 alone would be unreliable due to small sample sizes. The back-transformation ensures that the final estimate is returned to the original scale of poverty by consumption after fitting the model.

This model improves the estimates of consumption poverty at smaller geographic areas by leveraging the detailed auxiliary information available from the census (CPV 2010), while correcting for small sample sizes in the survey (LCS 2014) through the log transformation and random effects adjustments.

2.6 APPLYING THE SAE METHODOLOGY IN ECUADOR

In the study by [43], he used the advanced statistical technique known as Small Area Estimation (SAE), summarized in Figure 1, to analyze consumption and poverty in specific areas of Ecuador. This technique is especially useful when trying to make precise estimates in small geographic areas where sample sizes are too small to provide reliable estimates.

Figure 1.
SAE scheme

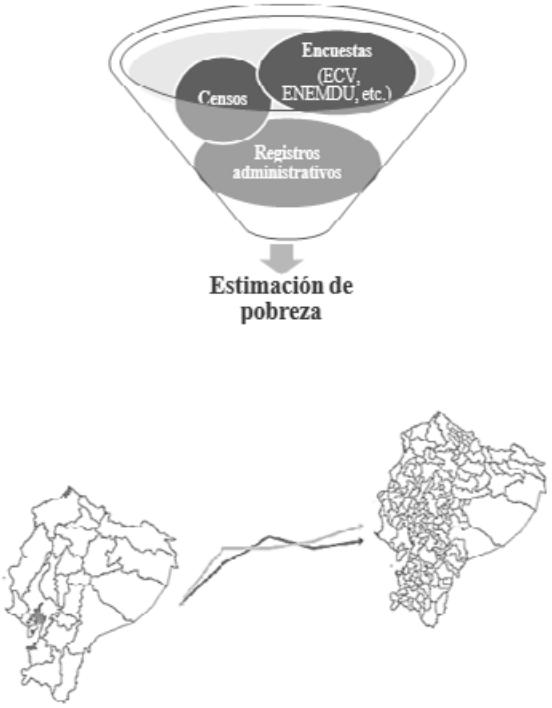

For the application of the SAE in [43], we used the Indirect method called Multiple Regression Estimator at the geographic area level of the natural logarithm of poverty by consumption, whose mathematical formulation is described in the previous section. In this initial process we used the Guide for the use of databases of the National Institute of Statistics and Census [44], this involved several important steps to analyses and effectively use data from two main sources: the Living Conditions Survey (LCS) 2013 - 2014, and the VII Population Census and VI Housing Census (CPV) 2010.

Step 1: Data collection was conducted using the Living Conditions Survey (LCS) for the years 2013-2014. This survey provided a wide range of information on the living conditions of the inhabitants of Ecuador, covering aspects such as income, expenditure, education and health, among others. In parallel, data from the VII

Population Census and VI Housing Census (CPV) conducted in 2010 were used. In addition, dummy variables were generated for each category. Dummy variables are binary variables that represent categories or groups in a statistical analysis. For example, a dummy variable could be used to code gender, assigning a value of 1 for "male" and 0 for "female". These variables allow categorical information to be included in the analysis, which generally only accepts numerical data [45].

Dummy variables are fundamental in statistical analysis, as they allow the inclusion of qualitative variables in models that require numerical data. These variables take binary values (0 or 1) and are used to represent specific attributes or categories within the data set. For example, when analyzing the impact of gender in a regression model, a dummy variable can be created to indicate whether an individual is female (1) or not (0), in [22]. This makes it easier to interpret how categorical differences affect the dependent variable in the model [46]. In summary, the creation of dummy variables is a crucial step in statistical analysis that allows for the integration of qualitative information into quantitative models. This approach not only improves the analytical power of the model, but also allows for more precise conclusions about how different categories influence the variables of interest [47].

Step 2: The homogenization of the databases was carried out in this process. In [24], he explains that reconciliation involves aligning or correlating data from different sources so that they are comparable with each other. In this case, the aim was to identify common variables between the Living Conditions Survey (LCS) and the Population and Housing Census (CPV). This means that variables that were present in both databases were selected for further analysis.

Standardization is an essential step in data analysis, as it ensures that information extracted from different sources is consistent and comparable. By identifying common variables between the LCS and the LCP, joint analysis of the data is facilitated, leading to more robust and informed conclusions about living conditions in Ecuador. Once homogenization is complete, aggregation at the household level follows, followed by a critique of the data. This step is crucial in any analysis, as it involves checking the data for errors, inconsistencies or outliers that may distort the results. In this case, outliers were removed and the database was cleaned, preparing it for the next phase of the process [48]. Table 1 presents the homologous variables obtained. In addition, in [43], the code necessary to carry out the homologation and aggregation of variables at the household level can be found.

Step 3: After standardizing and cleaning the two databases at the household level, the dependent and independent variables were identified. Dependent variables are those variables that we seek to predict or explain, while independent variables are used to make that prediction or explanation. In this analysis, the dependent variable was consumption poverty, while the independent variables were demographic and socio-economic in nature. It should be noted that only variables included in both databases were considered, as presented in Table 1 [24]. Simultaneously, econometric models were developed with data from both sources to predict per capita consumption. Econometric models are fundamental statistical tools in economics that allow for the examination of relationships between different variables. In this case, the variables selected for the models were similar to those used in the VII Population and VI Housing Census (2010), which ensured consistency in the analysis across data sources [49].

Once the models were developed, they were applied to census data, allowing for predictions of per capita consumption in specific geographic areas. These predictions were then used to calculate the consumption poverty rate in the districts of interest. In this case, poverty was determined by considering as poor those individuals whose per capita consumption was below a pre-established threshold [43] study provided a clear picture of consumption poverty in specific areas of Ecuador. By employing the Small Area Estimation (SAE) technique, accurate estimates were achieved even in areas with small sample sizes, highlighting the importance of advanced statistical techniques in economic and social studies [48].

In summary, the process allowed us to extract valuable information from the Living Conditions Survey (LCS) and the Population and Housing Census (CPV), facilitating a better understanding of consumption poverty at the household level in Ecuador. Subsequently, econometric models were estimated using Ordinary Least Squares (OLS) and Generalized Least Squares (GLS), following the SAE methodology. In addition, heteroskedasticity issues were analyzed using non-constant variance models, as recommended in the literature [40]. Finally, these parameters were applied to the census data, allowing us to predict consumption and construct the consumption poverty rate in small areas, robust to the level of the 365 Ecuadorian districts [49].

Step 4: Coding and application of the SAE methodology was carried out. This process began with the use of the Living Conditions Survey (LCS) standardized at household level. From this database, an explanatory model was created for each province, modelling the natural logarithm of per capita consumption. This approach is common in econometric analysis, as it allows transforming the data to make it more manageable and reduce the influence of extreme values on the results [49]. Subsequently, we integrated the analysis of heteroskedasticity, a common feature in economic data, which refers to the non-constant variation of errors in a regression model. This step was essential to fit the models appropriately, as heteroscedastic errors can influence the precision of

Table 1.

Indicators and/or standardized variables included in the methodology

Nº	Variable Name	Description	Azuay	Bolívar	Cañar	Carchi	Cotopaxi	Chimborazo	El Oro	Esmeraldas	Guayas	Imbabura	Loja	Los Ríos	Manabí	Morona Santiago	Napo	Pastaza	Pichincha	Tungurahua	Zamora Chinchipe	Galápagos	Sucumbíos	Orellana	Santo Domingo de los Tsáchilas	Santa Elena
1	C	Constant -	1	1	1	1	1	1	1	1	1	1	1	1	1	1	1	1	1	1	1	1	1	1	1	1
2	Analfabeto	Head of household is illiterate	1	1	0	1	1	1	0	1	1	1	1	0	0	0	1	1	0	1	1	0	1	0	0	0
3	analfabeto_cl	Percentage of heads of household who cannot read and write at cluster level	1	0	1	1	1	0	1	1	1	0	0	1	0	1	1	0	0	1	1	0	1	1	0	0
4	cocina_ex	The household has a kitchen exclusively for the use of the household.	1	0	0	0	0	0	1	1	1	0	0	1	0	0	0	0	1	0	0	0	0	0	1	0
5	cocina_ex_cl	Percentage of households that have a kitchen exclusively for household use at cluster level	0	0	1	1	0	1	1	0	0	0	0	0	1	1	1	0	1	0	1	0	1	1	0	1
6	edad_p	Average household age	1	1	1	0	0	1	1	0	1	1	0	0	1	0	1	0	1	1	1	0	1	0	0	0
7	edad_p_cl	Average household age at cluster level	1	1	1	0	1	1	0	1	1	0	0	1	1	0	1	1	0	1	0	0	1	1	1	1
8	edad2	Age squared of the household	0	1	0	0	0	0	1	1	1	0	1	0	0	0	0	0	0	0	0	0	1	0	0	0
9	edad2 cl	Age squared average household age at cluster level	1	0	1	0	0	1	1	0	0	0	1	1	1	1	1	0	0	1	1	1	0	1	0	0
10	edad2_p	Average age of the household squared	1	0	1	1	1	1	1	1	1	1	0	0	1	0	1	0	1	1	1	0	1	1	1	1
11	edad2_p_cl	Mean squared household age at cluster level	1	1	1	0	1	1	0	0	1	0	1	1	0	1	1	0	1	1	1	1	1	1	1	0
12	h01	Number of bedrooms in the dwelling	1	1	1	1	1	1	1	0	1	1	1	1	1	1	0	1	1	1	0	1	0	1	1	1
13	h01_cl	Average number of bedrooms in the dwelling at the cluster level	1	1	1	1	0	1	1	0	1	0	0	0	0	0	1	1	1	0	0	0	0	0	0	1
14	h04_2	The shower is shared with other households	0	1	0	0	0	0	0	0	0	1	0	0	0	1	0	0	1	1	0	0	0	0	0	0
15	h04_3	No shower	1	1	1	1	1	0	1	1	1	0	1	0	1	0	0	1	1	1	1	0	0	0	1	0
16	h15_3	You own the house and you are paying for it	0	0	0	0	1	0	1	1	1	0	0	0	1	0	1	0	1	1	0	0	0	0	1	0
17	h15_4	Housing is owned and fully paid for	1	0	1	1	0	0	1	0	0	0	0	1	0	0	0	0	1	1	0	1	0	0	1	0
18	h15_5	The house is ceded	0	0	0	1	0	0	1	0	0	0	0	0	0	0	1	0	0	0	1	0	0	0	0	0
19	h15_6	Housing is received by services	0	0	0	1	0	1	1	0	0	0	0	0	1	0	0	0	0	1	0	1	0	0	1	0
20	internet	The household has internet service	1	1	1	1	1	1	1	0	1	1	1	1	1	0	0	1	1	1	1	1	0	1	1	1
21	internet_cl	Percentage of households having internet service at cluster level	1	1	1	1	0	1	0	0	1	0	1	0	1	1	0	0	1	0	0	0	1	0	0	0
22	migra_d	Household received money from friends or relatives abroad in the last 12 months	0	1	0	0	0	0	1	0	1	0	1	1	0	0	0	0	0	0	0	0	1	1	0	1
23	migra_d_cl	Percentage of households that in the last 12 months received money from friends or relatives abroad at cluster level	0	0	0	0	1	1	0	0	0	0	0	0	0	1	0	0	0	0	1	0	1	0	0	0
24	mujer	If the head of household is female	0	0	1	0	0	1	0	0	0	0	0	1	0	0	1	0	0	1	0	0	0	1	1	0
25	mujer_cl	Percentage of female heads of household by cluster	0	1	0	0	0	0	0	1	0	0	0	0	0	1	0	0	0	1	1	0	1	0	1	0
26	nivel_2	Level of education of the head of household: GBS	0	0	1	0	0	1	1	0	0	0	0	1	0	0	0	1	1	0	0	1	0	0	1	1
27	nivel_3	Level of education of the head of household: incomplete secondary education	0	0	1	0	0	1	1	0	1	0	1	1	1	0	0	1	1	1	0	1	0	0	1	1
28	nivel_4	Level of education of the head of household: medium	1	1	1	1	1	1	1	1	1	1	1	1	1	1	1	1	1	1	1	1	0	0	1	1
29	nivel_5	Level of education of head of household: non-university tertiary education	1	0	1	0	0	1	1	0	1	1	0	1	0	1	1	0	1	1	1	1	1	0	1	0
30	nivel_6	Level of education of the head of household: university education	1	1	1	1	1	1	1	1	1	1	1	1	1	1	1	0	1	1	1	0	1	1	1	1
31	no_empleo	Head of household is unemployed	0	0	0	1	1	1	0	0	0	0	1	0	1	0	0	0	0	0	0	0	0	1	1	0
32	no_empleo_cl	Percentage of unemployed household heads	1	1	1	0	0	1	1	0	0	1	1	0	0	0	0	1	0	1	1	0	1	0	0	0
33	p03	Age of head of household	0	1	0	1	0	0	1	0	1	0	1	0	0	0	1	0	0	0	0	0	1	0	1	0
34	p03_cl	Average age of heads of households at cluster level	1	0	1	0	1	1	1	0	0	1	1	1	1	1	1	1	0	1	1	0	0	1	0	1
35	p16_2	Ethnicity of head of household: Afro-descendant	1	0	1	1	1	0	1	0	0	0	0	0	0	0	0	0	0	0	0	0	0	0	0	0
36	p16_3	Ethnicity of head of household: Montubio	1	0	1	1	0	0	1	0	0	0	0	0	0	1	0	1	0	0	0	1	0	0	0	0
37	p16_4	Ethnicity of the head of household: mixed race	0	0	1	0	1	0	0	1	0	1	0	0	0	1	1	0	0	1	1	0	0	0	0	0
38	p16_5	Ethnicity of head of household: white or other	1	0	0	0	0	1	0	1	0	1	1	0	0	1	1	1	0	1	0	0	1	1	0	0
39	p34_2	Marital or conjugal status of the head of household: common-law union	0	0	1	0	0	1	1	0	0	0	1	1	0	0	0	1	1	0	0	0	1	1	0	0
40	p34_3	Marital or conjugal status of the head of household: separated	0	0	0	0	0	1	0	0	0	1	0	0	1	0	1	0	0	0	0	0	0	0	0	1
41	p34_4	Marital or conjugal status of the head of household: divorced	0	0	0	0	0	0	0	0	1	1	0	1	1	0	0	0	0	1	0	0	0	0	0	0
42	p34_5	Marital or conjugal status of the head of household: widowed	0	1	0	0	0	1	0	1	1	0	0	0	0	0	0	0	1	1	0	0	0	0	0	0
43	p34_6	Marital or conjugal status of the head of household: single	0	0	0	1	0	0	0	1	0	0	0	0	0	0	1	1	0	0	0	0	0	1	1	1
44	pa_ad	Suitable housing wall materials	1	0	1	0	0	0	0	0	0	0	0	0	1	1	1	0	0	0	1	0	0	0	1	1
45	pa_ad_cl	Percentage of dwellings with adequate wall materials at cluster level	1	0	1	1	1	1	0	0	0	0	0	0	0	0	1	0	0	0	0	0	0	0	0	0
46	pi_ad	Suitable flooring materials	1	0	0	1	1	1	0	0	0	1	1	0	0	0	0	0	0	1	0	0	0	0	0	0
47	pi_ad_cl	Percentage of dwellings with adequate flooring materials at cluster level	0	0	1	1	0	1	0	1	1	0	0	0	1	0	0	0	1	0	1	0	0	0	0	0
48	rat_dp	Male/Female Ratio at household level	1	1	1	1	1	1	1	1	1	1	1	1	1	1	0	1	1	1	1	1	1	1	1	1
49	rat_dp_cl	Average Male/Female Ratio at cluster level	1	0	0	0	0	1	0	0	1	0	1	0	1	1	0	0	0	1	0	0	0	0	0	0
50	rural	Rural areas	0	0	0	1	0	0	1	0	1	0	1	1	1	0	0	0	1	0	1	0	1	0	0	1
51	T_am	Number of persons over 65 per household	0	0	1	1	0	1	1	0	1	0	0	1	1	1	1	1	0	0	1	1	1	0	0	0
52	T_am_cl	Percentage of people aged 65+ at cluster level	1	0	1	1	0	1	1	0	1	1	0	0	1	1	0	0	0	1	0	0	1	0	0	0
53	T_me	Number of persons aged 5-17 per household	1	1	1	1	1	1	1	1	1	1	1	1	1	1	0	1	1	1	1	1	1	1	1	1
54	T_me_cl	Percentage of households with 5–17-year-olds at cluster level	1	0	1	1	1	0	1	1	1	0	1	0	1	1	1	0	1	0	1	0	1	1	0	0
55	T_nn	Number of persons under 5 per household	1	1	1	1	1	1	1	1	1	1	1	1	1	1	0	1	1	1	1	1	1	1	1	1
56	T_nn_cl	Percentage of households with persons older than 5 years old at cluster level	0	1	1	1	1	0	0	0	1	0	0	0	0	0	1	1	0	1	0	0	1	1	0	0
57	T_ped	Number of persons with disabilities per household	1	1	1	0	1	0	1	0	1	1	1	0	1	0	0	0	1	1	0	0	1	1	1	0
58	T_ped_cl	Percentage of households with persons with disabilities at cluster level	0	0	1	0	0	1	0	0	1	0	0	0	0	1	0	0	0	1	1	0	0	0	0	0
59	T_per	Number of persons per household	1	1	1	1	1	1	1	1	1	1	1	1	1	1	1	1	1	1	1	1	1	1	1	1
60	T_per_cl	Average number of people at cluster level	1	0	0	1	0	1	1	0	1	0	0	0	0	0	1	1	1	0	1	0	1	1	0	1
61	te_ad	Adequate roofing materials	0	0	0	0	0	0	0	0	0	0	0	0	1	1	0	1	0	0	0	0	0	1	0	1
62	te_ad_cl	Percentage of dwellings with adequate roofing materials at cluster level	0	1	0	0	1	1	0	0	1	0	0	0	0	1	0	0	0	0	0	0	1	1	0	0
63	telef_f	Household has conventional telephone service	1	1	1	1	1	1	1	1	1	1	1	1	1	0	1	0	1	1	1	1	1	1	1	1
64	telef_f_cl	Percentage of households with conventional telephone service at cluster level	0	0	0	0	0	1	1	1	0	0	0	1	1	0	0	0	1	1	1	0	0	1	0	0
65	tvcable	The household has cable television service	1	1	1	1	1	1	1	1	1	1	1	1	1	1	1	1	1	1	1	1	1	1	1	1
66	tvcable_cl	Percentage of households with cable TV service at cluster level	0	0	0	1	0	0	1	1	0	0	0	0	1	1	0	0	0	0	1	0	0	0	0	0
67	v08_2	The water supply is piped outside the house but on the lot.	0	1	1	1	1	1	1	0	0	1	0	0	1	0	1	1	1	1	0	0	1	1	1	1
68	v08_3	Water supply is piped outside the dwelling, lot or land	0	0	0	0	1	0	0	0	0	0	0	0	1	0	1	0	1	1	0	0	1	0	0	0
69	v08_4	Water supply is not piped but received by other means.	1	0	1	0	1	1	0	0	0	0	0	1	1	1	1	1	1	1	0	1	1	1	1	1
70	v09_2	Type of toilet facilities: toilet and septic tank	0	0	1	0	1	0	0	0	0	0	0	0	0	1	0	1	1	0	1	0	0	0	0	0
71	v09_3	Type of toilet facilities: toilet and cesspool	0	0	0	1	1	0	0	1	0	0	0	0	0	1	0	0	1	1	1	0	0	1	0	0
72	v09_4	Type of toilet: latrine	1	0	0	0	0	1	1	0	0	0	0	0	0	0	0	0	1	0	0	0	1	0	0	0
73	v09_5	Type of toilet: none	0	0	0	1	0	1	0	0	0	1	0	1	0	1	0	0	0	0	1	0	1	1	0	1
74	v12a	Number of energy-saving light bulbs used by the household	1	1	1	1	1	1	1	1	1	1	1	1	1	1	1	1	1	1	1	1	1	1	1	1
75	v12a_cl	Average number of saved light bulbs used by households at the cluster level	1	0	1	1	0	1	1	1	0	1	0	1	0	1	1	0	1	0	1	0	1	0	1	1
76	vap_2	Main access to the house: cobblestones	0	0	0	0	0	0	0	1	0	1	1	1	1	1	0	0	1	1	1	0	1	1	1	0
77	vap_3	Main access to the dwelling: ballasted/dirt road	1	1	1	0	0	0	1	0	1	1	1	0	0	0	1	0	1	0	0	0	0	1	1	0
78	vap_4	Main access to the dwelling: pathway/walkway/other	1	1	1	0	0	0	0	0	1	1	1	0	0	0	0	0	1	0	0	1	0	1	0	0
79	vap_5	Main access to the dwelling: river/sea/lake	1	0	0	0	0	0	0	0	1	0	0	1	1	0	1	0	0	0	0	0	1	1	0	0
80	vtv_2	Type of housing: flat in house or building	0	0	0	0	1	0	1	1	1	0	1	1	0	0	0	1	1	0	0	0	1	0	1	1
81	vtv_3	Type of housing: room in a tenement house	1	0	1	0	0	0	0	0	0	0	0	0	0	0	0	0	0	0	0	1	1	0	0	0
82	vtv_4	Type of dwelling: half-hut, hut or hut	0	0	0	0	0	1	0	0	0	0	0	0	1	0	0	1	0	0	0	0	0	0	0	0
83	vtv_5	Type of dwelling: ranch	0	0	0	1	0	0	0	0	1	0	1	1	1	0	0	0	0	0	0	0	0	0	1	1

Source: [15]

the estimated coefficients and thus the reliability of per capita consumption predictions [48].

The output of these routines was a matrix of estimated coefficients, which was subsequently used to estimate consumption poverty in Ecuador's Census of Population and Housing CPV database. This step allowed us to apply the models fitted in the LCS to the CPV, thus generating more accurate predictions about the distribution of consumption poverty at the provincial level, which is key for planning effective public policies in the country. The coding used in [43] is shown below:

```
* ------------------------------------------------------------- *
* Small Sample Estimation (SAE)
                    *
* Consumption Poverty Estimation from LCS 2014 in CPV 2010 * *
* General Estimation Syntax *
* *------------------------------------------------------------- *

clear all
set more off
set matsize 11000
set maxvar 30000
set seed 1234

/* ------------------------------------------------------------- *
Declare Programme in Mata for GLS estimation
* ------------------------------------------------------------- */

mata
void sigma(real scalar N, real scalar Ncl){

//*** 1. Construct the Omega matrix for GLS with clustered errors.
Si=J(N, N, 0)
M=st_matrix("max")
m=st_matrix("min")

sigma2_h=st_matrix("sigma2_h")
sigma2_cl=st_matrix("sigma2_cl")

for (cl=1; cl<=Ncl; cl++)  {
m_=m[cl,1]
M_=M[cl,1]
for (i=m_; i<=M_; i++) {
for (j=m_; j<=M_; j++) {
        if (j==i){
                Si[j,i]=sigma2_h[i,1];
        }
        if (j!=i){
                Si[j,i]=sigma2_cl[i,1];
        }
    }
  }
}

//*** 2. Estimation v'a GLS

y=st_matrix("y")
X=st_matrix("X")

// Estimation of coefficients
inv_Si=invsym(Si)
b_gls=invsym(X'*inv_Si*X)*X'*inv_Si*y

// Variance-Covariance Coefficient Variance Matrix Estimation
V_gls=invsym(X'*inv_Si*X)

// Adjustment Estimation (R^2)
e=y-X*b_gls
sse=e'e
iota=J(N,1,1)
y_=y-iota*mean(y)
sst=y_'y_
R2=1-sse/sst

// Matrix of Coefficients and Standard Errors
se = sqrt(diagonal(V_gls))
report=(b_gls, se, b_gls:/se)

// Extract matrices back to Stata
st_matrix("report", report)
st_matrix("R2", R2)
st_matrix("b_gls", b_gls)
st_matrix("V_gls", V_gls)
}
end

/* ------------------------------------------------------------*
        Call database
* ------------------------------------------------------------*/
```

```
use "C:/SAE_2/1. Databases /base_hogares.dta", clear
forv d=1/24{  /* Start of loop for provinces */
preserve
*local d=1
keep if dominio==`d'

/* ---------------------------------------------------------------*
        Definitions
* ---------------------------------------------------------------*/
*gen ln_con=ln(cpcf)
* Declare dependent variable (dep) and independent variable (ind)
global dep ln_con
global ind      T_per T_nn T_me T_am T_pcd rat_dp p03 edad2_ ///
                edad_p edad2_p rural p16_2-p16_5 mujer nivel_2-nivel_6 p34_2-p34_6 analfabeto no_empleo ///
                migra_d vap_2-vap_5 v09_2-v09_5 h01 v08_2-v08_4 h04_2-h04_3 telef_f internet tvcable h15_3-h15_6 v12a ///
                te_ad pa_ad pi_ad vtv_2-vtv_5 cocina_ex T_per_cl-cocina_ex_cl

* Declare cluster level
gen cluster=ciudad

/* ---------------------------------------------------------------*
Estimation of the Consumption Model for each domain
* ---------------------------------------------------------------- */

***     1. Initial adjustment by OLS
reg $dep $ind, vce(r)

* Eliminate omitted variables in OLS (Must run more than once for some provinces)
global ind: colnames(e(b))
global ind= subinstr("$ind", "_cons", "", .)

forv r=1/100 {
foreach x of global ind {
local a = substr("`x'",1,2)
        if "`a'" == "o." {
        global ind = regexr("$ind", "`x'", "")
        }
}
}

* Selecting independent variables with 10% significance or less using a backward stepwise
sw, pr(.10): reg $dep $ind, vce(r)
keep if e(sample)

* Extract variables used effectively
global ind: colnames(e(b))
global ind= subinstr("$ind", "_cons", "", .)

* Create matrix X with actually used variables including a column of 1's
gen c=1
global ind2 "${ind} c"

*** 2. Decompose errors between parts of each household and cluster.
scalar K=colsof(r(table))
predict res, residual
egen res_cl=mean(res), by(cluster)
gen  sigma2_cl=res_cl^2
gen  res_h=res-res_cl
gen  e2=res_h^2

mkmat $dep, mat(y)
mkmat $ind2, mat(X)

/* ---------------------------------------------------------------*
Estimation of the Heterocedasticity Model for each domain
* ---------------------------------------------------------------*/

qui sum e2
scalar A=1.05*r(max)
gen het=ln(e2/(A-e2))
reg het $ind, vce(r)
scalar K_a=colsof(r(table))
scalar sigma_r=e(rss)/(e(N)-K_a)
predict xb if e(sample), xb
gen B=exp(xb)
gen  sigma2_ch=(A*B/(1+B))+0.5*sigma_r*(A*B*(1-B)/((1+B)^3))
gen sigma2_h=sigma2_ch+sigma2_cl

* Output matrices
mat a_het`d'=e(b)
mat a_V`d'=e(V)
```

```
/* ----------------------------------------------------------------*
        Estimation of the Model v'a GLS
* ----------------------------------------------------------------*/

*** 1. Construction of estimated sigma matrix of variance covariance of errors **Diagonal elements equal to variance of each household + variance of the cluster component **Off-diagonal elements equal to variance of the cluster component within the cluster

** 1.1 Initial definitions *Order the clusters
egen ncl=group(cluster)
sort ncl
*Identify the number of clusters
qui sum ncl
local Ncl=r(max)
*Identify the size of each cluster
bysort cluster: gen s_cl=_N
*Identify the starting position of each cluster
gen m_cl = 1 if ncl == 1
forval po = 2 / `Ncl' {
        local i = `po' - 1
        qui sum s_cl if ncl == `i'
        local max1 = r(max)
        qui sum m_cl if ncl == `i'
        local max = `max1'+r(max)
        replace m_cl = `max' if ncl == `po'
}
*Set upper limit for each cluster
gen M_cl=m_cl+s_cl-1

*Minimum and Maximum Matrices to fill clusters in the variance-covariance matrix
qui mean m_cl, over(ncl)
mat min=e(b)'

qui mean M_cl, over(ncl)
mat max=e(b)'

** 1.2 Filling in the estimated sigma matrix
mkmat sigma2_cl, mat(sigma2_cl)
mkmat sigma2_h, mat(sigma2_h)
local N=_N

** 1.3 Estimation of the declared function in Mata
mata sigma(`N', `Ncl')

** 1.4 Output matrices
mat b`d'=b_gls'
mat V`d'=V_gls'

mat dom=J(K,1,`d')
mat mod`d'=(dom, report)
mat rownames mod`d'=$ind2
mat R2_=(nullmat(R2_)\(`d',R2))
mat N=(nullmat(N)\(`d',_N))
mat msigma_r=(nullmat(msigma_r)\(`d',sigma_r))
mat mA=(nullmat(mA)\(`d',A))

**1.5 Extract cluster variance matrices
collapse (mean)sigma2_cl, by(cluster)
cd "C:/SAE_2/3. Estimacion/Resultados"
save "eta_`d'.dta", replace

/* ----------------------------------------------------------------*
        Simulations of coefficients
* ----------------------------------------------------------------*/

/* Create 100 random vectors of coefficients for each province averaging the vector estimated by GLS (or OLS in case of the alpha model) and their respective variance-covariance matrices. */

** Alpha Model (Heteroscedasticity Model)
local d1= colsof(a_het`d')
drawnorm a_het1-a_het`d1', n(100) mean(a_het`d') cov(a_V`d') clear
local i=0
macro drop inda
        foreach x of global ind2 {
        local i = `i'+1
        rename a_het`i' a_`x'
        global inda "$inda a_`x'"
        }
gen dominio = `d'
gen sim = _n
reshape wide $inda, i(dominio) j(sim)
tempfile alpha_`d'
save `alpha_`d"

**Beta Model (Model of the mean)
drawnorm b1-b`d1', n(100) mean(b`d') cov(V`d') clear
local i=0
macro drop indb
```

```
        foreach x of global ind2 {
        local i = `i'+1
        rename b`i' b_`x'
        global indb "$indb b_`x'"
        }
gen dominio = `d'
gen sim = _n
reshape wide $indb, i(dominio) j(sim)
tempfile beta_`d'
save `beta_`d"
restore
} /* Loop closure for provinces */

* Create a single coefficient file for all 24 provinces after running the loop.
global var "alpha beta"
foreach x of global var {
use ``x'_1', clear
        forval p = 2 / 24 {
        append using ``x'_`p"
        }

cd "C:/SAE_2/3. Estimation/Results "
save `x', replace
}

cd "C:/SAE_2/3. Estimation/Results "

use beta, clear
merge 1:1 dominio using alpha
drop _m
order dominio, first

cd "C:/SAE_2/3. Estimation/Results "
save "sim_b.dta", replace

*Crear matriz de etas por cluster
use eta_1, clear
        forval p = 2 / 24 {
        append using eta_`p'
        }

cd "C:/SAE_2/3. Estimation/Results "
save "eta_T.dta", replace

* Create matrix of variance parameters per household
clear
svmat msigma_r
svmat mA
drop mA1
rename msigma_r1 dominio
rename msigma_r2 sigma_r
rename mA2 A
save "A_sigma.dta", replace

**Extract model matrices, fit levels and sample sizes
mat2txt2 R2_ N using Ajuste.txt, replace
mat2txt2 R2_ N using Ajuste.txt, replace

mat2txt2 mod1 ///
mod2 ///
mod3 ///
mod4 ///
mod5 ///
mod6 ///
mod7 ///
mod8 ///
mod9 ///
mod10 ///
mod11 ///
mod12 ///
mod13 ///
mod14 ///
mod15 ///
mod16 ///
mod17 ///
mod18 ///
mod19 ///
mod20 ///
mod21 ///
mod22 ///
mod23 ///
mod24 using modelos.txt, replace
```

Step 5: Corresponding simulations were carried out using the standardized Census of Population and Housing (CPV) base together with the matrices and coefficients obtained in Step 4. These simulations allow for the inherent variability in the models, and are a common approach in econometrics to assess the robustness of estimates. In this case, 100 simulations were run to estimate per capita consumption poverty at the household level, which is essential to obtain a more accurate and detailed picture of the distribution of poverty [50].

Each of these 100 simulations generated a different estimate of consumption poverty, capturing possible fluctuations in the data and ensuring that the predictions are more representative of reality. These multiple simulations approach is useful when working with estimates in econometrics, as it allows for more reliable results to be obtained by averaging the different simulations, thus reducing uncertainty in the models [51]. From these estimates, the population of children aged 0-3 living in consumption poverty at the household level was selected. This step was key to identifying the most vulnerable groups and targeting more effective public policies. The precise estimates obtained through this process allow the design of targeted interventions that have a direct impact on improving the living conditions of the child population [43]. The coding is presented below:

```
* ------------------------------------------------------------ *
* Small Sample Estimation (SAE)                    *
*Estimation of Consumption Poverty from LCS 2014 in CPV 2010 *
*Simulations in the CPV
* ------------------------------------------------------------*

clear all
macro drop _all
set more off
set matsize 11000
set maxvar 30000
set seed 1234

/* ------------------------------------------------------------ *
        Create simulation bases
* ------------------------------------------------------------*/

* For speed of calculation, each simulation of coefficients needs to be separated (100 bases are created - 1 for each simulation).
cd "C:/SAE_2/3. Estimation/Results "
use sim_b, clear
forval y = 1 / 100 {
        foreach x of varlist b_T_per1 - a_te_ad100 {
        local v : var label `x'
        tokenize "`v'"
                                if `y' == `1' {
                                global var "$var `2'`1'"
                                }
        }
        preserve
        keep dominio $var
        cd "C:/SAE_2/3. Estimacion/Temp"
        recode b_* a_* (.=0)
        save sim_`y'.dta, replace
        restore
        macro drop var
}
/* ------------------------------------------------------------*
        Call CPV database
* ------------------------------------------------------------*/
use "C:\SAE_2\1. Databases \base_trabajo_cpv.dta", clear
*sample 10

gen cluster=ciudad

*Demographic composition of the household
egen T_per=sum(numpers), by(id_hogar)
gen menor=(p03>=5 & p03<=17)
egen T_nn=sum(p_5), by(id_hogar)
egen T_am=sum(p_65), by(id_hogar)
egen T_me=sum(menor), by(id_hogar)
egen T_h=sum(num_hom), by(id_hogar)
egen T_m=sum(num_muj), by(id_hogar)
gen rat_hm=T_h/T_m
gen rat_dp=(T_nn+T_me+T_nn)/T_per
egen edad_p=mean(p03), by(id_hogar)
gen edad2_p=edad_p^2
gen edad2_=p03^2
gen pcd=(p08==1)
egen T_pcd=sum(pcd), by(id_hogar)

* Ethnic recoding
recode p16 (2/4=2)

* Recoding level of education
gen       nivel=0 if p23==1
replace  nivel=1 if p23>=2 & p23<=4
replace nivel=1 if p23==5 & p24<=3
replace nivel=1 if p23==6
replace nivel=2 if p23==5 & p24>3 & p24<6
replace nivel=2 if p23==7 & p24<3
replace nivel=3 if p23==5 & p24==6
replace nivel=3 if p23==7 & p24==3
replace nivel=4 if p23==8
replace nivel=5 if p23==9 | p23==10
```

```
label define nivel 0"Ninguna" 1"EGB" 2"Media Incompleta" 3"Media" 4"Superior no Universitaria" 5"Universitaria"
label val nivel nivel

* Identification of suitable housing materials
gen te_ad=(v01>=1 & v01<=4)
gen pa_ad=(v03>=1 & v03<=4)
gen pi_ad=(v05>=1 & v05<=5)

* Keeping only the head of household and household information
keep if p02==1

*** Create dummies for each variable to create the X matrix of the GLS model.
foreach v in p16 nivel p34 vap v09 v08 h04 h15 vtv {
qui tab `v', gen(`v'_)
}

* Correct ethnicity others for few remarks. Joins whites
replace p16_5=1 if p16_6==1

* Correct housing access others for few remarks. Joins *a sendero
replace vap_4=1 if vap_6==1

* Correct antichresis housing tenure for few observations. Joins *a  arriendo
replace h15_1=1 if h15_2==1

* Correct dwelling type shack and hut for few observations. Joins *a mediagua
replace vtv_4=1 if vtv_6==1 | vtv_7==1
gen rural=(urp==2)
gen mujer=(p01==2)
gen analfabeto=(p19==2)
gen no_empleo=(p27==2)
gen migra_d=(m1==2)
gen telef_f=(h07==1)
gen internet=(h09==1)
gen tvcable=(h11==1)
gen cocina_ex=(h02==1)

* Cluster level average variables
foreach v in T_per T_nn T_me T_am T_pcd rat_dp edad_p edad2_p p03 edad2_ mujer ///
                analfabeto no_empleo migra_d h01 telef_f internet tvcable v12a ///
                te_ad pa_ad pi_ad cocina_ex {
                egen `v'_cl=mean(`v'), by(ciudad)
                }

clonevar dominio=provincia

*Keep only variables to be used
keep cluster id_hogar dominio T_per T_nn T_me T_am T_pcd rat_dp p03 edad2_ ///
        edad_p edad2_p rural p16_2-p16_5 mujer nivel_2-nivel_6 p34_2-p34_6 analfabeto no_empleo ///
        migra_d vap_2-vap_5 v09_2-v09_5 h01 v08_2-v08_4 h04_2-h04_3 telef_f internet tvcable h15_3-h15_6 v12a ///
        te_ad pa_ad pi_ad vtv_2-vtv_5 cocina_ex T_per_cl-cocina_ex_cl

*Identifying the independent (explanatory) variables
global  ind T_per T_nn T_me T_am T_pcd rat_dp p03 edad2_ ///
        edad_p edad2_p rural p16_2-p16_5 mujer nivel_2-nivel_6 p34_2-p34_6 analfabeto no_empleo ///
        migra_d vap_2-vap_5 v09_2-v09_5 h01 v08_2-v08_4 h04_2-h04_3 telef_f internet tvcable h15_3-h15_6 v12a ///
        te_ad pa_ad pi_ad vtv_2-vtv_5 cocina_ex T_per_cl-cocina_ex_cl

*Keep only remarks with complete information.
foreach v in $ind{
drop if `v'==.
}

order dominio cluster id_hogar, first

/* ---------------------------------------------------------------*
        Simulations
* ---------------------------------------------------------------*/

* Run each of the 100 simulations
forv s=1/100{
disp `s'
preserve

cd "C:/SAE_2/3. Estimacion/Temp"
destring dominio, replace
```

```
* Call the normalisation parameters of heteroscedasticity per domain
merge m:1 dominio using "C:/SAE_2/3. Estimacion/Resultados/A_sigma.dta"
drop _m

* Call eta estimates (cluster-level heteroscedasticity)
merge m:1 cluster using "C:/SAE_2/3. Estimacion/Resultados/eta_T.dta"
drop if _m==2
drop _m
egen sigma2_cl_=mean(sigma2_cl), by(dominio)
replace sigma2_cl=sigma2_cl_ if sigma2_cl==.

* Call the model coefficients Alpha and Beta for each simulation.
merge m:1 dominio using sim_`s'
keep if _m==3
drop _m

* Estimate the logarithm of per capita consumption according to the beta model (ln_con_d)
*Estimate the heteroscedasticity according to the alpha model (B_)
gen ln_con_d=b_c`s'
gen B_=a_c`s'
foreach v of varlist $ind {
di "`v'"
replace ln_con_d=ln_con_d + `v'*b_`v'`s'
replace B_=B_ + `v'*a_`v'`s'
}

gen B=exp(B_)

gen  sigma2_ch=(A*B/(1+B))+(0.5*sigma_r*(A*B*(1-B)/((1+B)^3)))

* Randomly estimate assuming normality the error components (at household level u_h and cluster level u_c).
gen u_h=rnormal(0, sqrt(sigma2_ch))
gen u_c=rnormal(0, sqrt(sigma2_cl))

* Bringing together the three components of estimated per capita consumption
egen ln_con=rsum(ln_con_d u_h u_c)
gen con_pc`s'=exp(ln_con)
keep id_hogar con_pc`s'

* Store a baseline of the results for each household of the 100 simulations of the estimated per capita consumption.
cd "C:/SAE_2/3. Estimation/Results "
if `s'==1{
        save cpv_con_.dta, replace
        }
else{
        merge 1:1 id_hogar using cpv_con_.dta, nogen
        save cpv_con_.dta, replace
        }

restore
}

/* ----------------------------------------------------------------*
        Poverty Estimation
* ----------------------------------------------------------------*/
cd "C:\SAE_2\1. Databases "
use "base_trabajo_cpv.dta", clear
gen id_sector=substr(id_hogar,1,12)

merge m:1 id_sector using "id_hogar-circuitos.dta"
drop if _m==2
drop _m

keep id_hogar izodec idist ciudad urp p01 p03 p08

cd "C:/SAE_2/3. Estimacion/Resultados"
merge m:1 id_hogar using "cpv_con_.dta"

keep if _m==3
drop _m

gen canton=substr(ciudad, 1, 4)
gen prov_=substr(ciudad, 1, 2)

*sample 2

*Define the poverty line of the LCS 2014
scalar lp=83.22367

* Estimate for each household 100 poverties according to its estimated per capita income in each of the 100 simulations.
forv s=1/100{
```

```
        gen pobre`s'=(con_pc`s'<lp)
}

* Creating care populations
gen cnh=(p03>=0 & p03<=3)
gen cibv=(p03>=1 & p03<=3)
gen joven=(p03>=15 & p03<=29)
gen ad_m=(p03>=65 & p03!=.)
gen pcd=(p08==1)
gen nac=1

*Create planning area with prefix Z
tostring izodec, replace
gen z="Z"
egen zonap=concat(z izodec)

* Create province with prefix P
cap tostring prov_, replace
gen p="P"
egen prov=concat(p prov_)

keep pobre* cnh cibv joven ad_m pcd nac zonap idist canton prov

* Create poverty for each population for each simulation
foreach p in cnh cibv joven ad_m pcd nac {
        foreach d in nac zonap idist canton prov {
                foreach stat in mean sum {
                        preserve
                        collapse (`stat') pobre* if `p'==1, by(`d')
                        cd "C:/SAE_2/3. Estimation/Results "
                        tempfile `p'_`d'_`stat'
                        rename `d' id
                        capture tostring id, replace
                        forv i=1/100{
                                rename pobre`i' pobre_`p'_`i'
                        }
                        save "``p'_`d'_`stat'"", replace
                        restore
                }
        }
}

foreach stat in mean sum {
        foreach p in cnh cibv joven ad_m pcd nac {
                use "``p'_nac_`stat'"", clear
                foreach d in zonap idist canton prov {
                        append using "``p'_`d'_`stat'""
                        }
                cd "C:/SAE_2/3. Estimacion/Temp"
                save `p'_`stat'.dta, replace
        }
}

foreach stat in mean sum {
        cd "C:/SAE_2/3. Estimacion/Temp"
        use cnh_`stat', clear
        foreach p in cibv joven ad_m pcd nac {
                append using `p'_`stat'
        }
        cd "C:/SAE_2/3. Estimation/Results "
        collapse (sum) pobre*, by(id)
        save "pobreza_res_`stat'.dta", replace
}
/* ------------------------------------------------------------*
Output files
* ------------------------------------------------------------*/
foreach stat in mean sum {
        cd "C:/SAE_2/3. Estimation/Results "
        use "pobreza_res_`stat'.dta", clear
        reshape long pobre_cnh_ pobre_cibv_ pobre_joven_ pobre_ad_m_ pobre_pcd_ pobre_nac_, i(id) j(s)

collapse (mean) cnh=pobre_cnh_ cibv=pobre_cibv_ joven=pobre_joven_ ad_m=pobre_ad_m_ pcd=pobre_pcd_ nac=pobre_nac_ ///
 (sd) cnh_sd=pobre_cnh_ cibv_sd=pobre_cibv_ joven_sd=pobre_joven_ ad_m_sd=pobre_ad_m_ pcd_sd=pobre_pcd_ nac_sd=pobre_nac_, by(id)

        gen l=length(id)
        sort l id
        drop l

        foreach u in cnh cibv joven ad_m pcd nac{
                gen `u'_cv=`u'_sd/`u'*100
        }
        export excel using "C:/SAE_2/3. Estimation/Results/Base_final_`stat'.xls", firstrow(variables) replace
}
```

2.7 LOGARITHMIC FAY-HERRIOT MODEL FOR INDIRECT ESTIMATION AND ITS RELATION TO THE MULTIPLE LINEAR REGRESSION MODEL FOR THE LOGARITHM OF CONSUMPTION POVERTY

The Fay-Herriot model [42], is a methodology used for indirect estimation in small areas, where sample size is limited. It is generally applied in situations such as censuses or national surveys, where data are scarce in certain geographic areas or sub-populations. The model assumes that direct estimates of a target variable for a small area can be improved by using auxiliary variable information and empirical models. From the above syntax, the Fay-Herriot model is identified mainly in the estimation structure using the generalized least squares (GLS) method and in the way variance components are handled. The model is presented in the following form:

2.7.1 Fay-Herriot mathematical model (logarithmic).

In [31], the Fay-Herriot model for small area estimation is given in (6).

2.7.2 Parameter estimation

In the syntax provided, generalized least squares (GLS) methods are used to estimate the coefficients and the variances of the model components (heteroscedasticity and cluster variance). This is observed in the following code fragment the application of the formula for the estimated coefficients by GLS is: , donde is the variance-covariance matrix of the errors, which in this case has been estimated by separating the variance of each household and the errors at the cluster level.

// Coefficient estimation using GLS
inv_Si = invsym(Si)
b_gls = invsym(X'*inv_Si*X)*X'*inv_Si*y

Here, the inversion of the variance-covariance matrix is performed that this represented as ( ) and it is estimated , the fitted coefficients of the model.

2.7.3. Decomposition of errors

The Fay-Herriot model takes into account the decomposition of errors into two components:

- Within-household variance : individual variance for each unit within an area or cluster.
- Inter-cluster variance : variance between the different areas or clusters. This treatment is evident in the syntax with the creation of the variance matrices:

gen sigma2_cl = res_cl^2
gen res_h = res - res_cl
gen e2 = res_h^2

2.7.4 Logarithmic model

The dependent variable modelled is the natural logarithm of per capita consumption. This is stated with:

gen ln_con = ln(cpcf)

This suggests that the Fay-Herriot model is being fitted to a log-transformed dependent variable. Model summary, the model implemented is a GLS-adjusted Fay-Herriot model, considering heteroskedasticity and variance effects at the cluster level, and applying a log transformation to the dependent variable to model per capita consumption in small areas. In mathematical terms, the model can be expressed as:

$$ln\left(Consumo_i\right)=X_i'\beta+u_i+e_i \qquad i=1,\ldots,m \tag{12}$$

Where the coefficients are estimated and variances (cluster) and (household) using generalized least squares, and an adjustment for heteroskedasticity is included using , the diagonal variance-covariance matrix.

2.8 RESULTS OBTAINED FROM THE APPLICATION OF THE FAY-HERRIET MODEL IN THE PARAMETER ESTIMATION AND THE ADJUSTED MODEL

When applying the Fay-Herriot model in parameter estimation, it is essential to verify that the assumptions of the model are met to ensure the validity and reliability of the results. The Analysis of Variance - ANOVA, indicates that the Fay-Herriot model has proven to be a valuable tool in the analysis of complex data, particularly in contexts where estimation for small areas is crucial. As shown in table 2, the variability decomposition shows that the sum of squares of the regression reaches a value of 9,634.1391, reflecting the portion of variability explained by the model. With 82 degrees of freedom, the mean square of the regression stands at 117.490, indicating a considerable explanation of the variability in the data [42]. On the other hand, the residuals present a sum of squares of 4,698.2966, with 27.696 degrees of freedom, suggesting a considerable sample size and a mean square of residuals of 0.16963809, a value that evidences the accuracy of the model in minimizing estimation errors [24]. The R^2 of approximately 0.67 (67.2%) underlines the relevance of the included auxiliary variables, as they explain more than two-thirds of the variability in the data, which is remarkable in small-area estimation contexts where data are often sparse and of higher variability [27]. This model not only provides reliable estimates, but also offers a solid basis for evidence-based decision-making, especially in situations where precision in geographically defined areas is essential for social and economic interventions [52]. Table 3 (annexes) presents the estimation of the consumption poverty parameters obtained by the Fay-Herriot model.

Table 2.
ANOVA - Analysis of Variance

Source of variation	SS	Df.	MS
Regression	9,634.1391	82	117,490
Residues	4,698.2966	27696	0.16963809
Total	14,332.4357	27778	0.51596356

Number of obs.	=	27.779
F(82, 27696)	=	692.59
Prob > F	=	0,0000
R^2	=	0.6722
R^2 – Adjusted	=	0.6712
Root MSE	=	0.41187

Source: [15]

The following graph presents the kernel density estimate of the model residuals together with a theoretical normal distribution for comparison. The solid curve represents the estimated distribution of the observed residuals, while the dotted line shows a normal distribution with the same mean and standard deviation.

Regarding the shape of the curve, it is observed that the kernel estimate closely resembles a normal distribution, which is a good sign for the Fay-Herriot model. However, there are some interesting details:

- The higher part of the kernel curve looks a bit flatter compared to the theoretical normal distribution.
- The tails of the kernel curve seem to spread out a bit more, suggesting that there might be more extreme values than we would expect in a standard normal distribution.

The bandwidth used in the kernel estimation is 0.0457, which determines how much the data is smoothed. A smaller bandwidth would make the curve follow the raw data more closely, while a larger one would produce a smoother curve.

In summary, the residuals of the Fay-Herriot model are approximately normally distributed, which is essential for the model to be valid. The similarity between the kernel curve and the theoretical normal distribution indicates that the residuals comply quite well with the assumption of normality. However, the small differences in the shape of the curve suggest that the residuals might have a slightly leptokurtic distribution, i.e. with heavier tails than those of a standard normal distribution. Although this slight deviation from normality is noticeable, it does not invalidate the model completely [40], [53].

Figure 2.
Kernel density estimation

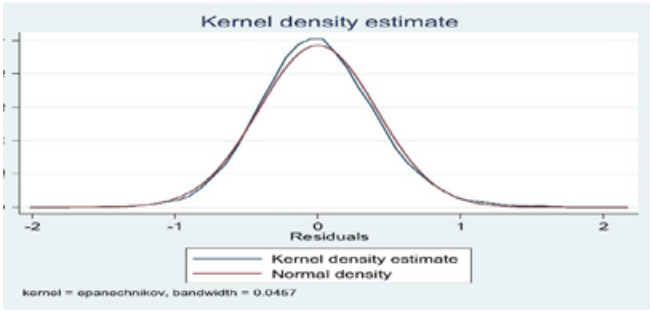

Source: [15]

Figure 3 presents a visual comparison between the quantiles of the residuals of the Fay-Herriot model and the corresponding quantiles of a theoretical normal distribution. In this graph, each point represents an observed residual, while the straight line shows the normal distribution expected under the assumption of normality.

In general, most of the points align quite well with the reference line, suggesting that the residuals follow an approximately normal distribution. This alignment is especially noticeable in the central range of the data, where the residuals fit well to the expected theoretical distribution.

However, at the extremes of the distribution, particularly at the bottom left of the graph, a slight deviation of the points from the straight line is observed. This deviation can be interpreted as an indication that the residuals have slightly heavier tails than those of a standard normal distribution, which is consistent with the previous observation of a leptokurtic distribution in the kernel density curve analysis.

In conclusion, the residuals of the Fay-Herriot model reasonably comply with the assumption of normality, which is fundamental for the validity of the statistical inferences of the model. Although there is a slight trend towards heavier tails, this deviation is not sufficient to invalidate the model. However, it may be beneficial to perform a more detailed analysis of the residuals to identify possible outliers or patterns not captured by the current model. Overall, the model proves adequate for the data analyzed, providing a solid basis for estimates and predictions in small area contexts [40], [54].

Figure 3.

Distribution of Residuals for the Fay-Herriot Model

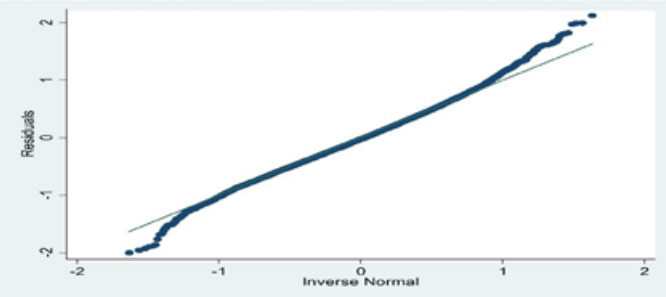

Source: [15]

Figure 4, which presents the residuals versus fitted values, provides a detailed insight into the behavior of the Fay-Herriot model. The residuals, which represent the differences between the observed values and those predicted by the model, are randomly distributed around the reference line (zero), which is a positive sign. This dispersion around zero suggests that the model is not systematically biased, i.e. it does not tend to consistently underestimate or overestimate the true values.

Homoscedasticity, i.e. the constancy of the variance of the residuals over the fitted values, is clearly seen in the graph. This feature is fundamental in regression models, as violations of this assumption could indicate problems in the specification of the model or the need for transformations in the variables.

Furthermore, the absence of discernible patterns in the distribution of residuals (such as systematic curves or trends) indicates that the model has adequately captured the relationship between the explanatory variables and the dependent variable. This suggests that the auxiliary variables included in the model are relevant and that the functional form of the model is appropriate.

Finally, no extreme residuals are identified that could distort the results, which is important for the robustness of the estimates. Taken together, these features of the residual plot versus fitted values support the validity of the Fay-Herriot model for these data, fulfilling the assumptions necessary for statistical inference to be reliable in small-area estimation contexts [40], [54].

Figure 4.

Residuals versus Fitted Values in the Fay-Herriot Model

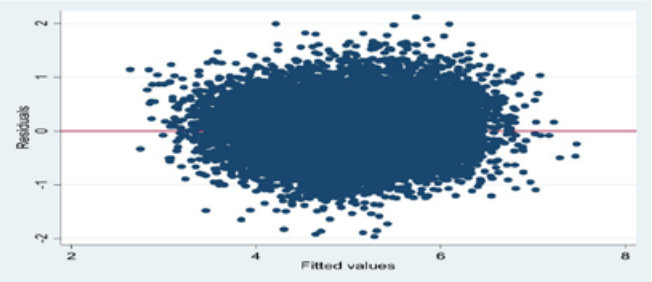

Source: [15]

Table 3 (Annexes) presents a GLS-adjusted Fay-Herriot model obtained in [43], with the logarithm of consumption as the dependent variable. Household characteristics and their impact on consumption are analyzed, showing estimated coefficients, standard errors, t-values, and confidence intervals for each independent variable and the intercept. The table shows that consumption is influenced by various socio-demographic and economic characteristics, providing a broad picture of the determinants of welfare in terms of household consumption.

From the results obtained, a thorough and detailed analysis was carried out which considers the following:

- **Household size and composition:** Household size and composition, in particular the number of children aged 0-3 years, have significant effects on consumption poverty. As the number of dependents increases, be they children or older adults, per capita consumption tends to decrease, suggesting greater economic pressure on larger households or households with more dependents.
- **Education:** Education emerges as a key driver of consumption, with higher levels of education associated with higher levels of consumption, highlighting the importance of education in the fight against poverty.
- **Technological and housing conditions:** Ownership of technological goods such as fixed telephone, internet, and cable TV is positively related to consumption, reflecting a higher standard of living in households with access to these technologies.
- **Gender:** Households where the reference person is female tend to have slightly lower consumption, which could point to differences in economic opportunities between men and women.
- **Regional differences:** Households in rural areas have slightly higher consumption compared to urban areas, although this effect is small, suggesting that geographical differences are not as pronounced in this sample.

Additionally, Table 4 and Map 1, presents the goodness of fit R^2 of the econometric models used through the SAE methodology for each of the domains analyzed. The R^2 of the models, as a whole, are above the 50% recommended in the literature [42], [55]. Next, we include the values corresponding to the coefficient of determination - goodness of fit, which is obtained in the estimation of small areas at the National level where we observe that: The R^2 measures what percentage of the variability in the dependent variable (e.g. consumption) is explained by the independent variables included in the Fay-Herriet Model. This is in the multiple regression model [42]. An R^2 value close to 1 indicates that the model explains the variability of the data well. A value close to 0 indicates that the model does not explain the variability well. In the table, the R^2 values vary from 0.60 (Carchi) to 0.82 (Napo), indicating that the model has different levels of explanatory power depending on the region. A higher R^2 suggests that the model is more appropriate for that region.

In addition to this the number of observations (n) refers to how many data were used to estimate the model in each domain. Regions with more observations, such as Guayas (2973) and Pichincha (2880), tend to have more robust models because the sample is larger. Regions with fewer observations, such as Morona Santiago (611) or Galápagos (556), might have less precise estimates due to the smaller sample size. Consequently, we look at the

quality of the model by region: Where Regions with good fit: Napo ($R^2 = 0.82$), Morona Santiago ($R^2 = 0.79$), Pastaza ($R^2 = 0.75$), Orellana ($R^2 = 0.76$). The model explains more than 75% of the variability in these regions, indicating that the model is highly predictive. Regions with moderate fit: Azuay ($R^2 = 0.70$), Chimborazo ($R^2 = 0.69$), Loja ($R^2 = 0.67$), among others. The model performs well in these regions, but there could still be factors not captured by the model. Regions with the lowest fit: Carchi ($R^2 = 0.60$), El Oro ($R^2 = 0.62$), Guayas ($R^2 = 0.61$), Galápagos ($R^2 = 0.62$). Although the model still explains a significant proportion of the variability, there is room for improvement in these regions, perhaps by considering additional variables or adjusting the model.

Adicionalmente, en el anexo se incluyen resultados obtenidos

Table 4.

Goodness-of-fit R_2 of econometric models

Dominio	R^2	Number of observations
AZUAY	0.70	1929
BOLÍVAR	0.63	855
CAÑAR	0.66	923
CARCHI	0.60	858
COTOPAXI	0.63	1089
CHIMBORAZO	0.69	1117
EL ORO	0.62	1950
ESMERALDAS	0.66	1037
GUAYAS	0.61	2973
IMBABURA	0.72	1051
LOJA	0.67	1139
LOS RÍOS	0.62	1219
MANABÍ	0.67	1231
MORONA SANTIAGO	0.79	611
NAPO	0.82	681
PASTAZA	0.75	570
PICHINCHA	0.68	2880
TUNGURAHUA	0.67	1151
ZAMORA CHINCHIPE	0.67	682
GALÁPAGOS	0.62	556
SUCUMBÍOS	0.67	735
ORELLANA	0.76	652
SANTO DOMINGO DE LOS TSÁCHILAS	0.65	976
SANTA ELENA	0.66	914

Source: [15]

It is crucial to recognize that child poverty is not a one-dimensional phenomenon, but is influenced by a complex interaction of socio-economic and demographic factors. While our analysis has focused on variables such as consumption and unmet basic needs, it is important to consider the possible influence of other factors not considered that could affect children's vulnerability. For example, parental education, especially that of the mother, has been shown to be a key factor in reducing child poverty, as it influences employment opportunities and household income [21].

In addition, access to basic services such as quality health, nutrition and education plays a critical role in child development and long-term poverty prevention [56]. The availability and quality of these services can vary significantly across regions and communities, which may explain some of the observed differences in child poverty levels. In addition, factors such as domestic violence, child abuse and lack of access to a safe and stimulating environment can have a negative impact on children's well-being and increase their risk of falling into poverty [57].

For future research, it would be advisable to explore the inclusion of these additional variables in the small area estimation model in order to gain a more complete and accurate understanding of the factors contributing to child poverty. This may require additional data collection through targeted surveys or the use of administrative data sources such as health and education records. By broadening the scope of our analysis, we will be able to identify more effective and targeted interventions to break the cycle of poverty and ensure a better future for all children.

3. Results and discussion

As mentioned in the methodological section, once the multiple linear regression models were estimated for each of the domains, simulations were carried out for each domain. It should be noted that methodologically, the estimation of consumption poverty using the SAE Small Area Estimation, particularly in the Fay-Herriet model involved most of the time and work. Finally, once the consumption poverty levels were calculated down to the smallest geographical disaggregation, i.e. the districts, we proceeded to make projections for the population of children aged 0-3 years, up to the year 2030 [43].

3.1 ANALYSIS OF THE INCIDENCE OF CONSUMPTION POVERTY

Consumption poverty is analyzed at different geographical levels, showing significant variations between provinces, cantons and districts. At the national level, the consumption poverty rate is 25.8%, but varies considerably in regions such as the highlands and the coast, where rates can be up to 30% higher in rural areas [14]. This geographical heterogeneity is crucial for the implementation of public policies, as it allows targeting resources to areas of greatest need and designing interventions adapted to local conditions. For example, conditional cash transfer programs that have proven effective in reducing child poverty can be applied in areas with high poverty rates [3]. Heterogeneity of poverty helps in policy implementation by allowing better allocation of resources to the most vulnerable populations, which can improve the effectiveness of social interventions [2].

Table 5.

Consumption poverty for children aged 0-3 years, by Province

Province	Incidence	Children from 0 to 3 years old	Standard deviation	Coefficient of variation
Napo	81,3%	7.121	2,0%	2,5%
Chimborazo	79,1%	24.929	3,1%	3,9%
Santa Elena	67,4%	17.726	6,4%	9,5%
Bolívar	66,1%	8.078	4,4%	6,7%
Zamora Chinchipe	60,9%	4.532	6,6%	10,9%
Esmeraldas	59,8%	25.358	2,3%	3,9%
Imbabura	55,4%	16.440	2,0%	3,6%
Morona Santiago	54,4%	6.142	2,5%	4,6%
Manabí	53,1%	51.156	3,5%	6,5%
Los Ríos	48,2%	28.339	2,0%	4,1%
Sucumbíos	45,6%	6.081	6,2%	13,5%
Cotopaxi	45,4%	13.494	2,9%	6,3%
Loja	42,4%	13.794	3,7%	8,6%
Tungurahua	40,6%	13.843	2,3%	5,8%
Azuay	39,4%	20.734	3,3%	8,4%
Guayas	37,6%	99.474	3,0%	8,0%
Carchi	37,4%	4.301	2,4%	6,4%
Pastaza	36,9%	2.124	4,0%	10,9%
Orellana	36,3%	4.035	2,7%	7,5%
Santo Domingo de los Tsáchilas	34,1%	10.371	2,8%	8,2%
Pichincha	25,1%	46.329	1,9%	7,5%
El Oro	18,5%	7.867	2,5%	13,4%
Cañar	15,2%	2.635	3,1%	20,2%
Galápagos	1,2%	20	0,7%	61,0%
National total	**41,1%**	**434.926**	**0,9%**	**2,3%**

Source: [15]

It is important to mention that the incidence of consumption poverty shows significant variations across age groups. In this case, consumption poverty in children aged 0-3 years was 41.1% respectively at the national level. The provincial disaggregation is shown in Table 5 on the incidence of poverty in children aged 0-3 years in different provinces of Ecuador, together with the standard deviation and the coefficient of variation (CV), which indicate the precision and variability of the estimates.

- Poverty incidence: Represents the percentage of children aged 0-3 living in poverty in each province. The provinces with the highest incidence of child poverty are Napo (81.3%), Chimborazo (79.1%) and Santa Elena (67.4%), while Galápagos (1.2%) has the lowest incidence.
- Number of children: Shows the total number of children aged 0-3 affected by poverty in each province. The provinces with the highest number of children in poverty are Guayas (99,474), Manabí (51,156) and Pichincha (46,329), due to their larger child population. On the other hand, Galapagos has the lowest number of children aged 0 to 3 (20), which coincides with its low incidence of poverty.
- Standard deviation: A measure of dispersion that indicates how much estimates of poverty incidence vary. Provinces with a higher standard deviation, such as Santa Elena (6.4%) and Zamora Chinchipe (6.6%), have greater uncertainty in their estimates, while provinces such as Pichincha (1.9%) and Esmeraldas (2.3%) show less variability in estimates.
- Coefficient of variation (CV): The CV is a measure that reflects the ratio of the standard deviation to the mean, indicating the relative precision of the estimates. A lower CV suggests greater precision. The table shows that Gálapagos (61%), Cañar (20.2%) and El Oro (13.4%) have high coefficients of variation, suggesting that poverty estimates in these provinces have greater uncertainty. In contrast, Napo (2.5%) and Esmeraldas (3.9%) have lower Coefficients of Variation, indicating greater reliability in their estimates.

Below, in Map 2, the distribution of consumption poverty for children aged 0-3 years is presented at the disaggregation level as Planning Zones [43], Planning Zone 1 (53.9%) and Planning Zone 3 (53.1%) show the highest consumption poverty scores for children aged 0-3 years. On the other hand, planning zone 9 (22.3%) reflects the best situation at the level of this entire population and for the country as a whole. Planning zones 2, 4 and 8 show rates below the national average (see Annex Table 6).

Map 1.

Consumption poverty for children aged 0-3 years, by Province

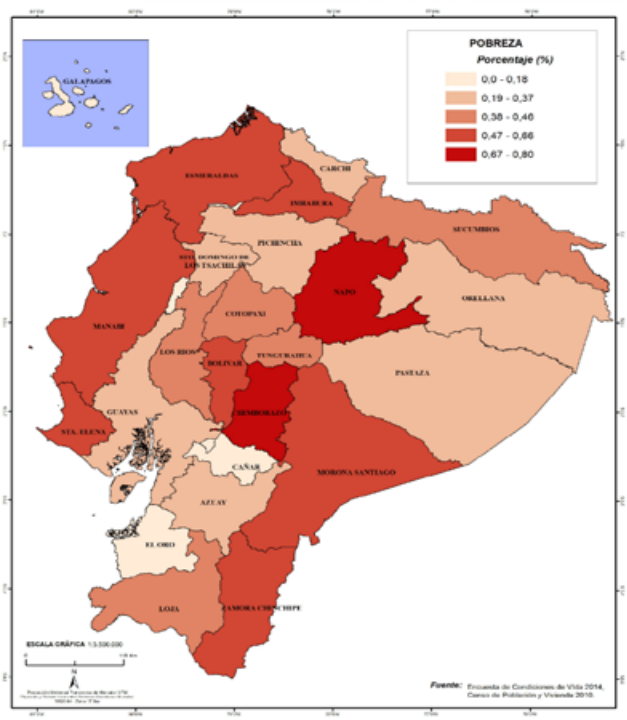

Map 2.

Consumption poverty for children aged 0-3 years, by Planning Area

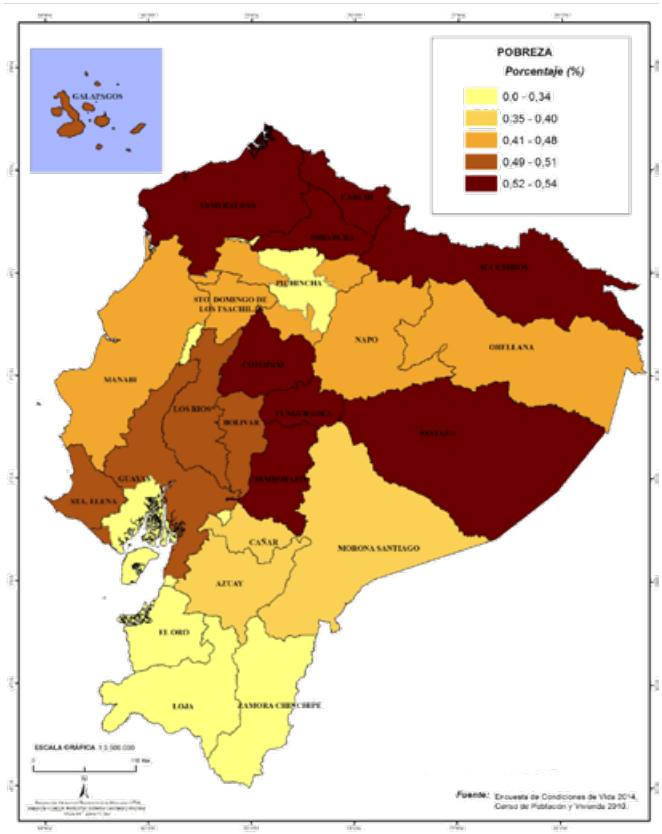

Map 3.

Consumption poverty for children aged 0-3 years, by Canton

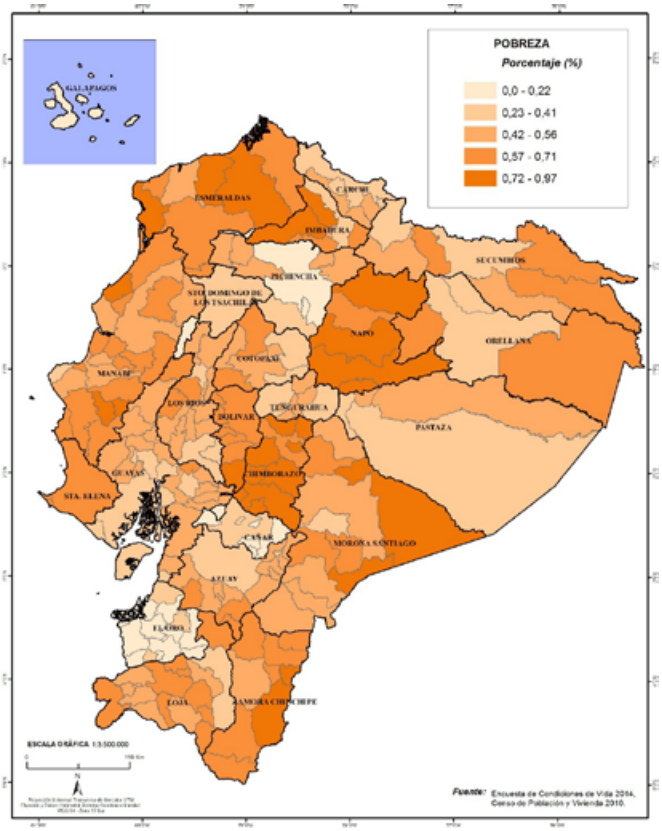

Source: [15]

Map 4.

Consumption poverty for children aged 0-3 years, by Distrito

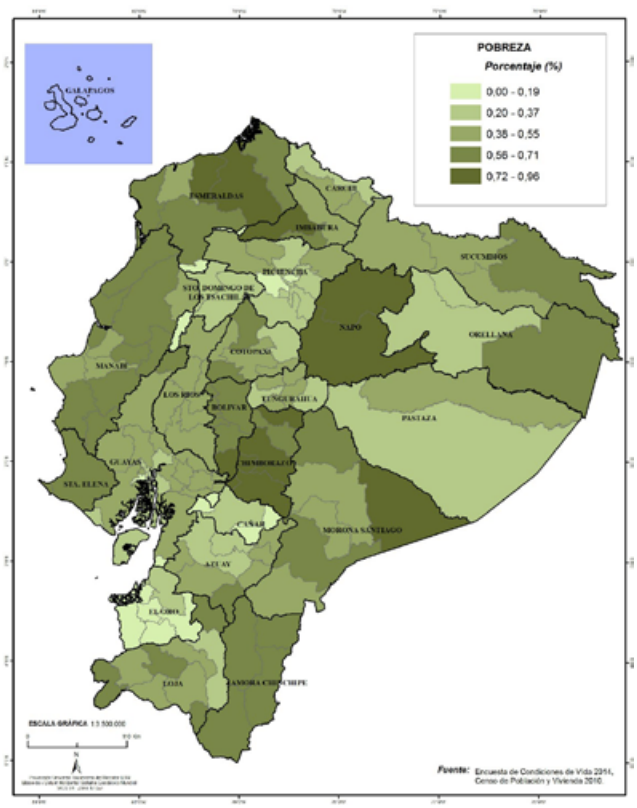

Source: [15]

In addition, Map 3 shows the distribution of poverty by consumption for children aged 0 to 3 years, at the cantonal level, where it was observed that the cantons with the highest incidence of consumption poverty are: Guamote (97.8%), Colta (95.5%), Carlos Julio Arosemena Tola (92.7%). Meanwhile, the cantons with the lowest incidence of consumption poverty are: Santa Cruz (1.4%), Isabela (0.6%), San Cristóbal (0.3%).

Finally, Map 4 shows the distribution of consumption poverty for children aged 0 to 3 years old at the district level, where the districts with the highest consumption poverty rates are: 06D04 (96.9%), 14D05 (87.5%), 06D05 (83.8%) and the districts with the lowest rates are: 03D03 (10.2%), 03D01 (6.2%), 20D01 (1%). In summary, the results show that there is significant heterogeneity in consumption poverty within territorial units in Ecuador. This allows for better targeting of public policies at the disaggregated level [43], (see Annex Estimation of consumption poverty for children 0-3 years old, according to the SAE methodology).

3.2 ESTIMATED POPULATION OF CHILDREN AGED 0 TO 3 YEARS OLD UP TO 2030, BY CONSUMPTION POVERTY.

The projection of the child population up to 2030 was made using the SAE methodology, which allows estimating consumption poverty in small areas. However, the lack of updated Living Conditions Survey (LCS) data introduces uncertainty into the projections, as recent economic changes can significantly affect consumption levels [2]. To mitigate this problem, econometric models were used that adjust the projections according to current economic trends. In addition, a homogeneous distribution of poverty in the areas studied was assumed, which could affect accuracy if not met. It is important to consider methodological adjustments to reflect possible variations in the distribution of poverty and improve the accuracy of the projections [58].

The methodology used to project the population of children aged 0-3 until 2030 is based on the use of advanced statistical techniques. These techniques allow for more precise estimates in small geographic areas where sample sizes are insufficient to provide reliable data. This methodological approach is particularly relevant in contexts where traditional data sources cannot accurately capture child population dynamics at the local level [59].

It is important to note that there is no update of the Living Conditions Survey (LCS), only the one conducted in the years 2013-2014. This survey is crucial as it provides detailed information on the living conditions and demographic structure of the Ecuadorian population. The lack of updating of this data source limits the ability to make more accurate projections on the child population. Population estimates depend on current data, and the absence of such data can compromise the accuracy of the results [60].

In addition, the demographic projections are based on the latest available information, including socio-economic and demographic data. If these sources are not up to date, projections may not adequately reflect recent changes in population structure, which could lead to less effective or inefficient public policy decisions [61].

A relevant aspect to highlight is that, despite the update of the VII Population and VI Housing Census of 2010 to the VIII Population, VII Housing and I Communities Census of 2022, the use of the latter census is not recommended for the application of the Small Area Estimation (SAE). This is because differences in the methodologies used in the 2010 and 2022 censuses may significantly affect the accuracy and validity of the SAE. The SAE relies on consistent and representative data to generate reliable estimates at the local level [4]. One of the main considerations is the change in data collection methodology. While the 2010 Census was conducted on a single day with student participation, the 2022 Census adopted a mixed approach, including both virtual and face-to-face collection. This change may have an impact on the coverage and representativeness of the data at the local level, which is critical for the proper functioning of SAE models, which require homogeneous and reliable data [62].

In addition, the 2022 Census incorporated new variables in its questionnaire, such as questions on sexual identity, pet ownership and female fertility. These variables open up new possibilities for analysis and estimation at the small area level. However, they also imply the need for adjustments to previously employed SAE models, as these must be adapted to the new types of data collected [63]. Finally, comparability of data between the 2010 and 2022 censuses will be a significant challenge. Differences in methodologies and variables collected could hinder longitudinal analyses and, consequently, the efficient application of the SAE. This challenge requires detailed evaluation to ensure that estimates remain valid and accurate [64]. Methodological changes, especially in the questionnaire for the 2010 and 2022 Censuses in Ecuador, could have important implications for the implementation of the Small Area Estimation (SAE). These modifications affect both the coverage and representativeness of the data, as well as the variables available for analysis at the local level. As a result, the accuracy of population projections may be limited. In particular, when working with models that rely on consistent data, any variation in data sources can compromise the reliability of estimates [40].

Going forward, it will be essential to closely monitor the quality and comparability of census data to ensure accurate application of the SAE. Methodological changes must be carefully managed to avoid distortions in the results obtained from the new data. Consistency in data

collection and comparability with previous censuses are critical to ensure that estimates remain reliable and useful for decision-making [63]. Despite these limitations, the present study successfully used the methodology of [43] to make annual projections of the population of children aged 0-3 years until 2030. These projections provide a valuable tool for planning in key sectors such as education, health and social services. In these areas, accurate population estimates are crucial for allocating resources and designing services efficiently.

From a methodological perspective, the projection of the population of children aged 0-3 towards 2030 required the use of alternative data sources and was developed in two different scenarios. In both cases, data derived from income poverty were used as the fundamental basis. Income poverty is an economic indicator that measures the ability of an individual or household to meet their basic needs from their income. This measure is crucial because it provides an accurate picture of the economic constraints faced by families, which is critical for accurate demographic projections [65]. The information on income poverty used for these projections comes from the National Survey of Employment, Unemployment and Underemployment (National Survey on Employment, Unemployment and Underemployment, ENEMDU). This survey, which is administered periodically by the National Institute of Statistics and Census (INEC) of Ecuador, collects data on the employment situation of the population, including employment, unemployment and underemployment. Given that the economic situation of households significantly influences demographic dynamics, the ENEMDU becomes a key source for the analysis and construction of long-term population estimation models [66].

We decided to use the income poverty measure instead of consumption poverty because of limitations in the data available to calculate the latter. Consumption poverty is calculated from the Living Conditions Survey (LCS), which is conducted on a non-periodic basis. There was an 8-year gap between the last LCS rounds, which implies that the data may be outdated and not adequate for reliable annual forecasting. This represents a significant challenge for long-term projections [67]. In contrast, the National Survey of Employment, Unemployment and Underemployment (ENEMDU) is conducted periodically, which provides more recent and relevant information for annual population projections. This is crucial when considering the evolution of income poverty, which can directly influence population dynamics. Therefore, we have chosen to use ENEMDU data to obtain more accurate estimates of the population of children aged 0-3 years around 2030 [66].

The use of income poverty as an indicator of the economic situation of an individual or household is a common practice in population projection studies. This measure allows for a more accurate capture of the economic fluctuations that directly affect households, which in turn impacts on demographic trends. In this sense, income poverty becomes a suitable proxy for assessing the current socio-economic situation and projecting future scenarios [65].

In economic terms, an individual income can be broken down into two main components: consumption and savings. This can be expressed by the equation Y=C+A, where Y represents total income, C consumption and A savings. A person's consumption is strongly influenced by his or her level of income, which can be modelled by the equation C=kY, where k is the marginal propensity to consume. This propensity indicates the fraction of an increase in income that is spent on consumption rather than saving. There is a direct and positive relationship between income and consumption: as income increases, so does consumption. Generally, changes in income lead to changes in consumption in similar proportions. However, in some contexts, such as in Ecuador, savings can be very limited. In such cases, income becomes a good proxy for consumption, which means that it can be used to represent the level of economic well-being of an individual or household [68].

The relationship between income, savings and consumption is fundamental to understanding the economic situation of a household. Income poverty is a measure based on this relationship and is used to make accurate poverty estimates for small geographic areas and specific population groups. By considering how income affects both consumption and savings, it is possible to obtain a clearer picture of the economic well-being of different segments of the population [69]. This methodology is particularly relevant for designing public policies to address the economic needs of the most vulnerable communities. Therefore, by analyzing consumption behavior and its relationship to income, it is possible to deduce how variations in income impact people standard of living. Accurate estimates of poverty and well-being are crucial for implementing effective strategies to promote social and economic development [70].

3.2.1.First scenario

The first scenario (see Annex Table 4), which is based on the following assumptions to estimate the population of children aged 0-3 years according to consumption poverty:

1. The variation in the growth rate of income poverty is constant at -8.87%, according to the latest data from the National Survey of Employment, Unemployment and Underemployment [71].
2. Poverty is evenly distributed across the country. - The incidence of poverty in the five self-reported cities does not show statistically significant variations.

3. This scenario uses the ENEMDU data, and the SAE methodology to predict consumption and construct the consumption poverty rate for the different population subgroups defined in the districts.

3.2.2.Second scenario

An approach based on growth rates derived from Ecuador Gross Domestic Product (GDP) is used to estimate the population of children aged 0-3 until 2030. This analysis assumes that variations in the level of production, and hence economic income, influence poverty levels in different regions of the country. This is considered to be a conservative scenario (see Annex Table 5), given that the country has relatively low annual growth rates. The methodology is based on several assumptions:

- **Income elasticity of poverty reduction:** Defined as the percentage change in poverty resulting from a 1% increase in per capita income. This elasticity is held constant and is calculated using the most recent data on income poverty variation provided by the National Survey of Employment, Unemployment and Underemployment (ENEMDU), as well as ECLAC growth projections for the same year.
- **Homogeneous distribution of poverty:** Poverty is assumed to be evenly distributed across the territory.
- **Minimum thresholds in the projections:** No projection is lower than an established minimum threshold. In this context, rates of change of GDP per capita are calculated using growth estimates provided by ECLAC and population projections published by INEC. The paper includes poverty elasticity calculations and projections for the child population aged 0-3 years, considering consumption poverty at the district level [72].

This approach allows for a deeper understanding of how economic changes affect vulnerable populations. Income elasticity is crucial for assessing the impact of economic policies on poverty, as a higher elasticity indicates that an increase in income has a significant effect on poverty reduction. Moreover, by considering a homogeneous distribution, it aims to simplify the analysis, although in practice there may be significant variations between different regions [73]. Finally, by setting lower limits on the projections, it ensures that the estimates do not underestimate the real needs of the child population. This is essential for designing effective policies to address deprivation and promote social well-being. The resulting projections provide valuable information for planning resources and services for this critical age group [74].

3.2.3.Additional clarifications:

- Adjustments to the SAE methodology: To improve accuracy, additional variables reflecting recent economic changes could be incorporated or the model could be adjusted to account for possible biases in the distribution of poverty [4].
- Homogeneous distribution of poverty: A homogeneous distribution was assumed to simplify the model, but if poverty is not evenly distributed, this could affect the precision of the estimates. It would be useful to explore models that incorporate geographical variations in the distribution of poverty [75].
- Projection scenarios: In the first scenario, historical data were used without significant adjustment to reflect current trends. In the second scenario, adjustments were included to reflect recent economic changes, allowing for a more realistic projection of the child population [9].

3.3 ANALYSIS OF THE RESULTS OBTAINED IN THE SCENARIOS.

CELADE estimates of the child population in Latin America are relevant to this analysis, as they provide a comparative framework for assessing regional demographic trends [76]. Figure 5 compares Ecuador child population projection scenarios with CELADE estimates, showing significant differences in the population growth rate. Factors such as education and birth control are crucial to explain these differences, as they directly influence population dynamics and poverty reduction [77]. The two projections differ in their approach: the first is based on historical trends, while the second incorporates adjustments to reflect recent economic changes, resulting in a more conservative projection of the child population in high-poverty areas.

In Figure 5 illustrates that a decline in the population of children aged 0-4 years is anticipated in all projected scenarios between 2022 and 2030. This trend can be attributed to a number of factors, such as declining birth rates, changes in population policies, as well as improvements in education and increased knowledge about birth control. CELADE estimates, which cover children up to the age of 4, show a more gradual decline. This might suggest that ECLAC foresees a slow change in the current conditions affecting the child population. In contrast, estimates from other scenarios, obtained using the SAE methodology, show more rapid reductions for children aged 0-3 in consumption poverty. This suggests that these scenarios anticipate more significant or rapid changes in the conditions impacting this age group [78].

It is crucial to note that these projections are merely hypothetical scenarios and that future reality may be subject to multiple unforeseen factors. While downward trends may cause concern, they may also reflect positive outcomes, such as increased access to education and birth control. Therefore, while the graph provides valuable insight into child population projections, it is critical to

Figure 5.

Estimation of girls and boys from 0 to 3 years old according to the SAE methodology, vs. Estimation of the population of girls and boys from 0 to 4 years old according to ECLAC until 2030.

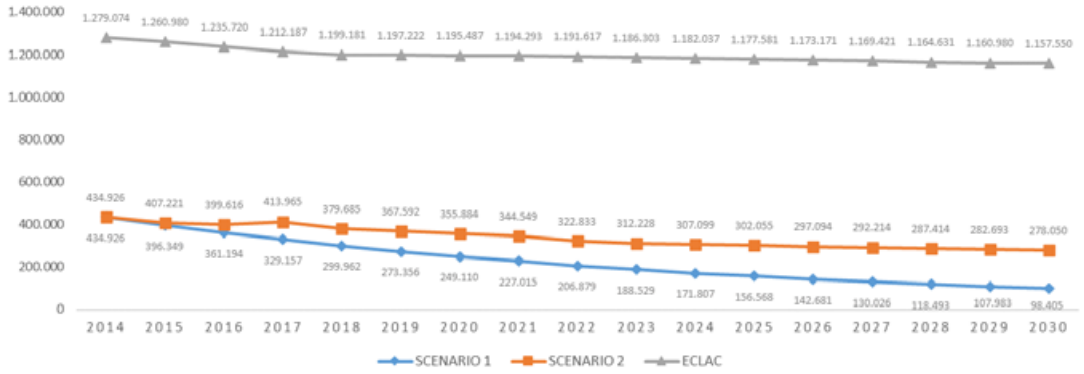

Source: [15]

contextualize these data with other metrics and socio-economic factors to gain a full understanding of the situation [79]. Finally, in assessing these projections, it is essential to consider how they relate to public policies and social programs aimed at supporting families and fostering a favorable environment for child growth. The interaction between demographic changes and the policies implemented will be critical in addressing future challenges related to population and social well-being [80].

To facilitate understanding of the results obtained, it is useful to make clearer comparisons between the different scenarios considered in the study. In particular, the simulation to estimate consumption poverty and project the child population up to 2030 (see Annex Table 6) reveals significant differences between the baseline, pessimistic and optimistic scenarios [35]. In the baseline scenario, child poverty is projected to increase moderately compared to current levels, while the pessimistic scenario shows a considerable increase due to factors such as the economic slowdown and rising unemployment. In contrast, in the optimistic scenario, child poverty is projected to decline due to the implementation of effective public policies and inclusive economic growth. These comparisons provide a better understanding of the potential impact of different factors and policies on the evolution of child poverty in Ecuador.

3.4 DISCUSSION

The application of the Small Area Estimation (SAE) methodology in this study has overcome the limitations of traditional estimation methods, providing accurate results at the local level. However, it is important to recognize that the utility of SAE is not without its challenges. One of the main advantages of SAE is its ability to integrate survey and census data, which facilitates obtaining reliable estimates in small areas [13]. However, the transition between positive results and limitations needs to be smoothed to maintain a clear thread.

Variations in census questions and collection methodology can introduce biases or errors in the data used for EDC, affecting the precision of estimates [58]. To mitigate these problems, strategies such as cross-validation of data and adjustment of models to reflect changes in local conditions can be implemented [75]. In addition, the lack of updating of the Living Conditions Survey (LCS) hinders the application of the methodology, as recent economic changes may not be reflected in the data, affecting the accuracy of the projections [2].

Undetected variations at the community level or within ethnic groups can have significant implications for the accuracy of estimates. For example, if community-specific cultural or socio-economic differences are not considered, models may not adequately capture local needs [39]. In terms of model performance, a good fit was observed in urban areas, but limitations affected rural areas more, where the lack of updated data was more pronounced [23].

A fundamental aspect to consider in the interpretation of the results obtained through SAE lies in the inherent limitations of this methodology. While SAE offers a valuable tool for generating estimates at the disaggregated level, it is crucial to recognize that its accuracy and validity depend to a large extent on the selection of auxiliary variables and their representativeness in the different geographical contexts analyzed [4]. The choice of variables that are not strongly correlated with the variable of interest, or that have measurement biases, can compromise the reliability of the estimates and lead to erroneous conclusions about the distribution of child poverty. It is also important to bear in mind that the SAE is based on statistical models that simplify the complexity of social reality, which can lead to the omission of relevant factors that influence children's vulnerability [75].

The discussion of the results of this study is enriched by linking them closely to their practical and theoretical implications, as well as by contrasting them with findings from another relevant research in the field [9]. For example, our results on the impact of maternal education on child poverty are consistent with previous studies that have shown a strong correlation between these two factors [81]. However, we also found some significant differences compared to research conducted in other geographical contexts, suggesting the importance of considering the specific characteristics of the Ecuadorian population when designing public policies aimed at reducing child poverty [82]. By analyzing these similarities and differences, we can gain a deeper understanding of the factors that influence child poverty and design more effective interventions tailored to local needs.

The results obtained by applying the SAE methodology make it possible to generate precise estimates of the incidence of consumption poverty for different age groups, especially for children aged 0-3 years, at provincial, cantonal, parish and district levels (see Annex Table 6). This level of disaggregation is not possible with traditional statistical methods, which makes the SAE methodology a crucial tool for planning and decision-making in public policy. The ability to estimate poverty rates more accurately at the district level provides government institutions with a solid basis for designing more effective and targeted strategies [4].

The usefulness of the SAE methodology is particularly evident when considering the limitations of current data sources, which do not allow reliable statistical inferences to be generated in small areas using conventional methods. SAE overcomes these limitations by exploiting both census and survey data and allows for the creation of tight and robust predictions in small population domains. The results of this approach show significant variations in consumption poverty levels between different planning areas, provinces, cantons and districts, highlighting the geographical heterogeneity of the poverty phenomenon. This underlines the need for specific and targeted policies to address these regional disparities [80].

At the district level, the results obtained through SAE are a valuable tool to visualize and understand consumption poverty gaps in the country. However, the unavailability of certain household-level socio-economic variables in the Census restricts the use of some predictors, which may limit the precision of the estimates. Moreover, methodological differences between the 2010 and 2022 censuses present additional challenges in the implementation of the SAE. These changes may affect the consistency and comparability of the data, underscoring the importance of adjusting methodologies to maintain the reliability of the analyses [83].

Comparison of the 2010 and 2022 Ecuadorian censuses reveals important methodological discrepancies that compromise the accuracy of small area estimates (SAE). Changes in questionnaire design, data collection techniques, population size and composition, and the amount of information collected affect the comparability of data and the accuracy of SAE estimates. Alterations in the questionnaires make direct comparison with the 2022 census difficult, introducing potential biases. Demographic changes also influence the accuracy of estimates if they are not adequately considered. To ensure the validity and reliability of the SAE estimates, it is essential to take these differences into account and adjust the methodology [84].

The lack of an update of the National Living Conditions Survey (LCS) hinders the application of the SAE methodology, limiting the possibility of integrating auxiliary information to improve the precision of the estimates. While acknowledging the limitations of the data sources used in this study, the models employed showed a good fit to the available data [40]. Finally, the limited spatial resolution of the data sources may prevent the detection of minor variations at the community or ethnic group level. Despite this limitation, the methodological approach used is useful for small area-level analysis [52].

While our study has revealed significant variations in consumption poverty levels between different regions, it is crucial to delve deeper into the underlying reasons for these disparities. Factors such as the economic structure of each region, the availability of employment, levels of education and the public policies implemented can influence the distribution of wealth and the vulnerability of households. For example, regions with a higher concentration of informal agricultural activities may be more susceptible to poverty due to commodity price volatility and lack of access to financial services and training [84].

Likewise, regions with a higher proportion of indigenous or Afro-descendant populations may face additional barriers to accessing employment and education opportunities due to discrimination and social exclusion [85]. Lack of investment in infrastructure and basic services in rural and marginalized areas can also contribute to perpetuating poverty and limiting economic development. To better understand these dynamics, it would be advisable to conduct detailed case studies in some of the regions with the highest levels of poverty, in order to identify the specific factors that are contributing to the situation and design more effective interventions tailored to local needs.

It is important to recognize the inherent limitations of any study based on statistical data, especially in areas where the available information presents a higher level of uncertainty. In our case, the representativeness of the LCS data may be limited in some regions, which could affect the validity of our projections. In addition, there may be measurement errors or biases in the data, which could influence the results. It is therefore essential to interpret our findings with caution and to recognize that there are margins of error associated with our estimates.

To improve the accuracy and reliability of future research, it would be advisable to explore the possibility of combining different data sources, such as administrative records, household surveys and satellite data, in order to obtain a completer and more accurate picture of the child poverty situation. It is also important to invest in training local staff in data collection and analysis to ensure the quality and relevance of the information. By addressing these limitations, we will be able to generate more solid and useful evidence for decision-making and the implementation of public policies aimed at the most vulnerable population.

It is essential to recognize that the SAE methodology has certain limitations that must be considered when interpreting the results and designing public policies based on them. One of the main challenges of SAE lies in the potential bias introduced by the selection of auxiliary variables, which may not be representative of the socio-economic reality of all the geographical areas analyzed [25]. To mitigate this risk, it is crucial to conduct a thorough analysis of the quality and relevance of the variables used, as well as to assess their ability to capture the specific dynamics of each local context.

It is also important to bear in mind that the SAE relies on survey data that may not be updated frequently enough to reflect the socio-economic changes occurring in society [86]. In this sense, it is advisable to complement survey data with information from other sources, such as administrative records and geographic information systems, in order to obtain a completer and more accurate picture of the child poverty situation [86].

Furthermore, it is crucial to recognize that poverty dynamics can vary significantly over time and in different geographical contexts, which can influence the effectiveness of policy programs designed on the basis of these data [87]. Therefore, it is necessary to conduct regular evaluations of implemented programs and adjust strategies based on the results obtained, in order to ensure that interventions are relevant and effective in reducing child poverty.

Living Conditions Surveys (LCS) play a crucial role in policy formulation by providing detailed information on the socio-economic characteristics of households and their access to basic services [88]. LCS data can influence the design of policy interventions for social inclusion and poverty reduction by identifying the most vulnerable groups and targeting resources where they are most needed. However, it is important to bear in mind that LCA are only one tool among many, and that their effectiveness depends on the quality of the data collected, the thoroughness of the analysis carried out and the political will to implement the recommendations derived from the results.

The findings of this study, which estimate the population of children in poverty in Ecuador using SAE, provide a notable advance in knowledge about this problem at the local level. Compared to previous research in Latin America, such as that of [10], which used SAE to measure rural poverty, our work stands out for focusing specifically on children aged 0-3 years in Ecuador, a group little studied at this scale. The results show great diversity in poverty levels across regions, provinces, cantons and districts, highlighting the need for detailed data to target resources efficiently. Furthermore, when comparing our projections with those of ECLAC, we find a reasonable alignment, which reinforces the reliability of our estimates in the face of the scarcity of updated territorial data in the country [2]. This innovative approach not only improves the precision of estimates in small areas, but also establishes a starting point for future studies on child poverty and vulnerability, providing policy makers with a key tool to prioritize interventions where they are most needed [10].

4. Conclusions

This study has demonstrated the usefulness of the SAE methodology for estimating consumption poverty in small areas, specifically contributing to this end by providing accurate estimates at the district level. The results obtained allow for a more specific identification of the target population required for decision-making regarding the implementation of specific public policies. By using recent data from 2014 to 2025 and projections up to 2030, a clear picture of demographic trends and child poverty in Ecuador is provided. This approach is particularly useful for the country economic and social planning, as it allows targeting resources in areas of greatest need and designing interventions tailored to local conditions.

One of the main contributions of this study is the ability to optimize the use of available information, combining survey and census data to generate accurate estimates. The numerical values of the estimates and indicators provide evidence of the credibility and precision of the SAE methodology, which allows for better public policy decision-making [53]. Furthermore, this study sets an important precedent for future research by demonstrating the feasibility of the SAE in the Ecuadorian context.

Limitations of the study, such as the lack of updated Living Conditions Survey (LCS) data, suggest the need for additional research to validate the results and explore new methodologies. It is recommended that future studies consider incorporating updated administrative data and conducting sensitivity analyses to assess the impact of the assumptions used in the projections [2]. The identification of vulnerable groups has been consolidated in this study, allowing for a better understanding of social and economic inequalities in Ecuador.

Emphasize the importance of replication of the method and its relevance in the field of social change. In a context of constant social and economic change, the SAE methodology offers a valuable tool for monitoring and evaluating the impact of public policies on child poverty reduction. Its replication in different geographical and social contexts can contribute to a better understanding of the dynamics of poverty and the identification of effective strategies to overcome it [8].

The SAE methodology provides accurate and reliable estimates of population variables at detailed geographical levels, which is essential for national socio-economic planning [89]. In the Ecuadorian context, the application of the SAE has made it possible to estimate consumption poverty at the district level between 2014 and 2030, facilitating the precise identification of populations requiring priority attention for the design of targeted public policies [86]. This analysis reveals considerable variability in consumption poverty levels between different regions, provinces, cantons and districts, highlighting the need for disaggregated data for efficient resource allocation [90]. Heterogeneity at the district level is particularly significant, and the availability of reliable data at this scale allows for better management of social inclusion programs [91]. In summary, the SAE methodology proves to be an effective tool for generating reliable estimates, even for small geographical areas, thus fulfilling a crucial need in public planning and management.

This study identifies, with great geographical precision, the most vulnerable population groups, which facilitates the efficient allocation of public resources for social assistance programs [92]. The integration of gender and ethnic perspectives is crucial for designing interventions that promote equity and social inclusion [93]. By applying econometric models to data from the 2014 Living Conditions Survey (LCS) and the 2010 Population Census, vulnerability estimates have been obtained at the district level, maximizing the use of available information [94]. The SAE methodology has proven to be a valuable **tool** for identifying unmet needs at the local level, enabling more informed and effective public decision-making [89]. The possibility of replicating this study periodically would allow for monitoring socio-economic evolution and adapting strategies to changing social realities [95].

The regression model employed shows a good fit in most geographical regions, with R^2 values generally above 0.60, indicating that the model explains more than 60% of the variability in consumption [96]. However, a less satisfactory fit is observed in some specific regions, such as Carchi and Guayas, suggesting the need for improvements or the incorporation of additional variables to optimize the model in these areas [97]. To improve the fit of the model in regions with R^2 values close to 0.60, it is recommended to explore the inclusion of additional explanatory variables or to re-evaluate the model specification. This could involve the consideration of region-specific socio-economic or geographical factors [98].

In regions with a limited number of observations, even if the R^2 is high, the uncertainty in the results can be considerable. In these cases, further data collection or the application of additional statistical techniques is recommended to strengthen the conclusions [99]. The model performs better in regions with higher R^2 values and a larger number of observations, such as Napo and Orellana, which increases the reliability of the results obtained in these areas. This contrast highlights the importance of data quality and quantity for the accuracy of econometric models [100]. The provinces of Napo and Chimborazo have a high prevalence of child poverty, which justifies the prioritization of resources and public policies in these regions. Targeted intervention is required to improve socio-economic and infrastructure conditions, with the aim of significantly reducing child poverty levels in these areas [101].

The high variability in poverty estimates in provinces such as Galápagos, Cañar and Zamora Chinchipe demands special attention. The lower precision of estimates in these areas suggests the need to improve the quality of data collection and the design of more targeted interventions to ensure a more reliable assessment of the situation and the effectiveness of implemented policies [102]. Despite having relatively moderate poverty rates (Guayas: 37.6%, Manabí: 53.1%, Pichincha: 25.1%), the provinces of Guayas, Manabí and Pichincha are home to a high number of children in poverty. This indicates that the implementation of programs aimed at this vulnerable population would have a significant impact on poverty reduction at the national level. It is crucial to develop and implement specific programs that address the particular needs of this population [103].

Provinces such as El Oro and Cañar, despite exhibiting low child poverty rates (18.5% and 15.2%, respectively), show high variability in their estimates, indicating considerable uncertainty in the data. It is essential to continue monitoring these provinces to confirm whether the low incidence of poverty is a real trend or an artefact of measurement imprecision. Rigorous monitoring will help determine the need for targeted interventions [58]. The formu10lation of effective child poverty reduction policies must consider not only the magnitude of the problem in each province, but also the quality and reliability of the available data. Prioritizing interventions based on accurate and reliable data is crucial to ensure that resources are allocated efficiently and that the strategies implemented are truly effective [104].

In order to enrich the comparative analysis and contextualize our findings, we have expanded the references section to include relevant international studies that have applied the SAE methodology in other contexts [105]. These studies address a variety of issues related to child poverty,

such as the measurement of food insecurity, access to health and education services, and the impact of public policies on poverty reduction [106]. By examining this research, we can gain a broader perspective on the challenges and opportunities associated with implementing SAE in different geographical and socio-economic contexts, and adapt best practices to the Ecuadorian reality [107].

References

[1] A. Gutiérrez, X. Mancero, and S. Guerrero, "Poverty mapping in Latin America: ECLAC experiences on small area estimation," *Statistical Journal of the IAOS*, vol. 38, no. 3, pp. 1021–1033, 2022.

[2] Comisión Económica para América Latina y el Caribe (CEPAL), *Panorama social de América Latina y el Caribe 2024: Desafíos de la protección social*, [Online]. Available: https://www.cepal.org/es/publicaciones/80858-panorama-social-america-latina-caribe-2024-desafios-la-proteccion-social .

[3] Banco Mundial, *Panorama de la pobreza y la desigualdad en América Latina y el Caribe* , Washington, D.C.: Banco Mundial, 2024.

[4] J. N. Rao and I. Molina, *Small Area Estimation*, John Wiley & Sons, 2015.

[5] DANE, *Encuesta Nacional de Calidad de Vida 2023* , Departamento Administrativo Nacional de Estadística de Colombia, 2023. [Online]. Available: https://microdatos.dane.gov.co/index.php/catalog/827 .

[6] INEGI, *Censo de Población y Vivienda 2024*, Instituto Nacional de Estadística y Geografía de México, 2024. [Online]. Available: https://www.inegi.org.mx/app/buscador/default.html?q=SAE .

[7] A. Sen, *Development as Freedom* , Oxford University Press, 1999.

[8] Banco Mundial, *Pobreza: Panorama general* , 2024. [Online]. Available: https://www.bancomundial.org/es/topic/poverty/overview .

[9] W. H. Greene, *Econometric Analysis* (8th ed.), Pearson Education, 2018.

[10] A. Arias-Salazar, A. Gutiérrez, S. Guerrero-Gómez, X. Mancero, N. Rojas-Perilla, and H. Zhang, "Small area estimation for composite indicators: the case of multidimensional poverty incidence," *Journal of Official Statistics* , 0282423X241300751, 2023.

[11] Eurostat, *City Statistics - Small Area Estimation* , European Commission, 2024. [Online]. Available: https://ec.europa.eu/eurostat/statistics-explained/index.php?title=City_statistics_-_small_area_estimation

[12] Statistics Canada, *Canadian Community Health Survey - Annual Component (CCHS)*, [Online]. Available: https://www23.statcan.gc.ca/imdb/p2SV.pl?Function=getSurvey&SDDS=3226 .

[13] A. Molina, J. Rosero, M. León, R. Castillo, F. Jácome, D. Rojas, et al., *Reporte de pobreza por consumo Ecuador 2006-2014*, 2016.

[14] INEC-BM, *Reporte de Pobreza por Consumo Ecuador 2006-2014*, Quito: Instituto Nacional de Estadística y Censos, 2014.

[15] S. Dercon, *Assessing Vulnerability* , World Bank Publications, 2001.

[16] Z. Villa Juan-Albacea, *Small Area Estimation of Poverty Statistics* , No. 2009-16, PIDS Discussion Paper Series, 2009.

[17] D. M. Stukel and J. N. K. Rao, "Estimation of regression models with nested error structure and unequal error variances under two and three stage cluster sampling," *Statistics & Probability Letters* , vol. 35, no. 4, pp. 401–407, 1997.

[18] Y. You and J. Rao, "A pseudo-empirical best linear unbiased prediction approach to small area estimation using survey weights," *Canadian Journal of Statistics*, vol. 30, no. 3, pp. 431–439, 2002.

[19] J. N. K. Rao and I. Molina, *Small Area Estimation: A Review of Methods Based on the Application of Mixed Models*, 2015. [Online]. Available: https://www.researchgate.net/publication/252669243_Small_Area_Estimation_A_Review_of_Methods_Based_on_the_Application_of_Mixed_Models .

[20] C. Elbers, J. O. Lanjouw, and P. Lanjouw, *Small Area Estimation of Poverty Indicators*, ResearchGate, 2003. [Online]. Available: https://www.researchgate.net/publication/230806613_Small_Area_Estimation_of_Poverty_Indicators .

[21] UNICEF, *The State of the World's Children 2023* , [Online]. Available: https://www.unicef.org/reports/state-worlds-children-2023 .

[22] Studocu, *Variables dummy de estadística* , [Online]. Available: https://www.studocu.com/ec/document/instituto-tecnologico-bolivariano-de-tecnologia/administracion/variables-dummy-de-estadistica/15406065 . [23]J. Jiang and P. Lahiri, "Mixed model prediction and small area estimation," *Test* , vol. 15, pp. 1–96, 2006.

[24] I. Molina, J. N. K. Rao, and G. S. Datta, "Small area estimation under a Fay-Herriot model with preliminary testing for the presence of random area effects," *Survey Methodology* , vol. 41, no. 1, pp. 1–20, 2015.

[25] M. Ghosh and J. N. Rao, "Small area estimation: an appraisal," *Statistical Science* , vol. 9, no. 1, pp. 55–76, 1994.

[26] W. Lutz, W. P. Butz, and K. E. Samir (Eds.), *World Population and Human Capital in the Twenty-First Century* , OUP Oxford, 2014.

[27] A. Van Delden, B. J. Du Chatinier, and S. Scholtus, "Accuracy in the application of statistical matching methods for continuous variables using auxiliary data," *Journal of Survey Statistics and Methodology* , vol. 8, no. 5, pp. 990–1017, 2020.

[28] M. Ghosh and J. N. Rao, "Small area estimation: an appraisal," *Statistical Science* , vol. 9, no. 1, pp. 55–76, 1994.

[29] I. Molina and Y. Marhuenda, *Small Area Estimation for Mapping Local Indicators* , 2019. [Online]. Available: https://www.makswell.eu/attached_documents/3_small-area-estimation-for-mapping-local-indicators.pdf .

[30] P. Corral, I. Molina, A. Cojocaru, and S. Segovia, *Guidelines to Small Area Estimation for Poverty Mapping* , Washington: World Bank, 2022.

[31] United Nations Population Fund, *Small Area Estimation for Mapping Local Indicators* , 2019. [Online]. Available: https://www.unfpa.org/sites/default/files/pub-pdf/19-310_SAE_Brochure_A4-SINGLE-PROOF6.pdf .

[32] [14] Asian Development Bank, *Introduction to Small Area Estimation Techniques: A Practical Guide for National Statistics Offices* , 2020. [Online]. Available: https://www.adb.org/publications/small-area-estimation-guide-national-statistics-offices .

[33] World Bank, *Guidelines to Small Area Estimation for Poverty Mapping* , 2023. [Online]. Available: https://www.worldbank.org/en/events/2023/02/07/guidelines-to-small-area-estimation-for-poverty-mapping .

[34] RTI International, *Small Area Estimation* , [Online]. Available: https://www.rti.org/brochures/small-area-estimation .

[35] A. de Mesa, *Los sistemas de pensiones en América Latina: institucionalidad, gasto público y sostenibilidad financiera en tiempos del COVID-19* , 2020.

[36] J. M. Wooldridge, *Introductory Econometrics: A Modern Approach* (6th ed.), Cengage Learning, 2016.

[37] M. C. Nguyen, P. A. C. Rodas, J. P. W. De Azevedo, and Q. Zhao, "Small area estimation and Poverty map in Stata," in *2017 Stata Conference* , No. 20, 2017.

[38] M. H. Boyle et al., "The influence of economic development level, household wealth and maternal education on child health in the developing world," *Social science & medicine* , vol. 63, no. 8, pp. 2242–2254, 2006.

[39] F. F. J. Bogliaccini, *Metas del milenio y desarrollo: las configuraciones del desarrollo social en América Latina* , Documento de Trabajo del IPES, Montevideo, 2008.

[40] J. N. K. Rao and I. Molina, *Small Area Estimation: A Review of Methods Based on the Application of Mixed Models* , 2015. [Online]. Available: https://www.researchgate.net/publication/252669243_Small_Area_Estimation_A_Review_of_Methods_Based_on_the_Application_of_Mixed_Models .

[41] E. A. Herrera Herrera, *Comparación de estimadores directos e indirectos en estimación de áreas pequeñas* , Universidad Santo Tomás, 2018. [Online]. Available: https://repository.usta.edu.co/bitstream/handle/11634/12530/2018edgarherrera.pdf?sequence=1

[42] R. E. Fay and R. A. Herriot, "Estimates of income for small places: An application of James-Stein procedures to census data," *Journal of the American Statistical Association* , vol. 74, no. 366, pp. 269–277, 1979.

[43] G. N. López Fuertes, *Estimación de la población de niñas y niños de 0 a 3 años del ecuador, según Pobreza por Consumo, mediante la metodología Small Area Estimation (SAE) hasta el año 2021* , Master's thesis, Quito: UCE, 2019.

[44] Instituto Nacional de Estadística y Censos (INEC), *Guía de Uso de Base de Datos* , 2021. [Online]. Available: https://www.ecuadorencifras.gob.ec/documentos/web-inec/EMPLEO/2021/Febrero-2021/202102_%20Guia%20de%20usuario%20BDD_ENEMDU.pdf

[45] J. Parra, *Introducción a las variables ficticias o variables dummy* , [Online]. Available: https://www.javierparra.net/ecoknowmic/introduccion-a-las-variables-ficticias-o-variables-dummy/ .

[46] Studocu, *Variables dummy de estadística* , [Online]. Available: https://www.studocu.com/ec/document/instituto-tecnologico-bolivariano-de-tecnologia/administracion/variables-dummy-de-estadistica/15406065 .

[47] M. C. Howard, *Regresión con Variables Dummy en Jamovi* , [Online]. Available: https://mattchoward.com/regresion-con-variables-dummy-en-jamovi/ .

[48] M. Carvajal, *Análisis de datos y detección de valores atípicos en econometría* , Quito: Ediciones Económicas, 2004.

[49] T. Hastie, R. Tibshirani, J. H. Friedman, and J. H. Friedman, *The Elements of Statistical Learning: Data Mining, Inference, and Prediction* , vol. 2, New York: Springer, 2009.

[50] A. C. King, M. P. Rao, and C. D. Tregillis, "Econometric Analysis," in *Litigation Services Handbook: The Role Of The Financial Expert* , 2017, pp. 1–62.

[51] R. McElreath, *Statistical Rethinking: A Bayesian Course with Examples in R and Stan* , Chapman and Hall/CRC, 2018.

[52] D. Pfeffermann, "New important developments in small area estimation," *Quality control and applied statistics* , vol. 59, no. 1, pp. 103–106, 2014.

[53] B. W. Silverman, *Density Estimation for Statistics and Data Analysis* , Routledge, 2018. [54] J. Fox, *Applied Regression Analysis and Generalized Linear Models* , Sage Publications, 2015.

[55] N. Tzavidis et al., "A framework for producing small area estimates based on the Fay-Herriot model," *Statistical Modelling* , vol. 19, no. 4, pp. 309–328, 2019.

[56] World Health Organization (WHO), *Global Strategy Data: Maternal, Newborn, Child, Adolescent and Ageing* , [Online]. Available: https://platform.who.int/data/maternal-newborn-child-adolescent-ageing/global-strategy-data .

[57] Save the Children, *World more dangerous than ever for children* , [Online]. Available: https://www.savethechildren.org.uk/news/media-centre/press-releases/world-more-dangerous-than-ever-for-children#:~:text=Save%20the%20Children%20report%20reveals,day%20were%20killed%20or%20maimed .

[58] A. F. Correa, *On the measurement of multidimensional poverty as a policy tool: empirical applications to Chile, Colombia, Equador and Peru* , 2017.

[59] S. K. Smith, J. Tayman, and D. A. Swanson, *State and Local Population Projections: Methodology and Analysis* , Springer, 2019.

[60] United Nations, *Principles and Recommendations for Population and Housing Censuses* , United Nations Statistics Division, 2020.

[61] S. H. Preston, P. Heuveline, and M. Guillot, *Demography: Measuring and Modeling Population Processes* , Blackwell Publishing, 2022.

[62] National Research Council, *Reengineering the 2020 Census: Risks and Challenges* , National Academies Press, 2020.

[63] D. Pfeffermann, "Small Area Estimation: A Review and Some Directions," *Statistica Sinica* , vol. 29, no. 1, pp. 289–326, 2019.

[64] OECD, *Challenges of the 2022 Census and the Implications for Data Comparability* , Organisation for Economic Co-operation and Development, 2022.

[65] J. Foster, J. Greer, and E. Thorbecke, "A class of decomposable poverty measures," *Econometrica: journal of the econometric society* , pp. 761–766, 1984.

[66] Instituto Nacional de Estadística y Censos (INEC), *Encuesta Nacional de Empleo, Desempleo y Subempleo (ENEMDU)* , Quito, Ecuador: INEC, 2023.

[67] P. Samaniego, "Evolución de la pobreza y la desigualdad en Quito," *Questiones Urbano Regionales. Revista del Instituto de la Ciudad* , vol. 1, no. 2, pp. 77–94, 2013.

[68] N. G. Mankiw and M. P. Taylor, *Economía* , Cengage Learning, 2021.

[69] J. De Gregorio, *Macroeconomía* , McGraw-Hill, 2007.

[70] R. Prebisch, *El desarrollo económico de América Latina y sus principales problemas* , Naciones Unidas, 2012.

[71] Instituto Nacional de Estadística y Censos (INEC), *Boletín de pobreza: Encuesta Nacional de Empleo, Desempleo y Subempleo (ENEMDU), Junio 2024* , Quito, Ecuador: INEC, 2024. [Online]. Available: https://www.ecuadorencifras.gob.ec/documentos/web-inec/POBREZA/2024/Junio/202406_Boletin_pobreza_ENEMDU.pdf .

[72] J. Andrade, E. Marinho, and G. Lima, "Crecimiento económico y concentración del ingreso: sus efectos en la pobreza del Brasil," *CEPAL* , 2017. [Online]. Available: https://repositorio.cepal.org/bitstream/handle/11362/42693/1/RVE123_Araujo.pdf .

[73] del Ecuador, O. S., *Situación de la niñez y adolescencia en Ecuador. Una mirada a través de los ODS* , 2019.

[74] INEC, *Proyecciones Demográficas 2022-2030* , 2024. [Online]. Available: https://www.ecuadorencifras.gob.ec/proyecciones-poblacionales/ .

[75] R. L. Chambers and R. Clark, *An Introduction to Model-Based Survey Sampling with Applications* , Oxford University Press, 2012.

[76] CELADE-División de Población de la CEPAL y División de Población de las Naciones Unidas, *Estimaciones y proyecciones de población a nivel nacional, de los 20 países de América Latina* , CEPAL, 2023. [Online]. Available: https://www.cepal.org/es/temas/estimaciones-proyecciones-poblacion/estimaciones-proyecciones-poblacion-nivel-nacional-los-20-paises-america-latina .

[77] UNICEF, *Estado Mundial de la Infancia 2024* , Fondo de las Naciones Unidas para la Infancia, 2024.

[78] Institute for Health Metrics and Evaluation, *TL Capstones global fertility* , 2024. [Online]. Available: https://www.healthdata.org/sites/default/files/2024-03/TL%20Capstones%20global%20fertility_ES.pdf .

[79] Dialoguemos, *¿Cuáles son los países de América Latina con la natalidad más baja y más alta?* , 2024. [Online]. Available: https://dialoguemos.ec/2024/10/cuales-son-los-paises-de-america-latina-con-la-natalidad-mas-baja-y-mas-alta/ .

[80] P. Corral, I. Molina, A. Cojocaru, and S. Segovia, *Guidelines to Small Area Estimation for Poverty Mapping* , Washington: World Bank, 2022.

[81] T. Lynch et al., "Definitions, theories, and measurement of stress in children," *Journal of Pediatric Nursing* , vol. 66, pp. 202–212, 2022.

[82] G. D. E. Loaiza, "Impacto de la inversión social en la reducción de la pobreza y la desigualdad en Ecuador: Análisis de políticas públicas y resultados 2010-2023," *Ciencia y Educación* , vol. 5, no. 12, pp. 122–138, 2024

[83] N. Tzavidis, L. C. Zhang, A. Luna, T. Schmid, and N. Rojas-Perilla, "From start to finish: a framework for the production of small area official statistics," *Journal of the Royal Statistical Society: Series A (Statistics in Society)* , vol. 181, no. 4, pp. 927–979, 2018.

[84] Food and Agriculture Organization of the United Nations (FAO), *[Título del recurso]* , [Online]. Available: https://openknowledge.fao.org/items/65139780-d06c-4b7c-a2cd-3ed4256eaa1c .

[85] Economic Commission for Latin America and the Caribbean (ECLAC), *Social Panorama of Latin America and the Caribbean 2024: Accessible Version* , [Online]. Available: https://www.cepal.org/en/publications/81294-social-panorama-latin-america-and-caribbean-2024-accessible-version .

[86] S. Parandekar, R. Vos, and D. Winkler, *Ecuador: Crisis, poverty, and social protection* , 2002.

[87] A. V. Banerjee and E. Duflo, *Poor Economics: A Radical Rethinking of the Way to Fight Global Poverty* , Public Affairs, 2011.

[88] A. Deaton, *The Analysis of Household Surveys: A Microeconometric Approach to Development Policy* , World Bank Publications, 1997.

[89] C. Elbers, J. O. Lanjouw, and P. Lanjouw, "Micro–Level Estimation of Poverty and Inequality," *Econometrica* , vol. 71, no. 1, pp. 355–364, 2003.

[90] M. F. M. Macías and M. M. B. Salinas, "Programas de servicios sociales para erradicar la pobreza en el Ecuador," *ECA Sinergia* , vol. 12, no. 1, pp. 59–69, 2021.

[91] G. Wan, "Regional income inequality in rural China, 1985–2002: Trends, causes and policy implications,"

in *Understanding Inequality and Poverty in China: Methods and Applications* , London: Palgrave Macmillan UK, 2008, pp. 89–116.

[92] I. A. Eyzaguirre, A. Y. Iwama, and M. E. Fernandes, "Integrating a conceptual framework for the sustainable development goals in the mangrove ecosystem: a systematic review," *Environmental Development* , p. 100895, 2023.

[93] W. Naudé, M. McGillivray, and S. Rossouw, *Measuring the vulnerability of subnational regions* , No. 2008/54, WIDER Research Paper, 2008.

[94] S. Alkire and M. E. Santos, "Measuring acute poverty in the developing world: Robustness and scope of the multidimensional poverty index," *World Development* , vol. 59, pp. 251–274, 2014.

[95] A. Ahrens, C. Aitken, and M. E. Schaffer, "Using machine learning methods to support causal inference in econometrics," in *Behavioral Predictive Modeling in Economics*, 2021, pp. 23–52.

[96] P. R. Voss, D. D. Long, R. B. Hammer, and S. Friedman, "County child poverty rates in the US: a spatial regression approach," *Population Research and Policy Review* , vol. 25, pp. 369–391, 2006.

[97] N. Shrestha, "Factor analysis as a tool for survey analysis," *American journal of Applied Mathematics and statistics* , vol. 9, no. 1, pp. 4–11, 2021.

[98] J. Cohen, *Statistical Power Analysis for the Behavioral Sciences* , Routledge, 2013.

[99] A. Field, *Discovering Statistics Using IBM SPSS Statistics* , Sage Publications Limited, 2024.

[100] J. Hentschel, *Combining census and survey data to study spatial dimensions of poverty: A case study of Ecuador* , vol. 1928, World Bank Publications, 1998.

[101] C. Elbers, J. O. Lanjouw, and P. Lanjouw, *Micro-level estimation of welfare* , vol. 2911, World Bank Publications, 2002.

[102] UNICEF, *The state of the world's children 2006: excluded and invisible* , UNICEF, 2005.

[103] D. Pfeffermann, "New important developments in small area estimation," *Quality control and applied statistics* , vol. 59, no. 1, pp. 103–106, 2013.

[104] Economic Commission for Latin America and the Caribbean (ECLAC), *Small area estimation (SAE): Resources* , [Online]. Available: https://statistics.cepal.org/portal/sae/resources.html?lang=en .

[105] F. O. Rico, C. F. T. Piñerez, and N. Ramirez-Vargas, "A Review of the Use of Small Area Estimation in Colombia," *Revista Colombiana de Estadística* , vol. 47, no. 2, p. 407, 2024.

[106] A. Zgodic et al., "Estimates of childhood overweight and obesity at the region, state, and county levels: a multilevel small-area estimation approach," *American journal of epidemiology* , vol. 190, no. 12, pp. 2618–2629, 2021.

[107] T. F. Crossley and L. J. Curtis, "Child poverty in Canada," *Review of Income and Wealth* , vol. 52, no. 2, pp. 237–260, 2006.

Annexes

Table 3.

Estimation of consumption poverty parameters

ln_con	Coef.	Std. Err.	t	P>|t|	[95% Conf. Interval]	
_cons	5,054579	0,1943018	26,01	0,0000	4,673738	5,435420
T_per	-0,1849809	0,004099	-45,13	0,0000	-0,1930151	-0,1769466
T_nn	0,1968746	0,0107344	18,34	0,0000	0,1758347	0,2179145
T_me	0,1011308	0,0057637	17,55	0,0000	0,0898337	0,1124279
T_am	-0,0602178	0,0076539	-7,87	0,0000	-0,0752198	-0,0452159
T_pcd	-0,064163	0,0067434	-9,51	0,0000	-0,0773804	-0,0509455
rat_dp	-0,5575776	0,0270586	-20,61	0,0000	-0,6106139	-0,5045413
p03	-0,0042259	0,0015088	-2,8	0,0050	-0,0071832	-0,0012685
edad2_	0,0000331	0,0000139	2,39	0,0170	5,94E-06	0,0000603
edad_p	0,0125164	0,0015418	8,12	0,0000	0,0094944	0,0155383
edad2_p	-0,0001247	0,0000134	-9,32	0,0000	-0,0001509	-0,0000985
rural	0,0212506	0,0074766	2,84	0,0040	0,0065961	0,0359052
p16_2	0,0929644	0,0144991	6,41	0,0000	0,0645455	0,1213832
p16_3	0,1053171	0,0151142	6,97	0,0000	0,0756924	0,1349418
p16_4	0,0987475	0,0092817	10,64	0,0000	0,0805549	0,11694
p16_5	0,1496131	0,0168492	8,88	0,0000	0,116588	0,1826383
mujer	-0,0398968	0,0086264	-4,62	0,0000	-0,056805	-0,0229886
nivel_2	0,0463438	0,0150709	3,08	0,0020	0,016804	0,0758836
nivel_3	0,1248864	0,0194194	6,43	0,0000	0,0868235	0,1629493
nivel_4	0,1692531	0,0170471	9,93	0,0000	0,1358399	0,2026662
nivel_5	0,2381168	0,0273787	8,7	0,0000	0,1844531	0,2917805
nivel_6	0,3887886	0,0177058	21,96	0,0000	0,3540843	0,423493
p34_2	-0,031441	0,0070084	-4,49	0,0000	-0,0451778	-0,0177042
p34_3	0,0290773	0,0112747	2,58	0,0100	0,0069783	0,0511762
p34_4	0,0906552	0,0154005	5,89	0,0000	0,0604695	0,1208409
p34_5	0,0514007	0,0122753	4,19	0,0000	0,0273404	0,075461
p34_6	-0,0121323	0,0115162	-1,05	0,2920	-0,0347047	0,01044
analfabeto	-0,063958	0,0126419	-5,06	0,0000	-0,0887368	-0,0391793
no_empleo	-0,0158142	0,008339	-1,9	0,0580	-0,0321591	0,0005306
migra_d	0,0422481	0,0081524	5,18	0,0000	0,0262689	0,0582272
vap_2	-0,0722079	0,0111353	-6,48	0,0000	-0,0940337	-0,050382
vap_3	-0,0586908	0,0064927	-9,04	0,0000	-0,0714168	-0,0459648
vap_4	-0,0938256	0,0105939	-8,86	0,0000	-0,1145902	-0,073061
vap_5	-0,0520068	0,0411179	-1,26	0,2060	-0,1325999	0,0285863
v09_2	0,0242875	0,0074351	3,27	0,0010	0,0097144	0,0388606
v09_3	-0,0393046	0,011603	-3,39	0,0010	-0,0620472	-0,0165621
v09_4	-0,0308275	0,0185361	-1,66	0,0960	-0,0671593	0,0055042
v09_5	-0,0369643	0,0129003	-2,87	0,0040	-0,0622495	-0,0116791
h01	0,0552463	0,0032684	16,9	0,0000	0,0488401	0,0616525
v08_2	-0,0914424	0,0073258	-12,48	0,0000	-0,1058013	-0,0770835
v08_3	-0,0396555	0,0264744	-1,5	0,1340	-0,0915467	0,0122356
v08_4	-0,1080225	0,0104776	-10,31	0,0000	-0,128559	-0,0874859
h04_2	-0,0503693	0,0129574	-3,89	0,0000	-0,0757663	-0,0249722
h04_3	-0,0933007	0,0085004	-10,98	0,0000	-0,1099619	-0,0766394
telef_f	0,125342	0,007444	16,84	0,0000	0,1107514	0,1399326
internet	0,1345116	0,0081625	16,48	0,0000	0,1185126	0,1505105
tvcable	0,177595	0,00684	25,96	0,0000	0,1641884	0,1910017
h15_3	0,0781627	0,0166848	4,68	0,0000	0,0454597	0,1108656
h15_4	0,0516225	0,0087074	5,93	0,0000	0,0345555	0,0686895
h15_5	0,0231404	0,0096073	2,41	0,0160	0,0043095	0,0419712
h15_6	0,0555352	0,0195722	2,84	0,0050	0,0171727	0,0938978
v12a	0,0252396	0,0008545	29,54	0,0000	0,0235647	0,0269146
te_ad	0,0254308	0,0211323	1,2	0,2290	-0,0159896	0,0668512
pa_ad	-0,0574557	0,0254689	-2,26	0,0240	-0,107376	-0,0075354
pi_ad	0,0507765	0,0120756	4,2	0,0000	0,0271077	0,0744453

vtv_2	0,0669437	0,0085981	7,79	0,0000	0,0500909	0,0837965
vtv_3	-0,0113254	0,0155061	-0,73	0,4650	-0,0417182	0,0190673
vtv_4	-0,0328144	0,0115216	-2,85	0,0040	-0,0553972	-0,0102316
vtv_5	-0,0803702	0,0277981	-2,89	0,0040	-0,1348559	-0,0258845
cocina_ex	0,0300794	0,0059608	5,05	0,0000	0,0183959	0,0417629
T_per_cl	-0,0773363	0,0203935	-3,79	0,0000	-0,1173087	-0,037364
T_nn_cl	0,1625616	0,0536592	3,03	0,0020	0,0573869	0,2677364
T_me_cl	-0,0034573	0,0282182	-0,12	0,9020	-0,0587665	0,0518518
T_am_cl	0,0593213	0,0449806	1,32	0,1870	-0,0288428	0,1474854
T_pcd_cl	-0,1433981	0,0350462	-4,09	0,0000	-0,2120905	-0,0747058
rat_dp_cl	-0,5178252	0,1589009	-3,26	0,0010	-0,8292788	-0,2063715
edad_p_cl	0,0075774	0,0097266	0,78	0,4360	-0,0114873	0,0266421
edad2_p_cl	-0,0002427	0,0000813	-2,99	0,0030	-0,000402	-0,0000834
p03_cl	-0,00767	0,0095427	-0,8	0,4220	-0,0263743	0,0110342
edad2__cl	0,0000665	0,0000851	0,78	0,4340	-0,0001003	0,0002334
mujer_cl	-0,111091	0,0342351	-3,24	0,0010	-0,1781936	-0,0439884
analfabeto_cl	0,1662323	0,0369349	4,5	0,0000	0,093838	0,2386265
no_empleo_cl	-0,0140697	0,0450944	-0,31	0,7550	-0,1024571	0,0743176
migra_d_cl	0,1869325	0,041368	4,52	0,0000	0,1058491	0,268016
h01_cl	-0,1104284	0,01241	-8,9	0,0000	-0,1347527	-0,0861041
telef_f_cl	0,1285071	0,0255726	5,03	0,0000	0,0783834	0,1786307
internet_cl	0,1339712	0,0407815	3,29	0,0010	0,0540374	0,213905
tvcable_cl	-0,0778569	0,0216295	-3,6	0,0000	-0,1202519	-0,035462
v12a_cl	0,0341016	0,0034544	9,87	0,0000	0,0273309	0,0408724
te_ad_cl	0,7739045	0,058824	13,16	0,0000	0,6586066	0,8892025
pa_ad_cl	-0,1189062	0,0333034	-3,57	0,0000	-0,1841826	-0,0536298
pi_ad_cl	-0,0504654	0,0288163	-1,75	0,0800	-0,1069468	0,0060159
cocina_ex_cl	-0,019565	0,017731	-1,1	0,2700	-0,0543185	0,0151886

Source: [15]

Table 4.

SCENARIO 1: Estimated consumption poverty of children aged 0-3 years, according to the methodology (SAE) up to 2030

Income elasticity of poverty reduction			-0,0887	-0,0887	-0,0887	-0,0887	-0,0887	-0,0887	-0,0887	-0,0887	-0,0887	-0,0887	-0,0887	-0,0887	-0,0887	-0,0887	-0,0887	-0,0887
Geographical Identifier	id	2014	2015	2016	2017	2018	2019	2020	2021	2022	2023	2024	2025	2026	2027	2028	2029	2030
National	1	434.926	396.349	361.194	329.157	299.962	273.356	249.110	227.015	206.879	188.529	171.807	156.568	142.681	130.026	118.493	107.983	98.405
Esmeraldas, Imbabura, Carchi, Sucumbíos.	Z1	52.180	47.551	43.333	39.489	35.986	32.794	29.885	27.234	24.818	22.617	20.611	18.783	17.117	15.599	14.215	12.954	11.805
Pichincha (excepto el cantón Quito), Napo, Orellana	Z2	22.378	20.393	18.584	16.936	15.434	14.065	12.817	11.680	10.644	9.700	8.840	8.056	7.341	6.690	6.097	5.556	5.063
Cotopaxi, Tungurahua, Chimborazo, Pastaza	Z3	54.391	49.566	45.170	41.164	37.513	34.186	31.154	28.391	25.873	23.578	21.487	19.581	17.844	16.261	14.819	13.505	12.307
Manabí, Santo Domingo de los Tsáchilas	Z4	61.528	56.070	51.097	46.565	42.435	38.671	35.241	32.115	29.266	26.670	24.304	22.148	20.184	18.394	16.762	15.275	13.920
Santa Elena, Guayas (excepto los cantones de Guayaquil, Samborondón y Durán), Bolívar, Los Ríos y Galápagos	Z5	89.586	81.639	74.398	67.799	61.785	56.305	51.311	46.760	42.612	38.832	35.388	32.249	29.389	26.782	24.406	22.241	20.268
Cañar, Azuay, Morona Santiago.	Z6	29.512	26.894	24.509	22.335	20.354	18.549	16.904	15.405	14.039	12.794	11.659	10.625	9.683	8.824	8.041	7.328	6.678
El Oro, Loja, Zamora Chinchipe	Z7	26.193	23.869	21.752	19.823	18.065	16.463	15.003	13.672	12.459	11.354	10.347	9.429	8.593	7.831	7.136	6.503	5.926
Guayaquil, Samborondón y Durán	Z8	64.053	58.372	53.195	48.477	44.177	40.259	36.688	33.434	30.468	27.766	25.303	23.059	21.014	19.150	17.451	15.903	14.492
Distrito Metropolitano de Quito.	Z9	35.107	31.993	29.155	26.569	24.212	22.064	20.107	18.324	16.699	15.218	13.868	12.638	11.517	10.495	9.564	8.716	7.943
AZUAY	P01	20.734	18.895	17.219	15.692	14.300	13.032	11.876	10.823	9.863	8.988	8.191	7.464	6.802	6.199	5.649	5.148	4.691
BOLÍVAR	P02	8.078	7.362	6.709	6.114	5.572	5.078	4.628	4.218	3.844	3.503	3.192	2.909	2.651	2.416	2.202	2.007	1.829
CAÑAR	P03	2.635	2.401	2.188	1.994	1.817	1.656	1.509	1.375	1.253	1.142	1.041	949	865	788	718	654	596
CARCHI	P04	4.301	3.919	3.571	3.254	2.965	2.702	2.462	2.244	2.045	1.864	1.699	1.548	1.411	1.286	1.172	1.068	973
COTOPAXI	P05	13.494	12.297	11.206	10.212	9.306	8.481	7.729	7.043	6.418	5.849	5.330	4.857	4.426	4.033	3.675	3.349	3.052
CHIMBORAZO	P06	24.929	22.718	20.703	18.867	17.194	15.669	14.279	13.012	11.858	10.806	9.848	8.975	8.179	7.454	6.793	6.190	5.641
EL ORO	P07	7.867	7.169	6.533	5.954	5.426	4.945	4.506	4.106	3.742	3.410	3.108	2.832	2.581	2.352	2.143	1.953	1.780
ESMERALDAS	P08	25.358	23.108	21.058	19.190	17.488	15.937	14.523	13.235	12.061	10.991	10.016	9.128	8.318	7.580	6.908	6.295	5.737
GUAYAS	P09	99.474	90.651	82.610	75.283	68.606	62.521	56.976	51.922	47.317	43.120	39.295	35.810	32.634	29.739	27.101	24.697	22.506
IMBABURA	P10	16.440	14.982	13.653	12.442	11.338	10.332	9.416	8.581	7.820	7.126	6.494	5.918	5.393	4.915	4.479	4.082	3.720
LOJA	P11	13.794	12.570	11.455	10.439	9.513	8.669	7.900	7.199	6.560	5.978	5.448	4.965	4.525	4.124	3.758	3.425	3.121
LOS RÍOS	P12	28.339	25.826	23.535	21.447	19.545	17.811	16.231	14.791	13.479	12.283	11.194	10.201	9.296	8.471	7.720	7.035	6.411
MANABÍ	P13	51.156	46.619	42.484	38.716	35.282	32.153	29.301	26.702	24.334	22.176	20.209	18.417	16.783	15.294	13.937	12.701	11.574
MORONA SANTIAGO	P14	6.142	5.598	5.101	4.649	4.237	3.861	3.519	3.207	2.923	2.664	2.428	2.213	2.017	1.838	1.675	1.526	1.391
NAPO	P15	7.121	6.490	5.914	5.389	4.911	4.475	4.078	3.716	3.386	3.086	2.812	2.563	2.336	2.129	1.940	1.768	1.611
PASTAZA	P16	2.124	1.936	1.764	1.608	1.465	1.335	1.217	1.109	1.011	921	839	765	697	635	579	528	481
PICHINCHA	P17	46.329	42.220	38.475	35.062	31.952	29.118	26.535	24.181	22.036	20.081	18.300	16.677	15.198	13.850	12.622	11.502	10.482
TUNGURAHUA	P18	13.843	12.615	11.496	10.476	9.547	8.700	7.928	7.225	6.584	6.000	5.468	4.983	4.541	4.138	3.771	3.437	3.132

ZAMORA CHINCHIPE	P19	4.532	4.130	3.764	3.430	3.126	2.849	2.596	2.366	2.156	1.965	1.791	1.632	1.487	1.355	1.235	1.125	1.025
GALÁPAGOS	P20	20	18	16	15	14	13	12	11	10	9	8	7	6	5	5	5	5
SUCUMBÍOS	P21	6.081	5.542	5.050	4.602	4.194	3.822	3.483	3.174	2.892	2.635	2.401	2.188	1.994	1.817	1.656	1.509	1.375
ORELLANA	P22	4.035	3.677	3.351	3.054	2.783	2.536	2.311	2.106	1.919	1.749	1.594	1.453	1.324	1.207	1.100	1.002	913
SANTO DOMINGO DE LOS TSÁCHILAS	P23	10.371	9.451	8.613	7.849	7.153	6.519	5.941	5.414	4.934	4.496	4.097	3.734	3.403	3.101	2.826	2.575	2.347
SANTA ELENA	P24	17.726	16.154	14.721	13.415	12.225	11.141	10.153	9.252	8.431	7.683	7.002	6.381	5.815	5.299	4.829	4.401	4.011

Table 5.

SCENARIO 2: Estimated consumption poverty of children aged 0-3 years, according to the methodology (SAE) up to 2030

Income elasticity of poverty reduction			-0,0637	-0,0187	0,0359	-0,0828	-0,0318	-0,0318	-0,0318	-0,0630	-0,0329	-0,0164	-0,0164	-0,0164	-0,0164	-0,0164	-0,0164	-0,0164
Geographical Identifier	id	2014	2015	2016	2017	2018	2019	2020	2021	2022	2023	2024	2025	2026	2027	2028	2029	2030
National	1	434.926	407.221	399.616	413.965	379.685	367.592	355.884	344.549	322.833	312.228	307.099	302.055	297.094	292.214	287.414	282.693	278.050
Esmeraldas, Imbabura, Carchi, Sucumbíos.	Z1	52.180	48.856	47.944	49.666	45.553	44.102	42.697	41.337	38.732	37.460	36.845	36.240	35.645	35.060	34.484	33.918	33.361
Pichincha (excepto el cantón Quito), Napo, Orellana	Z2	22.378	20.953	20.562	21.300	19.536	18.914	18.312	17.729	16.612	16.066	15.802	15.542	15.287	15.036	14.789	14.546	14.307
Cotopaxi, Tungurahua, Chimborazo, Pastaza	Z3	54.391	50.926	49.975	51.769	47.482	45.970	44.506	43.088	40.372	39.046	38.405	37.774	37.154	36.544	35.944	35.354	34.773
Manabí, Santo Domingo de los Tsáchilas	Z4	61.528	57.608	56.532	58.562	53.712	52.001	50.345	48.742	45.670	44.170	43.444	42.730	42.028	41.338	40.659	39.991	39.334
Santa Elena, Guayas (excepto los cantones de Guayaquil, Samborondón y Durán), Bolívar, Los Ríos y Galápagos	Z5	89.586	83.879	82.313	85.269	78.208	75.717	73.305	70.970	66.497	64.313	63.257	62.218	61.196	60.191	59.202	58.230	57.274
Cañar, Azuay, Morona Santiago.	Z6	29.512	27.632	27.116	28.090	25.764	24.943	24.149	23.380	21.906	21.186	20.838	20.496	20.159	19.828	19.502	19.182	18.867
El Oro, Loja, Zamora Chinchipe	Z7	26.193	24.524	24.066	24.930	22.866	22.138	21.433	20.750	19.442	18.803	18.494	18.190	17.891	17.597	17.308	17.024	16.744
Guayaquil, Samborondón y Durán	Z8	64.053	59.973	58.853	60.966	55.917	54.136	52.412	50.743	47.545	45.983	45.228	44.485	43.754	43.035	42.328	41.633	40.949
Distrito Metropolitano de Quito.	Z9	35.107	32.871	32.257	33.415	30.648	29.672	28.727	27.812	26.059	25.203	24.789	24.382	23.982	23.588	23.201	22.820	22.445
AZUAY	P01	20.734	19.413	19.050	19.734	18.100	17.524	16.966	16.426	15.391	14.885	14.641	14.401	14.164	13.931	13.702	13.477	13.256
BOLÍVAR	P02	8.078	7.564	7.423	7.690	7.053	6.828	6.611	6.400	5.997	5.800	5.705	5.611	5.519	5.428	5.339	5.251	5.165
CAÑAR	P03	2.635	2.467	2.421	2.508	2.300	2.227	2.156	2.087	1.955	1.891	1.860	1.829	1.799	1.769	1.740	1.711	1.683
CARCHI	P04	4.301	4.027	3.952	4.094	3.755	3.635	3.519	3.407	3.192	3.087	3.036	2.986	2.937	2.889	2.842	2.795	2.749
COTOPAXI	P05	13.494	12.634	12.398	12.843	11.779	11.404	11.041	10.689	10.015	9.686	9.527	9.371	9.217	9.066	8.917	8.771	8.627
CHIMBORAZO	P06	24.929	23.341	22.905	23.727	21.762	21.069	20.398	19.748	18.503	17.895	17.601	17.312	17.028	16.748	16.473	16.202	15.936
EL ORO	P07	7.867	7.366	7.228	7.488	6.868	6.649	6.437	6.232	5.839	5.647	5.554	5.463	5.373	5.285	5.198	5.113	5.029
ESMERALDAS	P08	25.358	23.742	23.299	24.136	22.137	21.432	20.749	20.088	18.822	18.204	17.905	17.611	17.322	17.037	16.757	16.482	16.211
GUAYAS	P09	99.474	93.138	91.399	94.681	86.840	84.074	81.396	78.804	73.837	71.411	70.238	69.084	67.949	66.833	65.735	64.655	63.593
IMBABURA	P10	16.440	15.393	15.106	15.648	14.352	13.895	13.452	13.024	12.203	11.802	11.608	11.417	11.229	11.045	10.864	10.686	10.510
LOJA	P11	13.794	12.915	12.674	13.129	12.042	11.658	11.287	10.928	10.239	9.903	9.740	9.580	9.423	9.268	9.116	8.966	8.819
LOS RÍOS	P12	28.339	26.534	26.038	26.973	24.739	23.951	23.188	22.449	21.034	20.343	20.009	19.680	19.357	19.039	18.726	18.418	18.115
MANABÍ	P13	51.156	47.898	47.004	48.692	44.660	43.238	41.861	40.528	37.974	36.727	36.124	35.531	34.947	34.373	33.808	33.253	32.707
MORONA SANTIAGO	P14	6.142	5.751	5.644	5.847	5.363	5.192	5.027	4.867	4.560	4.410	4.338	4.267	4.197	4.128	4.060	3.993	3.927
NAPO	P15	7.121	6.668	6.543	6.778	6.217	6.019	5.827	5.641	5.285	5.111	5.027	4.944	4.863	4.783	4.704	4.627	4.551
PASTAZA	P16	2.124	1.989	1.952	2.022	1.855	1.796	1.739	1.684	1.578	1.526	1.501	1.476	1.452	1.428	1.405	1.382	1.359
PICHINCHA	P17	46.329	43.378	42.568	44.096	40.444	39.156	37.909	36.702	34.389	33.259	32.713	32.176	31.647	31.127	30.616	30.113	29.618
TUNGURAHUA	P18	13.843	12.961	12.719	13.176	12.085	11.700	11.327	10.966	10.275	9.937	9.774	9.613	9.455	9.300	9.147	8.997	8.849
ZAMORA CHINCHIPE	P19	4.532	4.243	4.164	4.314	3.957	3.831	3.709	3.591	3.365	3.254	3.201	3.148	3.096	3.045	2.995	2.946	2.898
GALÁPAGOS	P20	20	19	19	20	18	17	16	15	14	14	14	14	14	14	14	14	14
SUCUMBÍOS	P21	6.081	5.694	5.588	5.789	5.310	5.141	4.977	4.818	4.514	4.366	4.294	4.223	4.154	4.086	4.019	3.953	3.888
ORELLANA	P22	4.035	3.778	3.707	3.840	3.522	3.410	3.301	3.196	2.995	2.897	2.849	2.802	2.756	2.711	2.666	2.622	2.579
SANTO DOMINGO DE LOS TSÁCHILAS	P23	10.371	9.711	9.530	9.872	9.055	8.767	8.488	8.218	7.700	7.447	7.325	7.205	7.087	6.971	6.856	6.743	6.632
SANTA ELENA	P24	17.726	16.597	16.287	16.872	15.475	14.982	14.505	14.043	13.158	12.726	12.517	12.311	12.109	11.910	11.714	11.522	11.333

Source: [15]

Table 6.

Estimation of consumption poverty of children aged 0-3 years, according to the methodology (SAE).

Geographical Identifier		Incidence (%)	Standard deviation (%)	Coefficient of variation (%)
1	National	41,1	1,03	2,54
1	Planning zone 1	53,9	1,20	2,23
2	Planning zone 2	47,7	1,70	3,58
3	Planning zone 3	53,1	1,53	2,89
4	Planning zone 4	48,0	2,54	5,28
5	Planning zone 5	50,3	1,71	3,39
6	Planning zone 6	35,2	2,70	7,69
7	Planning zone 7	31,6	2,59	8,21
8	Planning zone 8	33,6	2,72	8,10
9	Planning zone 9	22,3	1,95	8,75
1	Napo	81,3	4,23	11,15
6	Chimborazo	79,1	4,98	7,47
24	Santa Elena	67,4	3,18	22,72
2	Bolívar	66,1	3,54	9,42
5	Zamora Chinchipe	60,9	3,07	6,93
8	Esmeraldas	59,8	3,62	4,61
10	Imbabura	55,4	3,67	20,34
8	Morona Santiago	54,4	1,89	3,18
9	Manabí	53,1	2,67	7,16
10	Los Ríos	48,2	1,96	3,52
11	Sucumbíos	45,6	4,05	9,57
5	Cotopaxi	45,4	2,26	4,87
11	Loja	42,4	3,21	6,10
18	Tungurahua	40,6	2,56	4,67
1	Azuay	39,4	2,31	2,86
9	Guayas	37,6	4,34	12,27
4	Carchi	37,4	1,98	7,86
16	Pastaza	36,9	2,79	6,98
19	Orellana	36,3	6,06	9,66
23	Santo Domingo de los Tsáchilas	34,1	0,46	47,73
17	Pichincha	25,1	4,37	9,63
7	El Oro	18,5	4,09	11,55
3	Cañar	15,2	2,71	8,02
20	Galápagos	1,2	6,57	9,98
0101	Cuenca	32,6	3,72	11,43
0102	Girón	50,7	6,93	13,67
0103	Gualaceo	46,5	6,01	12,92
0104	Nabón	63,8	6,31	9,89
0105	Paute	46,3	5,89	12,73
0106	Pucara	62,4	8,13	13,02
0107	San Fernando	44,5	6,91	15,52
0108	Santa Isabel	46,4	5,57	12,01
0109	Sigsig	53,6	6,14	11,45

0110	Oña	69,4	7,18	10,35
0111	Chordeleg	42,7	5,95	13,93
0112	El Pan	48,1	9,82	20,39
0113	Sevilla de Oro	49,5	7,29	14,72
0114	Guachapala	38,8	10,65	27,49
0115	Camilo Ponce Enríquez	52,5	5,32	10,14
0201	Guaranda	67,1	4,40	6,56
0202	Chillanes	77,5	5,80	7,48
0203	Chimbo	65,5	5,99	9,16
0204	Echeandía	63,7	6,16	9,68
0205	San Miguel	64,2	5,79	9,01
0206	Caluma	57,3	6,84	11,94
0207	Las Naves	70,5	6,75	9,58
0301	Azogues	6,7	2,79	41,73
0302	Biblián	4,8	2,93	60,87
0303	Cañar	28,7	3,77	13,14
0304	La Troncal	10,2	4,40	42,96
0305	El Tambo	21,1	4,46	21,12
0306	Deleg	6,0	3,23	53,37
0307	Suscal	26,7	7,18	26,91
0401	Tulcán	30,2	3,79	12,54
0402	Bolívar	52,6	4,99	9,50
0403	Espejo	40,9	4,98	12,16
0404	Mira	54,3	4,44	8,18
0405	Montufar	45,9	4,18	9,10
0406	San Pedro de Huaca	28,2	5,71	20,26
0501	Latacunga	37,3	2,66	7,13
0502	La Maná	45,4	3,51	7,73
0503	Pangua	57,1	4,23	7,41
0504	Pujilí	51,7	4,99	9,66
0505	Salcedo	40,8	3,11	7,63
0506	Saquisilí	49,9	3,92	7,86
0507	Sigchos	61,6	5,05	8,20
0601	Riobamba	68,3	5,03	7,37
0602	Alausí	86,5	2,66	3,07
0603	Colta	95,5	1,80	1,88
0604	Chambo	78,8	4,23	5,37
0605	Chunchi	75,1	6,34	8,44
0606	Guamote	97,8	1,41	1,44
0607	Guano	84,5	3,99	4,72
0608	Pallatanga	84,4	3,90	4,62
0609	Penipe	79,1	6,19	7,82
0610	Cumanda	76,9	6,32	8,22
0701	Machala	14,5	3,35	23,15
0702	Arenillas	22,6	4,23	18,74
0703	Atahualpa	14,5	5,07	35,07
0704	Balsas	20,1	4,99	24,78

0705	Chilla	31,4	8,78	27,94
0706	El Guabo	27,1	4,28	15,76
0707	Huaquillas	16,8	3,90	23,26
0708	Marcabelí	26,6	5,57	20,91
0709	Pasaje	21,7	3,91	18,05
0710	Piñas	12,0	4,32	36,00
0711	Portovelo	20,1	4,69	23,35
0712	Santa Rosa	18,1	4,01	22,16
0713	Zaruma	19,9	5,28	26,48
0714	Las Lajas	22,6	6,05	26,81
0801	Esmeraldas	47,9	2,15	4,48
0802	Eloy Alfaro	73,3	2,77	3,78
0803	Muisne	75,1	2,95	3,92
0804	Quinindé	65,6	2,17	3,31
0805	San Lorenzo	62,5	3,22	5,15
0806	Atacames	59,1	2,70	4,58
0807	Rioverde	78,5	2,60	3,31
2302	La Concordia (*)	57,5	2,96	5,15
0901	Guayaquil	33,6	2,80	8,32
0902	Alfredo Baquerizo Moreno	57,9	3,92	6,77
0903	Balao	47,5	4,63	9,74
0904	Balzar	50,4	3,50	6,94
0905	Colimes	55,5	4,10	7,39
0906	Daule	37,0	2,29	6,19
0907	Duran	35,1	2,69	7,67
0908	Empalme	56,8	3,41	6,00
0909	El Triunfo	48,2	3,11	6,47
0910	Milagro	41,7	2,98	7,14
0911	Naranjal	48,2	3,28	6,80
0912	Naranjito	47,7	3,35	7,02
0913	Palestina	48,7	3,48	7,15
0914	Pedro Carbo	42,4	4,00	9,44
0916	Samborondón	26,3	1,91	7,26
0918	Santa Lucía	47,6	4,24	8,92
0919	Salitre	55,4	3,96	7,15
0920	San Jacinto de Yaguachi	47,8	3,21	6,72
0921	Playas	37,1	4,68	12,62
0922	Simón Bolívar	52,2	3,82	7,32
0923	Coronel Marcelino Maridueña	42,9	3,17	7,38
0924	Lomas de Sargentillo	39,2	4,32	11,03
0925	Nobol	44,9	4,01	8,92
0927	General Antonio Elizalde	45,7	2,99	6,54
0928	Isidro Ayora	42,9	4,12	9,60
1001	Ibarra	39,3	1,89	4,80
1002	Antonio Ante	52,7	2,06	3,91
1003	Cotacachi	74,6	2,49	3,34
1004	Otavalo	69,6	2,51	3,60

1005	Pimampiro	70,3	2,66	3,78
1006	San Miguel de Urcuquí	79,0	3,09	3,91
1101	Loja	29,3	3,88	13,26
1102	Calvas	49,3	4,50	9,14
1103	Catamayo	43,3	5,45	12,58
1104	Celica	51,7	4,73	9,15
1105	Chaguarpamba	59,5	5,07	8,52
1106	Espíndola	68,7	4,51	6,56
1107	Gonzanama	62,1	4,99	8,04
1108	Macara	42,6	5,02	11,78
1109	Paltas	58,3	4,05	6,96
1110	Puyango	52,7	5,00	9,48
1111	Saraguro	61,9	4,83	7,79
1112	Sozoranga	67,0	5,53	8,26
1113	Zapotillo	61,6	5,44	8,83
1114	Pindal	56,0	4,83	8,62
1115	Quilanga	59,4	5,75	9,68
1116	Olmedo	67,6	5,77	8,54
1201	Babahoyo	40,5	2,52	6,21
1202	Baba	55,0	2,69	4,89
1203	Montalvo	40,0	2,77	6,92
1204	Puebloviejo	47,5	3,20	6,75
1205	Quevedo	40,4	2,64	6,53
1206	Urdaneta	45,7	2,76	6,03
1207	Ventanas	43,7	2,85	6,53
1208	Vinces	48,7	2,44	5,01
1209	Palenque	61,7	2,74	4,44
1210	Buena Fe	52,6	2,96	5,62
1211	Valencia	56,1	2,90	5,18
1212	Mocache	57,6	2,50	4,34
1213	Quinsaloma	53,6	2,53	4,71
1301	Portoviejo	43,3	3,65	8,43
1302	Bolívar	59,3	2,90	4,89
1303	Chone	55,7	2,82	5,06
1304	El Carmen	47,8	3,56	7,46
1305	Flavio Alfaro	58,8	3,85	6,54
1306	Jipijapa	65,7	4,86	7,41
1307	Junín	63,5	4,02	6,33
1308	Manta	38,8	3,30	8,50
1309	Montecristi	50,0	5,85	11,69
1310	Paján	71,4	3,56	4,99
1311	Pichincha	64,8	3,39	5,23
1312	Rocafuerte	48,9	4,43	9,07
1313	Santa Ana	68,0	3,01	4,42
1314	Sucre	57,2	4,10	7,16
1315	Tosagua	56,9	3,96	6,97
1316	24 de Mayo	75,6	2,98	3,94

1317	Pedernales	63,1	3,25	5,15
1318	Olmedo	73,8	3,00	4,06
1319	Puerto López	63,0	5,45	8,66
1320	Jama	75,9	4,12	5,42
1321	Jaramijó	57,3	6,86	11,97
1322	San Vicente	55,5	4,70	8,46
1401	Morona	47,1	3,38	7,17
1402	Gualaquiza	50,5	2,47	4,89
1403	Limón Indanza	53,3	2,87	5,39
1404	Palora	56,0	3,25	5,81
1405	Santiago	59,5	3,64	6,12
1406	Sucúa	34,9	3,94	11,29
1407	Huamboya	86,7	2,91	3,36
1408	San Juan Bosco	51,7	4,11	7,96
1409	Taisha	87,5	2,38	2,72
1410	Logroño	68,9	3,57	5,18
1411	Pablo Sexto	59,7	5,48	9,19
1412	Tiwintza	77,0	2,72	3,53
1501	Tena	77,8	2,18	2,80
1503	Archidona	89,7	2,10	2,34
1504	El Chaco	77,9	5,17	6,64
1507	Quijos	68,0	5,37	7,89
1509	Carlos Julio Arosemena Tola	92,7	3,43	3,70
1601	Pastaza	35,2	4,23	12,03
1602	Mera	30,4	4,34	14,29
1603	Santa Clara	44,1	6,41	14,55
1604	Arajuno	47,3	8,31	17,56
1701	Quito	22,3	1,95	8,75
1702	Cayambe	53,3	2,73	5,13
1703	Mejía	35,5	3,07	8,65
1704	Pedro Moncayo	51,1	3,35	6,56
1705	Rumiñahui	21,8	1,96	9,00
1707	San Miguel de los Bancos	53,0	4,41	8,31
1708	Pedro Vicente Maldonado	49,9	3,92	7,85
1709	Puerto Quito	55,0	3,74	6,81
1801	Ambato	38,2	2,56	6,70
1802	Baños de Agua Santa	26,7	2,98	11,16
1803	Cevallos	31,0	4,00	12,89
1804	Mocha	39,2	5,16	13,16
1805	Patate	48,1	3,65	7,58
1806	Quero	52,3	4,79	9,15
1807	San Pedro de Pelileo	45,1	3,86	8,55
1808	Santiago de Pillaro	45,4	3,81	8,40
1809	Tisaleo	44,5	4,25	9,56
1901	Zamora	53,4	6,62	12,39
1902	Chinchipe	61,2	9,14	14,92
1903	Nangaritza	81,2	5,83	7,18

1904	Yacuambi	71,8	6,39	8,90
1905	Yantzaza	65,1	5,91	9,08
1906	El Pangui	60,4	4,84	8,02
1907	Centinela del Cóndor	59,9	5,98	9,99
1908	Palanda	65,1	9,07	13,93
1909	Paquisha	74,4	9,19	12,35
2001	San Cristóbal	0,3	0,33	131,97
2002	Isabela	0,6	0,85	145,36
2003	Santa Cruz	1,4	0,68	48,17
2101	Lago Agrio	40,7	4,63	11,39
2102	Gonzalo Pizarro	43,1	5,03	11,66
2103	Putumayo	63,0	4,84	7,69
2104	Shushufindi	47,8	4,48	9,36
2105	Sucumbíos	35,7	5,97	16,72
2106	Cascales	56,5	5,30	9,37
2107	Cuyabeno	59,6	5,40	9,05
2201	Orellana	27,5	4,38	15,95
2202	Aguarico	69,2	4,59	6,64
2203	La Joya de los Sachas	32,6	4,81	14,74
2204	Loreto	63,3	3,66	5,78
2301	Santo Domingo	33,8	2,71	8,02
2401	Santa Elena	66,7	6,63	9,94
2402	La Libertad	64,2	7,55	11,76
2403	Salinas	66,6	6,05	9,08
9901	Las Golondrinas (**)	65,6	2,17	3,31
9903	Manga del Cura (**)	47,8	3,56	7,46
9904	El Piedrero (**)	48,2	3,11	6,47
01D01	01D01	31,5	3,86	12,25
01D02	01D02	33,5	3,63	10,83
01D03	01D03	51,1	6,28	12,30
01D04	01D04	45,7	5,91	12,94
01D05	01D05	64,9	6,30	9,71
01D06	01D06	46,3	6,47	13,97
01D07	01D07	52,5	5,32	10,14
01D08	01D08	53,6	6,14	11,45
02D01	02D01	67,1	4,40	6,56
02D02	02D02	77,5	5,80	7,48
02D03	02D03	64,7	5,79	8,94
02D04	02D04	62,1	6,32	10,19
03D01	03D01	6,2	2,72	43,68
03D02	03D02	27,6	3,85	13,95
03D03	03D03	10,2	4,40	42,96
04D01	04D01	30,1	3,86	12,84
04D02	04D02	48,0	3,93	8,19
04D03	04D03	46,9	4,45	9,49
05D01	05D01	37,3	2,66	7,13
05D02	05D02	45,4	3,51	7,73

05D03	05D03	57,1	4,23	7,41
05D04	05D04	51,2	4,61	9,01
05D05	05D05	61,6	5,05	8,20
05D06	05D06	40,8	3,11	7,63
06D01	06D01	68,8	4,95	7,19
06D02	06D02	83,9	3,45	4,11
06D03	06D03	80,3	5,08	6,32
06D04	06D04	96,9	1,44	1,49
06D05	06D05	83,8	4,11	4,91
07D01	07D01	24,3	4,00	16,49
07D02	07D02	14,5	3,35	23,15
07D03	07D03	19,3	4,74	24,58
07D04	07D04	15,9	4,26	26,87
07D05	07D05	19,0	3,87	20,37
07D06	07D06	18,1	4,01	22,16
08D01	08D01	47,9	2,15	4,48
08D02	08D02	73,3	2,77	3,78
08D03	08D03	65,0	2,46	3,79
08D04	08D04	65,6	2,17	3,31
08D05	08D05	62,5	3,22	5,15
08D06	08D06	78,5	2,60	3,31
08D07	08D07	57,5	2,96	5,15
09D01	09D01	32,9	2,70	8,20
09D02	09D02	35,2	2,87	8,15
09D03	09D03	24,6	2,54	10,31
09D04	09D04	32,7	2,87	8,79
09D05	09D05	11,6	1,47	12,65
09D06	09D06	27,4	2,68	9,77
09D07	09D07	32,8	2,84	8,65
09D08	09D08	51,4	3,80	7,39
09D09	09D09	18,3	1,64	8,99
09D10	09D10	47,3	4,53	9,56
09D11	09D11	55,0	3,64	6,62
09D12	09D12	48,0	3,54	7,37
09D13	09D13	51,3	3,39	6,61
09D14	09D14	41,7	3,91	9,37
09D15	09D15	56,8	3,41	6,00
09D16	09D16	47,7	2,98	6,26
09D17	09D17	41,7	2,98	7,14
09D18	09D18	46,6	3,14	6,73
09D19	09D19	40,1	2,76	6,89
09D20	09D20	55,4	3,96	7,15
09D21	09D21	47,8	3,21	6,72
09D22	09D22	37,1	4,68	12,62
09D23	09D23	26,3	1,91	7,26
09D24	09D24	35,1	2,69	7,67
10D01	10D01	44,4	1,85	4,17

10D02	10D02	64,8	2,27	3,51
10D03	10D03	74,6	2,49	3,34
11D01	11D01	29,3	3,88	13,26
11D02	11D02	48,2	5,15	10,69
11D03	11D03	58,3	4,05	6,96
11D04	11D04	53,0	4,59	8,65
11D05	11D05	68,7	4,51	6,56
11D06	11D06	53,3	4,51	8,46
11D07	11D07	50,0	4,92	9,84
11D08	11D08	61,9	4,83	7,79
11D09	11D09	61,6	5,44	8,83
12D01	12D01	43,2	2,37	5,48
12D02	12D02	46,8	2,81	6,02
12D03	12D03	43,5	2,41	5,55
12D04	12D04	45,7	2,64	5,78
12D05	12D05	51,8	2,36	4,55
12D06	12D06	54,0	2,83	5,24
13D01	13D01	43,4	3,66	8,43
13D02	13D02	42,7	3,95	9,25
13D03	13D03	64,9	4,90	7,55
13D04	13D04	71,1	2,80	3,94
13D05	13D05	47,8	3,56	7,46
13D06	13D06	60,7	3,09	5,10
13D07	13D07	56,2	2,88	5,13
13D08	13D08	64,8	3,39	5,23
13D09	13D09	71,4	3,56	4,99
13D10	13D10	66,9	3,27	4,88
13D11	13D11	56,8	4,18	7,36
13D12	13D12	52,9	4,03	7,61
14D01	14D01	47,1	3,38	7,17
14D02	14D02	71,7	2,59	3,61
14D03	14D03	41,7	3,57	8,56
14D04	14D04	50,7	2,57	5,07
14D05	14D05	87,5	2,38	2,72
14D06	14D06	60,0	2,65	4,41
15D01	15D01	81,8	2,05	2,51
15D02	15D02	73,8	5,03	6,81
16D01	16D01	34,7	4,19	12,08
16D02	16D02	47,3	8,31	17,56
17D01	17D01	47,0	3,73	7,95
17D02	17D02	22,2	2,75	12,37
17D03	17D03	23,1	1,92	8,32
17D04	17D04	24,2	2,09	8,65
17D05	17D05	16,4	1,51	9,24
17D06	17D06	18,6	1,88	10,13
17D07	17D07	26,2	2,27	8,67
17D08	17D08	24,1	2,15	8,91

17D09	17D09	26,8	2,40	8,98
17D10	17D10	52,6	2,83	5,38
17D11	17D11	29,0	2,44	8,40
17D12	17D12	52,9	3,65	6,89
18D01	18D01	40,9	2,42	5,92
18D02	18D02	36,2	2,72	7,52
18D03	18D03	26,7	2,98	11,16
18D04	18D04	45,7	3,72	8,14
18D05	18D05	45,4	3,81	8,40
18D06	18D06	44,6	4,15	9,30
19D01	19D01	57,0	6,11	10,71
19D02	19D02	70,6	6,26	8,87
19D03	19D03	63,3	8,86	14,01
19D04	19D04	63,7	5,44	8,54
20D01	20D01	1,0	0,46	47,73
21D01	21D01	48,0	4,58	9,53
21D02	21D02	40,7	4,63	11,39
21D03	21D03	61,5	4,86	7,91
21D04	21D04	47,8	4,48	9,36
22D01	22D01	32,6	4,81	14,74
22D02	22D02	35,2	4,02	11,43
22D03	22D03	69,2	4,59	6,64
23D01	23D01	31,9	2,70	8,46
23D02	23D02	35,9	2,78	7,76
23D03	23D03	57,5	2,96	5,15
24D01	24D01	66,7	6,63	9,94
24D02	24D02	65,2	6,67	10,23

(*) Updated code

(**) Aggregates, value of nearby locality is assumed.

Source: [15]

FACULTAD DE INGENIERÍA Y CIENCIAS APLICADAS
UNIVERSIDAD CENTRAL DEL ECUADOR

INGENIO
2025, VOL 8(2), JULIO - DICIEMBRE, PP. 53-66

REVISTA INGENIO

Implementation of a Weather Station using FPGA with Real Time Data Access and Analysis

Implementación de una Estación Meteorológica Mediante FPGA con Acceso y Análisis de Datos en Tiempo Real

Holger Santillán | Universidad Politécnica Salesiana, UPS -Ecuador
José Ochoa | Universidad Politécnica Salesiana, UPS -Ecuador
José Ordoñez | Universidad Politécnica Salesiana, UPS -Ecuador
Peregrina Wong | Universidad Politécnica Salesiana, UPS -Ecuador

Recibido: 6/11/2024
Recibido tras revisión: 14/4/2025
Aceptado: 26/5/2025
Publicado: 10/07/2025

KEY WORDS
FPGA, Weather Station, Raspberry Pi 4, LabVIEW, Sensors.

ABSTRACT
The present study develops a weather station with the Fiel-Programmable Gate Array (FPGA) technology to obtain meteorological data in educational environments, but that can be adapted to any real scenario, using ADM1001 sensors for temperature and humidity, amount of rain, wind direction and wind speed. The proposed design aims to improve the accuracy and speed with which weather data is obtained in real time. For this purpose, the Elvis II+ platform together with the Xilinx Spartan 3E FPGA was used for the connections of the different types of sensors. In addition, the LabVIEW programming environment was used for the design and control of the system ensuring a user-friendly interface for the users. To present the collected data, a Node-Network solution was developed to efficiently visualize the data, the algorithms used achieved an accuracy of 85% under normal conditions, the root mean square error (RMSE) was 0.2 °C for temperature and 1.5% for humidity. This visualization is achieved through a Raspberry Pi since it facilitates the access and management of the meteorological information collected in real time, which endorses the quality of the prototype designed in the present work.

PALABRAS CLAVE
FPGA, Estación meteorológica, Raspberry Pi 4, LabVIEW, Sensores.

RESUMEN
El presente estudio desarrolla una estación meteorológica con la tecnología Fiel-Programmable Gate Array (FPGA) para obtener datos meteorológicos en entornos educativos, pero que puede adaptarse a cualquier escenario real, utilizando sensores ADM1001 de temperatura y humedad, cantidad de lluvia, dirección y velocidad del viento. El diseño propuesto pretende mejorar la precisión y rapidez con la que se obtienen los datos meteorológicos en tiempo real. Para ello, se ha utilizado la plataforma Elvis II+ junto con la FPGA Xilinx Spartan 3E para las conexiones de los diferentes tipos de sensores. Además, se utilizó el entorno de programación LabVIEW para el diseño y control del sistema asegurando una interfaz fácil de usar para los usuarios. Para presentar los datos recogidos, se desarrolló una solución Node-Network que permite visualizar los datos de forma eficiente, los algoritmos empleados alcanzaron una precisión del 85% en condiciones normales, el error cuadrático medio (RMSE) fue de 0.2 °C para la temperatura y de 1.5% para la humedad. Esta visualización se consigue a través de una Raspberry Pi ya que facilita el acceso y la gestión de la información meteorológica recogida en tiempo real, lo cual avala la calidad del prototipo diseñado en el presente trabajo.

1. Introduction

The country is currently experiencing more extreme climate changes, and this makes it increasingly necessary to monitor and predict these phenomena more accurately. According to, in Ecuador, several natural phenomena significantly affect the climate. The factors are measured thanks to current technology, and the data obtained in real time allows us to understand and react more effectively to changes [1].

Field-Programmable Gate Arrays, or FPGAs, are integrated circuits that can be programmed after manufacture. They are ideal for implementing complex handling algorithms and maintenance activities on electronic devices. The parallel processing and efficiency of these devices make FPGAs more efficient than microcontrollers and digital signal processors, delivering higher performance for real-time applications [2], [3].

https://doi.org/10.29166/ingenio.v8i2.7449

pISSN 2588-0829
eISSN 2697-3243
fing.revista.ingenio@uce.edu.ec

A real-time weather station has sensors and electronics, such as sensors for basic weather variables, such as temperature, humidity, uva ultraviolet radiation, and wind direction. Learning Objects form another part of the support for the educational process which facilitates their understanding [4], [5].

In this project, an experimental methodology is proposed to allow the use of the weather station, which involves an analysis of the functionality. The purpose is to evaluate significant parameters, such as humidity, temperature, the amount of rainfall, wind speed and direction. Real-time analytics is made possible by FPGAs' ability to collect and process data instantly [6].

The system uses LabVIEW as a simulation tool for development. LabVIEW is an acronym for Laboratory Virtual Instrument Engineering Workbench. It allows the development of a user interface that interacts with the simulation equipment in an intuitive way by presenting data in real time using boxes, graphs and specific markers for the reading of data from each sensor of the weather station. Therefore, the system is educational for any user who wishes to understand [7], [8].

Traditional weather stations often contend with slow data collection and limited processing. FPGA-based systems, in contrast, provide real-time data handling and high-speed parallel processing capabilities. While IoT-based weather stations offer remote connectivity and cloud integration, their common reliance on microcontrollers or single-board computers may not match the speed or hardware-level customization FPGAs deliver. Consequently, FPGA weather stations effectively combine local data processing with system reconfigurability, presenting a robust solution for responsive and accurate climate monitoring.

To augment system functionality, technologies such as Node-RED and CERN-ROOT are incorporated for data flow control and scientific data analysis, respectively. Node-RED supplies a user-friendly visual programming interface for managing sensor data, whereas CERN-ROOT facilitates complex statistical processing and visualization. The inclusion of these tools equips the FPGA-based system with potent software capabilities that complement its hardware strengths, supporting both immediate responses and detailed data insights.

From an educational standpoint, FPGA-based weather stations function as valuable learning platforms. They expose students and researchers to interdisciplinary content covering electronics, programming, signal processing, and environmental science. Engaging with real-time data and reconfigurable hardware allows learners to achieve a deeper understanding of embedded systems and their practical applications in contemporary environmental monitoring.

Weather stations play a vital role in collecting climate data that affects many sectors, from agriculture to disaster management. They help farmers make decisions by implementing accurate weather conditions, and to predict extreme events, they help reduce damage. Data is also necessary for inclusion in the climate change agenda, allowing environmental policy to be evaluated and adjusted [9].

In many respects, traditional weather stations face several notable challenges. The high cost associated with installation and maintenance can make the stations prohibitive for many. Similarly, data handling accuracy and speed are generally low, seemingly unable to respond quickly to events that occur around the weather. In addition, real-time data analysis is absent in many traditional systems, ultimately limiting its effectiveness in extreme events [10].

The application of FPGAs in weather stations provides several notable advantages. Due to the increase in computing resources, a rapid reaction to changing weather conditions is achieved. The system is improved in terms of accuracy by customizing the hardware for the particular sensors used. In addition, additional upgrades and upgrades are constant due to the adaptability of the FPGA, ensuring that the system can be modified or upgraded to newer specifications as needed [11].

The main purpose of the FPGA-based weather station is to work with various sensors and collect environmental parameters including temperature, humidity, direction, and wind speed. One of the most important features of this functionality is the ability to calculate and analyze such data accurately. In addition, there are also educational materials such as simulations and teaching tools that are available for students to understand the concept and application of the weather station.

This research expands the capabilities of real-time meteorology by taking the implementation of software built specifically around FPGA technology to the next level. It equips weather stations with computerized systems that improve the efficiency of their use as provided by general systems using normal approaches. This system can really help us control the weather better and is a great start to creating even more interesting things in the future.

Using FPGAs in a weather station greatly affects both study and real-world use. This platform is a high-tech tool that helps scientists better study weather and climate. This method changes real-time weather tracking and can be used in many situations, providing a flexible way to monitor different things.

Within a detailed review of the technologies, current methods of weather stations and real-time data processing. The analysis situates the project in the field of meteorological technologies, demonstrating how current innovations, such as the use of FPGAs, overcome the limitations of traditional systems. By understanding the existing environment, one can see how the proposed project

will improve the accuracy and speed of collecting and analyzing weather data.

The various sensors of the weather station stand out, being the fundamental AMT1001 to collect accurate measurements of critical hydroclimatic variables, such as temperature and relative humidity. Integrated into the IoT weather station layer, the AMT1001 offers level readings to enable monitoring of environmental conditions. The article used 65 samples, presented a correlation of 100% in the data and a transmission efficiency of 95.3%, validating the usefulness of AMT1001 in planning agriculture and resource management systems [12].

The PRS-1 sensor, a compact rain gauge designed to measure the amount of rainfall accurately by location. This sensor is important for collecting the amount of rainfall that covers rainfall, something that is necessary for Bangladeshi agriculture, where the lack of timely information has resulted in crop losses, as PRS-1 not only gives accurate measurements, but also stores and allows data to be shared online, facilitating the estimation of rainfall and agriculture based on historical and current data [13].

Ultrasonic cup anemometers are employed for wind measurement, as wind speed is a key component in evaluating a generation site before installing a wind farm. The low-cost anemometer was created using 3D addition technology and manufacturing instructions with an encoder and phototransistor to convert rotation into wind speed data using the Arduino Uno. The test results and the 0.968 showed that its level of accuracy is high and it may be a viable and economical option for future wind projects [14].

The FPGA-based weather station uses the Xilinx Artix7 array and the Verilog HDL language to accurately measure weather parameters. It uses a FT2232H USB-UART interface to record atmospheric pressure, temperature, and humidity, and allows the interconnection of various sensors. Data acquired in Nilgiri, Tamil Nadu, India, is visualized using the CERN-ROOT data analysis framework, providing a detailed and efficient graphical representation of weather conditions [15], [4].

The transceiver schemes MPSK (Mary-Phase Shift Keying) and MQAM (Mary-Quadrature Amplitude Modulation) are implemented in LabVIEW, considering the effect of noise. These schematics are reproduced with the SDR NI-USRP 2920 kit, and the strength of the received signal is measured with the R&S (Rohde & Schwarz) sensor. The results show good agreement with the simulations, and the detailed procedure serves as reference material for prototyping and hands-on teaching of communication systems [16].

The NI ELVIS II system facilitates the study of these characteristics, allowing the analysis of tunable filters in both the time and frequency domains. This educational equipment is essential to understand the behavior of filters of various orders, providing practical and detailed examples that enrich learning in electrical engineering. Its use in the curriculum is essential for a complete training in filter analysis and design [17].

The topology for FPGA based on a systolic structure, suitable for forward neural networks such as the multilayer perceptron (MLP). Implemented on the Zynq-7000 board with the MNEST dataset, the proposed architecture improves accuracy and performance using specific activation functions. This solution optimizes hardware efficiency in neural network applications, outperforming traditional structures [18].

The proposed design uses the Spartan-3E FPGA to generate and control a PWM signal with variable duty cycle using a rotary encoder. The Spartan-3E, with its internal clock of 50 MHz, allows you to adjust the PWM signal duty cycle from 0 to 100% by turning the encoder and changing the signal frequency. This approach offers high speed, customization and low cost, being suitable for applications in power control and electronics. The generated PWM signal is analyzed with an oscilloscope to ensure its accuracy at various frequencies [19].

The Raspberry Pi 4 has been employed to develop a low-cost disk imaging device useful in digital forensics for copying evidence before direct analysis. Using Python, the device allows digital evidence to be handled accurately and efficiently, minimizing the risk of tampering. Tests show that the Raspberry Pi 4 delivers solid performance in speed and accuracy, providing an economical alternative to more expensive equipment on the market [20].

Implementing an I2C controller on an FPGA to connect the BH1750FVI light sensor and transmit data to Simulink using an I2C bridge to UART. Using VHDL and a finite state machine (FSM), the I2C controller and UART have been developed. The verification is performed with a hardware I2C analyzer, ensuring accurate acquisition of sensor data. The UART controller then sends this data serially to the COM port for analysis and processing in Matlab-Simulink [21].

This protocol is ideal for systems with many distributed sensors, although the topology can become complex in large networks. Deploying switched networks, which divide the network into electronically managed segments, helps handle this complexity without increasing weight or radius. In this study, a long-line 1-Wire network with a data switch integrated into a master microcontroller is proposed, providing a reliable and economical solution for temperature sensor monitoring [22].

The Modbus protocol facilitates communication in industrial systems by connecting control devices through a simple interface. This article discusses how Node-Red, a flow-based visual programming tool, integrates with Modbus to control robots, such as Epson's 6-axis and SCARA robots. The combination of Modbus with Node-Red enables efficient and visual management of robotic systems, demonstrating that visual programming can simplify the

development and implementation of control software in industrial environments [23].

Both conventional manual and automatic weather stations rely on physical models and satellite data to make their predictions. However, in extremes with complex microclimates such as Quito, these methods are often inaccurate, in part due to local factors such as the Intertropical Convergence Zone that these structures are not armed to deal with. Given the inability to adapt to these specificities, their prognoses are often wrong [24].

The study by Asanza proposes a weather monitoring station with FPGA-based embedded systems. This system acquires high-resolution data and predicts real-time samples accurately. Additionally, a web application with user-friendly interface presents the collected data [11].

These stations are also inefficient because they cannot process information in real time and are expensive to expand in number to improve accuracy. Therefore, these shortcomings argue the need for economical and novel approaches, such as low-cost computers and advanced machine learning techniques, that can guarantee the accuracy of weather forecasts in extremes with complex microclimates [25].

The AASIP (Adaptive Arithmetic Significance Inference Prediction) algorithm, which optimizes the accuracy of the correction factor in the Sparse Implicit Projection (SIP) by correcting based on the arithmetic mean. AASIP improves accuracy in RC network list reduction by overcoming the limitations of traditional SIP and adjusting high-order moments. The effectiveness of the algorithm is validated through practical examples, demonstrating its ability to offer a more accurate approximation compared to previous methods [26].

Equation (1) of the arithmetic mean is:

$$\bar{X} = \frac{1}{n}\sum_{i=1}^{n} a_i = \frac{a_1 + a_2 + a_3 + \ldots + a_n}{n} \quad (1)$$

Where

$\bar{X}$***:*** *arithmetic mean*

a_n***:*** *number of data*

Σ*:* *sumatoria*

n: *Total number of data*

The article highlights the need to modernize weather monitoring in Ecuador due to the lack of advanced technology. The National Institute of Meteorology and Hydrology (INAMHI) is implementing a program to replace traditional stations with more advanced technologies, such as FPGAs, that would improve accuracy and efficiency in the collection of environmental data, such as temperature, humidity and atmospheric pressure [11].

Similarly, the study recommends considering alternatives such as static stations and wireless sensor networks to automate and monitor data. It also suggests comparing different data acquisition technologies, such as SRAM FPGA memory, to reduce response times and take into account environmental factors to improve the accuracy of the monitoring system.

FPGAs have proven to be very effective in improving accuracy and reducing response time in the acquisition of meteorological data. Compared to DDR3 memory, FPGAs can accelerate data reading by up to five times. In addition, systems using FPGAs with neural networks and the VHDL language have shown high accuracy in monitoring variables such as humidity and light intensity.

The article states that an Arduino Uno was initially used to connect the sensors and transmit data, which was replaced by Raspberry Pi due to its higher processing power. FPGAs are used in our thesis due to their high performance and energy efficiency, which makes them suitable for managing sensor data at high speed [11].

Therefore, this article is about the technological outdatedness of Ecuador's weather stations and an innovative solution based on FPGA systems. FPGA technology has demonstrated its impressive number of abilities to improve accuracy and efficiency in the acquisition of environmental data, including temperature, humidity, rainfall, and light intensity. Therefore, FPGA implementation can modernize existing systems and make data acquisition extremely efficient and high-quality.

The article describes the weather station that the Xilinx Artix 7 FPGA used. This station included the following temperature, humidity and pressure sensors and was programmed with VHDL. Then, the data that emerges from the station is processed and analyzed and visualized with CERN-ROOT from tests carried out in Nilgiri, Tamil Nadu, India [11].

When comparing the Xilinx Artix 7 and the Xilinx Spartan 3E, it is observed that the Xilinx Artix 7 demands more logical capabilities and memory, but its high price can be a challenge. On the other hand, the Spartan 3E costs relatively less and is accessible, it does not need a high additional technical demand compared to the other. Both are great for doing a project, but the most suitable solution depends on the particular case and budget.

The article introduces a system called Weather Station Monitoring, which uses IoT to provide weather data anywhere. This system, built with ESP32 microcontroller and MQTT broker, transmits data to the cloud and is displayed using NODE-RED in real time. It has temperature, humidity and wind speed sensors, with hydrological sensors monitoring water level and flow, allowing users to predict flooding [27].

This study uses NODE-RED for real-time visualization and recording of weather data, including

temperature, humidity, rainfall level, wind speed and direction. Although this system lacks hydrological data, the use of NODE-RED shows that there is still room for future expansions. NODE-RED and LabVIEW ensure accurate handling of the flow of weather data, providing an environment monitoring solution that is effective and easy to adapt.

The article describes a weather monitoring system that uses IoT and LabVIEW to collect and analyze data on temperature, humidity, vent velocity, pressure, and light intensity. The recording of this microcontroller data is stored in an Excel macro file and displayed on an LCD screen. In addition, the system uses a 4G module, the data is sent to the IoT cloud, allowing data to be accessed from remote locations via the mobile network [28].

In comparison, the system is simpler than the FPGA-based studio system, which offers greater accuracy, but is more complex to program. Although the system has some limitations in processing, it stands out for its powerful ability to transfer data to the cloud through 4G, which is still a significant advantage.

Tools such as LabVIEW and CERN-ROOT are effective for accurately processing and visualizing scientific data. LabVIEW facilitates real-time acquisition and monitoring; ROOT enables complex analysis of large volumes of data and integrates well with architectures such as FPGA. Thus, these tools improve the interpretation of environmental phenomena and optimize system performance [29].

Countries with complicated geographies such as Peru, Bolivia or Colombia have challenges similar to ours here in Ecuador with the coverage and accuracy of their weather stations. Recent studies show that using FPGA platforms for environmental monitoring in difficult to access areas is more efficient, as they take less time to respond and are more reliable [30].

Modernizing meteorological stations with advanced technology is key to the technological and scientific sovereignty of developing countries. For Ecuador, this means promoting technical and engineering education, training specialists and designing local solutions. This work, then, aims to help build a more resilient scientific infrastructure of our own [31].

2. Method

The development of the weather station is done by using FPGA technology to capture, process and analyze weather data in real time. FPGAs are chosen because of their ability to provide high accuracy and speed in data processing based on need. This is required for applications that need to constantly monitor various data points and be up-to-date with the latest information in an instant. Therefore, FPGA technology is necessary to enable efficient and fast processing, given its need in advanced meteorological applications.

The methodology of this project was mainly experimental. It means that a series of tests were performed to adjust the respective sensors and verify whether the FPGA could handle the real-time data effectively. Therefore, an adjustment of the system's parameters and an evaluation of its performance under various environmental conditions were performed. This ensured that the data collected was considered accurate and reliable in practical situations.

On the other hand, the implementation of the weather station with FPGA technology for monitoring environmental conditions such as temperature, humidity, wind direction and speed in real time, allowed a highly accurate and fast data processing, which was the right choice for advanced applications. LabVIEW was used to program the FPGA, which provides a welcoming graphical interface for designing and managing the data acquisition system, making it very easy to install and read the data.

It was decided to include a Raspberry Pi 4 in the system design to improve data transfer speed and connectivity. This device serves as a bridge to send information from the FPGA to other systems over a network, making it easy to access and analyze the data using programs such as Matlab-Simulink. In this way, an efficient solution for remote communication and information processing is achieved.

The project goes beyond simple climate monitoring. It also has an educational component designed for students, who can recreate the prototype and experiment with the weather station. This offers them a hands-on opportunity to learn about FPGA technology and meteorological principles. By combining LabVIEW and Raspberry Pi 4 in the design, an enriching educational experience is provided. Figure 1 shows the diagram of the weather station, which makes it easier to understand.

The following are the components for the project:

1. Humidity and temperature sensor AMD1001.
2. Directional anemometer.
3. Ultrasonic cup anemometers.
4. Tilting bucket rain gauge.
5. NI Elvis II+.
6. NI Digital Electronics FPGA Board.
7. Raspberry pi 4.
8. Screen.
9. Laptop.
10. Database.

Fig 1.

Weather station schematic with FPGA.

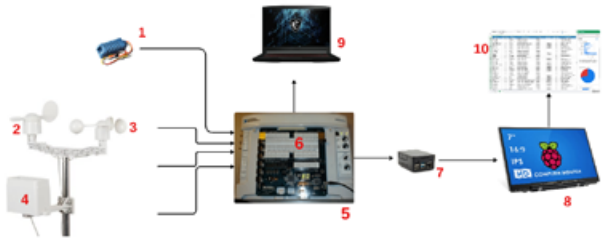

The development of the weather station using FPGA technology will be carried out in five phases to ensure the correct process. Information gathering and initial planning is a key section to understanding objectives clearly. Then, in the phase of study and selection of components, the parts such as sensors and other devices are selected. It ensures that everything is in order for the system to run smoothly.

The next phase, development and implementation of the project, where the FPGA is programmed and all the components are connected. Once everything is assembled, the calibration phase and adjustment of sensors and components is carried out where the respective adjustments and modifications are made, finally, in the data generation and analysis phase, the data obtained are collected and examined to evaluate the performance of the system and make final adjustments, figure 2 shows the phases for the implementation of the weather station.

Fig 2.

Phases for the implementation of the weather station

In the information gathering and initial planning phase, you do thorough research to understand the project requirements and set clear goals. Different types of weather sensors and FPGA technology are explored, as well as programming and connectivity needs. This research process allows the project scope, the necessary resources, and the timeline to be defined, creating a solid foundation for the next stages of development.

During the study and selection of components, the variety of available sensors, such as temperature, humidity and wind speed, is analyzed in detail to choose the ones that best suit the needs of the project. The technical specifications, FPGA compatibility, and cost of each component are reviewed. This phase is key to ensuring that the selected elements are suitable, efficient and reliable for the system.

The weather station employs high-precision sensors to ensure effective environmental monitoring. Temperature and humidity sensors AMD1001 noted for their accuracy and stability, providing reliable real-time data and quickly adapting to variations in the environment. This capability is crucial for obtaining accurate information about atmospheric conditions.

Directional and ultrasonic anemometers are used to measure the wind. The former records the wind direction accurately, while ultrasonic anemometers, with no moving parts, provide fast and accurate data, even in adverse conditions. This combination allows for a complete and accurate evaluation of wind behavior.

The tilting bucket rain gauge measures precipitation with high accuracy and durability, while maintaining a low maintenance requirement. Its robust design ensures accurate measurements of rainfall accumulation in real time, which is critical for water management and prediction of extreme weather events.

The integration of the sensors with the FPGA is done using standard communication protocols such as I2C and SPI, ensuring accurate and efficient data transmission. Sensors employing I2C connect to the FPGA's data pins (SDA) and clock (SCL), allowing for easy connection of multiple devices on a single bus, which is ideal for temperature and humidity sensors.

Sensors that use the SPI protocol connect to the clock pins (SCK), input data (MOSI), output data (MISO), and chip selection (CS). This protocol is especially suitable for sensors that require high transmission rate, such as certain anemometers and rain gauges, providing efficient performance in communicating fast and accurate data.

The FPGA receives signals from the sensors through these protocols, processing and converting the data when necessary, and preparing the information for real-time analysis. This initial processing ensures that the data is accurate and ready for immediate interpretation and use.

The NI Digital Electronics FPGA Board model was chosen for this project in combination with the NI ELVIS II+, due to its robust processing power and compatibility with the sensors used. This FPGA offers powerful processing power essential to efficiently handle real-time data acquisition and analysis.

When choosing the FPGA, we decided on the Spartan 3E because of its low cost, because it is readily available in academic labs, and because it is compatible with the NI ELVIS II+ platform. However, we also considered the Artix 7, which has significant technical advantages: many more DSP blocks (740 versus the Spartan 3E's 20), more LUTs (52,160 compared to 9,312), uses less power (thanks to its 28 nm technology versus the Spartan's 90 nm), and offers higher communications bandwidth. While the Artix 7 is better for processor-intensive tasks, Spartan 3E met our needs for the project, offering a good balance of performance, simplicity and cost for an educational environment ended reliably to environmental changes.

The NI Digital Electronics FPGA Board stands out for its wide availability of resources, such as Look-Up Tables (LUTs), registers, and digital signal processing (DSP) blocks. LUTs allow for the implementation of combinational logic and custom functions, while logs facilitate efficient data management. DSP blocks are key to performing complex calculations and advanced analysis, crucial for interpreting data accurately.

The compatibility of this FPGA with project sensors, which include devices for measuring temperature, humidity, wind, and rainfall, ensures seamless integration. This choice ensures that the FPGA can communicate and process data smoothly and effectively, meeting the speed and accuracy requirements needed for the project.

In the development and implementation phase of the project, the FPGA is programmed using tools such as LabVIEW as shown in Figure 3, to build the data acquisition system. The selected sensors are integrated and configured to work together. This stage includes both building the hardware and programming the software, ensuring that all components collaborate effectively to capture and process real-time weather data.

Fig 3.

Diagram of blocks made in LabVIEW.

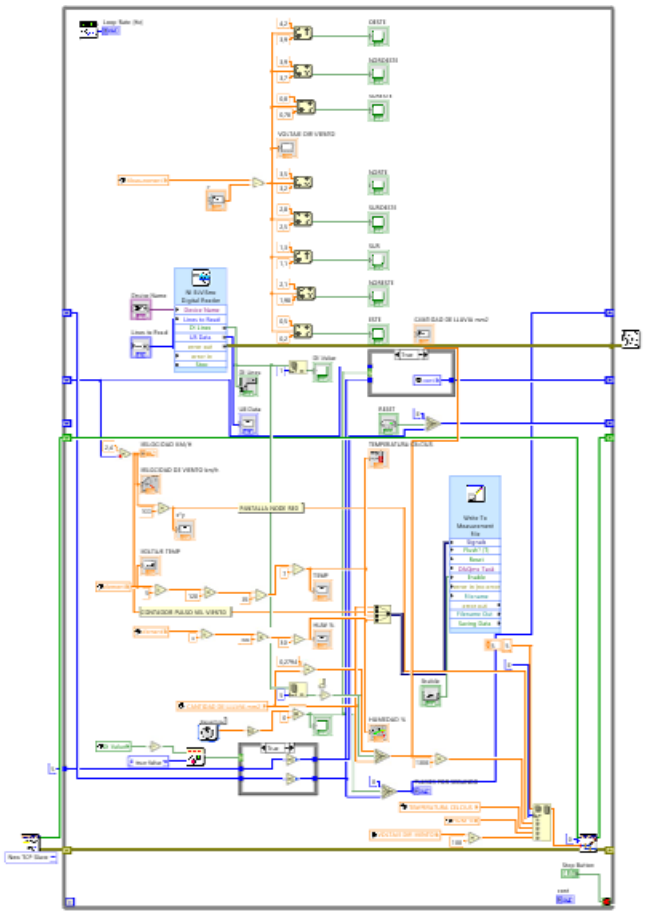

The FPGA architecture is designed with specialized modules that efficiently manage the flow of data from acquisition to transmission. The data acquisition module receives signals from the sensors and converts them to digital format. This module, programmed with LabVIEW, ensures accurate and fast capture of information, which is critical for proper processing.

The signal processing module, also developed with LabVIEW, uses DSP blocks to perform complex calculations and filter digital signals. This module transforms raw data into actionable information, enabling accurate, real-time interpretation. Programming in LabVIEW makes it easy to implement advanced algorithms and fine-tune analysis processes.

The processed data is temporarily stored in a storage module, which preserves the intermediate information for later analysis. For external communication, a Raspberry Pi 4 is used, which receives the data from the FPGA and sends it to analysis platforms. The integration of LabVIEW into FPGA programming ensures a smooth and efficient setup, allowing for effective and continuous data transfer.

The collected data is managed by a combined system of local storage on the FPGA and transmission to a server for further analysis. The FPGA temporarily stores the data, and a Raspberry Pi 4 acts as an intermediary to send the information to an external database. In addition, the data is exported to Excel files, providing an additional option for review and analysis.

Data visualization and access is facilitated by a graphical interface implemented with LabVIEW. This tool allows you to create an intuitive user interface that provides real-time visualizations as shown in Figure 4. Users can consult and manage weather information clearly and efficiently, optimizing data interpretation and decision-making.

Fig 4.

Weather station LabVIEW interface.

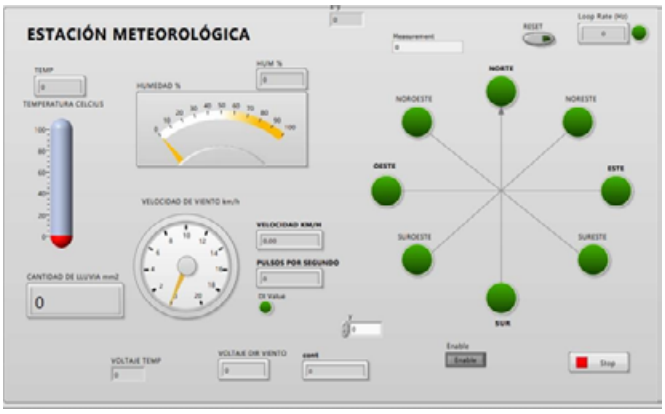

Calibrating and adjusting sensors and components involves making precise adjustments to improve measurement accuracy. Various tests are carried out to verify that the system works correctly under different conditions. This calibration process is essential to ensure that the data collected is accurate and that the system is optimi-

zed for the environment in which it was used, Figure 5 shows the weather station with each sensor.

To calibrate the sensors, we used certified reference equipment and data from official INAMHI weather stations, which allowed us to validate the accuracy of the measurements. We conducted tests for a week in different environments and at different times, comparing real-time readings with standard values. With the AMD1001 sensor, for example, we created a calibration curve using linear regression in LabVIEW. This allowed us to adjust its digital output according to the actual humidity and temperature, achieving a margin of error of less than ±2%. This ensured that the system responded reliably to environmental changes.

Fig 5.

Connection of each sensor to the weather station.

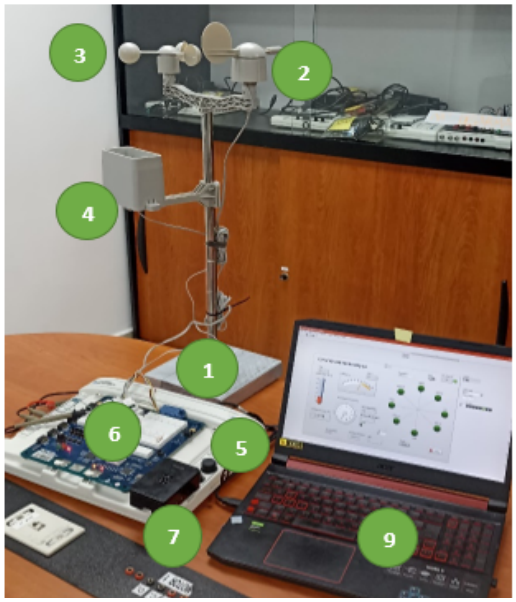

Finally, in the data generation and analysis phase, the operational data of the system is collected and analyzed to evaluate the performance of the weather station. The measurements are reviewed to ensure that the system is working as expected, making final adjustments, if necessary, in figure 6 the project is shown from the scheme proposed in figure 1.

Fig 6.

Weather station.

The methodology for developing the weather station with FPGA technology is divided into five essential stages: data collection and initial planning, selection and study of components, development and implementation of the system, calibration and adjustment of the sensors, and finally, generation and analysis of the data. This approach ensures that the project progresses in an organized and effective manner, achieving the stated objectives in an orderly and detailed manner.

3. Results and discussion

3.1. RESULTS

The results are presented in a table of data collected by the FPGA-based weather station. This table shows the measurements obtained for various environmental parameters, such as temperature, humidity, wind direction and speed, at different time intervals. The data have been recorded in real time, reflecting the environmental conditions throughout the observation period. This information is crucial for evaluating system performance and for performing detailed analyses on observed weather variations.

At the weather station using an FPGA, the data obtained is sent to a Raspberry Pi for management. After being processed by the FPGA, the Raspberry Pi stores this data in an Excel file, which facilitates its analysis and manipulation, using a common tool for the treatment of meteorological information.

In addition, the Raspberry Pi allows you to store and send the data to a server or database for more detailed analysis. Using Excel as a storage format simplifies the organization of information and the creation of charts, making it easier to identify trends and weather patterns effectively.

To assess the accuracy of the system, the data obtained was compared with those reported by Google Weather for the same region. The comparison showed a high correlation, with a Pearson correlation coefficient of 0.98 for temperature and 0.95 for humidity. The mean square error (RMSE) was 0.2°C for temperature and 1.5% for humidity, confirming the accuracy of the system relative to the data provided by Google Weather.

Table 1 provides data obtained by the weather station, where it details the temperature, humidity, wind direction, and amount of rain in the telecommunications club, each entry in the table corresponds to a set of each sensor facilitating the review and analysis of the environmental information collected. This data will serve as a basis for adjusting and optimizing the system, as well as for conducting studies on recorded weather trends and patterns.

The rain and wind measurements showed little variation because we tested in an enclosed location where the weather remained stable at all times. Since it did not rain while we were taking the data, the rain sensor always read the same. Similarly, the wind barely changed direction or speed, which is normal for a site with little air movement like the one we used for testing. This does not mean that the system failed, but that it accurately measured the actual ambient conditions during the experiment.

The tests sought to validate the system under stable conditions, to ensure the correct capture, transmission and storage of data in real time. This allowed testing the accuracy and consistency of each sensor before confronting them with more demanding conditions. Comparison with Google Weather showed high correlation, reinforcing the validity of the measurements despite the low variability. Future tests will be conducted in more dynamic environments to evaluate the system in the face of abrupt weather changes.

Real-time analysis made it possible to identify trends and predict short-term weather conditions with remarkable accuracy. The algorithms used reached an accuracy of 85% under normal conditions, which reflects a high effectiveness in anticipating typical climatic changes. Under extreme conditions, the accuracy was 75%, indicating a slight decrease in predictive capacity under severe events. These results show that, despite the variations, the system is effective in weather prediction in different scenarios.

Fig 7.

Graph of each sensor of the weather station.

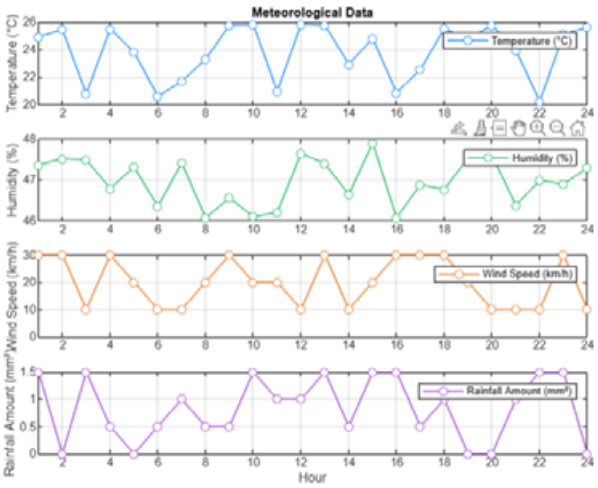

Figure 7 shows the measurements of each of the sensors in 4 graphs, in the graph for the temperature it shows that it remained constant, with slight variations around 23.7°C. Likewise, humidity remained at an average of 46.4%. These data indicate that the climate was fairly stable during the time it was measured. In the case of wind

Table 1.

Data obtained from the weather station.

WEATHER STATION				
Temperature	**Humidity**	**Dir. Wind**	**Cant. Of rain**	
1	**23,710937**	**46,386719**	**4,8**	**1,397**
2	23,59375	46,386719	4,8	1,397
3	23,59375	46,386719	4,8	1,397
4	23,59375	46,386719	4,8	1,397
5	23,710937	46,386719	4,8	1,397
6	23,710937	46,386719	4,8	1,397
7	23,710937	46,386719	4,8	1,397
8	23,710937	46,386719	4,8	1,397
9	23,710937	46,386719	2,4	1,397
10	23,710937	46,386719	2,4	1,397
11	23,710937	46,386719	2,4	1,397
12	23,59375	46,386719	2,4	1,397
13	23,710937	46,386719	2,4	1,397
14	23,710937	46,386719	2,4	1,397
15	23,710937	46,386719	2,4	1,397
16	23,710937	46,386719	4,8	1,397
17	23,710937	46,386719	4,8	1,397
18	23,710937	46,386719	4,8	1,397
19	23,710937	46,386719	4,8	1,397
20	23,710937	46,386719	4,8	1,397

speed, two variations are observed; Most measurements show a speed of 4.8 km/h, but there is a period when it decreases to 2.4 km/h. This variation suggests that the wind was variable.

As for rainfall, a graph shows that it remained at a constant level of 1,397 in all measurements. This indicates that the rain, although present, was uniform and constant, without major changes in its intensity. Figure 8 shows all the measurements taken.

Fig 8.

Measurements from the weather station.

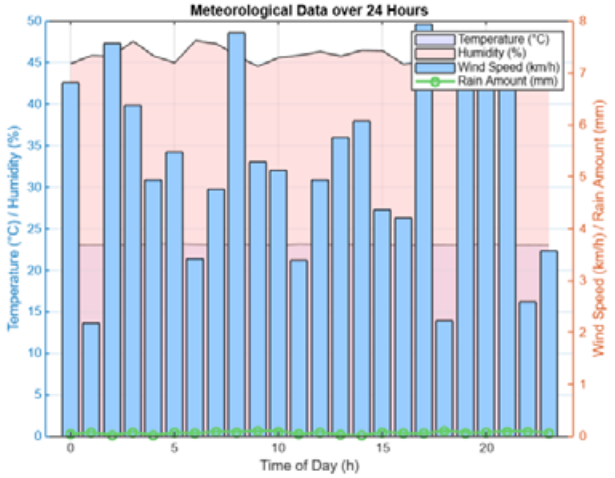

Figure 1 shows all the measurements combined, which shows how different meteorological variables can behave independently or show little relationship with each other during the same period of time. This suggests that the weather was fairly stable in the data collected and variations in one parameter, such as wind direction, did not necessarily translate into changes in other parameters, such as temperature or humidity.

For the evaluation and prediction of the system, data were collected for five continuous days (20 records/day, 100 in total). Seventy percent was used to train the prediction algorithm and 30% for testing and verification, which facilitated a reliable assessment of its accuracy under controlled conditions.

Measurement intervals of 15 minutes were defined for the timely capture of diurnal environmental changes. This frequency was selected to balance detailed monitoring with storage and processing efficiency, especially in stable weather.

The low variability of the data reflects the controlled testing environment. This initial phase focused on ensuring consistent sensor performance and system stability before transitioning to dynamic outdoor conditions, which will be explored in future phases for further validation.

3.2. DISCUSSION

The article describes a weather station built with a Xilinx Artix7, whose code is written in Verilog and used with Xilinx ISE software. This system performs read, write and control operations through the FT2232H module and a computer, thus facilitating the development and compilation of designs. The integration of sensors such as TMP36, HS1101 LF, and BMP180 demonstrates the versatility of the design, although working with Xilinx ISE requires advanced knowledge in digital design and VHDL programming [4].

On the other hand, the work carried out uses LabVIEW software for its design and programming since it offers a better platform to work ideal for data processing in addition to an intuitive graphical interface which facilitates the development of applications since it is faster and more accessible, especially for systems that integrate several types of sensors and require humidity, temperature, atmospheric pressure and UV light in addition to the extensive library and tools it offers and facilitated the integration of these sensors.

Although Xilinx ISE stands out for its accuracy and speed in data acquisition, it has been discontinued since 2013. However, its effectiveness in weather applications is still remarkable, according to the paper. Despite this, the transition to LabVIEW is recommended for its intuitive interface and ability to communicate with various protocols such as USB, serial, and Ethernet, which improves efficiency compared to Xilinx ISE [4].

The article addresses the technological challenges in meteorology for developing countries such as Ecuador, where many weather stations are inoperative due to the obsolescence of their equipment. Solutions such as static stations or wireless sensor networks (WSNs) are mentioned. However, a combination of FPGA technology for data processing and Arduino UNO for sensor connection is proposed, offering a reasonable cost and better performance in data monitoring [11].

Compared to the project carried out which focuses on the educational environment of the Salesian Polytechnic University, where a weather station will be developed using FPGA for data processing and Raspberry Pi for its visualization. In addition, manuals will be created detailing design and programming in LabVIEW. The goal is to not only build a weather station, but also to provide valuable educational resources for students interested in FPGAs, LabVIEW, and sensor integration.

The article presents an IoT-based weather station that uses the NodeMCU (12E) Wi-Fi ESP8266 microcontroller with DHT11 sensors for temperature and humidity and MQ135 for air quality. An app called VIT Weather Station was developed compatible with Android and iOS for real-time visualization of weather data. This project demonstrates how IoT can connect devices to collect and

disseminate environmental data, further addressing air pollution issues and providing essential information for public health [29].

Unlike the IoT-based solution, which uses a ESP8266 microcontroller and sensors to transmit data in real-time via a mobile app, the project focuses on FPGA technology. This choice allows for greater processing power and accuracy in the collection and analysis of weather data. The FPGA offers superior flexibility and efficiency, ideal for applications that require detailed and optimized handling of environmental data.

In the article a weather station is presented that provides real-time data which uses Raspberry Pi since this platform the use of this technology is due to the great cost of doing it with other devices, this system is based on Iot technology for the measurement of several environmental parameters such as temperature, Humidity, pressure and precipitation This data is collected and stored in Google Cloud SQL so that every person with internet availability can see it [30].

In contrast to the project, FPGAs are used for the collection of meteorological data, an option 80% more expensive than Raspberry Pi but which offers greater benefits in processing and accuracy. Although FPGA requires a higher investment, its ability to handle and optimize data with high accuracy is worth the cost. Unlike the Raspberry Pi, which has limitations in data processing and support, FPGA provides greater flexibility and performance, making it a better choice for applications that need high reliability.

The article presents a weather monitoring system based on a network of wireless sensors. It uses a Wi-Fi-capable ESP8266 microcontroller and transmits the data to a Raspberry Pi 3, which acts as a web server with a LAMP system (Linux, Apache, MySQL and PHP) for storing and viewing the information. The data can be extracted in Excel format for analysis [31].

In contrast, the project uses Node-Red for data visualization and storage, providing a graphical interface to design data flows without the need for extensive programming. In addition, Excel files created in LabVIEW are used to back up the data, offering a simple and effective solution for information management without relying on complex platforms.

Data obtained from the weather station indicate a constant temperature of 23.7°C and a humidity of 46.4%. Wind direction measurements vary between 2.4 km/h and 4.8 k/h, while the amount of rain remains fixed at 1,397. This uniformity in the data suggests that the system provides stable and reliable readings for environmental monitoring during the period evaluated.

The results meet expectations for consistency and accuracy. However, the lack of variability in wind direction and in the amount of rainfall could indicate limitations in sensor sensitivity or system configuration. It is advisable to investigate these aspects to improve the responsiveness and accuracy of the system.

When comparing the project of the system with the one described in the article, which uses a Xilinx Artix7 with advanced sensors and programming in Verilog, it was found that both systems present stability in data collection. However, the system in the aforementioned article offers greater flexibility and integration capacity, highlighting how advanced technologies can optimize accuracy and functionality in weather stations [4].

4. Conclusions

The information collected showed a stability of temperature, humidity and the amount of rainfall during the observation period. The temperature was approximately 23.71 °C and the humidity was around 46.39%. The wind direction varied between 2.4 km/h and 4.8 km/h, with a predominance of 4.8 km/h, which means moderate winds. The amount of rain has always been the same, 1,397 throughout the period.

These observations suggest that the measurement environment has been stable and that the FPGA-based data collection system. Slight variations in wind direction could reflect minor weather changes or sensor fluctuations. Taken together, the data collected demonstrates the system's effectiveness in real-time monitoring, providing a solid foundation for future analysis and applications.

The system has the capacity to generate a new measurement every 5 seconds, an attribute derived from its FPGA-based architecture and its integration with LabVIEW, which enables high-resolution environmental monitoring. However, for the initial validation and training of the prediction model, 20 records were acquired daily for five days. This approach was adopted in order to ensure the stability of the environment and efficiency in the subsequent data analysis.

Comparing the temperature and humidity data taken with the FPGA and the Arduino, it is observed that the FPGA offers greater accuracy compared to the Arduino, which can be attributed to its superior processing capacity and the quality of the sensors used. In addition, one notable change is the sampling rate: while the Arduino recommends that readings should not be taken more frequently than once every two seconds, the FPGA is capable of taking data every 0.5 seconds. This allows for faster changes in environmental conditions, providing more detailed and real-time monitoring.

For future work, an improvement in the resources used is recommended where sensors for air quality and solar radiation could be added to obtain more data. The GUI (Graphical User Interface) could be optimized to create a more intuitive and user-friendly visualization. In

addition, more advanced data transmission functions and technologies could be automated for autonomous maintenance applications. These improvements will increase the efficiency and versatility of the system.

In short, this project highlights the excellence of the technology used in weather stations with high precision of capture and processing of data in real time. Education, especially thanks to the use of Raspberry Pi and Node-RED, considers it a valuable experience with a wide range of applications. In addition, the recommendations to improve this system through the acquisition of new advanced sensors are practical. The project takes environmental work to an advanced level and promises to be a springboard for future innovations in the sector.

The FPGA is suitable for real-time weather and data processing applications due to its high accuracy and efficiency. This paper outlines how environmental data collection and analysis can benefit from this technology. As the need for real-time data grows, this component is the key to future advanced weather systems. The works provided here enable exponential growth in this field.

Seeking to have artificial intelligence present in an FPGA-based weather station has many benefits. This includes real-time data processing, AI algorithm optimization, and reducing energy consumption. In addition, with the help of AI, abnormalities can be easily detected, weather predictions can be improved, and automated maintenance tasks can be enabled. Such integration improves the weather system, making it more accurate and adaptable; This makes it reliable and useful for all users.

To extend the coverage and accuracy of weather data, a network connecting weather stations with FPGAs should be created. This integration would allow for more detailed data collection to analyze climate patterns at the regional and global levels in depth. With more complete and reliable data, research and decision-making on climate would be improved, facilitating a better understanding and management of climate variability.

This would mean that future research should include cutting-edge sensors in air quality measurement and explore networks of distributed sensors. Climate prediction can be improved by developing machine learning algorithms. On the other hand, it should be studied how using emerging communication technologies such as 5G and its contribution to disaster management could be efficient when it comes to addressing extreme events.

References

[1] R. Llugsi, "Climatic Challenges of Quito," in *2023 IEEE 13th International Conference on Pattern Recognition Systems, ICPRS 2023*, Institute of Electrical and Electronics Engineers Inc., 2023. https://doi.org/10.1109/ICPRS58416.2023.10179029

[2] Z. Zhang, Q. Yu, L. Njilla, and C. Kamhoua, "FPGA-oriented moving target defense against security threats from malicious FPGA tools," *Proceedings of the 2018 IEEE International Symposium on Hardware Oriented Security and Trust, HOST 2018*, 2018, pp. 163–166, https://doi.org/10.1109/HST.2018.8383907

[3] Y. Luo, M. A. Awal, W. Yu, and I. Husain, "FPGA implementation for rapid prototyping of high performance voltage source inverters," *CPSS Transactions on Power Electronics and Applications*, vol. 6, no. 4, 2021, pp. 320–331, https://doi.org/10.24295/CPSSTPEA.2021.00030

[4] K. Ramesh, "High-Precision and Low-Latency FPGA-Based Weather Station," in *2022 International Conference on Computer, Power and Communications (ICCPC)*, IEEE, Feb. 2022, pp. 77–82. https://doi.org/10.1109/ICCPC55978.2022.10072196

[5] A. B. Mourão and J. F. D. M. Netto, "Inclusive model application using accessible learning objects to support the teaching of mathematics," *Informatics in Education*, vol. 18, no. 1, pp. 213–226, 2019, https://doi.org/10.15388/infedu.2019.10

[6] S. Stoyanov, Z. Kuzmanov, and T. Stoyanova, "Weather Monitoring System Using IoT-based DIY Automatic Weather Station," in *2024 9th International Conference on Energy Efficiency and Agricultural Engineering, EE and AE 2024 - Proceedings*, Institute of Electrical and Electronics Engineers Inc., 2024. https://doi.org/10.1109/EEAE60309.2024.10600523

[7] H. Santillán, A. Mantilla, D. Cárdenas, and P. Wong, "Design of a low-cost portable electrocardiograph for telemedicine application," *Memoria Investigaciones en Ingeniería*, no. 26, pp. 244–264, Jul. 2024, https://doi.org/10.36561/ing.26.15

[8] T. Barathkumar, S. Divya Dharshin, J. Richard, and T. Sathiyabalan, "Battery Monitoring System using Labview Interface for Arduino," in *Proceedings of 2024 International Conference on Science, Technology, Engineering and Management, ICSTEM 2024*, Institute of Electrical and Electronics Engineers Inc., 2024. https://doi.org/10.1109/ICSTEM61137.2024.10561237

[9] Y. Adalberto and S. Casadiego, "Importance of meteorological stations for decision making in agriculture.", https://doi.org/10.13140/RG.2.2.33323.46886

[10] J. Mabrouki, M. Azrour, D. Dhiba, Y. Farhaoui, and S. El Hajjaji, "IoT-based data logger for weather monitoring using arduino-based wireless sensor networks with remote graphical application and alerts," *Big Data Mining and Analytics*, vol. 4, no. 1, pp. 25–32, Feb. 2021, https://doi.org/10.26599/BDMA.2020.9020018

[11] V. Asanza, R. E. Pico, D. Torres, S. Santillan, and J. Cadena, "FPGA based meteorological monitoring station," in *2021 IEEE Sensors Applications Symposium, SAS 2021 - Proceedings*, Institute of Electrical and Electronics Engineers Inc., Aug. 2021. https://doi.org/10.1109/

SAS51076.2021.9530151

[12] L. Camargo A, B. Medina D, y J. Gómez R, "PROTOTIPO ELECTRÓNICO IoT PARA EL SEGUIMIENTO DE VARIABLES AMBIENTALES," *REVISTA AMBIENTAL AGUA, AIRE Y SUELO*, vol. 13, no. 2, pp. 1–9, Nov. 2022, https://doi.org/10.24054/raaas.v13i2.2723

[13] M. J. Alam, S. A. Rafi, A. A. Badhan, M. N. Islam, S. I. Shuvo, and A. M. Saleque, "Design and implementation of a low-cost IoT based tipping bucket rain gauge," in *2021 International Conference on Emerging Smart Computing and Informatics, ESCI 2021*, Institute of Electrical and Electronics Engineers Inc., Mar. 2021, pp. 279–283. https://doi.org/10.1109/ESCI50559.2021.9396954

[14] J. S. Gutarra, J. A. Gastelo-Roque, y J. Sulluchuco, "A cup anemometer using 3D additive manufacturing," in *2020 IEEE XXVII International Conference on Electronics, Electrical Engineering and Computing (INTERCON)*, IEEE, Sep. 2020, pp. 1–4. https://doi.org/10.1109/INTERCON50315.2020.9220193

[15] A. Almasoud, M. Abbas, M. Aboelola, and A. Alghaihab, "FPGA Based DCO With Fine Control Correlation Calibration Technique," in *Proceedings of the International Conference on Electrical Engineering and Informatics*, Institute of Electrical and Electronics Engineers Inc., 2022, pp. 157–161. https://doi.org/10.1109/IConEEI55709.2022.9972266

[16] B. H. Raghunandan, A. Mahesh, and M. Babu M.p, "Wireless Communication System Design Using Labview and Software Defined Radio," in *7th IEEE International Conference on Computational Systems and Information Technology for Sustainable Solutions, CSITSS 2023 - Proceedings*, Institute of Electrical and Electronics Engineers Inc., 2023. https://doi.org/10.1109/CSITSS60515.2023.10334108

[17] Y. M. Inshakov y E. B. Solovyeva, "Simulation of Tunable Electrical Circuits Using NI ELVIS II Complex," in *Proceedings of the 2020 IEEE International Conference "Quality Management, Transport and Information Security, Information Technologies", IT and QM and IS 2020*, Institute of Electrical and Electronics Engineers Inc., Sep. 2020, pp. 477–480. https://doi.org/10.1109/ITQMIS51053.2020.9322801

[18] V. A. Sumayyabeevi, J. J. Poovely, N. Aswathy, y S. Chinnu, "A New Hardware Architecture for FPGA Implementation of Feed Forward Neural Networks," in *ACCESS 2021 - Proceedings of 2021 2nd International Conference on Advances in Computing, Communication, Embedded and Secure Systems*, Institute of Electrical and Electronics Engineers Inc., 2021, pp. 107–111. https://doi.org/10.1109/ACCESS51619.2021.9563342

[19] M. Bilal, Razia, A. Hussain, M. Khan, A. Munaim, y M. Alim, "PWM Waveform Generation and Control Using Rotary Encoder on Spartan-3E Starter Board," in *IMTIC 2023 - 7th International Multi-Topic ICT Conference 2023: AI Convergence towards Sustainable Communications*, Institute of Electrical and Electronics Engineers Inc., 2023. https://doi.org/10.1109/IMTIC58887.2023.10178475

[20] C. A. Nugroho y A. Amiruddin, "A Low-cost Disk Imaging Device Using Raspberry Pi 4 for Digital Forensics," in *Proceedings - 2023 IEEE International Conference on Cryptography, Informatics, and Cybersecurity: Cryptography and Cybersecurity: Roles, Prospects, and Challenges, ICoCICs 2023*, Institute of Electrical and Electronics Engineers Inc., 2023, pp. 314–319. https://doi.org/10.1109/ICoCICs58778.2023.10276963

[21] P. Bagdalkar y L. Ali, "Interfacing of light sensor with FPGA using I2C bus," in *2020 6th International Conference on Advanced Computing and Communication Systems (ICACCS)*, IEEE, Mar. 2020, pp. 843–846. https://doi.org/10.1109/ICACCS48705.2020.9074372

[22] V. Nicolau, M. Andrei, y B. Olteanu, "Data Switch in Long Line 1-Wire Networks for Monitoring System of Large Sensor Arrays," in *IEEE International Symposium for Design and Technology of Electronics Packages, SIITME - Conference Proceedings*, Institute of Electrical and Electronics Engineers Inc., 2023, pp. 265–268. https://doi.org/10.1109/SIITME59799.2023.10430495

[23] A. Garbev, "Possibilities for Visual Programming in Robotics via Node-RED," in *International Conference Automatics and Informatics, ICAI 2022 - Proceedings*, Institute of Electrical and Electronics Engineers Inc., 2022, pp. 367–371. https://doi.org/10.1109/ICAI55857.2022.9960113

[24] H. J. Santillán Carranza, P. Wong Wong, K. E. R. Alvarado, y M. J. Huayamave Cordero, "Implementación de un Sistema Meteorológico Educativo Usando IoT y Rasperry PI," *INGENIO*, vol. 7, no. 2, pp. 4–17, Jun. 2024, https://doi.org/10.29166/ingenio.v7i2.5265

[25] R. L. Canar, A. Fontaine, P. L. Morillo, y S. El Yacoubi, "Deep Learning to implement a Statistical Weather Forecast for the Andean City of Quito," in *2020 IEEE ANDESCON*, IEEE, Oct. 2020, pp. 1–6. https://doi.org/10.1109/ANDESCON50619.2020.9272106

[26] Z. Peng *et al.*, "Average-Approximation SIP Algorithms Used to Improve Accuracy of RC Model Order Reduction," in *2023 International Symposium of Electronics Design Automation, ISEDA 2023*, Institute of Electrical and Electronics Engineers Inc., 2023, pp. 71–75. https://doi.org/10.1109/ISEDA59274.2023.10218670

[27] N. U. Khuzairi, S. Saon, A. K. Mahamad, M. S. M. Zainordin, S. Yamaguchi, y M. A. Bin Ahmadon, "Weather Station Monitoring System with Node-RED," in *GCCE 2023 - 2023 IEEE 12th Global Conference on Consumer Electronics*, Institute of Electrical and Electronics Engineers Inc., 2023, pp. 678–681. https://doi.org/10.1109/GCCE59613.2023.10315514

[28] H. Ma, Y. Qiao, J. Li, y X. Mao, "Design of an AI Small-Scale Meteorological Monitoring System," in *IMCEC 2024 - IEEE 6th Advanced Information Management,*

Communicates, Electronic and Automation Control Conference, Institute of Electrical and Electronics Engineers Inc., 2024, pp. 297–301. https://doi.org/10.1109/IMCEC59810.2024.10575073

[29] N. Tandan *et al.*, "Design and Implementation of IoT Based Local Weather Station - An Experimental Setup," in *IBSSC 2022 - IEEE Bombay Section Signature Conference*, Institute of Electrical and Electronics Engineers Inc., 2022. https://doi.org/10.1109/IBSSC56953.2022.10037309

[30] V. Mathur, Y. Saini, V. Giri, V. Choudhary, U. Bharadwaj, and V. Kumar, "Weather Station Using Raspberry Pi," in *Proceedings of the IEEE International Conference Image Information Processing*, Institute of Electrical and Electronics Engineers Inc., 2021, pp. 279–283. https://doi.org/10.1109/ICIIP53038.2021.9702687

[31] S. B. Merrah y A. Adane, "Meteorological sensor network based on ESP8266," in *2023 International Conference on Advances in Electronics, Control and Communication Systems, ICAECCS 2023*, Institute of Electrical and Electronics Engineers Inc., 2023. https://doi.org/10.1109/ICAECCS56710.2023.10105060

FACULTAD DE INGENIERÍA Y CIENCIAS APLICADAS
UNIVERSIDAD CENTRAL DEL ECUADOR

INGENIO
2025, VOL 8(2), JULIO - DICIEMBRE, PP. 67-75

REVISTA INGENIO

Diseño y Comparación Económica de una Superestructura de un Puente con Vigas de Hormigón Postensado o con Vigas-Losas-Cajón

Design and Economic Comparison of a Bridge Superstructure with Post-Tensioned Concrete Beams or with Box-Slab-Beams

John Alex Almeida Hernández | Escuela Politécnica Nacional -Ecuador
Alexis Eduardo Armas Herrera | Escuela Politécnica Nacional -Ecuador
Luis Tinerfe Hernández Rodríguez | Escuela Politécnica Nacional -Ecuador
María Belén Correa Vallejo | Escuela Politécnica Nacional -Ecuador
Diego Armando Arévalo Chafuel | Escuela Politécnica Nacional -Ecuador

Recibido: 10/2/2025
Recibido tras revisión: 10/3/2025
Aceptado: 2/4/2023
Publicado: 10/7/2025

PALABRAS CLAVE
Comparación económica, diseño estructural, hormigón postensado, puentes, superestructura.

RESUMEN
En este artículo se diseña, compara técnicamente y evalúa económicamente la superestructura de un puente de 30 metros de luz sin apoyos intermedios, usando dos variantes diferentes, con el objetivo de obtener la opción más ventajosa para su uso en Ecuador. En un caso, se utiliza losa de hormigón armado sobre vigas de hormigón postensado y, en la otra, vigas y losa unidas integralmente formando una sección cajón. El diseño se hizo siguiendo las normas actuales, tanto internacionales como del Ecuador. Para el puente con losa sobre vigas postensadas se usa una herramienta de cálculo desarrollada internamente. Para el puente con viga-losa-cajón, se realiza un prediseño basado en normas y se modela con software especializado. El análisis económico considera los costos actuales de Ecuador para materiales y mano de obra. Se establece un cronograma de actividades con diagramas de Gantt y cronogramas, ajustados a escalas de tiempo iguales para ambos puentes y condiciones similares, garantizando indicadores de comparación coherentes. Se concluye que, en base al diseño y análisis económico que se ha realizado para ambas variantes, para una longitud de 30 m, típica para puentes tipo paso elevados sobre avenidas, el puente losa sobre vigas postensadas representa la mejor opción desde el punto de vista constructivo y económico, sirviendo esto de guía para que los proyectistas puedan decidir qué solución van a utilizar.

KEY WORDS
Economic comparison, structural design, post stress concrete, bridges, superstructure.

ABSTRACT
In this article, the superstructure of a 30-meter-span bridge without intermediate supports is designed, technically compared, and economically evaluated using two different variants, with the objective of determining the most advantageous option for use in Ecuador. In one case, a reinforced concrete slab over prestressed concrete girders is used, while in the other, the girders and slab are integrally connected to form a box section. The design was carried out following current international and Ecuadorian standards.
For the bridge with a slab over prestressed girders, an internally developed calculation tool is used. For the box-section girder-slab bridge, a preliminary design is performed based on standards and modeled using specialized software. The economic analysis considers current material and labor costs in Ecuador. A schedule of activities is established using Gantt charts and timelines, adjusted to equal time scales for both bridge types and similar conditions, ensuring consistent comparison indicators.
The study concludes that, based on the design and economic analysis conducted for both variants, for a 30-meter span—typical for overpass bridges—the slab-over-prestressed-girder bridge represents the best option from a construction and economic standpoint. This serves as a guideline for designers in selecting the most suitable solution.

1. Introducción

Los puentes son uno de los elementos más importantes en la proyección de carreteras, aún más en Ecuador por su topografía, hay que sortear gran número de grandes depresiones y ríos no solo para comunicar ciudades, sino que en algunos casos acortar el tiempo de viaje en vías existentes y de esta manera fortalecer la red vial para fomentar el desarrollo productivo del país [1]. En otros países, especialmente países desarrollados, se han realizado grandes avances en el diseño y construcción de puentes viga losa cajón mediante dovelas unidas por postensado y de esta manera, se ha conseguido construirlos con mayores luces y optimizar los materiales al tener secciones estructurales más eficientes [2]. Un puente de carretera

https://doi.org/10.29166/ingenio.v8i2.7839

pISSN 2588-0829
eISSN 2697-3243
fing.revista.ingenio@uce.edu.ec

debe estar diseñado para soportar de forma segura todas las cargas previstas durante su vida útil [3]. Los diseñadores y calculistas estructurales de Ecuador generalmente toman como referencia la norma americana AASHTO [4] realizando sus propias interpretaciones y asunciones, lo que dificulta aún más el correcto desarrollo e implementación de puentes de hormigón postensado y vigas losa cajón [5].

El presforzado es una técnica de pre cargar el concreto en forma tal que se eliminen o reduzcan los esfuerzos de tensión que son inducidos por las cargas de gravedad. En el pretensado los cables están esforzados contra anclajes externos y el concreto es fraguado en contacto directo con los tendones, permitiendo así desarrollar el afianzamiento. En el postensado, cuando el concreto ha ganado suficiente resistencia, los tendones son esforzados directamente contra el concreto y son mecánicamente asegurados en anclajes empotrados en la fragua en cada extremo [6]. Los puentes de vigas presforzadas requieren peraltes menores que las de hormigón armado, siendo entonces menos pesados, logrando mayores luces. Utilizan acero y concreto de alta resistencia [7].

El postensado es una derivación del pretensado, pero en este caso se fabrica la pieza de hormigón dejando los conductos longitudinales con el perfil que se haya decidido para los tendones de postensado, generalmente poseen la forma del diagrama de momentos. La colocación de estos conductos se realiza previo al vaciado del hormigón. Una vez endurecido el hormigón se enhebran dichos conductos pasando por su interior los torones, y mediante equipos adecuados, como gatos de tesado, se procede a realizar el postensado de los mismos hasta alcanzar la tensión deseada [8].

El postensado tiene las ventajas de uniones sencillas y eficientes entre losas, vigas, muros y columnas, que eliminan problemas de juntas entre dichos elementos. Permite el acortamiento significativo de plazos de ejecución de la obra de aplicarse eficientes cronogramas de construcción. El sistema de encofrado se puede retirar inmediatamente concluido el tensado. Por lo general hay siempre eficientes programas de ejecución debido a que los moldes se pueden reusar [9]. Además, se logran estructuras livianas y resistentes que permiten reducir las cargas y alcanzar mayores luces entre vanos. Cuando el trazado de los tendones deja de ser recto, lo que resulta muy frecuente con este sistema, aparece un componente vertical de cortante que se opone ventajosamente al esfuerzo de corte originado por las cargas externas, permitiéndose un incremento del espaciamiento de la armadura pasiva transversal, con el consecuente ahorro de acero. Muy útil para la construcción en dovelas o prefabricados que luego pueden ser unidos en la obra. Aplicable a estructuras hiperestáticas o continuas, en las que incluso pueden existir cambios de curvatura en la directriz de los cables o alambres [8].

El postensado tiene las desventajas que, a diferencia del hormigón armado común, se requiere de mano de obra y maquinaria especializada. El postensado es más caro que el de hormigón pretensado. Los anclajes no se recuperan y quedan perdidos en el hormigón. Precisa una vaina o ducto por dónde van los cables e inyección posterior de gran complejidad de ejecución en el caso de no utilizarse el acero engrasado, el cual ya viene envainado y engrasado de fábrica. El acero utilizado es un acero especial, más caro que el acero de refuerzo común [9]. Al tener trazados curvos de los cables las pérdidas por fricción se incrementan durante el tesado [8].

En la Escuela Politécnica Nacional, en Ecuador, se han realizado varios estudios sobre la temática de evaluación y reforzamiento de puentes existentes con más de 30 años de construidos, debido a que las normas y cargas actuales son muy diferentes a cuando se diseñaron, destacándose los de Benavides [10], Mediavilla [11], Galarza [12] y Solís [13]. En este trabajo se aborda una temática diferente, siendo el objetivo determinar la variante más ventajosa para la construcción de puentes tipo paso elevados sobre avenidas en el Ecuador, al ser más conveniente no usar pilas intermedias, empleando vigas postensadas o viga losa cajón y realizándose un estudio comparativo entre el diseño de la superestructura de un puente de 30 m de longitud apoyado en ambos estribos y sin apoyos intermedios. Debido a que en Ecuador no existe una norma propia que trate lo abordado en este trabajo, se toma como referencia la norma AASHTO [4]. Primero se utilizará losa de hormigón armado y vigas de hormigón postensado y luego con vigas y losa unidas integralmente formando una sección cajón en volados sucesivos, llamados dovelas, unidos por postensado y refiriéndose como viga-losa-cajón. Al final, se efectúa un análisis económico entre las dos propuestas tomando como referencia los precios de los materiales, mano de obra y maquinaria en el Ecuador y así poder determinar la variante más ventajosa. En la metodología utilizada, además de la AASHTO [4], se tomaron en cuenta aspectos y criterios destacados por Rodríguez [14], Ministerio de Transporte y Comunicaciones de Perú [15] y la Norma Ecuatoriana de la Construcción NEC-SE-CG [16]. En términos de análisis sísmico se consideran criterios presentados en la Norma Ecuatoriana de la Construcción NEC-SE-DS [17], ASCE/SEI 41-23 [18], Gombosuren [19] y Wei et al. [20].

2. Método

2.1 MATERIALES

La AASHTO [4] expone que la resistencia a la compresión del hormigón a los 28 días () para postensado no

debe ser menor que 28 MPa y solo se podrán utilizar hormigones con resistencias de diseño mayores que 70 MPa si algún artículo específico así lo permite y se realizan ensayos físicos para establecer las relaciones entre la resistencia del hormigón y las demás propiedades y, además, si las condiciones locales lo permiten. Para determinar el módulo de elasticidad del hormigón) de peso normal, se usa una expresión matemática basada en investigaciones, la cual se presenta en la ecuación (1).

$$Ec = 9115 \cdot f'c^{0.33}[MPa] \quad (1)$$

Las barras para el acero de refuerzo deben ser corrugadas, excepto para estribos cerrados y mallas metálicas en los cuales se podrá emplear barras lisas. La fluencia nominal para acero de refuerzo (fy), no debe ser inferior de 420 MPa ni superior a 520 MPa. El módulo de elasticidad del acero de refuerzo no presforzado, (Es), puede asumirse como 200 000 MPa. El módulo de elasticidad para acero presforzado (Ep) puede ser considerado como de 197 000 MPa para torones y 207 000 MPa para barras, en algunos casos puede ser necesario valores más exactos obtenidos de ensayos de laboratorio o informes entregados por el fabricante [4].

En la Tabla 1 se presentan las características de mono torones de presfuerzo grado 270 – baja relajación que se usan en Ecuador.

Tabla 1.

Características torones de presfuerzo grado 270 – baja relajación en Ecuador

Diámetro (mm)	Número de Alambres	Tracción mínima a la rotura (kN)	Área mínima (mm^2)	Masa Aproximada (kN/km)
12.7	1x7	183.7	98.7	7.77
15.24	1x7	260.7	140	11.04

2.2 LÍMITES DE PRESFUERZO PARA EL ACERO DE PRETENSADO

La norma AASHTO [4] establece que el límite de esfuerzo a la tracción de los tendones debido al presforzado en los estados límites de resistencia, servicio y evento extremo no debe exceder los valores recomendados por el fabricante de los tendones o anclajes, y los valores especificados en la Tabla 2.

Tabla 2.

Límites de esfuerzo para tendones de pretensado y postensado [4]

Condición	Tipo de tendón		
	Barras lisas de alta resistencia.	Cables de baja relajación.	Barras de alta resistencia conformadas.
	Pretensado		
Inmediatamente antes de la transferencia	0.70 f_{pu}	0.75 f_{pu}	-
En estado límite de servicio después de las pérdidas	0.80 f_{py}	0.80 f_{py}	
	Postensado		
Antes del acuñamiento, se puede permitir a corto plazo	0.90 f_{py}	0.90 f_{py}	0.90 f_{py}
En anclajes y acoplamientos inmediatamente después del acuñamiento de los anclajes	0.70 f_{pu}	0.70 f_{pu}	0.70 f_{pu}
En otros sitios a lo largo de la longitud del miembro, alejado de los anclajes y acopladores inmediatamente después del acuñamiento	0.70 f_{pu}	0.74 f_{pu}	0.70 f_{pu}
En estado límite de servicio después de las pérdidas	0.80 f_{py}	0.80 f_{py}	0.80 f_{py}

Además, para el postensado, se permite utilizar durante cortos periodos de tiempo antes del acuñamiento para compensar las pérdidas por fricción y acuñamiento, solo si no se sobrepasan los valores expuestos en la Tabla 2, donde y se corresponden con el esfuerzo a tensión de fluencia y último respectivamente del acero de pretensado.

2.3 LÍMITES DE ESFUERZOS PARA EL HORMIGÓN

El límite de compresión antes de las pérdidas del hormigón presforzado, incluido los puentes construidos en voladizos sucesivos, será de , donde es la resistencia a

la compresión del hormigón en el momento del tensado de los cables o torones de presfuerzo. En ausencia de datos experimentales puede tomarse como . Los esfuerzos de compresión del hormigón inmediatamente después de las pérdidas se evaluarán utilizando la combinación de carga en estado límite de Servicio I, de acuerdo con la Tabla 3. El factor de reducción de carga, (), se podrá considerar igual a 1.0 cuando las relaciones de esbeltez de las almas y alas, determinadas conforme al Artículo 5.6.4.7.1 de la AASHTO [4], no sean mayores que 15. Cuando la relación de esbeltez es mayor a 15, el factor de reducción , deberá ser calculado de acuerdo con el Artículo 5.6.4.7.2.

Tabla 3 .

Límites para el esfuerzo de compresión del concreto presforzado después de las pérdidas [4]

Ubicación	Esfuerzo límite
Debido a la suma de tensión efectiva de presforzado y cargas permanentes	$0.45\sqrt{f'_c}\,(MPa)$

2.4 PÉRDIDAS TOTALES EN LA FUERZA DE POSTENSADO

Las pérdidas del presforzado se clasifican en pérdidas instantáneas y pérdidas diferidas, las cuales dependen del tiempo. El estudio de las pérdidas también se realiza con el fin de que se pueda determinar la fuerza del presforzado o tensión que actúa sobre la sección de hormigón en cualquier etapa de la vida útil del elemento. Además, cabe aclarar que las pérdidas se manifiestan en formas diferentes y con características propias que dependen del tipo de técnica de presforzado del hormigón. De este modo las pérdidas para el postensado pueden considerarse como se muestra en la ecuación (2), la cual es la presentada por la AASHTO [4]:

$$\Delta f_{pT} = \Delta f_{pF} + \Delta f_{pA} + \Delta f_{pES} + \Delta f_{pLT} \quad (2)$$

Donde:

Δf_{pT} Pérdidas totales (MPa)

Δf_{pF} Pérdidas iniciales por fricción (MPa)

Δf_{pA} Pérdidas iniciales por asentamiento o penetración de anclajes (MPa)

Δf_{pES} Suma de todas las pérdidas iniciales o ganancias debidas al acortamiento o extensión elástica en el momento de la aplicación del presforzado y/o cargas externas (MPa)

Δf_{pLT} Pérdidas debidas a la contracción a largo plazo y debido a la fluencia del hormigón, y relajación del acero (MPa)

Las pérdidas instantáneas suceden durante el proceso de tensado de la armadura activa e inmediatamente después de la transferencia de la fuerza de presforzado al elemento de hormigón, entonces para el postensado las pérdidas instantáneas más frecuentes son las siguientes:

a. Pérdidas del conjunto de anclaje debido al asentamiento o penetración los mismos (Δf_{pA}).
b. Pérdidas por fricción a lo largo de los ductos, o de las sillas de apoyo si se trata de postensado no adherente (Δf_{pF}).
c. Pérdidas por acortamiento elástico instantáneo del hormigón (Δf_{pES}).

Las pérdidas que dependen del tiempo (Δf_{pLT}) se producen debido a la fluencia lenta y contracción a largo plazo del hormigón, y a la relajación del acero de elementos postensados. En los Artículos 5.9.3.3 y 5.9.3.4 de la norma AASHTO [4], se establece un método aproximado y un método refinado respectivamente para el cálculo de las pérdidas dependientes del tiempo o al largo plazo. Estos métodos serán aplicables conforme a las condiciones de cada proyecto.

2.5 PUENTES VIGA-LOSA-CAJÓN

Las secciones de vigas y losa unidas integralmente formando una sección cajón son elementos de concreto postensado o pretensado, de peralte constante o variable dependiendo de la luz que se necesite cubrir y por su forma presentan un aspecto arquitectónico agradable a la vista. Estas secciones están conformadas por una losa superior, dos o más almas, y una losa inferior. Las secciones transversales de la superestructura de puentes viga-losa-cajón postensadas pueden ser de múltiples celdas o de celda única, como se muestra en la Figura 1.

Figura 1 .

Viga-losa-cajón de múltiples celdas (Arriba) y viga-losa-cajón de una celda (Abajo)

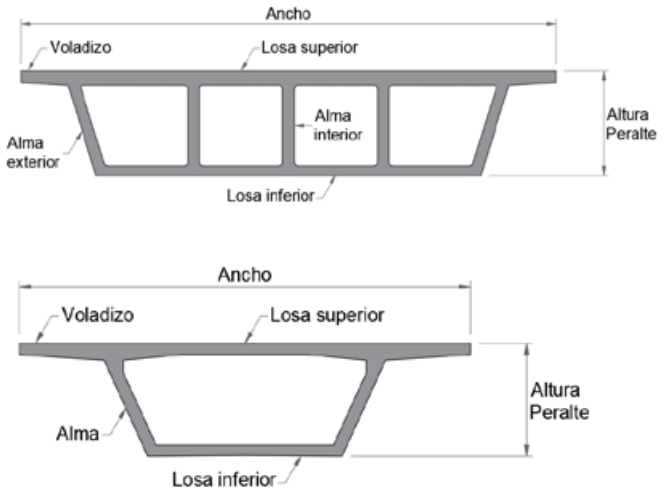

Los componentes básicos de la sección transversal son:

- Losa superior: toda la losa de hormigón incluidas las partes entre las almas internas y los voladizos fuera de las almas exteriores.

- Voladizos: salientes de la losa superior.
- Almas o vigas: pueden ser interiores o exteriores, verticales o inclinadas.
- Losa inferior: conecta las almas en la parte inferior y cierra la sección.

Este tipo de secciones, debido a su configuración estructural, son ideales para puentes de grandes luces y es así que a partir de los 30 m de longitud se empieza a compensar su dificultad constructiva frente a otras configuraciones de sección transversal de puentes. Son eficientes para resistir esfuerzos de flexión positivos y negativos puesto que las losas superiores e inferiores absorben la mayoría de estos esfuerzos, asimismo estas secciones poseen una mayor rigidez torsional debido a su condición de sección cerrada que en la mayoría de casos evita utilizar diafragmas intermedios [21]. Otra ventaja es que al tener una gran rigidez transversal permite reducir al mínimo el espesor de las paredes por lo que se logran secciones más delgadas y esbeltas [2].

Sin embargo, tiene como desventajas que para luces pequeñas las dificultades de ejecución y construcción, no se compensan con las ventajas estructurales y reducción de peso que ofrecen. Si la construcción se realiza in situ es necesario de mucha obra falsa, cimbras y encofrados trayendo complejidad en la construcción. De esta manera el rendimiento en la construcción de este tipo de puentes puede complicarse y en consecuencia se requiera emplear mucha mano de obra y maquinaria especializada. Además, si la construcción se realiza in situ mediante el método de volados sucesivos o construcción en voladizo es necesario contar con un encofrado móvil, a parte, si la sección es de peralte variable hay que tomar en cuenta esta variación haciendo más laboriosa su construcción en relación a puentes de otras tipologías como los puentes de losas sobre vigas. En el caso de construcción con elementos prefabricados se requiere de una superficie extra de trabajo para la construcción de los segmentos prefabricados, y si estas instalaciones no se encuentran cerca del sitio de construcción del puente se debe realizar mayores gastos de transporte. Adicionalmente, es preciso el uso de equipos tecnológicos avanzados como una estructura de soporte para la construcción y una grúa para instalar los elementos prefabricados [21].

3. Resultados y discusión

3.1 CONSIDERACIONES INICIALES

Partiendo que el objetivo del trabajo es determinar la variante más ventajosa empleando vigas postensadas o viga losa cajón para su uso en intercambiadores sobre avenidas del Ecuador, se diseñó un puente de 30 m de longitud considerando que se encuentra apoyado en los estribos y sin apoyos intermedios, permitiendo esto último que no existan pilas en el separador central. El ancho es de 9 m conformado por dos vías de 3.6 m cada una, un carril para cada sentido del tráfico vehicular, con barreras de 0.40 m de ancho a ambos lados del puente, bermas de 50 cm a cada lado, sin veredas y sin parterre intermedio. La sección longitudinal del puente se muestra en la Figura 2.

Figura 2

Sección longitudinal del puente

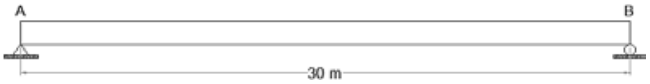

3.2 PUENTE LOSA SOBRE VIGAS POSTENSADAS

Para el diseño de cada miembro estructural de esta solución se ha tomado en cuenta lo explicado en la AASHTO [4] obteniéndose las siguientes dimensiones: una losa de 20 cm de espesor, vigas exteriores de 1.60 m de altura y 0.60 m de ancho y vigas interiores de 1.60 m de altura y 0.40 cm de ancho. Esto se muestra en la Figura 3. Para el cálculo resistente se ha utilizado una herramienta de cálculo con el fin de facilitarlos, la cual no es parte de este artículo. Los resultados del armado de la losa se presentan en la Figura 4.

Figura 3

Sección transversal del puente losa sobre vigas

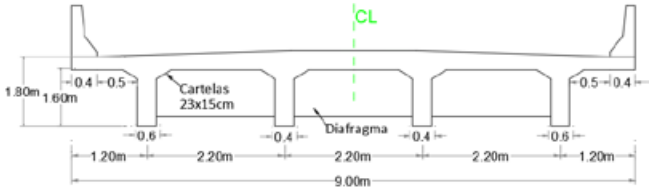

Figura 4

Armado de la losa

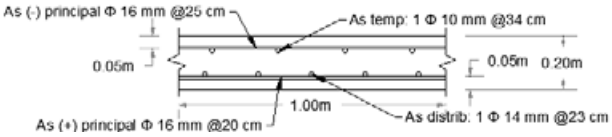

Para el trazado de vigas se tomó en cuenta el tipo de apoyo del puente, pues, el trazado de postensado debe seguir la forma del diagrama de momentos que soporta este. En este caso se tiene un puente simplemente apoyado en sus extremos con un diagrama de momentos de forma parabólica con un valor máximo en el centro de la longitud y cero en los extremos. Con esto en consideración, el tra-

zado de los cables de postensado es de forma parabólica empezando y terminando a la altura del eje neutro del puente y con valor máximo en el centro a una distancia de 15 m de los apoyos. El Trazado de cables de postensado se muestra en la Figura 5. Los resultados del armado de las vigas exteriores se presentan en la Figura 6 y de las interiores en la Figura 7. En el caso de la armadura de refuerzo, el armado mínimo resultó suficiente para cumplir con los requisitos de resistencia, además de favorecer el proceso constructivo al optimizar la disposición y colocación del refuerzo.

Figura 5

Trazado de cables de postensado. Dimensiones en metros

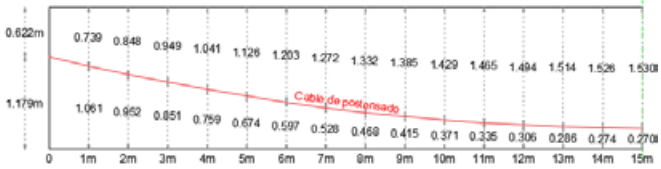

Figura 6

Armado de las vigas exteriores

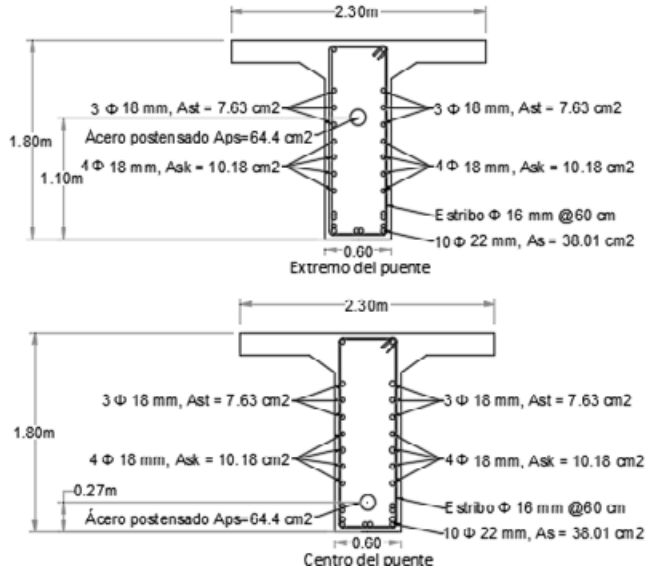

Figura 7

Armado de las vigas interiores

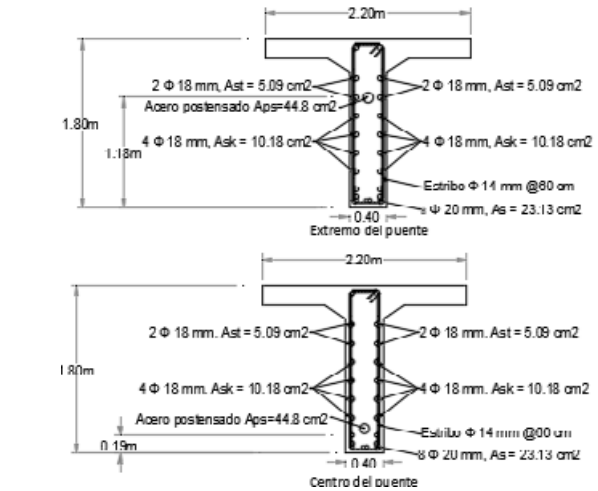

3.3 PUENTE VIGA-LOSA-CAJÓN

Las consideraciones iniciales, tanto de longitud como de carga, son las mismas que para el puente losa sobre vigas postensadas. Se ha realizado un prediseño de la sección del puente basándose en la norma AASHTO [4], quedando como resultado la sección que se muestra en la Figura 8. Para el diseño se ha utilizado el software CSI Bridge, versión de prueba [22], especializado en diseño de puentes, en el cual se ha introducido las dimensiones antes especificadas y las características de los materiales. El modelo puente viga-losa-cajón en software de diseño se presenta en la Figura 9.

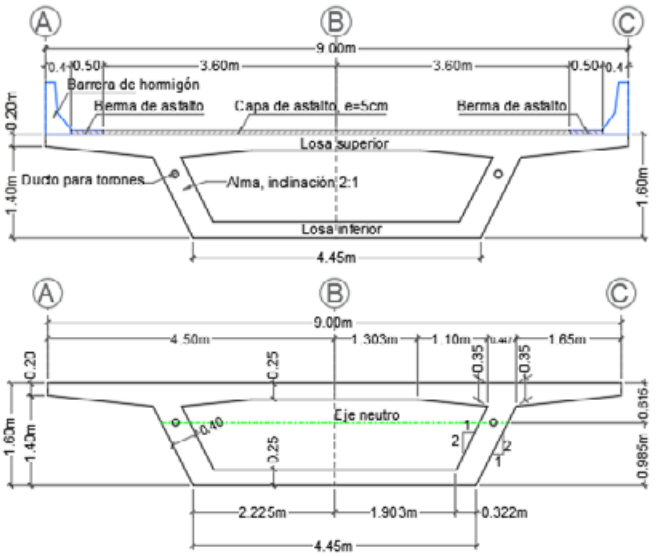

Figura 9

Modelo Puente viga-losa-cajón en software de diseño

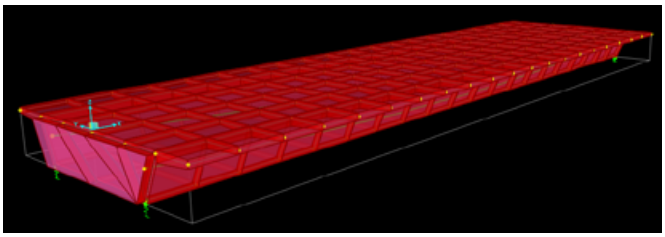

Una vez analizado se procede a calcular su armado realizándose un análisis transversal de la sección del puente para asegurarse de que este soporte las cargas requeridas. En la Figura 10 se muestra el armado. El trazado de los cables de postensado en esta solución toma la misma consideración respecto al tipo de apoyo del puente, sin embargo, en el caso de este el trazado también tiene una inclinación en sentido "x" además del sentido "y" como se muestra en la Figura 11, donde solo se representa la mitad de la viga, debido a que la otra mitad por simetría es igual.

Figura 10

Armado de sección transversal de puente viga-losa-cajón.

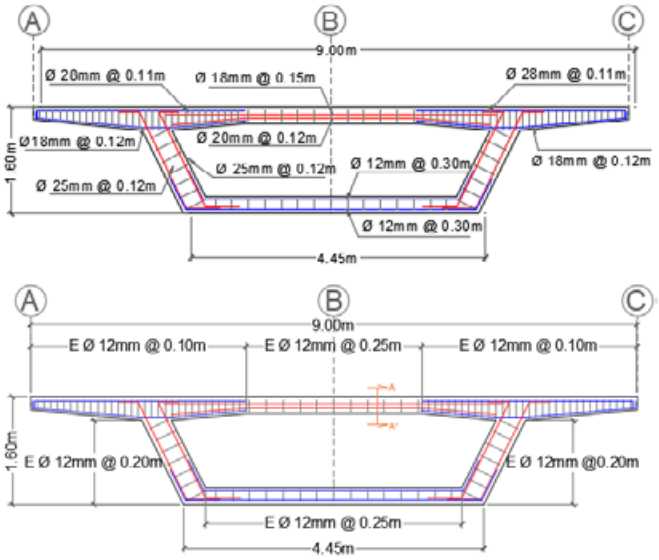

Figura 11

Vista superior y lateral del trazado de cables de postensado. Dimensiones en metros

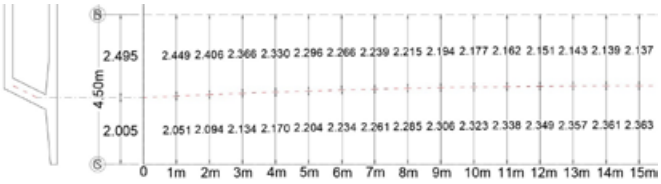

Vista superior.

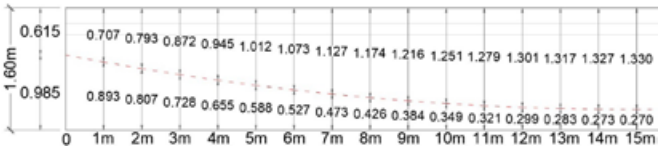

Vista lateral

En el modelo de la sección transversal se optó por utilizar puntos de inserción para realizar la conexión entre la losa superior y las almas, en lugar de hacer una conexión directa de eje a eje, ya que de este modo se pretende realizar una mejor aproximación a las condiciones reales de la unión entre estos elementos. Se hace hincapié en esta parte debido a que la losa superior tiene una sección transversal de peralte variable y las almas se conectan a la losa superior en la parte de mayor peralte de la losa, por lo que, realizar una conexión de eje a eje no es la opción más aconsejable debido a que se agrega más sección o material en las uniones, por ende, se aumenta el peso del modelo, y además no se consideran los efectos que produce la sección peraltada en los momentos. Por otro lado, para garantizar que las almas se conecten en la parte inferior de mayor peralte de la losa superior, en el modelo se utilizan puntos de inserción con el propósito de que se transmitan las mismas deformaciones entre los elementos en los puntos de interés y de esta manera tener conexiones que se asemejan a las condiciones constructivas reales.

3.4 COMPARACIÓN ECONÓMICA

El análisis del costo de ambas superestructuras obtiene un punto importante en el presente trabajo pues al comprobar que ambas opciones soportan de manera eficiente las cargas solicitadas, el tiempo de construcción y el costo final de la estructura juegan un papel determinante en la elección de la mejor variante de puente. En la tabla 4 se muestra la comparación económica entre las 2 soluciones usando los costos de Ecuador y considerando solo la parte estructural de la superestructura. Para el proceso de postensado multi torón es necesario importar los equipos y elementos necesarios como son: el gato hidráulico y los elementos de anclaje, debido a que, en Ecuador no existe disponibilidad de estos equipos, razón por la cual en el análisis de precios unitarios se ha considerado los costos de exportación desde una empresa ubicada en Colombia. La variante con vigas postensadas utilizó un volumen de hormigón de 164.30 m^3, un peso del acero de refuerzo de 146.97 kN y del acero de presfuerzo de 55.12 kN. En cambio, para el caso de la losa-viga-cajón fueron 137.11 m^3, 347.49 kN y 48.05 kN respectivamente.

Tabla 4

Presupuesto de general de ambas estructuras

Tipo de solución	Costo (USD)	Diferencia
Puente Losa sobre vigas postensadas	$117 089.36	$42 819.45
Puente Losa-viga-cajón	$159 908.81	

En lo referente a tiempo de construcción se ha determinado con ayuda de un diagrama de Gantt para cada tipo de puente. Los tiempos de ejecución finales se presentan en la Tabla 5.

Tabla 5

Tiempo de ejecución de general de ambas estructuras

Tipo de solución	Tiempo de Ejecución		
	Meses	Semanas	Días
Puente Losa sobre vigas postensadas	2.9	12	60
Puente Losa-viga-cajón	3.9	16.4	82

Observando el proceso de diseño y el análisis económico, se llega a cumplir el objetivo de esta investigación, obser-

vándose que la variante losa-viga-cajón, aunque tienen una apariencia arquitectónica mejor, es más costosa 1.36 veces mayor que usando vigas postensadas, sirviendo esto de guía para que los proyectistas puedan decidir qué solución van a utilizar

4. Conclusiones

En el diseño del puente losa sobre vigas postensadas se puede observar que las vigas internas tienen una base de 40 cm, mientras que las vigas exteriores poseen una base 60 cm, debido a que, si se mantiene una base de 40 cm para las vigas externas no se cumple con el chequeo de los módulos de sección mínimos y tampoco con el estado límite de Resistencia I, ya que los momentos que se producen en las vigas exteriores son mayores que en las vigas interiores. En consecuencia, se tuvo que aumentar la base de las vigas externas a 60 cm para no tener aumentar el peralte de la viga, opción poco factible, y tampoco aumentar el número de vigas principales que provocaría un rediseño total del puente. Esto conlleva a que el momento de diseño () de las vigas externas sea 1.46 veces mayor que el momento último actuante.

Para el análisis del puente losa sobre vigas postensadas se ha considerado unas pérdidas totales iniciales del 20 % en los cables y cuando se han realizado los cálculos respectivos para las pérdidas debido al postensado, éstas han variado al 19.95 % de pérdidas totales para las vigas internas y el 19.73 % para las vigas externas, por lo que, al ser menores que el porcentaje de pérdidas asumido inicialmente, no es necesario realizar un rediseño. En cambio, para la variante viga-losa-cajón el programa en el que se ha diseñado calcula automáticamente las pérdidas debido al postensado dando como resultado unas pérdidas totales del 18.75 %. Como se puede notar las pérdidas debido al postensado en puentes son relativamente altas en comparación con el 10 % de pérdidas para edificios que suele ser recomendado en varias bibliografías, por lo que es preciso realizar los cálculos correspondientes para determinar las pérdidas debido al postensado, ya que de otro modo si se toman porcentajes tan bajos de pérdidas el diseño de puentes en hormigón postensado sería incorrecto.

En lo referente a los tiempos de construcción, la solución viga-losa-cajón presenta cronograma que excede con 22 días laborables al cronograma de la variante losa sobre vigas postensadas. Esto se debe a la dificultad tanto en el encofrado como en la colocación de la armadura, por lo cual, la variante losa sobre vigas representa una mejor opción en este apartado, debido a que tiene un ahorro de tiempo del 29 % en comparación a la viga-losa-cajón.

Al momento de determinar los costos indirectos en el análisis de precios unitarios uno de los factores más importantes es la ubicación del proyecto, pues, de esto depende el aumento o disminución de los costos en logística, transporte de materiales y personal, arriendo de bodegas y terrenos durante la construcción, etc. Razón por la cual los costos indirectos pueden ir desde un 20 % en una buena ubicación hasta un 35 % en una ubicación desfavorable del proyecto.

El costo del puente viga-losa-cajón supera al costo del tipo losa sobre vigas en un 36.57 % y esta diferencia en costo se debe principalmente a que el viga-losa-cajón necesita más acero de refuerzo en sentido transversal. También el mayor costo de este último se debe a su geometría la cual implica que la construcción de este tipo de puentes sea más complicada y por esta razón, en el análisis de precios unitarios para rubros similares como es el caso del hormigón, encofrado, desencofrado y armado, el costo por rubro aumente.

En base al diseño y análisis económico que se ha realizado para el puente losa sobre vigas postensadas y el viga-losa-cajón en hormigón postensado, se ha evidenciado que, para una longitud de 30 m, típica para puentes tipo paso elevados sobre avenidas en el Ecuador, donde es más conveniente no usar pilas intermedias, el puente losa sobre vigas representa la mejor opción desde el punto de vista constructivo y económico. Sin embargo, en muchas ciudades se opta por la solución viga-losa-cajón por razones estéticas, ya que su forma o geometría es más atractiva arquitectónicamente y realza los espacios urbanos.

Referencias

[1] NEVI, *Especificaciones Generales Para la Construcción de Caminos y Puentes*, vol. III, Quito, Ecuador.

[2] J. C. Araújo, *Diseño de un puente de hormigón pretensado en volados sucesivos: comparación de diseño y costo de construcción entre el puente diseñado y el puente construido en acero y hormigón postensado sobre la quebrada de Gualo*, Universidad San Francisco de Quito, Ecuador, 2011.

[3] D. Huang y B. Hu, "Concrete Segmental Bridges: Theory, Design, and Construction to AASHTO LRFD Specifications", CRC Press, First Edition, Boca Raton, USA, 2020. https://doi.org/10.1201/9780429485473

[4] AASHTO, *LRFD Bridge Design Specifications*, American Association of State Highway and Transportation Officials, 9th Edition, Washington DC, USA, 2020.

[5] A. Arévalo, *Diseño y comparación económica de la superestructura de un puente de un solo vano considerando variantes de losa con vigas de hormigón postensado y vigas de acero*, Escuela Politécnica Nacional, Quito, Ecuador, 2023. http://bibdigital.epn.edu.ec/handle/15000/24955

[6] A. Rodríguez Serquén, *Puentes con AASHTO LRFD 2020*, 9na Edición, Perú, 2022.

[7] ACI CODE-318-19, *Building Code Requirements for*

Structural Concrete and Commentary, American Concrete Institute, USA, 2022.

[8] J. A. Hernández y J. J. Hernández, *Hormigón Estructural. Diseño por Estados Límites (Parte III),* Habana, 2011.

[9] A. Torres y F. Morales, *Sistemas constructivos: Hormigón pretensado y postensado*, Universidad de la República, Montevideo, Uruguay, 2011.

[10] J. Benavides, M. Díaz, L. Hernández y E. Mora, *"Evaluación estructural de un puente en la ruta Spondylus del Ecuador",* Revista Ciencia y Construcción, Vol. 3(3), pp. 6-18, 2022.

[11] J. C. Mediavilla, L. Hernández y M. Molina, "Reforzamiento de la superestructura de un puente tipo viga losa de hormigón armado", Revista Ciencia y Construcción, Vol.4(4), pp. 23-34, 2023.

[12] B. Galarza, M. Llumiquinga, L. Hernández, E. Mora y M. Molina, "Evaluación estructural de un puente sobre un río en la costa ecuatoriana", Ciencia, Ingenierías y Aplicaciones, Vol. 7(1), pp. 55-87, 2024.

[13] K. Solís, L. Hernández, I. Águas y P. Pinto, "Evaluación estructural de la superestructura de un puente existente tipo viga losa de hormigón armado en Ecuador", Ciencia, Ingenierías y Aplicaciones, 7(2), pp. 1-37, 2024. https://doi.org/10.22206/cyap.2024.v7i2.3273

[14] M. K. Rodríguez, *Diseño de un puente tipo losa y puente viga losa hasta 20m de luz, en el Distrito de Chilca-2017*, Escuela Académica Profesional de Ingeniería Civil, Universidad Continental, Huancayo, Perú, 2019. https://hdl.handle.net/20.500.12394/5486

[15] Ministerio de Transporte y Comunicaciones de Perú, *Manual de Puentes*, Dirección General de Caminos y Ferrocarriles, Perú, 2018.

[16] NEC-SE-CG, *Cargas Generales*, Norma Ecuatoriana de la Construcción, MIDUVI, Ecuador, 2024.

[17] NEC-SE-DS, *Peligro sísmico diseño sismo resistente,* Norma Ecuatoriana de la Construcción, MIDUVI, Ecuador, 2015.

[18] ASCE/SEI 41-23, *Seismic Evaluation and Retrofit of Existing Buildings*, American Society of Civil Engineers, Virginia, USA, 2023.

[19] D. Gombosuren y T. Maki, "Effect of Joint Flexibility on Seismic Performance of a Reinforced Concrete Ductile Moment-Resisting Frame", Advances in Materials Science and Engineering, Article ID 6858283, 2022. https://doi.org/10.1155/2022/6858283.

[20] F. Wei, H. Chen y Y. Xie, "Experimental study on seismic behavior of reinforced concrete shear walls with low shear span ratio", Journal of Building Engineering, Vol. 45, Article ID 103602, 2022. https://doi.org/10.1016/j.jobe.2021.103602

[21] H. Alosilla, *Proceso constructivo de viaducto con viga cajón postensada de sección variable, cimentado sobre pilotes excavados - proyecto tren eléctrico*, Vol. TOMO I: Universidad Nacional De Ingeniería, Lima, Perú, 2015.

[22] CSI Bridge, *Software*, versión de prueba, Computers and Structures, Inc., 2024 https://www.csiamerica.com/products/csibridge

FACULTAD DE INGENIERÍA Y CIENCIAS APLICADAS
UNIVERSIDAD CENTRAL DEL ECUADOR

INGENIO
2025, VOL 8(2), JULIO - DICIEMBRE, PP. 76-84

REVISTA INGENIO

Minecraft como Estrategia de Enseñanza para el Desarrollo de Habilidades Matemáticas de Estudiantes del Subnivel Elemental

Minecraft as a Teaching Strategy for the Development of Mathematical Skills in Elementary School Students

Atiaja López Betsayra Sherlin | Universidad Central del Ecuador, UCE -Ecuador
Moreno Liquinchana Jostin Paul | Universidad Central del Ecuador, UCE -Ecuador
Manzano Aguas Patricia Alexandra | Universidad Central del Ecuador, UCE -Ecuador

Recibido: 21/02/2025
Recibido tras revisión: 13/3/2025
Aceptado: 2/4/2025
Publicado: 10/7/2025

PALABRAS CLAVE
Minecraft education, habilidades matemáticas, espacios virtuales, enseñanza y aprendizaje

RESUMEN
El ciberespacio se presenta como una alternativa de mejora en los procesos educativos que existen en la actualidad, específicamente en el campo de la matemática. A lo largo de la historia, las personas han presentado dificultades en cuanto a los procesos lógicos y la resolución de problemas. Por eso, la investigación se elaboró con el objetivo de brindar una nueva oportunidad de aprendizaje actualizada y significativa, siendo el ciberespacio una estrategia de enseñanza para el desarrollo de habilidades matemáticas en los estudiantes de Subnivel Elemental. El nivel de investigación es descriptivo, donde puntualiza características principales del fenómeno, a su vez, es correlacional con lo que se favoreció la comparación entre las variables a fin de enriquecer la información. El tipo de investigación que se ocupó fue documental, dando la posibilidad de fundamentar teóricamente y extraer datos del INEVAL. Se aplicó un enfoque cuantitativo con una población de 1000 datos y una muestra de 516. Entre los resultados más destacables se descubrió que, los estudiantes sostienen un nivel bajo en matemáticas. Además, se subrayó que la tecnología ayuda en el aprendizaje, es ahí donde aparecen los espacios virtuales como el Minecraft Education para contribuir en el desarrollo de habilidades matemáticas.

KEY WORDS
Minecraft education, mathematical skills, virtual spaces, teaching and learning

ABSTRACT
Cyberspace is presented as an alternative to improve the educational processes that exist today, specifically in the field of mathematics. Throughout history, people have presented difficulties in terms of logical processes and problem solving. Therefore, the research was elaborated with the objective of providing a new, updated and meaningful learning opportunity, being cyberspace a teaching strategy for the development of mathematical skills in Elementary Sublevel students. The level of research is descriptive, where it points out main characteristics of the phenomenon, at the same time, it is correlational, which favored the comparison between variables in order to enrich the information. The type of research used was documentary, giving the possibility of providing a theoretical basis and extracting data from INEVAL. A quantitative approach was applied with a population of 1000 data and a sample of 516. Among the most noteworthy results, it was found that students have a low level in mathematics. In addition, it was emphasized that technology helps in learning, which is where virtual spaces such as Minecraft Education appear to contribute to the development of mathematical skills.

1. Introducción

En el Ecuador, el proceso de aprendizaje de las matemáticas ha presentado una gran serie de desafíos, dado que esta asignatura comprende un grado de complejidad alto, provocando que los estudiantes se encuentren envueltos con un sinfín de dificultades para comprender los conceptos, procesos y su adecuada solución. [1] menciona que los resultados que se obtienen de diferentes pruebas nacionales (Ser Bachiller, Ser Estudiante) e internacionales (pruebas PISA) dan cuenta que los estudiantes no alcanzan las competencias matemáticas requeridas [1, p.2]. Por tal motivo, esto refleja una problemática muy

https://doi.org/10.29166/ingenio.v8i2.7934

pISSN 2588-0829
eISSN 2697-3243
fing.revista.ingenio@uce.edu.ec

grave, pues no sostiene una buena compresión de la asignatura y esto a su vez da a entender que en la educación existen ciertas deficiencias para que los estudiantes desarrollen habilidades aptas para su buen desempeño.

En las instituciones educativas, se destaca el aprendizaje por medio de la memorización y deja a un lado el razonamiento y el potencializar las habilidades de los alumnos, siendo un factor muy preocupante, de tal forma que reduce el nivel de conocimientos. En una investigación en el año 2008 [2] autores dan a conocer esa reducción con datos que muestran una calificación de 508 sobre 1000 en cuarto año de Educación Básica [2, p. 6]. Esto evidencia el impacto con gran magnitud que se presenta en el área de matemática y es claro que el estudiantado no posee las competencias necesarias para aplicarlas.

Es ahí donde los estudiantes deben adquirir las bases necesarias para alcanzar un aprendizaje de calidad, sin embargo, la realidad es que gran parte de estos sujetos no adquieren las habilidades fundamentales en su proceso educativo. Según [3] sostienen que existen una gran problemática en cuanto al aprendizaje de las matemáticas y su rendimiento, puesto que los estudiantes conllevan ciertos conflictos durante su proceso en lo que va de aspectos simples a complejos, los cuales son: compresión conceptual, razonamiento lógico y la resolución de los problemas.

Por tal motivo, en la actualidad es fundamental que se utilice recursos o medios tecnológicos, que favorezca el entendimiento a las matemáticas, por ello, [4] menciona es primordial el uso de medios tecnológicos dentro de la educación, pues ofrecen una alta gama de posibilidades, por medio del juego o actividades creativas que permita la compresión de teoría, conceptos, reglas y actividades matemáticas. La implementación de espacios virtuales en la educación ha sido de gran ayuda para la enseñanza de las matemáticas, facilita a que los estudiantes tengan varias opciones para poder prepararse e investigar a fin de potencializar su capacidad intelectual.

En este contexto, se debe desistir de los métodos tradicionales para responder a la nueva realidad educativa, donde apliquen procesos que conlleven conseguir un aprendizaje significativo, por ello, el ciberespacio en la educación se presenta como una estrategia que potencialice el desarrollo de las habilidades matemáticas en los estudiantes. Se ha convertido en una herramienta digital muy crucial dentro del campo educativo, en virtud de que los estudiantes consigan desarrollar las habilidades matemáticas de forma más significativa en los diversos espacios virtuales. Mediante nuevas experiencias se visualiza y comprende de mejor manera los conceptos matemáticos y sus procesos.

1.1. CIBERESPACIO

El ciberespacio alude en términos simples a un entorno virtual que contribuye enormemente a desarrollar diferentes actividades tecnológicas en las redes y se lo efectúa a través de diversas aplicaciones informáticas para un determinado fin en concreto. Para [5] respaldan que el ciberespacio se considera como un espacio virtual que mantiene una conexión directa y constante de personas a través de redes [5, p. 347]. En ese sentido, es un espacio virtual que favorece notoriamente en el mundo, permite que las personas se comuniquen e intercambien información de manera más sencilla y rápida, mediante videojuegos, sitios web, redes sociales, entre otros.

El ciberespacio es un mundo digital que está en constante actualización y conecta a un sinfín de usuarios mediante el uso de aparatos electrónicos, entre los cuales están las computadoras, laptops y celulares. Su término tomo importancia debido a la capacidad de poder interactuar unos con otros con la ayuda del internet. El ciberespacio como concepto nace en la literatura, con la novela Neuromancer de Gibson (1984), y es acogido por la informática, dado el parecido de la obra con lo que sucede en el mundo actual y las redes [6]. Por esa razón, este término se popularizó, siendo los entornos virtuales una realidad que la sociedad experimenta, donde cada sujeto la utiliza para distintas acciones como las de comunicar, jugar o el entretenimiento.

1.1.1 Tipos

Los ciberespacios de la comunicación son un tipo de plataformas que se centran netamente en la interacción y comunicación de información entre las diferentes identidades que hacen uso de una red definida. Para [7] explica que los medios de comunicación que circulan en la Web (…) posibilitan la interacción, hay dominio sobre ellos y se encuentran ubicados en redes globales, sostenidos por computadoras, además que integran voz, imagen, video y texto [7, p. 46]. Esto indica que gracias a estas redes se consigue compartir ideas y pensamientos de un lugar a otro generando una determinada conversación de un tema en concreto con ayuda de recursos multimedia. Cabe indicar que para cumplir con esta función se ocupan las redes sociales, foros y plataformas de videoconferencia.

Un ciberespacio de juego alude a la representación de un ambiente virtual que es muy inevitable, estas plataformas tienen la finalidad de entretener y relacionarse con nuevas amistades. El autor [8] define que han permitido gran alcance orientadas muy especialmente a la inmersión y a la interactividad, que no hay que olvidar nunca que no son más que una dimensión de la interacción del cara a cara entre los humanos [8, p. 15]. Siguiendo esa lógica, tiene la facultad de hacer conectar a cualquier población a un mundo virtual de diversión en el que se coopera, compite y sobre todo se distrae la gente.

Los ciberespacios de realidad virtual son entornos digitales muy diferentes a lo común, ya que permite la posibilidad de simular cosas u objetos en 3D. [9] dice que

es un tipo de realidad, es decir, que existe una realidad material o física y una realidad intangible y que los seres humanos en el intento de construir representaciones simbólicas terminamos por virtualizar la realidad concreta [9, p. 96]. Por ello, son plataformas muy fundamentales para que las personas puedan experimentar de manera abstracta una determina realidad que no sea física, donde pueden conocer objetos y contextos a través de los casos VR.

1.1.2 Ciberespacio en la educación

El ciberespacio en la educación específica la capacidad de hacer uso de las diferentes plataformas en línea a fin de que se desarrolle un aprendizaje e integración dentro de los diferentes entornos virtuales. El autor [9] destaca que permite replantear las formas de pensar, actuar, relacionarse, enseñar y aprehender en la llamada sociedad red [9, p. 86]. Gracias a las nuevas tecnologías es que se puede alcanzar un mejor y avanzado aprendizaje, dado que los estudiantes y docentes tienen la posibilidad de ocupar un gran número de recursos digitales para emplearlos dentro del proceso de enseñanza-aprendizaje. Además, existen diversas plataformas que encaminan en la formación de los individuos, entre los cuales encontramos el *Minecraft Education*.

El *Minecraft Education* en el proceso de enseñanza-aprendizaje se ha convertido en una estrategia, para el desarrollo de habilidades matemáticas, así pues, [10] sostiene que Minecraft es un espacio virtual para los estudiantes donde la colaboración les permite acentuar la compresión de situaciones presentes en muchas de las disciplinas del conocimiento [10, p. 2]. Si bien esta herramienta de Minecraft ha proporcionado grandes beneficios en la educación en diversos contextos y ámbitos.

Además, existe una gran correspondencia entre el *Minecraft Education* y el desarrollo de las habilidades matemáticas, pues permite a los estudiantes, mediante un mundo virtual, construir más su conocimiento de manera creativa, así como lo menciona [11] busca promover la colaboración y creatividad. Es una herramienta digital que incrementa las competencias en los estudiantes, para responder a las exigencias tanto de la vida académica como laboral en los educadores [11, p. 12]. Esta herramienta proporciona grandes beneficios en el aprendizaje de los estudiantes, fortalece de manera innovadora los conocimientos matemáticos, potencializando procesos para un buen desarrollo de habilidades.

1.2. HABILIDADES MATEMÁTICAS

Las habilidades matemáticas son entendidas como el conjunto de capacidades cognitivas, que el estudiante desarrolla, con el fin de adquirir o potenciar sus conocimientos matemáticos. Según, [12] los estudiantes deben potenciar sus competencias matemáticas, con el propósito de ser personas críticas y analíticas que les permita resolver problemas matemáticos, empleando diversas estrategias para alcanzar su máximo potencial. Este conjunto de capacidades es fundamental, para el desarrollo de los estudiantes, permite cumplir con las destrezas del aprendizaje matemático y con ello lograr un aprendizaje significativo.

Es esencial el desarrollo de las habilidades matemáticas desde la etapa infantil, puesto que, profundiza en el desarrollo del razonamiento lógico y la resolución de problemas, además, el comprender los significados y su proceso que se ejecuta de manera organizada para alcanzar con lo que se requiere y dónde interviene la reflexión y toma de decisiones de un estudiante [13]. En este sentido, el desarrollo de estas habilidades son un proceso complejo, pues, se requiere de interés y disposición para comprender conceptos matemáticos y que estos sean entendidos y comprendidos.

Las habilidades matemáticas se caracterizan por las acciones que ejecutan en alguna actividad y sobre todo las que el estudiante debe desarrollar, por ende, este un proceso continuo que los estudiantes deben cumplir. Según Ferrer (2010) existen cuatro habilidades matemáticas de las cuales encontramos el entendimiento de conceptos y propiedades, en este primer apartado los estudiantes aprenden a comprender y entender conceptos matemáticos, seguido a eso se encuentra la compresión de pasos para la realización de un problema, para que los estudiantes puedan adaptarse a procedimientos heurísticos, que comprende el uso de reglas matemáticas junto con la metacognición, finalmente el estudiante se enfrenta a un análisis para resolver problemas en la vida cotidiana. Estas habilidades se desarrollan durante el proceso de aprendizaje del estudiante, cada una de estas tiene componentes necesarios, pues esto ayuda, a que los estudiantes cumplan y sigan desarrollando más su pensamiento matemático.

Las matemáticas son importantes en la toma de decisiones y resolución de problemas. Pues ayuda a pensar de forma razonada, donde interviene un proceso lógico de reflexión, comprensión, construcción, adquisición de habilidades y actitudes para un adecuado desempeño matemático en la sociedad [14]. Por ello, esta asignatura se convierte en un gran reto para los estudiantes, pues al desarrollar habilidades cognitivas enriquecen su pensamiento crítico y mejoran sus habilidades.

2. Método

2.1. TIPO DE INVESTIGACIÓN

La investigación se caracteriza por ser documental, en la que [15] la define como el proceso de la investigación científica y de la información preexistente antes de empezar la investigación, y que se publican tanto en fuentes

documentales tradicionales [15, p. 183]. En concordancia, este proyecto se fundamenta mediante la revisión y contraste de información proveniente de medios digitales y físicos, comparando fuentes y priorizando aquellas de origen primario.

Se hace uso del nivel descriptivo el cual permite recopilar datos e informaciones sobre las características, propiedades, aspectos o dimensiones de las personas, agentes e instituciones de los procesos sociales [16, p. 2]. Mediante este tipo de investigación se puede obtener características sobre qué estrategias metodológicas se aplica para que los estudiantes del subnivel elemental presenten un adecuado proceso de habilidades matemáticas.

La profundidad del estudio se centra en un nivel correlacional, debido a que este aspecto busca un carácter comparativo de variables para alcanzar una investigación enriquecedora. El autor [17] plantea que en este alcance de la investigación surge la necesidad de plantear una hipótesis en la cual se proponga una relación entre 2 o más variables [17, p. 3]. La correlación busca enlazar o conectar variables para observar la influencia que tiene la una con la otra; con la ayuda del Chi cuadrado se logra ejecutar dicho proceso.

2.2. ENFOQUE DE LA INVESTIGACIÓN

La investigación tiene un enfoque cuantitativo el cual representa un proceso sistemático de información, puesto que, mediante datos estadísticos, se va a describir el fenómeno que se está estudiando. Los autores [18] mencionan que el enfoque cuantitativo utiliza la recolección de datos para probar hipótesis con base en la medición numérica y el análisis estadístico [18, p. 4]. Así pues, este enfoque recolecta datos numéricos con el fin de que se pueda para analizar e interpretar variables, utilizado herramientas estadísticas.

2.3. POBLACIÓN Y MUESTRA

En este apartado se presenta la población y muestra de la investigación. La población es el conjunto total de personas u objetos de los que se requiere conocer en una investigación, [19] menciona que la población es un conjunto de elementos que contienen ciertas características que se pretenden estudiar [19, p. 648]. Es decir, la población se conceptualiza como un conjunto de fenómenos que tienen características similares para ser estudiados. En la presente investigación se utiliza una población de 1000 datos proporcionados por el INEVAL, que son recolectados a nivel nacional y permite reflejar la realidad del proceso educativo en el periodo académico 2023-2024, enfocándose en el área de matemática del Subnivel Elemental.

La muestra es la parte específica de una población total, según [20] la muestra es un subconjunto o parte del universo o población en que se llevará a cabo la investigación [20, p. 77]. En este sentido la muestra es el conjunto reducido en el que se aplica ciertos métodos para someterlos a estudios. Para definir un grupo representativo de la población total, se realiza el cálculo de la muestra.

2.3.1. Cálculo de la muestra

Es necesario efectuar un proceso mediante el cual se defina el grupo representativo de la población. Los autores [21] mencionan que consiste en encontrar una muestra que sea representativa del universo o población con cierta posibilidad de error (se pretende minimizar) y nivel de confianza (maximizar), así como probabilidad [21, p. 178]. Por ello, este cálculo permite brindar una muestra que sea efectiva y que cubra o generalice a toda la población. Cabe indicar que, hacer el cálculo de la muestra es fundamental para que la investigación sea infalible y minuciosa.

Los datos que se van a emplear para el cálculo de la muestra son proporcionados por el INEVAL [22]. Estos datos son recogidos a nivel nacional y permite reflejar la realidad del proceso educativo de cada nivel. En este caso, se tomará en consideración los aspectos que influyen en el área de Matemática específicamente del subnivel elemental. Para ello, se utilizará una población de 1000 de los estudiantes que rindieron la prueba Ser.

La fórmula para calcular la muestra es la siguiente:

$$n=\frac{N\times Z^2\times p\times q}{e^2\times(N-1)+Z^2\times p\times q}$$

n: Tamaño de la muestra

N: Tamaño de la población o universo

Z: Nivel de confianza

e: Margen de error

p: Probabilidad de que ocurra el evento

q: Probabilidad de que no ocurra el evento

Figura 1

Datos del cálculo de la muestra

Parámetro	Valor
N	1000
Z	1,96
P	50%
Q	50%
E	3%

Nota. Datos que calcula la muestra de esta investigación

Reemplazando los datos con la fórmula, el proceso del cálculo es el siguiente:

Figura 2

Cálculo de la muestra

$$n = \frac{N * Z^2 * p * q}{e^2 * (N-1) + Z^2 * p * q}$$

$$n = \frac{1000 * 1{,}96^2 * 0{,}5 * 0{,}5}{0{,}03^2 * (1000-1) + 1{,}96^2 * 0{,}50 * 0{,}50}$$

$$n = 516$$

Nota. Fórmula estadística para el cálculo de la muestra.

En el proceso del cálculo de la muestra se emplea: una población de 1000 estudiantes, un nivel de confianza del 1,96, y un margen de error del 3%. Al reemplazar todos los datos en la fórmula, se obtiene que la muestra total de 516, este resultado permite analizar los datos respectivos que corresponden al área de matemática del Subnivel Elemental. Estos datos sirven como pilar fundamental para el proceso estadístico de la investigación.

2.4. MATERIAL

2.4.1.Procesamiento de datos

Para el procesamiento de datos, se considera el uso de 1000 datos de los estudiantes que rindieron las Pruebas Ser, esta información es proporcionada y recogida por el Instituto Nacional de Evaluación Educativa. La información al ser brindada por esta entidad permite un proceso que sea seguro y real. Entonces, los datos no son desarrollados netamente por los participantes del presente proyecto, sino que son extraídos de fuentes externas que es el caso del INEVAL. Cabe destacar que no se utiliza el Alfa de Cronbach, puesto que se efectúa un proceso diferente y para que sea más efectivo de cálculo la muestra, la que es 516 a fin de que se pueda analizar e interpretar de manera apropiada los datos.

3. Resultados y discusión

3.1 RESULTADOS

3.1.1. Tabla de frecuencia para datos no agrupados

Las tablas de frecuencia son una herramienta que permite organizar y ordenar datos de una investigación. Así pues, [23] afirman que las distribuciones de frecuencias se presentan mediante tablas estadísticas que son agrupaciones de datos ordenados con arreglo a un criterio lógico [23, p. 47]. Estas tablas estadísticas, permite comprender la información de datos, de forma más concisa, debido a que, al elaborar una tabla se comprende de mejor manera la información estadista pues esta expresada de manera clara y sistematizada.

En la tabla 1, se presentan las tablas de frecuencia con datos no agrupados.

Tabla 1

Sexo del sustentante

		Frecuencia	Porcentaje	Porcentaje válido	Porcentaje acumulado
Válido	MUJER	253	49,0	49,0	49,0
	HOMBRE	263	51,0	51,0	100,0
	Total	516	100,0	100,0	

Nota. Resultado de tabla de frecuencia de datos no agrupados, datos obtenidos por el INEVAL 2023-2024

La tabla de frecuencia con datos no agrupados, perteneciente al sexo del sustentante, reflejan que se existen 253 mujeres que corresponde al 49%, por otra parte, se evidencia que hay 263 hombres que compete al 51% de los estudiantes del subnivel elemental. Es por ello, que existe una relación un tanto equilibrada entre los géneros, con una leve mayoría en lo que respecta a los hombres. Por tal virtud, mayoritariamente el género masculino marca cierta diferencia en el aprendizaje, ya que pueden desarrollar habilidades más rápido y efectiva en cuanto a la matemática.

3.1.2.Medidas de tendencia central

Las medidas de tendencia centrales son herramientas estadísticas, pues permiten conocer el estado del conjunto de datos obtenidos, en este contexto, [24] menciona que las medidas de tendencia central son medidas estadísticas que pretenden resumir en un solo valor a un conjunto de valores [24, p. 1]. Esto quiere decir, que estas medidas son fundamentales para identificar valores centrales o medios, además que proporcionan información de un valor único y representativo que puede ser útil para la investigación.

En la tabla 2, se presenta las medidas de tendencia central.

Tabla 2.

Nivel de logro alcanzado por los sustentantes en el campo de Matemática

		Nivel de logro alcanzado por los sustentantes en el campo de Matemática
N	Válido	492
	Perdidos	24
Media		1,23
Mediana		1,00
Moda		1
Mínimo		0
Máximo		3
Suma		606

Fuente [22]

Se puede observar las medidas estadísticas sobre el Nivel de logro alcanzado por los sustentantes en el campo de Matemática, en los datos obtenidos por el INEVAL tenemos un rango de 0 a 3 correspondientes al nivel de logro; entonces, se puede evidenciar que existe una similitud entre las tres medidas, de tal forma que la media representa el 1,23 en promedio, y con ello se define que los estudiantes presentan un nivel de logro bajo o medio, considerando que el logro máximo es el 3, el cual corresponde al nivel de logro más alto (excelente), mientras que el valor de la mediana y la moda es 1, esto quiere decir que en los sustentantes de matemáticas prevalece el nivel de logro elemental. Esto resulta que, los estudiantes no sostienen un rendimiento bueno o excelente, demostrando que existe un bajo nivel, en tanto las habilidades y el dominio que se refieren a la parte de la Matemática.

Tabla 3.

Promedio obtenido en el campo de matemática

		Promedio obtenido en el campo de Matemática
N	Válido	492
	Perdidos	24
Media		673,11
Mediana		659,00
Moda		635
Mínimo		540
Máximo		846
Suma		331168

Fuente: Resultado de las medidas de tendencia central, datos obtenidos por el INEVAL 2023-2024 [22]

En la tabla de las medidas de tendencia central del promedio del área de Matemática, se revela que es válido 492 y se perdió 24 datos de la muestra que se utiliza. Así pues, entre estas medidas marcan un rango correspondiente de semejanza, dado que la media equivale a 673,11 del promedio en general, la mediana a 650 y la moda a 635. Estos resultados demuestran que los estudiantes no se encuentran en una postura ni alta, ni baja en cuanto al rendimiento de la materia de Matemáticas, más bien se encuentran en un nivel medio alto, aunque no se alcanza con el rendimiento necesario para definir un nivel muy bueno o excelente.

3.1.3. Chi cuadrado

Dentro de la educación, es común analizar la relación entre diferentes aspectos uno de ellos es el quintil correspondiente al índice socioeconómico y el tipo de financiamiento de una institución educativa, sean públicas, privadas o mixtas, a la que una población pertenece, por ello se plantea lo siguiente:

Hi: ¿El quintil como índice socioeconómico, influye en el financiamiento de una institución educativa?

Ho: ¿El quintil como índice socioeconómico, no influye en el tipo financiamiento de una institución educativa?

En la tabla 4, se acepta la hipótesis alternativa y se rechaza la hipótesis nula, pues existe un valor menor al 5%, es decir en este análisis obtenido por el chi-cuadrado, demuestra un porcentaje del 0,000 y por ello se puede definir que el quintil socioeconómico si influye en el tipo de financiamiento de una institución educativa, lo que a su vez refleja el desempeño en el ámbito matemático. Los estudiantes que pertenecen a los quintiles más bajos que corresponden 1 y 2 por lo general asisten a instituciones públicas que sostienen recursos y materiales limitados para un aprendizaje de calidad. Por otra parte, los estudiantes que se encuentran en los quintiles 4 y 5 tienen más probabilidades de acceder a instituciones mixtas o privadas que suelen adaptarse a nuevas formas de enseñar para un mejor el desempeño en Matemáticas. Así pues, la diferencia es notable de un grupo y el otro para alcanzar con un rendimiento destacable o muy bueno.

Tabla 4.

Quintil como índice socioeconómico y el tipo de financiamiento de la institución educativa

	Valor	Df	Significación asintótica (bilateral)
Chi-cuadrado de Pearson	99,124[a]	8	,000

Fuente: Prueba de chi-cuadrado de los datos utilizados por el INEVAL 2023-2024 [22]

3.1.4. Tabla de doble entrada

La tabla de doble entrada es una herramienta muy crucial en el procesamiento de datos, debido a que ayuda a sintetizar la información más relevante de una investigación, además ayuda a mantener una visualización coherente y estructurada. Los autores [25] plantean que una tabla de doble entrada sirve para presentar la

distribución conjunta de dos variables estadísticas [25, p. 50]. En este contexto, la tabla de doble entrada facilita la comprensión de datos, puesto que estos están organizados y sirven para hacer una relación o comparación de la estadística.

Tabla 5.

Entornos virtuales en el sistema educativo.

Entornos virtuales en el aprendizaje.	Porcentaje
¿Sabe acerca de los entornos virtuales?	64,71 %
Los entornos virtuales son importantes en el aprendizaje	47,06 %
¿Qué tan ventajoso es que se implementen los espacios virtuales en el aprendizaje?	58,82%
La tecnología contribuye a la formación de los estudiantes	83,33%

Fuente: Datos estadísticos del impacto de los entornos virtuales en la educación *[26]*.

En la tabla 5, se revela la influencia positiva y efectiva de los espacios virtuales con relación a la educación. Se demuestra que el 64,71% de estudiantes conocen acerca de las plataformas virtuales, a su vez, el 47,06% indica que son muy cruciales en el aprendizaje y el 58,82% sostiene que los entornos virtuales tienen sus ventajas en la educación, dando abertura a que se experimente una formación diferente y actualizada acorde a la realidad de la nueva sociedad. Por añadidura, se evidencia un porcentaje del 83, 33 % que apunta a la capacidad que aporta los diferentes espacios virtuales al sistema educativo. Como se puede observar en los datos, existe una gran aceptación, donde se puede alcanzar mejores procesos de aprendizajes que sean creativos, significativos e innovadores.

Por su parte, el autor [27] menciona que los entornos virtuales de aprendizaje, favorecen los procesos de enseñanza-aprendizaje y contribuyen en la formación de los educandos, es por lo que resulta novedoso su uso en la enseñanza de las matemáticas en el nivel de educación secundaria [28] y por otro lado, afirma que los entornos virtuales de aprendizaje constituyen oportunidades que permiten potenciar los procesos de enseñanza aprendizaje mediante la interacción de los docentes y los estudiantes en relación a flexibilidad y accesibilidad de manera innovadora. Ambos autores reconocen la efectividad de los entornos virtuales de aprendizaje en la educación. Las nuevas formas de aprender, a través de entornos virtuales, permite que el estudiante pueda interactuar, comunicarse y sobre todo generar conocimientos relevantes, alcanzando una mayor productividad de sus saberes, capacidades y habilidades.

3.2 DISCUSIÓN

El sexo del sustentante de cierta manera influye en el desempeño del sujeto, cierto género puede desarrollar más pronto el aprendizaje de las matemáticas, en este caso, el 51% equivale a que los hombres, desarrollan un tanto más ágil las habilidades matemáticas que las mujeres (49%). Para [29] explica que los resultados de PISA 2009 y 2012 muestran que (…) en otros países latinoamericanos se observan pequeñas diferencias a favor de los hombres en el test de matemática [29, p. 21]. En ese sentido, se revela que no existe una diferencia notable entre la capacidad mental entre los géneros, sino que el hombre tiende a ser un poco más factible y hábil en la resolución de problemas.

El nivel de logro alcanzado por los sustentantes en el área de matemáticas refleja una duda acerca del aprendizaje que se efectúa, ya que en la medida de tendencia central; la media es 1,23; la mediana es 1,00 y la moda 1. Esto puntualiza que los estudiantes se encuentran en un nivel elemental y no alcanzan con los conocimientos necesarios [22]. Afirma que el 70,9% de los estudiantes de Ecuador no alcanzan el nivel 2, categorizado cómo el nivel de desempeño básico en matemáticas [22, p. 44]. Es decir, el desempeño es muy bajo, puesto a que los estudiantes disponen de conocimientos simples, ocasionando que el aprendizaje se convierta en un proceso complejo y que no se desarrollen las habilidades matemáticas como se deben.

Ahora bien, el quintil como factor socioeconómico y el financiamiento de una institución educativa, según datos obtenidos se constata que sí influye dentro del desarrollo del aprendizaje de los estudiantes. Como afirma [30] el quintil de alumnos más pobres solo se beneficia del 16% de la financiación pública destinada a la educación, en comparación con el quintil más rico, que se beneficia del 28% [30, p. 2]. En este contexto, el quintil socioeconómico es fundamental dentro de la educación, puesto que al obtener un quintil más alto, el estudiante está en la posibilidad de adquirir y potenciar sus conocimientos matemáticos, puesto que esto no limita a tener una educación más avanzada; sin embargo, los estudiantes que se encuentran en el quintil medio o más bajo, no están la posibilidad de que puedan acceder a una educación de calidad.

El uso de la tecnología como plataformas digitales, metaversos, juegos en línea, en la educación es valioso en el proceso de enseñanza de la matemática de los estudiantes, pues proporciona grandes beneficios y facilita en su aprendizaje. [31] dentro de su investigación demuestran que el 58,1 % de los estudiantes encuestados señaló que está de acuerdo con la utilización de las herramientas tecnológicas para el mejoramiento de las matemáticas en su vida estudiantil [31, p. 43]. Por ello, es importante que se utilice herramientas tecnológicas en este proceso, pues son de gran ayuda para el desarrollo de habilidades cognitivas de los estudiantes, además que posibilita un mejor desempeño en sus competencias.

Además, la herramienta de Minecraft en el ciberespacio juega un papel fundamental en la educación. Esta

nueva estrategia de enseñanza y aprendizaje ha contribuido al proceso de formación de los estudiantes, generando interés por aprender. Así pues, [32] afirma que el ciberespacio facilita nuevas formas de interacción, aprendizaje y creación. Los sistemas actuales despliegan posibilidades diversas de organización y explotación de la inteligencia colectiva [32, p. 2788]. El ciberespacio elimina barreras de aprendizaje, dando valor a las importantes, de tal froma que permite un conocimiento mas trasendental, el cual foemnta a un aprendizaje autónomo permitiendo al estudiante a trabajar a su propio ritmo y contribuir a la interación y creatividad de los estudiantes.

4. Conclusiones

Minecraft es una herramienta muy fundamental en el aprendizaje, debido a que, aparta los métodos tradicionales y se enfoca en impartir un aprendizaje más dinámico, creativo, innovador, significado y que se adapte a la nueva realidad de las personas del siglo 21. Por ello, los entornos virtuales tienen un gran impacto en el aprendizaje, ya que representa el 83,33%, siendo un aspecto positivo para que los estudiantes alcancen un buen desempeño en su proceso de formación educativa.

En síntesis, se evidencia que los estudiantes del subnivel elemental presentan un bajo rendimiento académico en la asignatura de matemática, lo que implica que durante su proceso de enseñanza y aprendizaje no desarrollan adecuadamente sus habilidades matemáticas y afecta su formación. El promedio de calificaciones de esta asignatura es de 673,11 esto determina que los estudiantes no alcanzan la puntuación necesaria para aprobar la materia, lo que puede generar varias consecuencias a lo largo de su vida académica.

Cabe indicar que, el índice socioeconómico juega un papel muy fundamental en la utilización de los entornos virtuales, en vista de que, puede llegar a existir una brecha en la formación digital. Por tanto, hay que considerar la realidad educativa y adaptar los recursos y acciones necesarios para alcanzar un aprendizaje moderno y duradero.

Finalmente, el uso de la tecnología en la educación ha sido de gran relevancia para la enseñanza de los estudiantes, el ciberespacio se ha convertido en una herramienta didáctica que facilita el desenvolviendo cognitivo. El diseño de ciberespacios contribuye a la educación de los estudiantes, pues el 83,1% está destinando a que los estudiantes se apasionen e incentiven por aprender matemática, si se hace uso de espacios interactivos.

Referencias

[1] D. V. Wampash Antuash, *El bajo rendimiento académico en matemáticas, con los estudiantes del sexto C de Educación General Básica de la Unidad Educativa Tres de Noviembre de la ciudad de Cuenca,* 2018.

[2] E. M. Orbea Jiménez, Y. M. García García, D. H. Martínez Rubio y J. M. Orbea García, «Incidencia de la discalculia en el aprendizaje de Matemática, estudiantes del Colegio "José María Velaz" del Cantón La Maná,» *Revista Latinoamericana de Ciencias Sociales y Humanidades,* vol. 5, nº 1, pp. 606-618, 2024.

[3] Y. Martínez y L. Mayorga, «Dificultades en torno al proceso de enseñanza aprendizaje de la matemática» *Mérito Revista de Educación* , vol. 2, nº 6, pp. 171-183, 2020.

[4] D. Mora, «Estrategias para el aprendizaje y la enseñanza de las matemáticas» *Revista de Pedagogía,* vol. 24, nº 70, pp. 181-272, 2003.

[5] L. Cháves y H. Vásquez, «El ciberespacio, fuente de control y vigilancia para los ciudadanos» *Perspectivas en inteligencia,* vol. 11, nº 20, pp. 347-357, 2019.

[6] E. Santana y Z. Báez, «Ciberespacio y Cibermundo: delimitaciones conceptuales desde el materialismo sistémico» *Ciencia y Sociedad,* vol. 47, nº 1, pp. 45-56, 2022.

[7] M. Montiel, «Los cibermedios como nuevas estructuras de comunicación social» *Revista de Ciencias Humanas y Sociales,* vol. 1, nº 33, pp. 34-48, 2000.

[8] F. García, «Videojuegos y virtualidad narrativa,» *ICONO 14,* vol. 4, nº 2, pp. 1-24, 2006.

[9] A. Hermann, «Pedagogía del Ciberespacio: hacia la construcción de un conocimiento colectivo» *Sophia, Colección de Filosofía de la Educación,* vol. 1, nº 11, pp. 83-103, 2011.

[10] J. Plaza, *Minecraft Education Edition: una forma didáctica para potenciar la agilidad de resolución de problemas matemáticos,* 2022.

[11] M. Saldaña, «Minecraft Education como herramienta de aprendizaje en la formación de estudiantes unversitarios» *REDHCS,* vol. 30, nº 20, pp. 1-18, 2022.

[12] D. Barrera y V. Urquizo, *Habilidades Matemáticas en los estudiantes de la Unidad Educativa Once de Noviembre,* 2020.

[13] M. Velasco, «Habilidades Matemáticas» *FEDUMAR,* vol. 8, nº 1, pp. 15-18, 2021.

[14] N. Herrera Villamizar, W. Montenegro Velandia y S. Poveda Jaimes, «Revisión teórica sobre la enseñanza y aprendizaje de las matemáticas» *Revista Virtual Universidad Católica del Norte* , vol. 1, nº 35, pp. 254-287, 2012.

[15] I. Chong de la Cruz, *Métodos y técnicas de la investigación documental*, México, 2007.

[16] E. Nieto, «Tipos de investigación,» *Universidad Santo Domingo de Guzmán,* vol. 2, nº 1, pp. 1-2, 2018.

[17] C. Ramos, «Los alcances de una investigación,» *Ciencia América,* vol. 9, nº 3, pp. 1-5, 2020.

[18] R. Sampieri, C. Fernández y L. Baptista, *Definiciones de los enfoques cuantitativo y cualitativo, sus similitudes y diferencias*, RH Sampieri, Metodología de la Investigación, 2014.

[19] L. Ventura, «¿Población o muestra?: Una diferencia necesaria» *Revista Cubana de Salud Pública,* vol. 43, nº 4, pp. 349-648, 2017.

[20] P. López, *Población muestra y muestreo,* vol. 9, nº 8, pp. 69-74, 2004.

[21] R. Hernández , C. Fernández y M. Baptista, *Metodología de la investigación*, 6th ed., Mc Graw Hi Education, 2014.

[22] Instituto Nacional de Evaluación Educativa, *Educación en Ecuador: Resultados de PISA para el desarrollo*, Quito: INEVAL, 2018.

[23] S. Fernández, J. Sánchez, A. Córdoba y A. Largo, *Estadística descriptiva*, Esic Editorial, 2002.

[24] F. Quevedo, «Medidas de tedencia central y dispersión» vol. 11, nº 3, pp. 1-20, 2011.

[25] A. Estrada y C. Díaz, «Errores en el cálculo de probabilidaddes en tablas de doble entrada en profesores en formación» *UNO, Didáctica de las matemáticas,* vol. 44, nº 1, pp. 48-58, 2007.

[26] D. Sánchez , P. Morales y E. Pico, «Entornos virtuales de aprendizaje para el fortalecimiento de la enseñanza-aprendizaje de la geometría analítica en educación básica superior», *Revista Latinoamericana de Ciencias Sociales y Humanidades,* vol. 4, nº 1, pp. 2054-2074, 2023.

[27] J. Ayil, «Entorno virtual de aprendizaje: una herramienta de apoyo para la enseñanza de las matemáticas» *RITI,* vol. 6, nº 11, pp. 34-39, 2018.

[28] T. Bermúdez, «Aportes de los entornos virtuales en educación secundaria», *Journal Scientific MQR Investigar,* vol. 7, nº 3, pp. 901-3918 , 2023.

[29] M. Río, K. Strasser y M. Superreguy, «¿Son las habilidades matemáticas un asunto de género? Los estereotipos de género acerca de las matemáticas en niños y niñas de Kínder, sus familias y educadoras», *Calidad en la educación,* vol. 1, nº 45, pp. 20-53, 2016.

[30] UNICEF, *Transformar la educación mediante una financiación equitativa,* 2023.

[31] W. Yaselga y C. Morocho, «Las Tics como estrategias para fortalecer el aprendizaje de las matemáticas de EGB subnivel básico superior», *Revista Multidisciplinaria Proyecto,* vol. 1, nº 1, pp. 29-46, 2024.

[32] F. Sánchez, «Educación, cibercultura e inteligencia colectiva», *Gazeta de antropología,* vol. 30, nº 1, pp. 2340- 2792, 2014.

[33] O. Vega, «De las TIC en la educación a las TIC para la educación», *Revista Vector,* vol. 11, nº 1, pp. 24-29, 2016.

[34] Y. Pérez y R. Ramírez, «Estrategias de enseñanza de la resolución de problemas matemáticos: Fundamentos teóricos y metodológicos», *Revista de investigación,* vol. 35, nº 73, pp. 169-194, 2011.

[35] J. Torres Guzmán, *Desarrollo de un entorno virtual en Minecraft Education para el aprendizaje de las tablas de multiplicar,* 2024.

FACULTAD DE INGENIERÍA Y CIENCIAS APLICADAS
UNIVERSIDAD CENTRAL DEL ECUADOR

INGENIO
2025, VOL 8(2), JULIO - DICIEMBRE, PP. 85-94

REVISTA INGENIO

Simulación Sincrofasorial con PMUs Virtuales en Sistema de Potencia Para Estudios Fuera de Línea

Synchrophasor Simulation With Virtual PMUs in Power System for Off-Line Studies

Armando Salvador Freire Freire | Universidad Técnica de Cotopaxi -Ecuador
Fernando Rafael Arias Atiaja | Universidad Técnica de Cotopaxi -Ecuador
Jennifer Nicole Bustos Arias | Universidad Técnica de Cotopaxi -Ecuador

Recibido: 25/4/2025
Recibido tras revisión: 1/5/2025
Aceptado: 20/5/2025
Publicado: 10/7/2025

PALABRAS CLAVE
WAMs, PMUs, Monitoreo dinámico, DIgSILENT PowerFactory, Python.

RESUMEN
Uno de los principales componentes que conforman el sistema de monitoreo de área extendida (WAMs) son las Unidades de Medición Fasorial (PMUs), dispositivos que permiten realizar análisis dinámico en el estado del sistema eléctrico. Estos equipos permiten la estimación de fasor representando las magnitudes de ángulos de tensión e intensidad y garantizando, mediante la sincronización temporal y frecuencia de muestreo, visualizar al sistema en tiempo real y comparar fasores medidos en distintos puntos de la red. Este estudio presenta una plataforma de monitoreo dinámico con PMUs para un sistema de potencia de dos áreas, el enfoque comienza con el desarrollo y verificación de un modelo de referencia ejemplo 12.6 (P. Kundur, Power system stability and control), simulado en el software de DIgSILENT PowerFactory, luego se realiza un estudio dinámico mediante la implementación de eventos de perturbación con la finalidad de extraer datos de voltajes y corrientes en magnitud y ángulo, además, se implementa un algoritmo mediante el software Python que sirve de PMU virtual para la lectura y envío de datos registrados mediante una red ip ficticia que será extraída por el software Pyscript para la visualización y uso de datos para su monitoreo, también se muestra el monitoreo dinámico sincrofasorial mediante el software PMU Connection Tester que se comunica por medio de la ip virtual enviada desde Python, como resultado se obtiene la gráfica de respuesta mediante la visualización de ángulos de PMUs virtuales.

KEY WORDS
WAMs, PMUs, Dynamic Monitoring, DIgSILENT PowerFactory, Python.

ABSTRACT
One of the main components that make up the wide area monitoring system (WAMs) are the Phasor Measurement Units (PMUs), devices that allow dynamic analysis of the state of the electrical system, these devices allow phasor estimation representing the magnitudes of voltage and current angles and guaranteeing by means of time synchronization and sampling frequency to visualize the system in real time and compare phasors measured at different points of the network. This study presents a dynamic monitoring platform with PMUs for a two-area power system, the approach starts with the development and verification of a reference model example 12.6 (P. Kundur, Power system stability and control), simulated in DIgSILENT PowerFactory software, then a dynamic study is performed by implementing disturbance events in order to extract data of voltages and currents in magnitude and angle, in addition, an algorithm is implemented using Python software that serves as a virtual PMU for reading and sending data recorded through a fictitious ip network that will be extracted by the Pyscript software for viewing and use of data for monitoring, also shows the dynamic monitoring synchrophasor by PMU Connection Tester software that communicates through the virtual ip sent from Python, as a result the response graph is obtained by displaying angles of virtual PMUs.

1. Introducción

Los grandes apagones eléctricos que han causado pérdidas económicas millonarias en diversas partes del mundo, propiciaron la necesidad de realizar un análisis dinámico y en tiempo real del estado del sistema de potencia [1].

El objetivo de los WAMs es mejorar el control y monitoreo en tiempo real de los sistemas eléctricos de potencia (SEP), proporcionando datos a través de las Unidades de Medición Fasorial (PMUs). Estas unidades permiten un muestreo sincronizado y una actualización de datos a altas velocidades, mediante la estimación fasorial de

https://doi.org/10.29166/ingenio.v8i2.8148

pISSN 2588-0829
eISSN 2697-3243
fing.revista.ingenio@uce.edu.ec

la frecuencia, magnitud y ángulo de fase de los componentes de voltaje y corriente. Esto se logra gracias a la sincronización temporal y la alta frecuencia de muestreo en tiempo real dentro del sistema eléctrico. Así, los sistemas WAMs en operación, junto con el sistema de posicionamiento global (GPS), facilitan la supervisión de los sistemas de energía bajo el mismo marco de referencia de tiempo, con una precisión de 1 ms [2].

Los dispositivos PMUs monitorizan, protegen y controlan el estado del sistema eléctrico, manejan una fuente mediante señales de tiempo GPS para adquirir información precisa de la red generando datos fasoriales en espacios separados por miles de kilómetros [3], la sincronización del tiempo, la alta precisión y su velocidad de respuesta hacen de que estos equipos sean oportunos tanto para el control y protección en tiempo real, como para el monitoreo global en estado estable y dinámico del sistema [4]. Estas unidades se encuentran conectados a un concentrador de datos fasoriales (PDC) para obtener observabilidad en un sistema de monitoreo de área amplia, así como para el monitoreo dinámico.

Dada la importancia que tiene la supervisión confiable del sistema, nuevos desafíos numéricos y algoritmos matemáticos se han estudiado y mejorado durante décadas, la creciente penetración de PMUs al sistema de transmisión introdujo un potencial de mejoras como la observabilidad al estimador de estado (SE) y las aplicaciones que permite la Evaluación de Seguridad Dinámica (DSA), aportando así información precisa a la toma de decisiones, a partir de ello se instalaron PMUs en líneas de transmisión de redes eléctricas en todo el mundo, volviendo una acción imperativa para avanzar en una red más inteligente [5], [6].

Pero, el desarrollo gradual y la complejidad operacional ha generado interés por la Sistema de Evaluación Dinámica de seguridad (DSA), que determina la capacidad en un sistema de potencia para sobrevivir a contingencias o perturbaciones imprevistas que podrían causar la violación de límites de seguridad dentro del sistema potencia. Los operadores de la red ante eventos inesperados muestran problemas para establecer el estado exacto del sistema eléctrico. Un sistema con grado de inseguridad conduce a la propagación de fallas afectando la dinámica del sistema que necesita de una acción de control vertiginosa para evitar situaciones críticas que puedan ocasionar inestabilidad o llegar al colapso total del sistema eléctrico de potencia [7], [8]implementation of power system dynamic security assessment (DSA).

Se ha identificado la necesidad de desarrollar una plataforma de simulación de estudio fuera de línea porque las nuevas tecnologías presentan desafíos significativos en términos de adaptación y conocimiento especializado para los operadores del sistema. Según [9] en el análisis de sistemas fuera de línea, los modelos se consideran probabilísticos para contingencias o condiciones operativas de la red. Su evaluación se realiza tanto en estado estacionario (SSA) como en estado dinámico (DSA). Este método de evaluación convencional, debido a la gran dificultad en su modelado, es inviable para su aplicación en tiempo real. Sin embargo, resulta adecuado para tareas como la planificación del sistema a largo plazo, ya que en este modo no se requiere una respuesta instantánea para evitar eventos críticos [10].

La intención de este trabajo se ve reflejado a través de las exigencias que presentan los sistemas eléctricos para operadores del sistema, donde las simulaciones van variando a la velocidad del cambio de la realidad, por lo que se determina la importancia de poseer plataformas necesarias de monitoreo dinámico implementadas con herramientas de software open source, que de un programa de simulación como DIgSILENT PowerFactory transmita información a diferentes programas o herramientas computacionales como Python, y de esta forma permita realizar similares funciones a las realizadas en programas principales, con el propósito de dotar una herramienta de entrenamiento offline y capacitación [11].

El objetivo es desarrollar una simulación digital en tiempo fuera de línea (modo estudio) mediante la integración de un software de simulación de sistemas eléctricos de potencia donde extraiga información fasorial de simulación en el dominio del tiempo de la red de dos áreas modelada en Power Factory DIgSILENT y se envíe mediante un script desarrollado en el lenguaje Python que haga la función de PMU virtual y esta información sea recibida mediante otro script en PyScripter que haga la función de PDC, donde se identifique una aplicación de diferencia angular, para crear una conciencia situacional de sistema eléctrico y establecer posteriormente medidas de protección y control.

1.1. Fundamento Teórico

Los sistemas de gestión de la energía (EMS) se hallan basados en estimadores de estado, teniendo en cuenta la importancia de este campo se hace un estudio de los adelantos conseguidos hasta la presente y las limitaciones existentes, por lo que se analiza las unidades de medición fasorial y tecnologías implicadas con la Norma IEEE C37.118.

1.2. ESTADO DEL ARTE

En la revisión de la normativa para sincrofasores, la primera norma establecida para los sistemas WAMs fue la IEEE 1344-1995, que introdujo los conceptos básicos para la medición sincronizada [12]. Esta norma fue posteriormente reemplazada por la IEEE C37.118-2005, la cual define la medición de fasores sincronizados utilizados en aplicaciones de sistemas de potencia, también define un protocolo de comunicación de datos, no se

abordó el monitoreo dinámico [13], hasta que aparece la IEEE C37.118.1-2011, de carácter informativo que establece la medición de sincrofasores para sistemas de potencia y define la medición de frecuencia, sincrofasorial y ROCOF [14]frequency, and rate of change of frequency (ROCOF, y la C37.118.2-2011 que establece la norma de trasferencia de datos de sincrofasores; en la IEEE C37.118.1aTM-2014 en su enmienda modifica algunos requisitos de rendimiento y actualizaciones para corregir incoherencias introducidas por IEEE Std C37.118.1-2011 [15]and Table 11 (formerly Table 12, mediante la IEC/IEEE 60255-118-1:2018 describe requisitos de marca de tiempo y sincronización para mediciones y establece métodos para evaluar las mediciones de sincrofasores para sistemas de potencia, requisitos para cumplir la norma en condición estática y dinámica.

La literatura muestra que [16] desarrolla e implementa en el centro de control de potencia de la compañía eléctrica de Chubu (Japón) una simulación dinámica para formación de despachadores, donde muestra interés tanto en la modelación, algoritmos de simulación y técnicas del software, ofreciendo a sus alumnos una simulación realista. En Irlanda de Norte [17] ejecuta una simulación en Python PSS/E que ofrece una excelente interface donde se genera gran cantidad de datos y evalúa las WAMs basadas en datos arrojados por PMUs, donde se encuentra la red de distribución acoplada a generación distribuida, concluyen que el control y la seguridad de la red a largo plazo mejora, mientras que a corto plazo se implementa una monitorización y modelado preciso del sistema.

En Tokyo [18] se desarrolla un simulador para entrenamiento de la operación del sistemas de energía que reproduzcan fenómenos eléctricos, ya que uno de los objetivos es mejorar la capacidad de adaptación de los operadores ante contingencias complicadas o catástrofes, también para el estudio de casos de gestión de riesgos en la operación diaria, lo que contribuye al suministro seguro y estable. En Suecia [19] se elabora una simulación en Simulink para modelos de control de alto nivel en sistemas de red VSC-HVDC para lo que realiza simulaciones tanto fuera de línea como en tiempo real para varios escenarios de prueba e indica que este modelado muestra la importancia para mejorar el control de la tensión de CC durante los fallos.

En Ecuador [20], indica que el Centro de Control del Operador Nacional de Electricidad (CENACE), para obtener una estimación del Sistema Nacional Interconectado (SNI), emplea un estimador de estado que proporciona resultados en formato tabular, debido a la falta de herramientas que permitan supervisar el ángulo en tiempo real. En [21], describe los principales compontes del sistema WAMs y en base al análisis establece elementos de estrategias para el diseño e implementación del sistema WAMs en el SNI del Ecuador y afirma que mediante los análisis posoperativos ha sido posible identificar el estado dinámico del sistema. Mientras [22], presenta la aplicación de herramientas de software libre entre otros, el lenguaje de programación Python y asegura ampliamente sus aplicaciones eficientes para análisis numéricos y aplicación en ciencias e ingenierías. En [23] se implementa un prototipo de PMU con el uso de la arquitectura RIO y el software (labVIEW) con el objetivo de proteger, monitorear y controlar el sistema eléctrico ya que cuenta con sistema de monitoreo en tiempo real, permitiendo controlar la inestabilidad de voltaje del sistema frente a contingencias. Mientras en el año 2016 en [24], se establece la regulación sobre requerimientos para la supervisión y control en tiempo real del Sistema Nacional Interconectado (SNI), además de determinar responsables al Sistema Eléctrico Ecuatoriano (SEE) y al Operador Nacional de Electricidad (CENACE).

En [25]es por ello que cada sistema eléctrico requiere de estudios y evaluaciones propias que permitan conocer su dinámica operativa y establecer índices o límites de seguridad con el fin prevenir colapsos totales o parciales.\r Este documento presenta una Metodología para Identificar límites seguros de diferencia angular en un sistema eléctrico de potencia conocidos también como límites de estabilidad estática de ángulo. Para la elaboración de este trabajo se resalta el uso de herramientas tecnológicas modernas de monitoreo y análisis de sistemas de potencia, como el Sistema de Monitoreo de Área extendida (WAMS se presenta una metodología para identificar límites de estabilidad estática de ángulo en el sistema eléctrico basándose en mediciones sincrofasoriales, conjuntamente con la técnica de minería de datos que permitió alertar al operador ante posibles problemas de estabilidad estática y con ello crear conciencia operativa del suministro de energía eléctrica. En [26] se implementa un hardware y un software para sistemas de control que utiliza una tarjeta F28379D de la serie C2000 de TI mediante la interfaz de la plataforma LabVIEW finalmente realiza pruebas convencionales para validar las mediciones realizadas por PMUs de acuerdo a la norma IEEE C37.118.1. En [11] se desarrolla una herramienta computacional para archivar información en una base de datos gratuita y realizar estudios relacionados con los sistemas eléctricos de potencia a través de la interfaz gráfica (GUI) y el programa DIgSILENT PowerFactory mediante programación en Python, importa y exporta datos para guardar dentro de la base de datos SQlite y luego ejecutar flujos de potencia usando formato de programas como Pypower. En [27] se integra los sistemas dinámicos a partir de Matlab y Simulin y DIgSILENT Power Factory en el entorno de co-simulación mediante el protocolo de comunicación OPC evitando que operen cerca de los límites y mejore la seguridad y la confiabilidad del estado estable y dinámico del sistema.

1.3. COMPONENTES DE LA PLATAFORMA WAMS

El sistema de monitoreo de área extendida (WAMS) permite mediciones en tiempo real, mediante combinaciones con tecnologías, sistemas y aplicaciones que suministran la observabilidad dinámica de un sistema de potencia [24], [2], en la Figura 1 se muestra la arquitectura de las WAMs.

Figura 1.

Diagrama de la arquitectura centralizada de las WAMs.

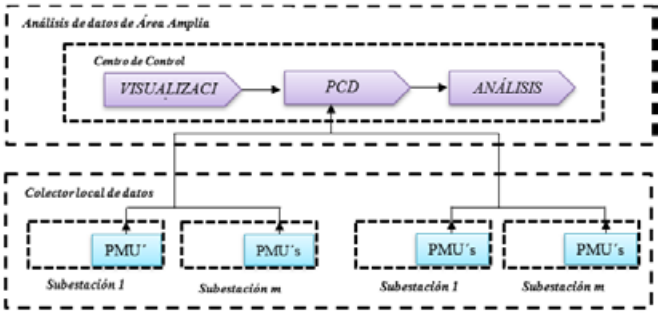

Nota. La figura muestra la estructura general de las WAMS (Wide Area Monitoring Systems).

El sistema WAMS y sus componentes [22].

- Unidad de medición fasorial - PMU
- Concentrador de datos del fasores - PDC
- Sistemas de telecomunicaciones del sistema WAMS
- Servidores de aplicaciones WAMS
- Sistemas de aplicaciones WAMS
- Sistemas registro Historial de información WAMS.

Un PMU es un equipo de medición de fasores de tensión y corriente de la red eléctrica, con periodos en el orden de los microsegundos [20], provoca estaciones de fasores sincronizados de frecuencia y de variación de frecuencia (ROCOF) a partir de señales de voltaje y corriente a través del sincronismo temporal [14]frequency, and rate of change of frequency (ROCOF, [28]based on local and remote voltage synchrophasor measurements through Phasor Measurement Unit (PMU).

El PDC o concentrador de datos de fasor es utilizado en sistemas de medición fasorial [14]frequency, and rate of change of frequency (ROCOF, recibe y almacena la información de datos medidos por los PMUs [21].

Un Sincrofasor es un fasor calculado mediante una señal muestreada que utiliza señal de tiempo estándar como referencia de medidas donde tienen una relación de fase definida [14], la ecuación de forma de onda indica en (1):

$$x(t) = X_m \cos\cos(Wt + \emptyset) \qquad (1)$$

Representado como el fasor como indica en (2)

$$X = \left(\frac{X_m}{\sqrt{2}}\right) e^{j\emptyset} \qquad (2)$$

$$X = \left(\frac{X_m}{\sqrt{2}}\right)(\cos\emptyset + j\sin\emptyset)$$

$$X = X_r + jX_i$$

Donde:

$\left(\frac{X_m}{\sqrt{2}}\right)$: Valor cuadrático medio (RMS)

$X_r + jX_i$: Parte real e imaginaria de un valor complejo

$\emptyset$: Ángulo de fase

φ: Valor que depende de la escala temporal

1.4. APLICACIÓN DE LA HERRAMIENTA COMPUTACIONAL

Disponer de aplicaciones que permitan almacenar paquetes de una base de datos gratuita es el objetivo de la herramienta Open source, permitiendo al usuario obtener una iteración amigable y segura al mismo tiempo, para una conversión de base de datos al sistema eléctrico de potencia, los requerimientos de los programas de simulación cambian a la velocidad del cambio de la realidad, lo que permite el traslado de información de programas de simulación principal a herramientas computacionales. DIgSILENT PowerFactory es un programa de cálculo de redes eléctricas y simulación digital, instrumento muy eficaz de diseño asistido por computadora (CAD) en el análisis de los sistemas eléctricos de potencia. El programa accede el análisis de sistemas heterogéneos para aplicaciones como: industriales de generación, transmisión, distribución, además tiene una peculiaridad especial de integración de funciones de cálculo mediante modelos matemáticos y base de datos, que acelera el procesamiento de datos, y combina capacidad de modelado flexible y altamente confiable con algoritmos de solución altamente eficientes [29].

1.4.1 Generalidades de lenguaje en Python

El lenguaje de programación Python de alto nivel es de interpretado, interactivo y orientado a objetos, de código, intuitivo y práctico fácil de asimilar. Trabaja con varios tipos de datos dinámicos utilizados en lenguaje de clase, en este sentido más allá de la programación orientada a objetos permite múltiples paradigmas de programación, como la programación de procedimientos y funcionales [30].

El script define como agregado de instrucciones escritas dentro de un lenguaje de programación que ordena al software qué hacer. Los lenguajes script utilizan una variable semejante para distintas tipologías de datos, ejecutando una facilidad para el desarrollo de la programación frente a lenguajes copilado en los que una variable es notoria para un tipo de datos fijados y solo puede ser

utilizada para datos de este tipo. De esta manera usando el lenguaje script los desarrolladores son capaces de mezclar códigos con diferentes grados de productividad y para ejecutar un script hay que indicarle al interprete el nombre del programa [31] .

2. MÉTODO

2.1. Flujo de potencia estático de 2 áreas

Se realiza el flujo de potencia en estado estacionario del ejercicio 12.8 del libro Power System Stability and Control, se analiza en detalle los efectos de estructura del sistema como modelado, tipo de excitación y las cargas para determinar características del sistema [32], en la Figura 2 se indica la metodología de estudio.

Figura 2.

Metodología del caso de estudio.

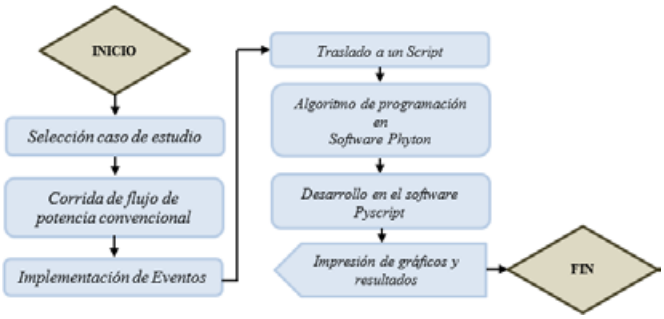

Nota. Representación gráfica de los pasos a seguir para desarrollar el sistema.

En el sistema de prueba para el detalle se procede a realizar el analisis del sistema de potencia, mediante parámetros presentados en el modelo de referencia ejemplo 12.6 (P. Kundur, Power system stability and control [32].

Se pretende simular y monitorear el sistema eléctrico a través de las PMU, el fenómeno en estabilidad estática y transitoria ya que debe tener la habilidad para mantener en sincronismo luego de que experimente un disturbio severo. A continuación, se ejecuta la implementación en el software de simulación Digsilent PowerFactory como se observa en la Figura 3.

Se procede a colocar PMU´s en las barras 1, 3, 7, 8, 9 y 2 para extraer la información fasorial (módulo y ángulo) de voltajes y corrientes para diferentes perturbaciones.

Figura 3.

Flujo de potencia de 2 áreas.

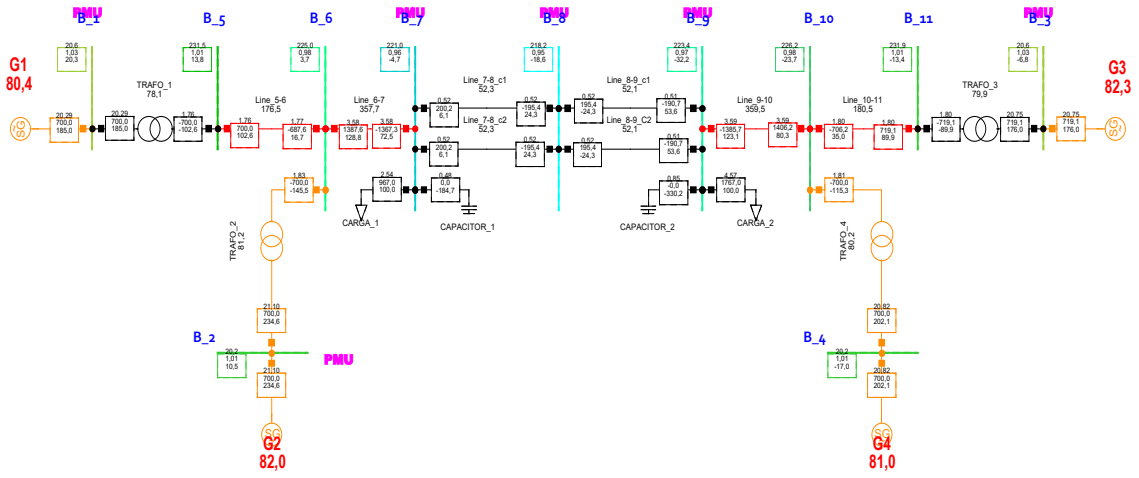

Nota. Caso de estudio implementado en el software Digsilent PowerFactory con la aplicación de PMUs.

A. Creación de eventos de perturbación

Para el análisis fasorial dinámico se procede a definir eventos de perturbación en el SEP como se muestra en la tabla 1.

Tabla 1.

Eventos de perturbación para SEP de 2 áreas.

NOMBRE DE EVENTOS	TIEMPO (s)	ELEMENTO SELECCIONADO
Short-circuit Event	20.	Line_8-9_C2
Swich Event	20.01	Line_8-9_C2
Short-circuit Event(1)	20.01	Line_8-9_C2
Swich Event	21.	Line_8-9_C2
Short-circuit Event(2)	60.	B_7
Short-circuit Event(3)	60.05	B_7
Load Event	100.	CARGA_1
Load Event(1)	110.	CARGA_1
Load Event(2)	150.	CARGA_2
Load Event(4)	155.	CARGA_2

Nota. En la tabla 1 muestra los eventos de perturbación definidos en el sistema para observar su comportamiento.

Se crea 4 eventos dinámicos como falla trifásica en línea de transmisión 8-9 del circuito 2, falla trifásica en barra 7, aumento de carga de 40 % en la carga 1 y un aumento de carga del 50% en la carga 2.

B. Exportación de datos fasoriales

Para el proceso de exportación de datos se realiza la simulación en estado dinámico donde extraemos las señales de voltajes, corrientes en magnitud y ángulo desde Digsilent en archivo .csv como se muestra en la Figura 4.

Figura 4.

Exportación de datos en archivo .csv

Nota. En la figura 4 muestra la extracción de datos, para guardarla en un formato determinado.

De manera de exportar con separación con comas y decimales con puntos en un periodo de registro de al menos 200 segundos.

Figura 5.

Archivo .csv

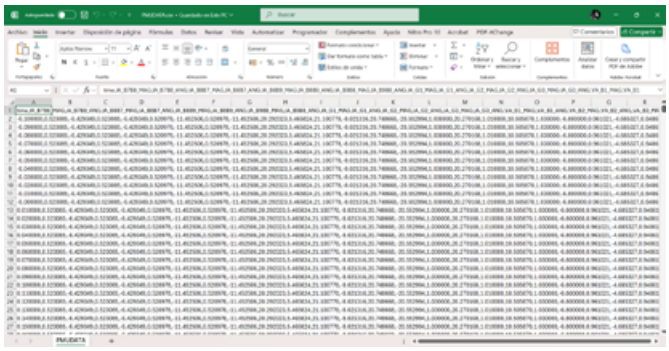

Nota. En la figura 5 apreciamos los datos extraídos del sistema en archivo excel csv, datos que sean fáciles de mover de un programa a otro.

En la Figura 5 podemos observar que los datos guardados se encuentran separados por comas y los decimales se encuentran con puntos, el archivo se encuentra apto para el manejo en el programa Python.

C. Desarrollar un script en Python que permita envió de información sincrofasorial

Para el siguiente código de envío de información se crea una ip ficticia 127.0.0.1 con puerto de enlace 1410.

Además, se implementa el uso de las señales extraídas del archivo .csv para el envío de valores como voltajes y corrientes en magnitud y ángulo en el código de Python.

D. Desarrollar un script en PyScripter que permita la recepción de información sincrofasorial enviada de Python

Como visualización de señales por parte del software Pyscripter colocamos en código la presentación de señales de deferencia angular de la barra 1-7 y 3-9 con su respectivo límite de operación (ver Figura 7), además, potencia activa y reactiva del generador 2.

Se realiza una prueba de conexión con la ip ficticia para visualizar las señales sincrofasoriales con el programa PMU Connection Tester, colocamos la siguiente configuración (ver Figura 8).

3. Resultados y discusión

A. Respuesta de eventos de perturbación

En la Figura 9 se muestra los eventos exportados en base al estudio dinámico del sistema de 2 áreas sin controladores, que muestran en gran magnitud los eventos definidos en el SEP.

A. Envío y recepción de eventos

Se corre la simulaci***ón tanto en*** Python y Pyscripter, dando como resultado la respuesta de diferencia angular B1-B7, B3-B9, potencia activa y reactiva del generador 2 (ver Figura 11).

Como se observa en las Figuras 11 y 12, la respuesta de potencia activa y reactiva del generador 2 dan el mismo resultado, definiendo de esta manera que nuestro sistema de envío y recepción sincrofasorial funciona y está bien programada. Para la visualización de ángulos de los PMU virtuales, se usa el software PMU Connection Tester que da el siguiente resultado (ver Figura 13).

4. Conclusiones

En resumen, los estudios fuera de línea son esenciales para realizar análisis profundos y detallados de eventos. Como se observó, permiten tener un historial de lo ocurrido en el sistema. Cuando un sistema de potencia experimenta una contingencia mientras opera, la prioridad principal es restablecerlo, no analizar el problema en detalle en ese momento. El análisis exhaustivo ocurre una vez que la urgencia de restablecer el sistema ha pasado,

con el objetivo de encontrar la causa raíz del problema y proponer posibles soluciones.

En definitiva, en el estudio se extrajeron datos de respuesta de voltaje y corriente en magnitud y ángulo del software DIgSILENT PowerFactory, tanto sin la implementación de controladores, debido a que se tiene una mejor respuesta en el análisis del sistema frente a los eventos definidos, como se observó en la figura 9, como con controladores. Cabe señalar que al implementar el AVR***´s*** el sistema mostró inestabilidad debido a que pierde amortiguamiento y es necesario la implementación de PSS´s que ayudaron aportar amortiguamiento al sistema y tener una mejor respuesta frente a los eventos definidos como se observó en la figura 10, de tal manera que los tiempos de estabilidad mejoran en comparación al sistema sin controladores que también es estable pero se prolonga en el tiempo.

Después de modelar un sistema eléctrico de dos áreas en el software DIgSILENT PowerFactory, se definieron eventos de perturbación para realizar simulaciones RMS. Luego de exportar la información de voltajes y corrientes a transmitir, se utilizó Python como herramienta de código abierto. Este lenguaje de programación permitió que el script de Python, actuando como PMUs (Unidades de Medición Fasorial), leyera el archivo exportado de DIgSILENT PowerFactory. A través del PMU Connection Tester, se verificó la transferencia de información al software Pyscript, que funcionó como un PDC (Concentrador de Datos Fasoriales). Esto simuló el monitoreo de una red, permitiendo observar la recopilación, procesamiento y transmisión de datos desde un concentrador.

En definitiva, el software desarrollado permitió detectar las características claves de la onda de las variables eléctricas como potencias, voltajes, corrientes que permitan mejorar la estabilidad y confiabilidad del sistema, como se pudo evidenciar en la figura 13, para así lograr la observabilidad del sistema eléctrico que sus aplicaciones le permiten y cumplir el objetivo que es adquirir conciencia situacional del sistema eléctrico.

Referencias

[1] Z. Huang *et al.*, "Performance evaluation of phasor measurement systems," *IEEE Power Energy Soc. 2008 Gen. Meet. Convers. Deliv. Electr. Energy 21st Century, PES*, pp. 1–7, 2008, doi: 10.1109/PES.2008.4596880.

[2] A. Shaobu Wang, R. Huang , X. Ke, J. Zhao, R. Fan, H. Wang, Z. Huang y D. V. Sathanur, "Risk-oriented PMU placement approach in electric power systems," vol. 14, no. 2, pp. 301–307, 2019, doi: 10.1049/iet-gtd.2019.0957.

[3] C. Mishra, K. D. Jones, A. Pal, y V. A. Centeno, "Binary particle swarm optimisation-based optimal substation coverage algorithm for phasor measurement unit installations in practical systems," *IET Gener. Transm. Distrib.*, vol. 10, no. 2, pp. 555–562, 2016, doi: 10.1049/iet-gtd.2015.1077.

[4] A. DelaTorre, "Análisis técnico para la Implementación de un Sistema de Monitoreo de Área Extendida (Wams) en el Sistema Nacional Interconectado del Ecuador," Universidad Politécnica Salesiana sede Quito, 2013.

[5] A. G. Phadke, "Synchronized phasor measurements a historical overview -," pp. 476–479, 2002.

[6] A. Jovičić, "COMPUTAT IONALLY EFF ICI ENT STATE ESTIMATION FOR POWER SYSTEMS WITH CONVENTIONAL AND SYNCHROPHASOR MEASUREMENTS," University of Belgrade, 2021.

[7] S. C. G. Cruz, "Esquema de Monitoreo Integrado de Seguridad de Sistemas de Potencia," Universidad de los Andes, 2016.

[8] U. Kerin, G. Bizjak, R. Krebs, E. Lerch, and O. Ruhle, "Faster than real time: Dynamic security assessment for foresighted control actions," *2009 IEEE Bucharest PowerTech Innov. Ideas Towar. Electr. Grid Futur.*, pp. 1–7, 2009, doi: 10.1109/PTC.2009.5282087.

[9] I. Chychykina, Z. A. Styczynski, C. O. Heyde, and R. Krebs, "Power system instability prevention and remedial measures with online Dynamic Security Assessment," *2015 IEEE Eindhoven PowerTech, PowerTech 2015*, 2015, doi: 10.1109/PTC.2015.7232303.

[10] Diego Aguas, "Implementación de una plataforma de simulación digital en tiempo real para entrenamiento de operadores ante fenómenos dinámicos," ESCUELA POLITÉCNICA NACIONAL, 2020.

[11] D. Pérez Llamuca, "Herramienta computacional en software libre para conversión de bases de datos del sistema eléctrico de potencia entre diferentes plataformas de simulación," 2021. [Online]. Available: https://bibdigital.epn.edu.ec/handle/15000/21575?mode=full

[12] IEEE, *IEEE Std 1344-1995(R2001) : IEEE Standard for Synchrophasers for Power Systems.*, vol. 1995. 1995.

[13] IEEE Power Engineering Society, *IEEE Std C37.118-2005*, vol. 2005, no. March. 2005. [Online]. Available: http://ieeexplore.ieee.org/xpls/abs_all.jsp?arnumber=660853

[14] IEEE-SA Standards Board, *IEEE Standard for Synchrophasor Measurements for Power Systems*, vol. C37.118.1™, no. December. 2011.

[15] P. System, R. Committee, I. Power, y E. Society, "IEEE Standard for Synchrophasor Measurements for Power Systems -- Amendment 1: Modification of Selected Performance Requirements," *IEEE Std C37.118.1a-2014 (Amendment to IEEE Std C37.118.1-2011)*, vol. 2014, pp. 1–25, 2014.

[16] K. Sato, Z. Yamazaki, T. Haba, N. Fukushima, K. Masegi, y H. Hayashi, "Dynamic simulation of a power system network for dispatcher training," *IEEE Trans. Power Appar. Syst.*, vol. PAS-101, no. 10, pp. 3742–3750, 1982, doi: 10.1109/TPAS.1982.317059.

[17] P. Brogan, J. Morrow, R. Best, y D. Laverty, "Python PSS/E simulation to test efficacy of proposed PMU based WAMS and potential WAMPAC applications," *Proc. Univ. Power Eng. Conf.*, pp. 1–5, 2013, doi: 10.1109/UPEC.2013.6714952.

[18] T. Kataoka, M. Shitsukawa, y A. Tajimi, "Improvement in coordinated restoration operation skills covering more than one area (Developing a power system operation training simulator that precisely reproduces electrical phenomena)," *44th Int. Conf. Large High Volt. Electr. Syst. 2012*, 2012.

[19] M. R. Hasan, L. Vanfretti, W. Li, y N. A. Khan, "Generic high level VSC-HVDC grid controls and test systems for offline and real time simulation," *9th Int. 2014 Electr. Power Qual. Supply Reliab. Conf. PQ 2014 - Proc.*, pp. 57–64, 2014, doi: 10.1109/PQ.2014.6866784.

[20] G. J. Araque y R. Barba, "Unidades de Medición Fasorial - PMU," pp. 247–253, 2010.

[21] G. Rivera y A. D. La Torre, "Estrategias para la Implementación de un Sistema de Monitoreo de Área Extendida WAMS en el Sistema Nacional Interconectado del Ecuador," *Rev. Técnica "Energía,"* vol. 9, no. 1, pp. 34–43, 2013, doi: 10.37116/revistaenergia.v9.n1.2013.134.

[22] R. C. H. Lara, "Herramientas de Software Libre para Aplicaciones en Ciencias e Ingeniería," *Rev. Politécnica*, vol. 32, no. 1, pp. 1–8, 2013, [Online]. Available: http://revistapolitecnica.epn.edu.ec/ojs2/index.p

[23] A. Villamarín, y D. Espín, "Diseño e Implementación de un Prototipo de Unidad de Medición, Fasorial (PMU - Phasor Measurement Unit) para el Monitoreo, Control y Protección de Sistemas Eléctricos". *Revista Técnica "Energía"* No. 11, pp. 127–135, 2015.

[24] E. Arconel, "REGULACIÓN No. ARCONEL – 003/16 Requerimientos para la supervisión y control en tiempo real del Sistema Nacional Interconectado," pp. 1–27, 2016.

[25] L. Bonilla y R. Cubillo, "Determinación de límites de seguridad estática de ángulo en el SNI a partir de mediciones sincrofasoriales," *Rev. Técnica "Energía,"* vol. 15, no. 1, pp. 90–97, 2018.

[26] P. M. Pozo, I. A. Pozo, and N. A. Pozo, "Design and Construction of a Low-Cost Phasor Measurement Unit (PMU) for Three-Phase Distribution Power Systems according to the norm IEEE Diseño e Implementación de una (PMU) de baja potencia para Sistemas," no. 16, pp. 8–16, 2019.

[27] L. L. Chiza, "Co-simulation between PowerFactory and Matlab / Simulink for the simulation of an HVDC link integrated to the 39-bus system Co-simulación entre PowerFactory y Matlab / Simulink para la simulación de un enlace HVDC integrado al sistema de 39 barras," no. 19, pp. 150–157, 2022.

[28] R. Franco, "Uso de Sincrofasores para la Detección de Oscilaciones de Potencia y Pérdida de Sincronismo . Aplicación al Sistema Eléctrico Uruguayo para la Separación Controlada en Islas" Universidad de la República de Uruguay, 2012.

[29] F. Gonzalez Longatt, "DIgSILENT PowerFactory (Manual de Usuario)," no. April, pp. 1–2, 2004, [Online]. Available: file:///C:/Users/Personal/Downloads/Manual_de_Usuario_DIgSILENT_Parte_I.pdf

[30] R. Gonzá and Lez, *Python Para todos*. 2015.

[31] M. Pérez Domínguez, "Extensión de Aplicaciones mediante Python embebido," ESCUELA TÉCNICA SUPERIOR DE INGENIERÍA Y SISTEMAS DE TELECOMUNICACIÓN, 2017.

[32] P. Kundur, "Power System Stability and Control - Prabha Kundur - McGraw-Hill Education." p. 1176, 1994. [Online]. Available: https://www.mheducation.co.in/html/9780070635159.html

ANEXOS

Figura 6.

Script para envío de información sincrofasorial.

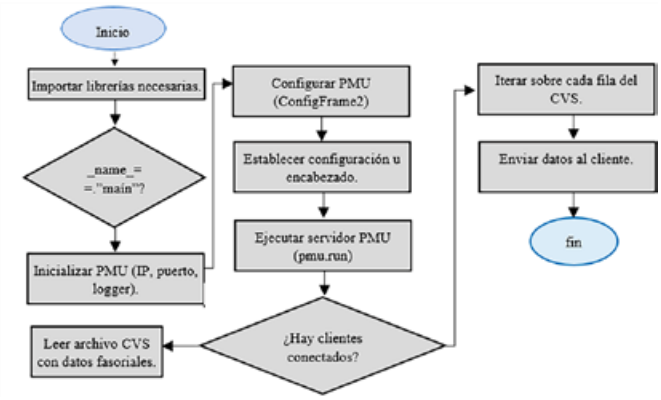

Nota. En la figura 6 hace referencia al protocolo TCP/IP de la máquina que esté funcionando correctamente y el puerto garantiza la entrega del paquete de datos en orden.

Figura 7

Script para recepción de información sincrofasorial.

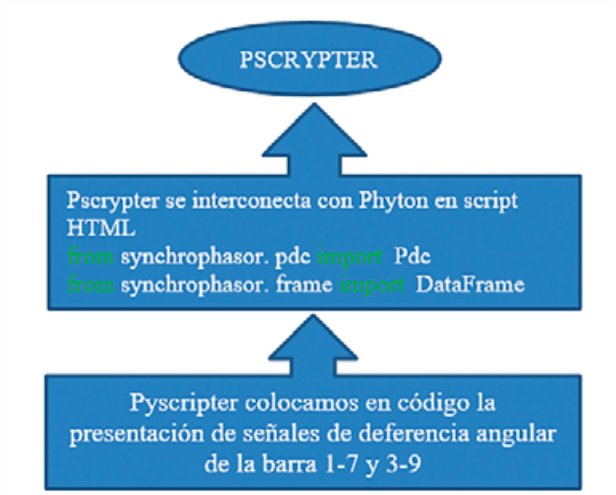

Nota. En la figura 7 muestra el sistema Pyscripter donde se interconecta el código Python en un script HTML.

Figura 8.

Configuración del PMU Connection Tester.

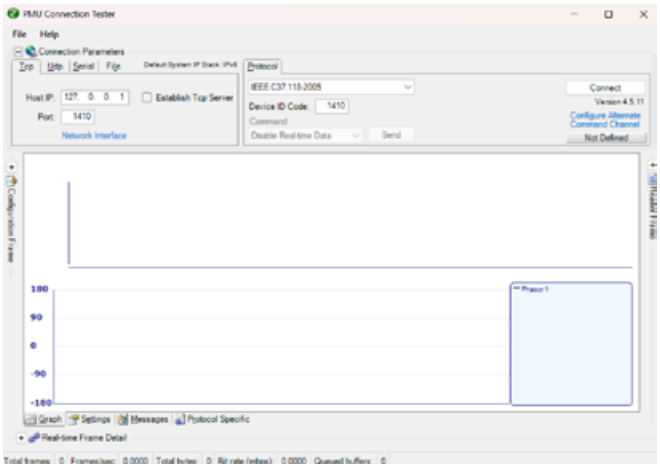

Nota. En la figura 8 se observa el ingreso de la IP en la dirección de internet del dispositivo probado y en el puerto, el número de puerto que se conecta al dispositivo y recibe datos del mismo.

Figura 9.

Eventos definidos de perturbación del SEP sin controladores.

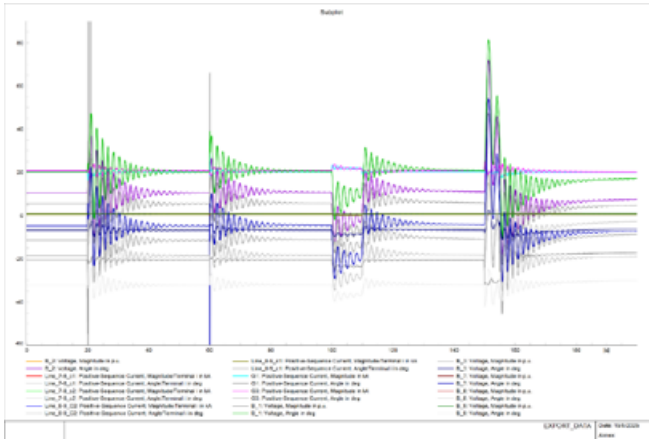

Nota. En la figura 9 se verifica los eventos provocados en el SEP sin controladores los mismos que podrían ser interrupciones, variaciones de voltaje, frecuencia o sobre corriente.

Figura 10.

Eventos definidos de perturbación del SEP con controladores AVR y PSS.

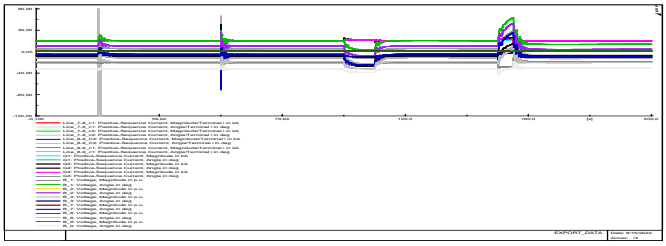

Nota. En la figura 10 se puede apreciar como el estabilizador del sistema de potencia y el regulador automático de voltaje controlan la tensión y las oscilaciones en el sistema eléctrico.

Figura 11.

Gráfica de respuesta por Pyscripter.

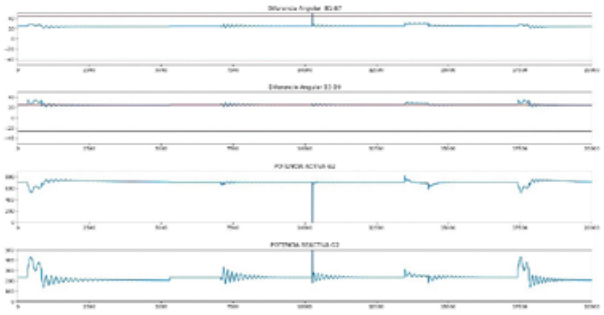

Nota. En la figura 11 se puede observar el grafico creado en Pyscript mediante la ejecución de Python donde se visualiza como resultado la diferencia angular de las barras seleccionadas.

Figura 12.

Gráfica de respuesta de potencia activa y reactiva del generador 2 por Digsilent.

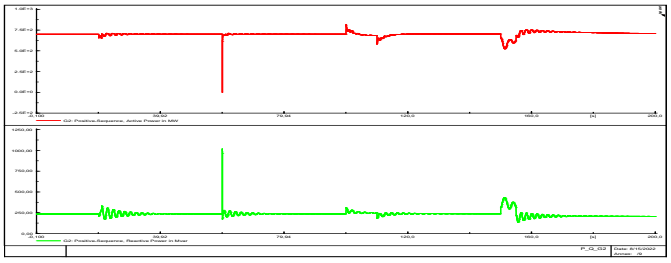

Nota. Mediante el software de gran alcance como digsilent se puede apreciar las gráficas de potencia activa y reactiva las mismas que fueron entregadas por el programa para su análisis.

Figura 13.

Gráfica de respuesta por PMU Connection Tester.

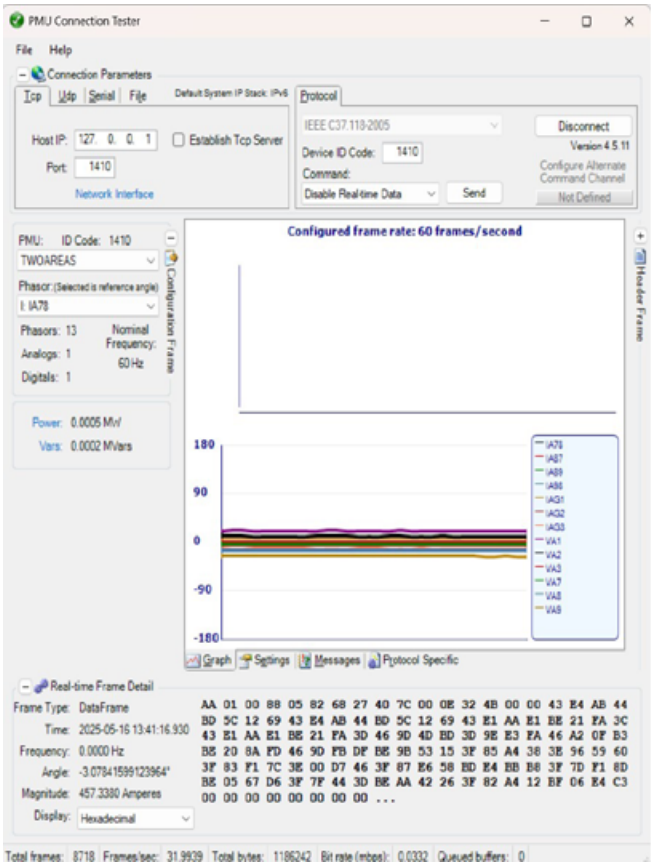

Nota. En la figura 13 se observa el probador de conexión PMU que verifica la recepción de flujo de datos de medición fasorial y valida la conexión de flujos de dispositivos, además se visualiza gráficamente los datos sincrofasoriales.

FACULTAD DE INGENIERÍA Y CIENCIAS APLICADAS
UNIVERSIDAD CENTRAL DEL ECUADOR

INGENIO
2025, VOL 8(2), JULIO - DICIEMBRE, PP. 95-106

REVISTA INGENIO

Valorization of Sugarcane Bagasse into Nano-Silica: Optimized Route for Enhancing Strength and Sustainability in Cement Mortars

Valorización del Bagazo de Caña de Azúcar en Nanosílice: Ruta Optimizada para Mejorar la Resistencia y la Sostenibilidad en Morteros de Cemento

Mohammadfarid Alvansazyazdi | Universitat Politécnica de Valencia - España
Jenny Estefany Chandi Paucar | Universidad Central del Ecuador- Ecuador
Fausto Enrique Chavez Guaman | Universidad Central del Ecuador- Ecuador
Pablo Mauricio Bonilla Valladares | Universidad Central del Ecuador- Ecuador
Debut Alexis Patrice Martial | Universidad de las Fuerzas Armadas - Ecuador
Jorge Luis Santamaria Carrera | Universidad Central del Ecuador- Ecuador
Hugo Alexander Cadena Perugachi | Universidad Central del Ecuador- Ecuador
Andrea Estefania Logacho Morales | Universidad Central del Ecuador- Ecuador

Recibido: 29/4/2025
Recibido tras revisión: 19/5/2025
Aceptado: 6/6/2025
Publicado: 10/7/2025

PALABRAS CLAVE
Nanomateriales, Partículas de nano-sílice, Morteros de cemento, Propiedades mecánicas, Hidrofobicidad del mortero

RESUMEN
La presente investigación tiene como objetivo evaluar la influencia de la adición de nanopartículas de sílice derivadas del bagazo de caña de azúcar, sintetizadas en el laboratorio mediante el método sol-gel, sobre las propiedades del mortero de cemento en estado fresco y endurecido. En el estado fresco, se analizan la trabajabilidad, la consistencia y la fluidez, mientras que en el estado endurecido se evalúan la resistencia a la compresión y la hidrofobicidad. Se prepararon especímenes utilizando cementos Tipo N y Tipo HS, con la adición de nanopartículas de sílice en proporciones de 0,25 %, 0,50 %, 0,75 %, 1,00 % y 1,50 % en peso, como reemplazo del cemento en el mortero de control. Los resultados revelaron que el 0,25 % de nano-sílice fue el porcentaje de adición óptimo para ambos tipos de mortero. Además, se observó que tanto las propiedades en estado fresco como en estado endurecido se vieron afectadas negativamente a medida que aumentaba el porcentaje de nano-sílice. La resistencia a la compresión aumentó en un 9 % a los 28 días y en un 12 % a los 56 días para el mortero con cemento Tipo N; mientras que, para el mortero con cemento Tipo HS, el incremento fue del 9 % a los 28 días, 10 % a los 56 días y 5 % a los 90 días. La prueba del ángulo de contacto indicó que las nanopartículas de sílice reducen la permeabilidad de los morteros, siendo los especímenes elaborados con cemento Tipo N los que presentaron una mayor impermeabilidad en comparación con aquellos elaborados con cemento Tipo HS.

KEY WORDS
Nanomaterials, Nano-silica particles, Cement mortars, Mechanical properties, Mortar hydrophobicity

ABSTRACT
The present research aims to evaluate the influence of adding silica nanoparticles derived from sugarcane bagasse, synthesized in the laboratory using the sol-gel method, on the properties of cement mortar in both its fresh and hardened states. In the fresh state, the study examines workability, consistency, and flow, while in the hardened state, it evaluates compressive strength and hydrophobicity.
Specimens were prepared using Type N and Type HS cement, with the addition of nano-silica particles at 0.25%, 0.50%, 0.75%, 1.00%, and 1.50% by weight as a replacement for cement in the control mortar. The results revealed that 0.25% nano-silica was the optimal addition percentage for both mortars. Moreover, it was found that both fresh and hardened properties were negatively affected as the percentage of nano-silica increased. The compressive strength increased by 9% at 28 days and 12% at 56 days for the Type N cement mortar, while for the Type HS cement mortar, the strength increase was 9% at 28 days, 10% at 56 days, and 5% at 90 days. The contact angle test indicated that nano-silica particles reduce the permeability of the mortars, with specimens made with Type N cement exhibiting greater impermeability compared to those made with Type HS cement.

1. Introduction

Construction is one of the industries that generates the most carbon footprint in the world, as the materials it relies on are mainly cement-based, which requires a considerable amount of energy and the exploitation of non-renewable resources for its production [1]. According to the UN, the construction sector is responsible for more than 34% of energy demand and around 37% of CO2 emissions during 2021 [2].

https://doi.org/10.29166/ingenio.v8i2.8164

pISSN 2588-0829
eISSN 2697-3243
fing.revista.ingenio@uce.edu.ec

In recent years, there has been a proposal to reduce cement use in construction by replacing it with industrial, agricultural, and other byproducts, one of which is sugarcane bagasse.

Sugarcane is produced worldwide, and according to the FAO, global sugar consumption is expected to increase over the next 10 years, with sugarcane continuing to account for more than 85% of sugar crop production [3]. Once the raw material is extracted from this plant, a residue is generated, the sugarcane bagasse [4].

Nanotechnology has been researched and introduced in the construction industry, specifically in the production of concrete and mortars, aiming to improve the physical and mechanical performance of cements added with certain types of nanometric particles such as silica dioxide, graphene, iron oxide, zinc oxide, carbon nanotubes, titanium dioxide, among others [5], [6], [7], [8], [9]. These have resulted in higher strength, greater durability, and more contributions to sustainable construction [10].

The integration of innovative methodologies, as seen with the application of information and communication technologies (ICTs) in educational settings, parallels the transformative impact of nanomaterials in enhancing the sustainability and efficiency of construction practices [10].

The development of advanced construction materials not only depends on material science innovations but also on the systematic management of experimental data and project progress, where tools such as web-based executive dashboards have proven to be critical [11].

Moreover, the ability of organizations to rapidly adapt and integrate emerging technologies, such as nano-silica derived from agricultural waste, is fundamental for innovation and competitiveness in sustainable construction [12].

A sustainable material with a wide range of applications is silica dioxide (SiO2), which occurs naturally as quartz and can be extracted from sand and other minerals. Another source of SiO2 is plants, and therefore, this compound can be extracted from agro-industrial waste, such as sugarcane bagasse [13]. According to the Ibero-American Agency for the Diffusion of Science and Technology (DICYT), the chemical composition of sugarcane bagasse ash is dominated by silica oxide, with alumina and iron oxide content, which can react with calcium hydroxide in cement hydration and produce materials that improve the mechanical and durability properties of concrete [14].

Nanosilica consists of nanometric-sized particles of SiO2, which possess pozzolanic properties that react with portlandite and improve its properties [15]. Due to its size, it can group together in the small pores of the cement paste, closing them or reducing their size, decreasing permeability by making the mortar denser and enhancing its mechanical properties [17]. The incorporation of this addition results in a reduction in cement requirements, while increasing the demand for mixing water due to the high specific surface area of the nanomaterial [16].

Studies on the incorporation of nanosilica in construction materials support the aforementioned benefits of this material on the properties of concrete [17], [18], [19], [20], [21], [22], paving stones [23], and mortars [24], [25], [26]. This improvement in properties positions nanosilica as an advanced solution for more durable and sustainable construction [29].

Given the above, this study aims to analyze the modification of the properties of mortars in both the fresh and hardened states, with additions of SiO2 nanoparticles derived from sugarcane bagasse in percentages of: 0.25%, 0.50%, 0.75%, 1.00%, and 1.50% by weight as a partial replacement for cement, as a positive factor in reducing the environmental impact generated by agro-industrial waste and the construction industry [30].

2. Materials y Methods

2.1 MATERIALS

2.1.1. Cement

Two types of cement were used: Maestro by Holcim (Type N cement) and Campeón by Selvalegre (Type HS cement).

2.1.2. Fine Aggregate

The fine aggregate was sourced from Santo Domingo, with a density of 2.69 g/cm³ and an absorption capacity of 1.7%. Its granulometry meets the grading limits for natural sand established in INEN 2536 [27].

Additionally, the organic impurities in the fine aggregate were assessed, revealing a low impurity content. The quantity of lightweight and friable particles was within the limits set by NTE INEN 699 and 698, respectively.

2.1.3. Nanosílice derived from sugarcane bagasse

The silica nanoparticles were obtained in the laboratory from sugarcane bagasse waste through a multi-step extraction process that includes: 1. Conditioning of the material: drying and grinding of sugarcane bagasse, 2. Calcination of the material: pyrolysis using a Bunsen burner and transformation into ashes using a muffle furnace, 3. Acid treatment of the ashes: reflux in HCl and HNO_3 acids, 4. Purification of the ashes: reflux in NaOH, and 5. Precipitation of the product: application of the sol-gel method to obtain silica particles [13], [28]. Figure 1 indicates the process carried out to obtain silica nanoparticles from sugarcane bagasse.

The mentioned procedure was performed four times (four cycles) to obtain the desired amount.

Table 1 shows the quantities of each material used per cycle, as well as the final amounts.

Table 1

*Quantities **o**f each material used per cycle*

Cycle	*Bagasse (kg)*	*Ashes (g)*	*HCl (ml)*	*HNO_3 (ml)*	*NaOH (ml)*
1	0.33	14.9	59.8	50.0	50.0
2	0.65	10.1	60.5	50.0	100.0
3	34.97	427.6	855.1	420.0	696.6
4	44.56	203.8	507.6	210.0	600.0
Total	80.51	656.4	1483.0	730.0	1446.6

Table 2 presents the quantities of nano-silica obtained from sugarcane bagasse in each cycle, as well as the yield per cycle and the overall yield of this material.

Table 2

Quantities of nanosilica obtained from sugarcane bagasse per cycle and its yield

Cycle	*Nanosilica obtained (g)*	*Yield (%)*
1	1.8	0.542
2	3.6	0.556
3	208.6	0.596
4	254.4	0.571
Total	468.4	0.566

Figure 1

Laboratory process for obtaining nanosilica derived from sugarcane bagasse

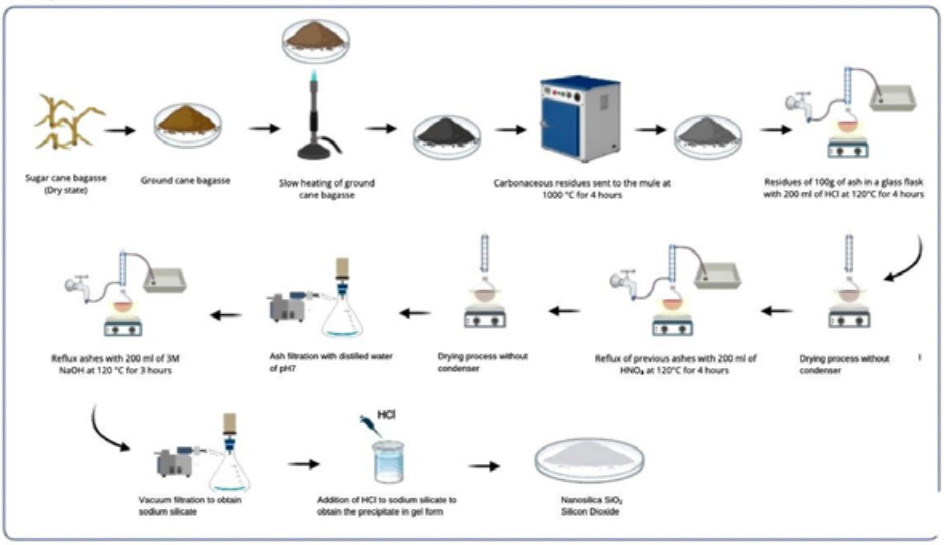

The optimization of the synthesis parameters, including acid concentration and reflux cycles, plays a crucial role in maximizing the quality and yield of nano-silica. Similar optimization strategies have been successfully applied in surface engineering through the use of NSGA-II algorithms [29]. The characterization of the nano-silica particles obtained from sugarcane bagasse was performed using the following laboratory techniques:

2.1.3.1. Scanning Electron Microscopy (SEM)

Figure 2 shows a surface with a rough and heterogeneous texture, composed of particles varying in size and shape. The distribution of shades suggests the presence of elevated areas (brighter) and deeper regions (darker). The highly agglomerated structure indicates a material with a high specific surface area, which is characteristic of nanoparticles.

Figure 2

SEM test conducted by the Microscopy Laboratory, ESPE, on the nanosilica sample obtained with a 1μm scale.

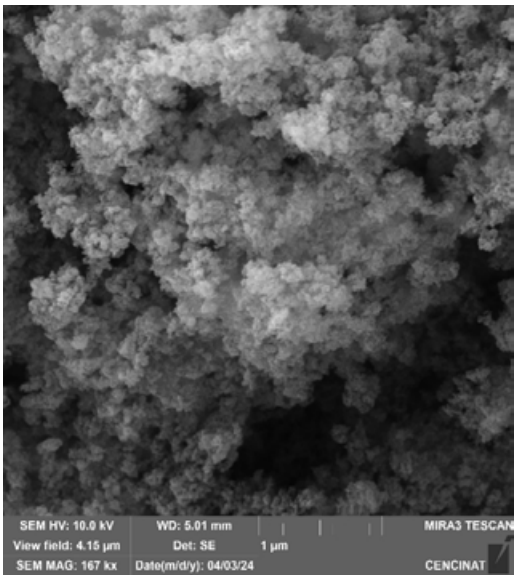

2.1.3.2. Transmission Electron Microscopy (TEM)

Figure 3 shows that the SiO_2 nanoparticles tend to agglomerate, possibly due to attractions generated by the differences in electronegativity between O and Si atoms. The 100 nm scale allows visualization of particles smaller than 100 nm, confirming that this material qualifies as a nanomaterial.

Figure 3

TEM test conducted by the Microscopy Laboratory, ESPE, on the nanosilica sample obtained with a 100 µm scale.

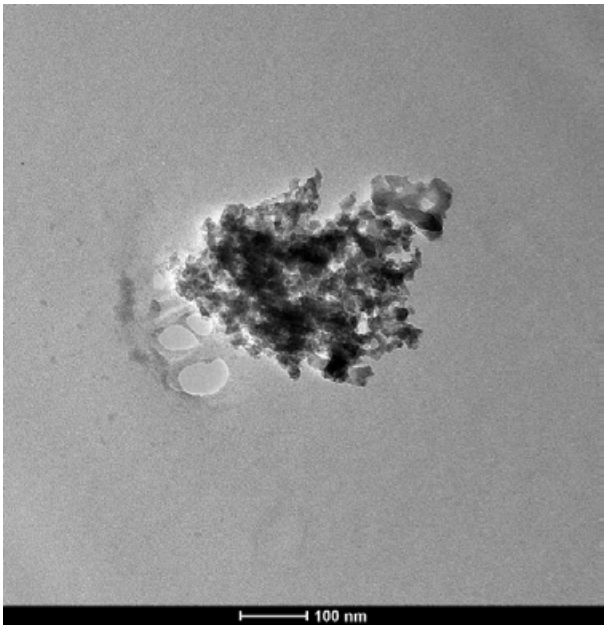

2.1.3.3. X-ray Diffraction (XRD)

Narrower peaks indicate larger crystals, while wider peaks may indicate smaller crystal sizes. However, it maintains the characteristic pattern of nano-silica proposed by Puerto Suárez. [17]

Figure 4

XRD analysis performed on the nanosilica sample.

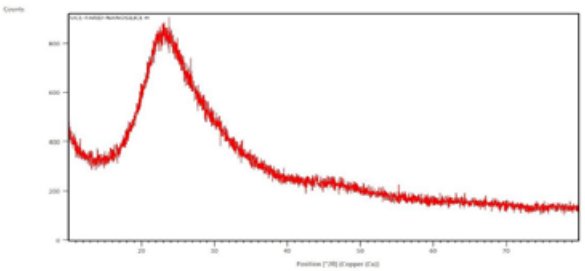

2.1.3.4. Energy Dispersive Spectroscopy (EDS)

The elements Si and O from SiO2 were identified in the sample. The percentages obtained for each element are close to the ratio that represents SiO2, with 2 parts of O for every part of Si (66.10% for O and 25.37% for Si).

Tabla 3

Components and percentages present in the sample.

Element	*Amount present in the sample.*
Oxygen (O)	66.10 %
Sodium (Na)	6.42 %
Aluminium (Al)	1.24 %
Silicon (Si)	25.37 %
Iron (Fe)	0.88 %
TOTAL	100 %

2.2 METHODS

2.2.1. Mixture Proportioning

The proportioning used was selected based on NTE INEN 1806 [30], which specifies the commonly used cement: sand ratio in construction of 1:3. The amount of water was selected based on mortar flow tests.

Two types of mortar were prepared: with type N cement and type HS cement. The proportions are shown in Table 4.

Table 4

Quantities for 9 specimens of standard mortar.

Material	Weight (g)	Ratio
Type N Cement		
Cement	740.0	1
Sand	2220.0	3
Water	437.3	0.54
Type HS Cement		
Cement	740.0	1
Sand	2220.0	3
Water	429.9	0.53

Once the weight quantities of each material for the reference mortar are determined, the weight of the cement is replaced with each percentage of nanosilica that is to be added to the mixture (see Table 5).

Table 5

Quantities for 9 specimens of mortar with the addition of nanosilica particles.

Material	Quantity in weight of the materials (g)				
	0.25%	0.50%	0.75%	1.00%	1.50%
Type N Cement					
Cement	738.1	736.3	734.4	732.6	728.9
Sand	2220	2220	2220	2220	2220
Water	437.3	437.3	437.3	437.3	437.3
Nanosilica	1.85	3.70	5.55	7.40	11.10
Type HS Cement					
Cement	738.1	736.3	734.4	732.6	728.9
Sand	2220	2220	2220	2220	2220
Water	437.3	437.3	437.3	437.3	437.3
Nanosilica	1.85	3.70	5.55	7.40	11.10

2.2.2. Mixing procedure

The nanosilica particles must undergo a predispersal to obtain stable suspensions before being integrated into the mortar mixture, as their high specific surface area can cause particle agglomeration that hinders the proper combination of the mortar materials [18]. To prepare the nanosilica suspension, a high-shear mixer was required. A portion of the mixing water, along with the nanosilica, was mixed for 120 seconds at 1000 rpm.

To prepare the mortar mixtures, the water and the nanosilica suspension were placed in the mixer, the cement was added and mixing continued for 3 minutes at low speed. The fine aggregate in a dry condition was then added to the mixer, mixing for 30 seconds at low speed, then for another 30 seconds at medium speed. The process was paused, and the mixture was allowed to rest for 90 seconds. After this time, the mixture was mixed again for an additional 60 seconds.

2.2.3. Optimal Nanosilica Addition Percentage

Immediately after mixing, the flowability of the fresh mixtures was measured according to NTE INEN 2502 [31], which specifies a flow of 110 ± 5 in 25 drops on the flow table.

The results of the fresh-state mortar tests, Table 4, show that with the incorporation of nanosilica particles into the mortar, there is a loss of workability as the percentage of nanosilica added increases. In other words, the higher the amount of nanosilica, the lower the flowability of the mixture. The mixtures with 0.25% and 0.50% nanosilica with type N and type HS cement exhibited medium workability and were found to be easy to handle and apply. However, starting from 0.75% addition, it was observed that the consistency of the mixtures shifted from plastic to dry over time. As the percentage of addition increased, this decreased the workability of the mixtures, making them more difficult to handle.

The analysis of the fresh-state properties indicates that the mixtures with both types of cement are negatively affected by the increase in nanosilica quantity added. However, the mixtures with 0.25% nanosilica addition presented the best results in terms of workability, consistency, and flowability.

Subsequently, a compressive strength test was performed according to NTE INEN 488 [32] on the hardened mortar specimens. Nine specimens were made for both the reference mixture and the mixtures with nanosilica addition using the two types of cement (Total 108 specimens). The tests were carried out at 1, 3, and 28 days for type N cement and 1, 3, and 7 days for type HS cement (The difference in testing ages is due to the strength each type of cement can achieve).

Graph 1

Incremento de la resistencia a la compresión (%) vs Tipo de mortero, cemento tipo N

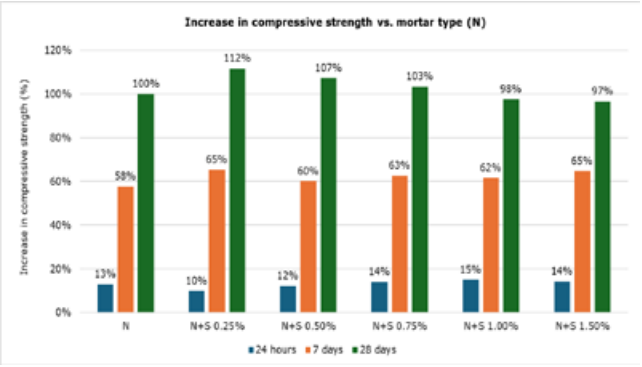

Graph 1 shows the compressive strength as a percentage for the different mixtures, taking the compressive strength of the reference mortar at 28 days as 100%. It can be observed that the greatest increase in strength for the mortar with type N cement is achieved with a 0.25% addition of nanosilica, reaching 12% more strength compared to the reference mixture.

Graph 2

Incremento de la resistencia a la compresión (%) vs Tipo de mortero, cemento tipo HS

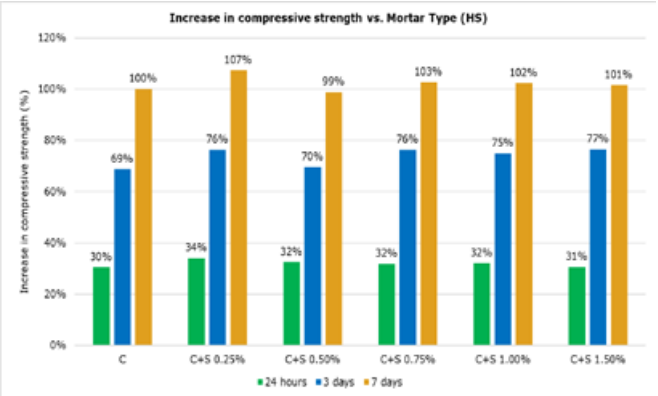

Graph 2 shows the compressive strength as a percentage for the different mixtures with type HS cement, taking the compressive strength of the reference mortar at 7 days as 100%. It can be observed that the greatest increase in strength for the mortar is achieved with a 0.25% addition of nanosilica, reaching 7% more strength compared to the reference mixture.

The analysis of the hardened-state specimens with the two types of cement used indicates that the addition of nanosilica improves compressive strength. However, it is observed that high percentages do not seem to generate significant improvements in strength and may even negatively affect it, suggesting that there is a limit to the amount of nanosilica that can be added. It is observed in both types of cement that the 0.25% nanosilica addition percentage is the one that allows for the highest strength in mortars.

Therefore, a 0.25% addition of nanosilica is established as the optimal percentage, and the preparation of the final specimens is carried out to obtain better statistics and confirm the results for comparison with the reference sample.

3. Results

3.1 MECHANICAL PROPERTIES

A total of 10 mortar specimens were prepared for each mixture type, i.e., reference mixture and mixture with 0.25% nanosilica addition for each testing age: 1, 3, 7, 28, 56, and 90 days, and each type of cement used (Total 240 specimens). Table 5 presents the arithmetic mean value of the compressive strength results for the reference mixture specimens and the mixture with 0.25% nanosilica addition from sugarcane bagasse.

Type N Cement

Table 7 shows that, at 24 hours, the mixture with 0.25% nanosilica exhibits a decrease of 0.6 MPa in strength compared to the reference mixture, which had a strength of 0.9 MPa. The same behavior was observed up to 3 days, with the reference mortar reaching 2.6 MPa and the mortar with 0.25% nanosilica reaching 2.1 MPa. This suggests that the initial decrease in the mortar's strength is attributed to the addition of nanosilica.

Starting from 7 days, the mortar with nanosilica addition shows higher strength than the reference mortar. The reference mortar achieved 3.7 MPa, while the mortar with nanosilica reached 4.2 MPa. At 28, 56, and 90 days, the trend of increased strength continued for the mixture with nanosilica addition, indicating that, in the long term, the addition of nanosilica provides positive benefits in terms of strength.

This behavior can be observed in Graph 3, which shows that the highest strengths over time were achieved by the mortar with 0.25% nanosilica.

Graph 3

Compressive strength vs. age of mortar (Type N)

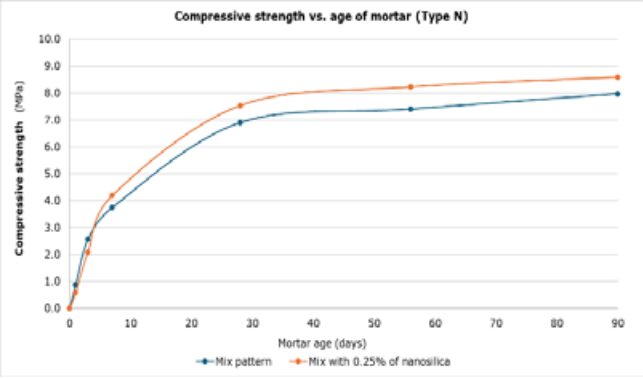

In Graph 4, the percentage increase in compressive strength between the reference mortar and the mortar with 0.25% nanosilica addition is shown. A strength increase of 9% was achieved at 28 days, 12% at 56 days, and 9% at 90 days.

Graph 4

Increase in compressive strength (%) vs. age of mortar (Type N)

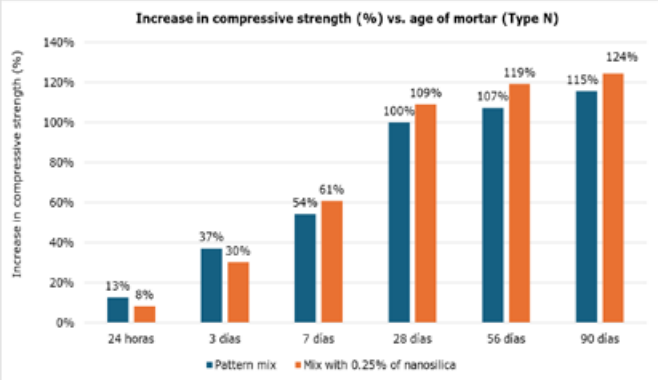

Type HS Cement

Graph 5 shows the increase in compressive strength of the mortar with nanosilica addition starting from the first day, where a strength of 5.9 MPa is observed compared to the 5.0 MPa reached by the reference mortar. This growth trend continues until the 90-day age, where the mortar with 0.25% nanosilica reaches a strength of 36.8 MPa, compared to the 34.0 MPa of the reference mortar.

This behavior can be observed in Graph 5, which shows that the highest strengths over time were achieved by the mortar with 0.25% nanosilica.

Graph 5

Compressive strength vs. age of mortar (Type HS)

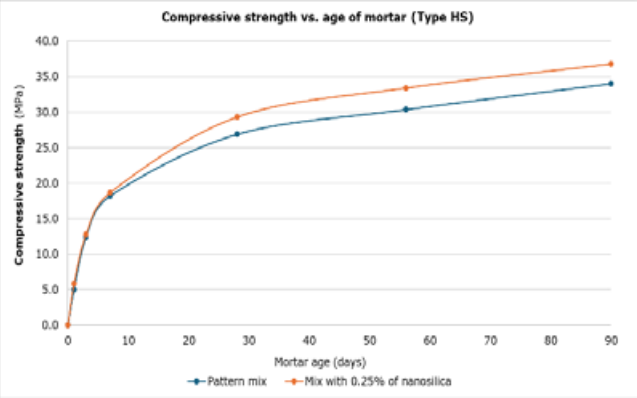

In Graph 6, the percentage increase in compressive strength between the reference mortar and the mortar with 0.25% nanosilica addition is shown. A strength increase of 9% was achieved at 28 days, 10% at 56 days, and 10% at 90 days.

The results presented demonstrate the benefits of nanosilica addition in this study, with 0.25% sugarcane bagasse nanosilica, in increasing the compressive strength of mortars with type N cement and mortars with type HS cement.

After performing the compressive strength tests, a contact angle test was conducted to determine the hydrophobicity of the specimens. It was decided that the test would be carried out at 28, 56, and 90 days for both the reference mortar specimens and those with sugarcane bagasse nanosilica addition, as the mortar reaches its maximum strength at this age.

To perform the contact angle test, the surface of the specimens was cleaned to remove any dust, impurities, or detachment. A drop of water was then placed on the smoothest and least porous surface of the specimen using a micro needle, which allowed a small drop to be placed. Using a laboratory microscope, the behavior of the water drop on the mortar surface was observed (whether it is absorbed or not). Images were captured with a smartphone camera, and through the ImageJ software, the angle formed between the water drop and the mortar surface was measured.

Angles less than 90° indicate that the material is hydrophilic (more permeable/more absorbent), and angles greater than 90° indicate that the material is hydrophobic (less permeable/less absorbent).

It can be seen in Table 8 that the mixtures with nanosilica addition for both types of cement used have higher values compared to the reference mixtures. This means that the addition of nanosilica reduces the mortar's absorption capacity, making it a more hydrophobic or less permeable material. This contributes to the durability of the mortar, as it helps prevent or reduce damage that may occur due to freeze-thaw cycles, as well as issues like efflorescence, internal moisture, presence of microorganisms, etc.

3.2 MICROSTRUCTURE OF MIXTURES WITH NANOSILICA

The SEM images of mortars with both Type N and Type HS cement and 0.25% nanosilica reveal a more uniform and dense structure, with smaller and better-distributed particles. At 56 and 90 days, a decrease in porosity is observed, indicating greater compaction of the mortar matrix.

Figure 5

SEM analysis of mortar mix with type N cement (a) and 0.25% nanosilica, at 28(b), 56(c) and 90 days(d).

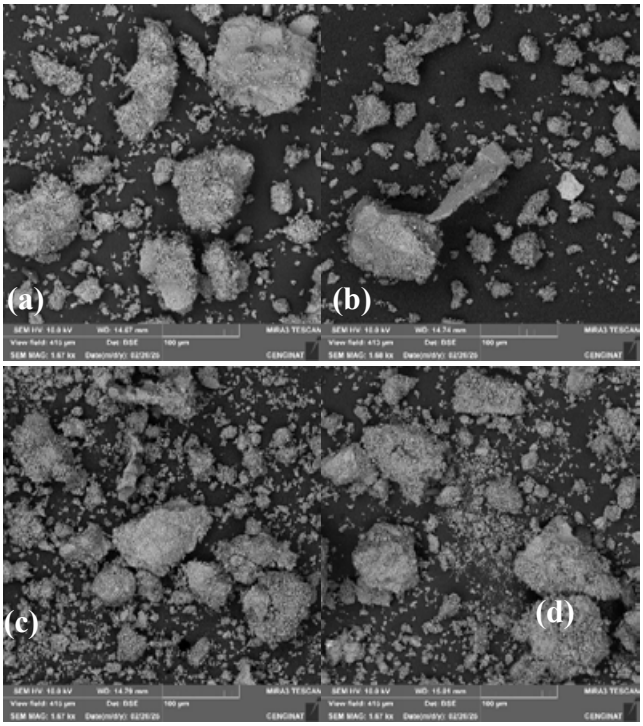

Previous studies have demonstrated that the incorporation of nano-silica into cementitious matrices leads to significant improvements in mechanical performance and microstructural densification, promoting greater durability and strength [26].

In addition to mechanical improvements, the introduction of functionalized nano-silica particles enhances the hydrophobic behavior of mortar, thus improving its resistance to water ingress and extending its service life [33].

The smaller pore size and the increase in hydration products, such as C-S-H (calcium silicate hydrate), contribute to improving the durability and strength of the mortar.

The incorporation of nanosilica significantly enhances the microstructure, reducing porosity and promoting the formation of cementitious products, which translates into higher mechanical strength and durability.

4. Conclusions

- The extraction of silica nanoparticles using the sol-gel method was carried out in four cycles, yielding a total production of 468.4 grams of nanosilica from 80.5 kg of sugarcane bagasse waste sourced from the Puyo canton, demonstrating a yield of 0.566%.
- The characterization of the nanosilica obtained from sugarcane bagasse reveals several structural and chemical properties that confirm it is a material with typical SiO_2 nanoparticle characteristics. The SEM test revealed a rough and heterogeneous surface with an agglomerated structure, indicating a high specific surface area, which is characteristic of nanoparticles. Meanwhile, the TEM test showed that the particle size is below 100 nm, confirming it as a nanomaterial. The XRD image indicated that the diffraction pattern matches the nanosilica structure reported in the literature, suggesting a crystalline phase consistent with the characteristics of a nanostructured material. Finally, the EDS analysis confirmed the presence of Si and O in proportions close to the stoichiometry of SiO_2, with 66.10% oxygen and 25.37% silicon.
- The fresh and hardened state properties of the reference mortar and mortar with nanosilica addition at different percentages, using two types of cement, determined that the optimal nanosilica addition percentage is 0.25%. This percentage does not affect the fluidity, workability, or consistency of the fresh-state mortar, allowing for easy handling and placement. In the hardened state, this percentage achieved the highest compressive strength compared to the reference mortar.
- It was observed that high nanosilica percentages can negatively affect fresh-state mortar mixtures with both Type N and Type HS cement, causing the mixtures to transition from a plastic state to a dry state (lower workability, dry consistency, and difficult handling).
- The contact angle test showed that the tested specimens, including conventional mortar with Type N and HS cement, exhibited a hydrophilic surface, except for the mortar made with Type N cement and 0.25% nanosilica addition, which presented a hydrophobic surface at 90 days of age. Additionally, the incorporation of nanosilica increased the contact angle in these specimens, confirming that nanoparticles reduce water absorption by filling the voids in the mortar.
- The incorporation of nanosilica synthesized from sugarcane bagasse in mortars not only contributes to the sustainable management of agricultural waste but also enhances construction efficiency and sustainability. By reducing cement dependency, CO_2 emissions are decreased, helping to mitigate the environmental impact of the construction industry. Moreover, the improvement in mechanical properties optimizes material usage, leading to lower resource consumption.

References

[1] M. Álvarez, J. Izquierdo y M. Rojas, «Uso de la ceniza de bagazo de caña (CBC) como reemplazo parcial del cemento Portland - Caso Colombia,» IBRACON, 2019.

[2] Organización de las Naciones Unidas (ONU), «Las emisiones históricas del sector de la construcción, lo alejan de los objetivos de descarbonización,» 2022. [En línea]. Available: https://news.un.org/es/story/2022/11/1516722.

[3] Organización de las Naciones Unidas para la Alimentación y la Agricultura (FAO), *OCDE-FAO Perspectivas agrícolas 2023-2032*, 2023.

[4] L. W. Morales, M. Alvansazyazdi y *et al*., «Prevención de la contaminación por la fabricación de hormigones con nanopartículas.,» Conference Paper, vol. ResearchGate, 2020.

[5] M. Alvansazyazdi y J. Rosero, «The pathway of concrete improvement via nano-technology,» *Revista Ingenio,* vol. 2, *N°1,* 2019.

[6] M. Alvansazyazdi, A. Villalba, S. Saltos, J. Santamaria, A. Cadena, M. Leon, L. Leon, P. Bonilla, B. Heredia, J. Bucheli, A. Debut y M. Feizbahr, «Enhancing Sustainable Construction: An Evaluation of Nano-Graphene's Effectiveness in Mortar Composition,» *International Journal of Engineering & Technology Sciences,* 2024.

[7] M. Alvansazyazdi, J. Fraga, E. Stalyn, R. Guevara, J. Santamaria, M. Leon, A. Cadena, P. Bonilla, B. Heredia, A. Debut y M. Feizbahr, «Comparative Analysis of a mortar for plastering with hydraulic cement type HS incorporating nano-iron vs cement-based mortar for masonry type N,» *International Journal of Engineering & Technology Sciences,* 2024.

[8] Y. Du, I. Pundiene, J. Pranckeviciene, A. Zujevs y A. Korjakins, «Study on the Pore Structure of Lightweight Mortar with Nano-Additives,» *MDPI, Nanomaterials,vol. 13, n° 2942,* 2023.

[9] M. Karakouzian, V. Farhangi, M. Farani, A. Joshaghani, M. Zadehmohamad y M. Ahmadzadeh, «Mechanical Characteristics of Cement Paste in the Presence of Carbon Nanotubes and Silica Oxide Nanoparticles: An Experimental Study,» *MDPI, Materials, vol. 14, n° 1347,* 2021.

[10] N. E. Lascano Robalino, E. I. Soledispa Pereira, J. O. Crespo Bravo, J. A. Bucheli García, M. F. Oleas Escalante, J. M. Carmita Guadalupe, A. M. Espinoza Cotera and B. G. Heredia Ayala, "Nanosilica: The Secret Ingredient for Enhanced Concrete Durability," *International Journal of Engineering & Technology Sciences,* vol. 2025, no. ISSN: 2289-4152, p. 9, 2025.

[11] N. Salgado, J. Guaña, C. Escobar y M. Alvansazyazdi, «Result of the Methodology for Learning English Distance with the Use of TICs. Case Study: Central University of Ecuador» *In Á. Rocha et al. (Eds.),* vol. WorldCIST', nº 19, pp. 227-233, 2019.

[12] M. Alvansazyazdi, N. Salgado, A. Borghei, S. Camino y M. Guzmán, «Web-Based Executive Dashboard Reports for Public Works Clients in Construction Industry.,» pp. 285-294, 2019.

[13] M. Alvansazyazdi, H. Alvansaz, M. Hakakian, N. Salgado y A. Camino Solórzano, «An Investigation and Presentation of a Model for Factors Influencing the Agility of Human Resources: A Case Study of Yazd Electricity Distribution Company,» In Á. Rocha et al. (Eds.), pp. 823-834, 2019.

[14] L. Cajero, M. E. Nicho, U. León, M. R. Díaz, R. Salgado, E. García y E. Díaz, «Caracterización de SiO2 obtenido a partir de fuentes naturales,» *Revista Politécnica de Aguascalientes, Vol 3, Año 3,* 2024.

[15] Agencia Iberoamericana para la difusión de la Ciencia y la Tecnología (DICYT), «Bagazo de caña, posible componente de concreto hidráulico,» 2014. [En línea]. Available: https://www.dicyt.com/noticias/bagazo-de-cana-posible-componente-de-concreto-hidraulico.

[16] N. León, «Influencia de la adición de nano sílice en el hormigón autocompactante,» Universidad Politécnica de Madrid, 2012.

[17] L. Morales, M. Alvansazyazdi, P. Landázuri y W. Vásconez, «Prevención de la contaminación por la fabricación de hormigones con nanopartículas,» *Iberian Journal of Information Systems and Technologies, RISTI, N°E30, 06,* pp. 297-312, 2020.

[18] J. Puerto, Efecto de la nanosílice sobre las propiedades reológicas de la matriz cementante y su influencia en el estado endurecido del concreto hidráulico, Bogotá: Universidad Nacional de Colombia, 2019.

[19] M. Alvansazyazdi, B. Claudio y R. Bagner, «Study of the Incorporation of nano-SiO2 in high-performance concrete (hpc),» *Revista Ingenio 2022,* vol. 5 (1), pp. 12-21, 2022.

[20] L. Loaiza, E. Díaz y M. Rojas, «Nanosílice como aditivo para el concreto - caso Colombia,» IBRACON, 2019.

[21] A. Khaloo, M. Mohammad y P. Hosseini, «Influence of different types of nano-SiO2 particles on properties of high performance concrete,» *ELSERVIER, Construction and Building Materials, vol. 113, pp. 188-201,* 2016.

[22] J. Tapia, M. Alvansazyazdi y A. Barrionuevo, «Study of an Environmentally Friendly High-Performance Concrete (HPC) Manufactured with the Incorporation of a Blend of Micro-Nano Silica,» *Revista Científica de Arquitectura y Urbanismo, EÍDOS, vol. 24,* pp. 95-110, 2024.

[23] M. Mobini, A. Khaloo, P. Hosseini y A. Esrafili, «Mechanical properties of fiber-reinforced high-performance concrete incorporating pyrogenic nanosilica with different surface areas,» *ELSEVIER, Construction and Building Materials, vol. 101, pp. 130-140,* 2015.

[24] M. Alvansazyazdi, B. Arévalo y J. Arévalo, «Adoquines de hormigón ecoamigables fabricados con la incorporación de una mezcla de micro-nano sílice,» *Revista Ingenio,* vol. 5 (1), pp. 34-42, 2022.

[25] G. Pérez, A. Guerrero, I. Jiménez y S. Abdul, «Estudio comparativo del efecto de dos tipos de nanosílice sobre las propiedades de pastas de cemento Portland y cemento belítico,» Instituto Ciencias de la Construcción "Eduardo Torroja", Madrid, 2012.

[26] M. Dávila, D. D. Costa y D. Duarte, «Efecto de la adición de nanosílice en cementos y concretos,» Universidad Simón Bolívar, Caracas, 2013.

[27] M. Alvansazyazdi, J. Figueroa, A. Paucar, G. Robles, M. Khorami, P. Bonilla, A. Debut y M. Feizbahr, «Nano-silica in Holcim General Use Cement Mortars: A Comparative Study with Traditional and Prefabricated Mortars,» 2024.

[28] NTE INEN 2536, «Áridos para uso en morteros para mampostería. Requisitos.,» Quito - Ecuador, 2010.

[29] Y. Ni'mah, Z. Muhaiminah y S. Suprapto, «Synthesis of Silica Nanoparticles from Sugarcane Bagasse by Sol-Gel Method,» *Nanoparticle, vol. 4, n°1, p. 10,* 2023.

[30] A. Golsha, M. Rezazadeh Shirdar, S. Gohery y M. Alvansazyazdi, «Optimization of Pre-Treatment Parameters before Diamond Coating using Non-Dominated Sorting Genetic Algorithm (NSGA-II),» Advanced Materials Research, vol 463-464, pp. 399-405, 2012.

[31] NTE INEN 1806, «Cemento para mampostería. Requisitos» Quito - Ecuador, 2015.

[32] NTE INEN 2502, «Cemento hidráulico. Determinación del flujo en morteros» Quito - Ecuador, 2009.

[33] NTE INEN 488, «Cemento hidráulico. Determinación de la resistencia a la compresión de morteros en cubos de 50 mm de arista» Quito - Ecuador, 2009.

[34] M. Alvansazyazdi, F. Alvarez-Rea, J. Pinto-Montoya, M. Khorami, P. M. Bonilla-Valladares, A. Debut y M. Feizbahr, «Evaluating the Influence of Hydrophobic Nano-Silica on Cement Mixtures for Corrosion-Resistant Concrete in Green Building and Sustainable Urban Development,» *Sustainability,* vol. 15, nº 21, p. 15311, 2023.

[35] M. Alvansazyazdi, F. Alvarez, J. Pinto, M. Khorami, P. Bonilla, A. Debut y M. Faizbahr, «Evaluating the Influence of Hydrophobic Nano-Silica on Cement Mixtures for Corrosion-Resistant Concrete in Green Building and Sustainable Urban Development,» *MDPI, Sustainability, vol. 15, n° 15311,* 2023.

[36] M. Alvansazyazdi, D. Farinango, J. Yaucan, A. Cadena, J. Santamaria, P. Bonilla, M. León, A. Debut, M. Feizbahr, L. León y B. Ayala, «Exploring Crack Reduction in High-Performance Concrete: The Impact of Nano-Silica, Polypropylene, and 4D Metallic Fibers,» *International Journal of Engineering & Technology Sciences,* 2024.

[37] M. Alvansazyazdi, J. Figueroa, A. Paucar, G. Robles, M. Khorami, P. M. Bonilla-Valladares, A. Debut y M. Feizbahr, «Nano-silica in Holcim General Use Cement Mortars: A Comparative Study with Traditional and Prefabricated Mortars.,» *Advances in Concrete Construction,* vol. 17, nº 3, pp. 135-150, 2024.

Annexes

Table 6

Properties of mortars in fresh state

Mix Type	Fluidity	
	Type N Cement	Type HS Cement
M control	113	112
M with 0.25% nanosilica	111	109
M with 0.50% nanosilica	110	105
M with 0.75% nanosilica	110	99
M with 1.00% nanosilica	100	96
M with 1.50% nanosilica	97	92

Table 7

Strength values of mortars at different ages

Mix	Compressive strength (MPa)					
	1 day	3 days	7 days	28 days	56 days	90 days
Type N Cement						
M control	0.9	2.6	3.7	6.9	7.4	8.0
M with 0.25% nanosilica	0.6	2.1	4.2	7.5	8.2	8.6
Type HS Cement						
M control	5.0	12.4	18.2	26.9	30.4	34.0
M with 0.25% nanosilica	5.9	12.8	18.7	29.3	33.4	36.8

Table 8

Hydrophobicity of mortars, contact angle test

Mortar	*Age (days)*		
	28	*56*	*90*
Type N Cement			
M control	62.8°	79.1°	84.2°
M with 0.25% nanosilica	63.4°	80.1°	98.2°
Type HS Cement			
M control	43.3°	47.6°	59.9°
M with 0.25% nanosilica	48.1°	51.2°	78.4°

Graph 6

Increase in compressive strength (%) vs. age of mortar (Type HS)

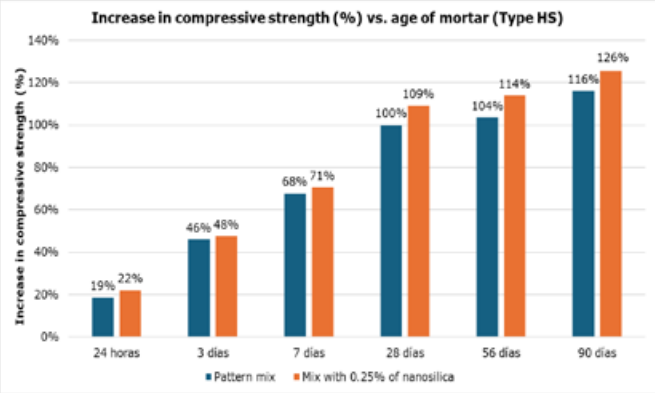

Figure 6

SEM analysis of mortar mix with HS type cement (a) and 0.25% nanosilica, at 28(b), 56(c) and 90 days(d).

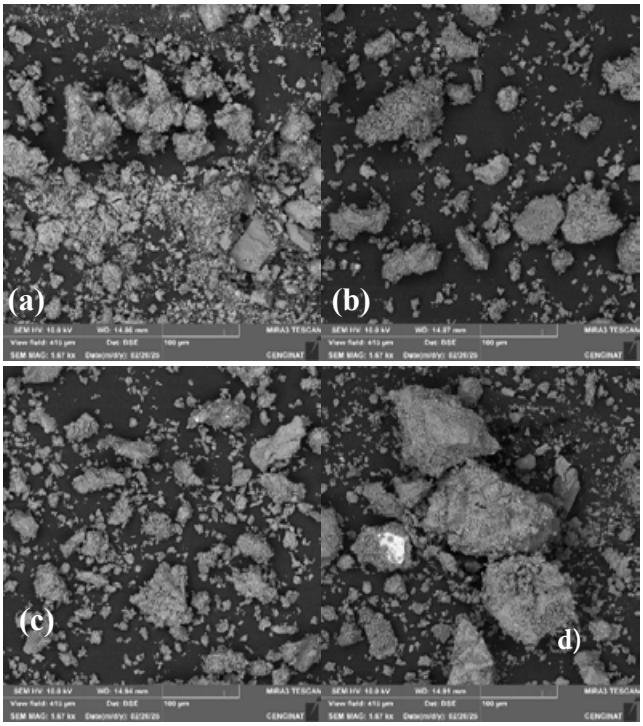

FACULTAD DE INGENIERÍA Y CIENCIAS APLICADAS
UNIVERSIDAD CENTRAL DEL ECUADOR

INGENIO
2025, VOL 8(2), JULIO - DICIEMBRE, PP. 107-114

REVISTA INGENIO

Improving Workplace Safety: A Delphi Study On OSH Monitoring And Management

Mejorar la Seguridad en el Trabajo: un Estudio Delphi Sobre la Supervisión y la Gestión de la SST

Ferenc Faragó | Óbuda University -Hungría
Fernando Rene Flores Benítez | Instituto Superior Universitario 17 de Julio -Ecuador
Gyula Szabó | Óbuda University -Hungría

Recibido: 1/4/2025
Recibido tras revisión: 24/5/2025
Aceptado: 11/6/2025
Publicado: 10/7/2025

KEY WORDS
Safety, Management, OSH management, Safety performance management, OSH performance monitoring, Decision-making

ABSTRACT
Improving OSH performance in today's rapidly changing technological and economic environment is a major challenge for organizations. While there are many studies on OSH practices and interventions, there is little research on the information used by managers to make effective decisions in this area. This study aims to address this by identifying the main sources of information used to make such decisions and the key factors influencing them. A 16-person panel of OSH professionals and managers were asked in three rounds of the Delphi method for their views. In the first round, they provided qualitative feedback on information sources and factors that influence decisions. These were analysed and used to create questions for the next rounds. A 70% agreement threshold was used to determine consensus. The panel agreed on four key sources of information for OSH decisions: compliance, employee feedback, risk assessments, and accident analysis results. The study identified influential factors affecting how this information is interpreted, including organisational culture, leadership commitment and resource availability. Effective OSH decision-making also depends on broader contextual and organisational factors, not just information availability.

PALABRAS CLAVE
Seguridad, gestión, salud ocupacional SSO, gestión en desempeño en seguridad, monitoreo, toma de decisiones

RESUMEN
Mejorar el desempeño en Seguridad y Salud Ocupacional (SSO) en el entorno actual, caracterizado por rápidos cambios tecnológicos y económicos, representa un gran desafío para las organizaciones. Aunque existen numerosos estudios sobre prácticas e intervenciones en SSO, hay poca investigación sobre la información que utilizan los directivos para tomar decisiones eficaces en este ámbito. Este estudio busca abordar esa brecha identificando las principales fuentes de información utilizadas para tomar decisiones en SSO y los factores clave que las influyen. Un panel de 16 personas, compuesto por profesionales y directivos en SSO, fue consultado en tres rondas mediante el método Delphi para conocer sus opiniones. En la primera ronda, proporcionaron comentarios cualitativos sobre las fuentes de información y los factores que influyen en la toma de decisiones. Estos comentarios fueron analizados y utilizados para elaborar preguntas para las siguientes rondas. Se utilizó un umbral de consenso del 70 % para determinar acuerdos. El panel coincidió en cuatro fuentes clave de información para la toma de decisiones en SSO: cumplimiento normativo, retroalimentación de los empleados, evaluaciones de riesgos y resultados del análisis de accidentes. El estudio también identificó factores que influyen en cómo se interpreta esta información, como la cultura organizacional, el compromiso del liderazgo y la disponibilidad de recursos. La toma de decisiones eficaz en SSO también depende de factores contextuales y organizacionales más amplios, y no solo de la disponibilidad de información.

1. Introduction

Evaluation of risks is a fundamental component of guaranteeing safe and healthy working conditions in addition to being required by law [1]–[3]. For OSH managers and professionals, enhancing occupational safety and health (OSH) in a quickly changing scientific and financial context continues to be a constant struggle. The number of work-related accidents in the European Union (EU) has decreased somewhat over the last ten years, but it is still alarmingly high. The substantial impact on workers, businesses, and society at large is highlighted by the over three million non-fatal and 3347

https://doi.org/10.29166/ ingenio.v8i2.8253

pISSN 2588-0829
eISSN 2697-3243
fing.revista.ingenio@uce.edu.ec

fatal work accidents that happened in EU nations in 2021 alone, according to Eurostat [4], [5].

Employers, particularly those in big companies, have a complicated and essential obligation to prevent workplace accidents and job-related disorders [6], [7]. Companies need to satisfy consumer demands with their goals to conduct sustainable operations, with these goals serving as a guide for operational decisions [8]–[10].

Employees, who want safe working conditions, are among the important consumers. These expectations are met, and operational performance is improved by excellent OSH management. In addition to improving productivity and lowering accident-related expenses, it also raises employee engagement. OSH is positioned as a competitive advantage and a crucial success factor due to its high safety culture and positive work environment, which also help to attract and retain talent [11]–[16].

It is imperative to regularly evaluate safety-related operations in a changing organizational structure. To evaluate hazards and comprehend the safety posture of the company, professionals need to handle complex data. Rapid, well-informed decision-making is necessary at all organizational levels due to the growing complexity of technology settings and changing production needs [17]–[19].

An essential ability for management is problem-solving, which starts with recognizing an undesirable circumstance and concludes with coming up with an innovative solution. Enough high-quality information is necessary to make effective decisions. Choosing the best course of action comes after recognizing and comprehending the situation, according to psychological theory. Therefore, decisions are the result of transforming information into actions or even more information [20]–[27].

The type and quality of information used depend heavily on the nature of the problem and the decision-maker's experience. Chikan describes two stages in corporate decision-making: preparing and making decisions [21]. These are often separated across organizational levels, resulting in interpretational differences and information gaps. The function and managerial level affect how information is perceived and utilized, especially in OSH, where risk minimization is paramount.

Continuous access to pertinent information is crucial for assessing risks and recognizing hazards in rapid production situations. Proactive and based on data corporate safety management is essential. Organizational decisions pertaining to safety are greatly impacted by the availability of timely, pertinent, and well-structured information. The organizational level at which the information is obtained and internal business elements like culture, structure, and communication flow that influence how information is interpreted and used both affect how effective these choices are.

Managing occupational safety and health (OSH) remains a constant challenge for companies operating in increasingly technologically advanced and economically unstable situations. However, while there are several frameworks and regulatory procedures in place to support OSH compliance, the quality and accessibility of relevant organisational data play a significant role in the effectiveness of managerial decision-making in this area. In contrast, little is known about the specific types of information that managers use, how this information is processed at different organisational levels, and which internal factors facilitate or hinder managers from making sound OSH decisions. This gap poses a significant difficulty in advancing proactive and evidence-based safety practices. The present study seeks to identify and analyse the key information sources and organisational factors that influence OSH decision-making. The aim is to support more effective and informed management strategies that will improve safety performance [17], [19].

2. Methodology

Expert opinions on monitoring and handling occupational safety and health (OSH) performance were gathered for this study using a modified electronic Delphi approach that was administered during three survey rounds (see Figure 1).

Figure 1.

Research methodology

Through anonymous and iterative communication, the Delphi technique is a systematic expert consultation procedure intended to promote consensus on complicated subjects [28], [29]. In contrast to conventional group discussions, the Delphi method guarantees anonymity, reducing the impact of dominating personalities and enabling participants to formulate their answers on their own. It usually consists of several rounds, in which par-

ticipants answer questions and get controlled feedback along with a rundown of the outcomes from the previous round before moving on to the next. Because experts can revise their answers considering group comments while retaining their unique viewpoints, this format promotes reflective thinking [30]–[33].

Expert opinions on the data and corporate variables that influence occupational safety and health (OSH) decisions are systematically gathered and refined using the three-round Delphi technique. This format was chosen in accordance with generally recognised scientific guidelines, which suggest that three rounds are typically sufficient to minimise participant fatigue and attrition, while also achieving a firm consensus among experts. In the first round, open-ended questions were used to gather qualitative data and pinpoint important ideas and variables. In the second round, these preliminary results were organised into more specific topics, enabling specialists to assess group input more effectively. The third round was then used to reach a consensus, clarify any remaining differences and confirm areas of agreement. A predetermined consensus threshold of 70% agreement among participants was set [34].

The initial phase of the Delphi study, which is shown in Figure 2, was to investigate the fundamental factors that affect occupational safety and health (OSH) management decision-making. In addition to evaluating organizational and individual factors that could have a positive or negative impact on these decisions, participants were asked to identify the kinds of information commonly used in corporate OSH decisions.

This round also aimed to gather actual instances of successful OSH practices and comprehend the perceived difficulty of OSH-related procedures within businesses. The notion of Key Performance Indicators (KPIs) was also introduced, and expert opinions regarding their influence on managerial choices were gathered. The study focused its attention to the methods and procedures for tracking OSH performance and sharing findings in the second round. To get their opinions on the kind of information middle and senior managers require to properly assess OSH, experts were asked to participate. The round looked at how best to share updates with leadership, how often to do so, and whether contemporary technology like artificial intelligence could improve present procedures. With special focus on the flow and display of information to assist strategic decision-making, this phase expanded the investigation into the operational aspects of OSH management. The final round focused on choosing and assessing Key Performance Indicators to improve knowledge of OSH performance measurement. In addition to determining if these indicators are in line with the organization's more general

Figure 2.

Research questions

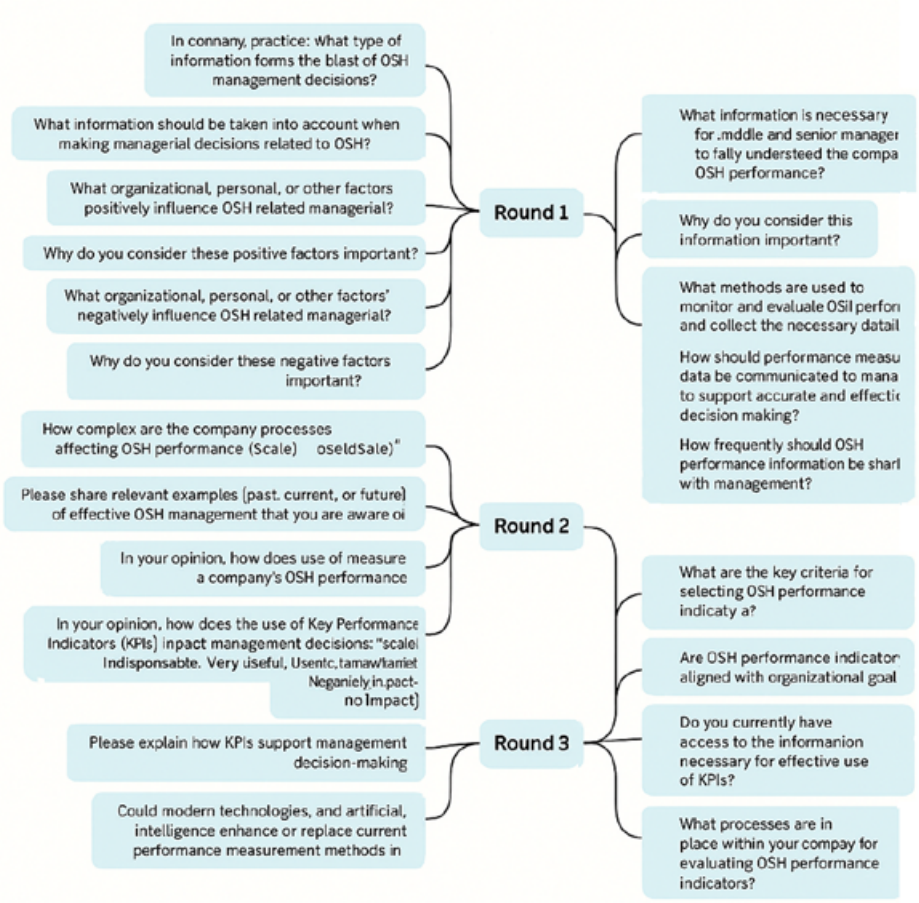

strategic objectives, experts were asked to provide criteria for selecting suitable KPIs. The availability of pertinent data needed for KPI use and the internal procedures used by businesses to evaluate these indicators were also examined in this round.

Between March and November 2023, two expert teams conducted the study. The four members of the preparatory team were an experienced audit specialist, two doctoral research students from the Doctoral School of Security Sciences at the University of Óbuda, and a senior associate professor. The design and coordination of the study fell within the purview of this group. The specialists on the second team were chosen based on their responses to the study questions. These specialists were either seasoned researchers, senior managers in big businesses, or those with significant OSH competencies. Participants had to have proven proficiency in OSH management, senior-level experience in major organizations, or noteworthy academic research credentials in the field in order to meet the inclusion criteria. A sample size of at least 15 was required to guarantee trustworthy consensus. The Delphi survey was accepted by 32 experts out of the 124 who were first invited in March 2023, and 16 completed all three rounds.

Questionnaires were developed based on a preliminary review of literature concerning occupational safety and health (OSH) and how company decisions are made. In the first round, open-ended questions were used to elicit qualitative insights and identify key categories of information and influencing factors. These responses were analysed using inductive content analysis and thematic coding. This process was supported using word cloud visualization to validate the prominence of recurring terms and themes. These initial findings informed the design of the second and third rounds, which employed structured questions and scale evaluations to assess levels of agreement. To ensure content validity, each version of the questionnaire was reviewed and refined by the research team, who were professionals with extensive experience in OSH and Delphi methodology.

Strict protocols were put in place to ensure that the study's participants remained anonymous. During the analysis and feedback phases, all replies were anonymised, and each expert was assigned a unique identification number. The identities of other participants weren't shown to the experts. To minimise the possibility of dominance bias or a hierarchical effect, communication took place online using Excel spreadsheets for the second and third rounds, and Survio for the first.

3. Results

The research identifies key types of information that influence managerial decisions in OSH. Experts reached consensus on four main sources: legal and standard compliance, employee feedback, risk assessment results, and accident data. Additional factors considered included cost-effectiveness, technical feasibility, audit findings, and employee satisfaction. Other responses touched on benchmarking, business impact, risk timelines, process integration, and sustainability.

In the first round, qualitative responses were categorized into 16 distinct informational themes. Quantitative aggregation of expert responses revealed consensus—defined as agreement by at least 70% of participants—for four key items: (1) compliance with legal and standard requirements (100% agreement), (2) employee feedback and suggestions (81%), (3) results from risk assessments (78%), and (4) accident statistics and analysis (70%). Additional factors such as cost-effectiveness (58%) and technical feasibility (52%) did not meet the consensus threshold but were retained for further evaluation in subsequent rounds. A total of 16 distinct statements summarising these observations were compiled and presented in Table 1.

Table 1.

Information underpinning OSH decisions, own-editing.

Information to inform decisions on OHS	Agreement (%)
compliance with legislation, standards	100
employee ideas, opinions, feedback, lobbies	81
risk assessments	78
accident statistics (events, near-misses) and analysis, root cause analysis	70
cost, cost-effectiveness and available resources	58
technical feasibility	52
results of management reviews, internal audits	39
employee skills, satisfaction	39
safety first philosophy, parent company expectations	19,5
reduce risks, new risks emerge	19,5
priority order of occupational safety and health	13
benchmark results	6,5
the achievement of occupational safety and health objectives and programmes	6,5
order, working environment	6,5
own professional judgement	6,5
training, education	6,5

A total of 36 elements were found after the positive and negative aspects were filtered out (e.g., lack of commitment, lack of good communication). A five-point Likert scale was used to gauge the experts' responses to questions about how complex business procedures impact OSH (Table 2). All the experts agreed that business pro-

cedures that impact OSH are intricate and difficult to understand.

Table 2.

Assessment of the complexity of company processes affecting OSH

Complexity of business procedure that impant OHS	No of repsonses
They are simple, easy to understand and easy to track	2
They are not very simple, but easy to understand and track	1
They are not simple; they are not easy to understand	1
Complex processes that are not easy to understand	11
Highly complex processes, not easy to understand and monitor	1

The significance of tracking and assessing OSH-related procedures was acknowledged by experts, who pointed out that it facilitates managerial decision-making, enhances information flow within the company, allows for comparisons, and aids in identifying key areas of attention. Key Performance Indicators (KPIs) were thought to be very useful for OSH management. Although one expert believed KPIs had little bearing on decision-making, two others thought they were crucial.

KPIs were found to serve five main purposes: (a) identifying problems and priority areas; (b) supporting decision-making; (c) managing processes and giving feedback; (d) improving communication; and (e) enabling comparison and long-term tracking. Regarding the utilization of KPIs, a total of 28 criteria were identified. Experts also underlined that for KPIs to be useful; they must be employed in certain circumstances. Among the worries were that KPIs might not provide enough context on their own and that their appropriate application necessitates professional knowledge, training, interpretation, and open, two-way communication across the organization.

In the second round, structured statements based on round one findings were presented to experts using closed-ended formats. The expert panel agreed on 20 of the 118 specific statements, with a consensus of more than 70%. Panellists were asked to reevaluate their answers for things that did not receive consensus in the first round, with the goal of promoting a range of opinions rather than coercing them into agreement. Requests for clarification followed differing viewpoints. Despite having been carried out, rounds two and three's specific results are not presented in this page. Lastly, for confirmation, the experts were given access to the combined results from all three rounds. Two of the sixteen participants did not reply, but fourteen of them acknowledged agreement with the results.

The third round further refined items that lacked clear consensus. Of the 92 items presented, 14 achieved the 70% consensus level. Notably, strong agreement was reached regarding the sources for defining OSH key performance indicators (e.g., OHSAS management systems and corporate expectations), and on the necessity of linking KPIs to organizational goals. However, participants expressed limited confidence in their own readiness to apply these indicators effectively, with only 37.5% affirming adequate knowledge. The main KPIs are presented in Table 3.

Table 3.

Key Performance Indicators (KPIs) for OSH Identified Through Expert Consensus.

KPI Source or Criterion	Description	Consensus Level
OHSAS Management Systems	KPIs should be based on standards from Occupational Health and Safety Assessment Series (OHSAS).	Achieved (>70%)
Parent Company Expectations	KPIs should reflect the expectations and strategic directions of the parent company.	Achieved (>70%)
Linkage to Organizational Objectives	KPIs should be aligned with company-level strategic goals.	Achieved (>70%)
Expert Knowledge and Experience	KPIs should be selected by professionals with expertise in OSH and process control.	Not Consensual
Usability Across Organizational Levels	KPIs must be understandable and applicable at all management levels.	Partial Support
Information Flow and Communication	KPIs should facilitate two-way communication and support decision-making transparency.	Partial Support
Complementarity with Other Business KPIs	OSH KPIs are not typically integrated with financial or production indicators.	Achieved (100%)
Supportive Tools and Training Required for Interpretation	Proper interpretation of KPIs requires training and documentation.	Partial Support

OSH management decisions are influenced by a number of firm aspects. A supportive business culture, managers' communication abilities, and effective two-way communication within the organization are the primary elements that favourably influence managers' dedication to OSH. The primary impediments include lack of resources, lack of expertise and knowledge management, lack of enthusiasm, and unprofessional decision-making. Both the company's and employees' personal opinions are impacted by wise OSH actions (Figure 3).

Figure 3.

Information and company factors influencing OSH decisions

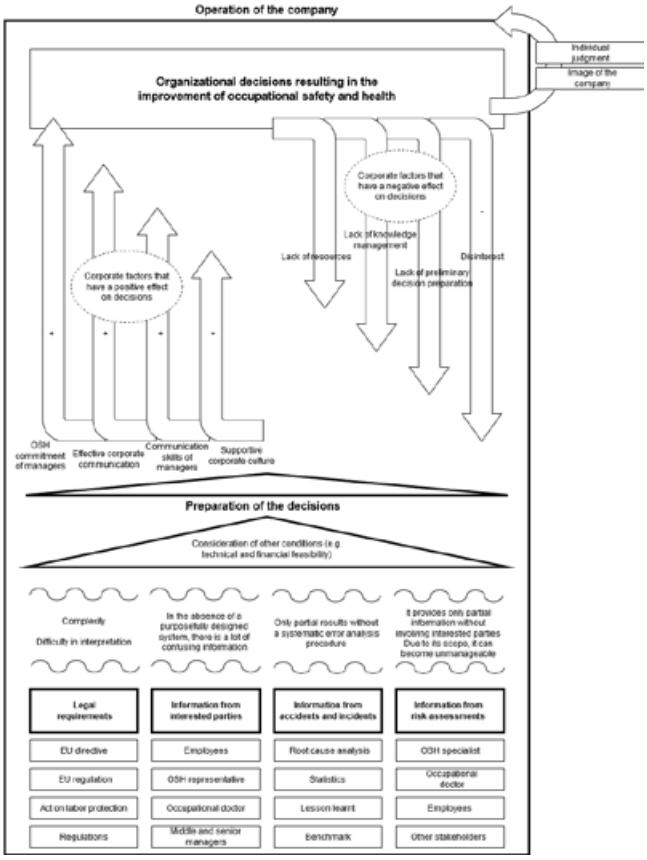

3.1. Discussion

The study highlights the multifaceted and complex nature of information sources that underpin OSH decision-making processes. One of the main results is that OSH managers base their judgments mostly on adherence to national and EU legislative frameworks. Despite providing a strong foundation for safety requirements, many companies find the legislation to be too complicated, indicating the need for improved support systems and more precise interpretation guidelines. Although it also highlights disparities in understanding and implementation across different firms, this is consistent with other research showing that legal compliance successfully enhances workplace safety [11], [19], [35], [36].

The significance of involving stakeholders in OSH decisions is another important subject. It is seen to be essential to get input from employees, occupational health specialists, and management, particularly in sophisticated technological workplaces where frontline staff frequently have the most practical experience. Frequent feedback systems allow for the early detection of risks and promote a preventive culture. However, OSH professionals may become overwhelmed and lose concentration if they receive too much unfiltered feedback, so this process needs to be handled carefully. The creation of organized and effective feedback mechanisms is therefore necessary to guarantee that pertinent information influences choices without becoming irrelevant.

All members of the expert panel agreed that risk assessments are the cornerstone of OSH strategy. The institutional significance of both qualitative and quantitative risk assessments is further supported by legislative requirements. A number of obstacles were identified, too, such as the inability to effectively handle intricate evaluations and convert results into administrative decisions that could be put into practice. Particularly in situations involving new or developing technology, experts underlined the necessity of trustworthy, transparent, and controllable risk assessment procedures.

The results of the research emphasize the importance of diversified, organized, and context-aware information flows in making OSH judgments of the highest caliber. Stakeholder participation, empirical accident data, legislative requirements, and thorough risk assessments interact to form the basis of good safety governance. The availability of resources, organizational communication, and managerial commitment are necessary to support these, nevertheless [2], [12], [37]–[39]. According to the research, the efficiency and sustainability of OSH procedures can be greatly increased by combining these components in a comprehensive way while taking confounding variables into account.

The findings of the Delphi study indicate the need to support a change in OSH management, shifting the focus from reactivity to proactivity and embracing data-driven decision-making, strategy alignment and cultural commitment. Implementing these insights could enhance employee satisfaction, operational effectiveness and safety performance, ultimately leading to long-term commercial success. The study shows that, in practical terms, good OSH governance necessitates an organizational culture that encourages candid communication, prompt feedback, and proactive risk management in addition to regulatory compliance. The general agreement that managerial commitment and effective internal communication are essential for facilitating safety decisions highlights the need of leadership development and internal communication procedures that are adapted to the information flows associated with safety [40].

4. Conclusions

Expanding the body of knowledge on the data supporting OSH choices and the business variables influencing them was the aim of this study. In order to make management decisions that result in better workplace health and safety, the experts agreed that information from many sources and at various organizational levels is required. Decision-making about OSH is also influenced by a few additional factors. Confounding variables that complicate the interpretation of data from many sources and the corporate elements that have the biggest impact on management choices have been brought to light by the study. The expert view that emerged from the process made clear that corporate efforts to enhance OSH performance enhance employee engagement and the company's reputation, both of which support long-term corporate success.

To make informed decisions, OSH practitioners will benefit from the study's findings. Guidelines for OSH practitioners, managers, and business decision-makers can be developed using them to enhance their OSH management decision-making procedures.

One of the study's main limitations is the expert panel's diversity and representativeness. Despite the participants' extensive backgrounds in occupational safety and health (OSH), the final group only included 16 experts, most of whom were connected to major Hungarian institutions and companies. The findings' applicability to different organizational sizes, cultural contexts, or industrial sectors is limited by the sample's modest size and geographic concentration. More varied viewpoints should be incorporated into future studies to improve the results' external validity and wider applicability.

References

[1] M. Peron, S. Arena, N. Paltrinieri, F. Sgarbossa, y G. Boustras, "Risk assessment for handling hazardous substances within the European industry: Available methodologies and research streams," *Risk Anal.*, vol. 43, no. 7, pp. 1434–1462, 2023, doi: 10.1111/risa.14010.

[2] G. Szabó, "The Characteristics of Industrial Safety Risk Management," *Advances in Intelligent Systems and Computing*, vol. 1204, pp. 47–52, 2020, doi: 10.1007/978-3-030-50946-0_7.

[3] B. Jahanvand, S. Bagher Mortazavi, H. Asilian Mahabadi, y O. Ahmadi, "Determining essential criteria for selection of risk assessment techniques in occupational health and safety: A hybrid framework of fuzzy Delphi method," *Saf. Sci.*, vol. 167, no. April, p. 106253, 2023, doi: 10.1016/j.ssci.2023.106253.

[4] Eurostat, "Accidents at work by sex and age, excluding road traffic accidents and accidents on board of any mean of transport in the course of work (NACE Rev. 2 activity A, C-N excluding H)" 2023. https://ec.europa.eu/eurostat/databrowser/view/hsw_mi03/default/table?lang=en.

[5] Eurostat, "Number of non-fatal and fatal accidents at work, 2021" 2024. https://ec.europa.eu/eurostat/statistics-explained/index.php?title=File:Number_of_non-fatal_and_fatal_accidents_at_work,_2021_(persons)_AAW2023.png.

[6] S. van den Heuvel *et al.*, Estimating the costs of work-related accidents and ill-health: An analysis of European data sources - European Risk Observatory. 2017.

[7] European Agency for Safety and Health at Work, "The value of occupational safety and health and the societal costs of work-related injuries and diseases," pp. 1–10, 2017, doi: 10.2802/986314.

[8] D. Dumitriu, G. Militaru, D. C. Deselnicu, A. Niculescu, y M. A. M. Popescu, "A perspective over modern SMEs: Managing brand equity, growth and sustainability through digital marketing tools and techniques," *Sustain.*, vol. 11, no. 7, 2019, doi: 10.3390/su10022111.

[9] A. D. Neely, C. Adams, y M. Kennerley, *The Performance Prism The Scorecard for Measuring and Managing Business Success*, 1era ed. Financial Times Management, 2002.

[10] T. Imre, *Stratégiai menedzsment a gyakorlatban*, 1era ed. Budapest: SpringMed Kiadó Kft., 2020.

[11] V. C. Erazo-chamorro, R. P. Arciniega-rocha, y G. Szabo, "Safety workplace: From of point of view of ergonomics and occupational biomechanics" vol. 65, pp. 669–676, 2022.

[12] V. C. Erazo-Chamorro, R. P. Arciniega-Rocha, N. Rudolf, B. Tibor, and S. Gyula, "Safety Workplace: The Prevention of Industrial Security Risk Factors," *Appl. Sci.*, vol. 12, no. 21, 2022, doi: 10.3390/app122110726.

[13] T. Dyllick y K. Hockerts, "Beyond the business case for corporate sustainability," *Bus. Strateg. Environ.*, vol. 11, no. 2, pp. 130–141, 2002, [Online]. Available: https://onlinelibrary.wiley.com/doi/abs/10.1002/bse.323.

[14] M. O'Toole, "The relationship between employees' perceptions of safety and organizational culture.," *J. Safety Res.*, vol. 33, no. 2, pp. 231–243, 2002, doi: 10.1016/S0022-4375(02)00014-2.

[15] C. Haslam, J. O'Hara, A. Kazi, R. Twumasi, and R. Haslam, "Proactive occupational safety and health management: Promoting good health and good business," *Saf. Sci.*, vol. 81, pp. 99–108, 2016, doi: 10.1016/j.ssci.2015.06.010.

[16] Z. C. Tan, C. E. Tan, y Y. O. Choong, "Occupational Safety & Health Management and Corporate Sustainability: The Mediating Role of Affective Commitment," *Saf. Health Work*, vol. 14, no. 4, pp. 415–424, 2023, doi: 10.1016/j.shaw.2023.10.006.

[17] R. K. Mitchell, B. R. Agle, y D. J. Wood, "Toward a Theory of Stakeholder Identification and Salience:

Defining the Principle of Who and What Really Counts," *Acad. Manag. Rev.*, vol. 22, no. 4, p. 853, 1997, doi: 10.2307/259247.

[18] R. P. Arciniega-Rocha, V. C. Erazo-Chamorro, P. D. Rosero-Montalvo, y G. Szabó, "Smart Wearable to Prevent Injuries in Amateur Athletes in Squats Exercise by Using Lightweight Machine Learning Model," *Inf.*, vol. 14, no. 7, pp. 1–12, 2023, doi: 10.3390/info14070402.

[19] R. P. Arciniega-Rocha, V. C. Erazo-Chamorro, y G. Szabo, "The Prevention of Industrial Manual Tool Accidents Considering Occupational Health and Safety," *Safety*, vol. 9, no. 3, 2023, doi: 10.3390/safety9030051.

[20] F. Dr. Lénárd, *A problémamegoldó gondolkodás*, 6ta ed. Budapest: Akadémiai Kiadó, 1987.

[21] A. Chikán, *Vállalatgazdaságtan*, II ed. Budapest: AULA Kiadó, 1999.

[22] D. K. Chikán, *Az értékteremtő folyamatok menedzsmentje*. AULA Kiadó, 1999.

[23] F. Faragó, "Teljesítménymutatók, mint menedzsment döntéselőkészítő eszközök alkalmazása a nagyvállalati munkavédelemben," Mérnöki Szimpózium a Bánkin Előadásai, pp. 124–134, 2022.

[24] T. H. Davenport y L. Prusak, *Tudásmenedzsment.* Budapest: Bőgel György, 2001.

[25] S. Hans, *From Dream to Discovery: On Being a Scientist*. New York: McGraw-Hill, 1964.

[26] F. Jay W., *Industrial Dynamics*, 1era ed. Massachusetts: Massachusetts Institute of Technology, 1961.

[27] V. Dr. Nemény, *A döntéshozatal alapelemei*. Budapest: Tankönyvkiadó, 1985.

[28] K. Korzon, "A Delphi módszer felhasználása a tájékoztatási tevékenység fejlesztésének prognosztizálásában," 1976.

[29] S. Keeney, F. Hasson, y H. McKenna, "Consulting the oracle: ten lessons from using the Delphi technique in nursing research" *J. Adv. Nurs.*, vol. 53, no. 2, pp. 205–212, Jan. 2006, doi: 10.1111/j.1365-2648.2006.03716.x.

[30] N. D. Uhl, "Delphi Technique," in *The International encyclopedia of curriculum*, A. Lewy, Ed. Oxford-New York: Pergamon Press, 1991, p. 453.

[31] H. A. Linstone y M. Turoff, *Delphi Method: Techniques and Applications*, 2da ed. Addison-Wesley Publishing Company, Advanced Book Program, 1975.

[32] M. Häder y S. Häder, "Delphi und Kognitionspsychologie: Ein Zugang zur theoretischer Fundierung der Delphi-Methode," *ZUMA Nachrichten*, vol. 37, no. 19, pp. 8–34, 1995, [Online]. Available: http://www.gesis.org/fileadmin/upload/forschung/publikationen/zeitschriften/zuma_nachrichten/zn_37.pdf.

[33] R. Boulkedid, H. Abdoul, M. Loustau, O. Sibony, y C. Alberti, "Using and reporting the Delphi method for selecting healthcare quality indicators: a systematic review.," *PLoS One*, vol. 6, no. 6, p. e20476, 2011, doi: 10.1371/journal.pone.0020476.

[34] H. A. von der Gracht, "Consensus measurement in Delphi studies: Review and implications for future quality assurance," *Technological Forecasting and Social Change*, vol. 79, no. 8, pp. 1525–1536, Oct. 2012, doi: 10.1016/J.TECHFORE.2012.04.013.

[35] "Work-related Musculoskeletal Disorders (WMSDs) - Risk Factors : OSH Answers." https://www.ccohs.ca/oshanswers/ergonomics/risk.html.

[36] R. P. Arciniega-Rocha, V. C. Erazo-Chamorro, P. D. Rosero-Montalvo, y G. Szabó, "Healthy and safe workplace definition: A friendly boundary for a complex issue.," in *Mérnöki Szimpózium a Bánkin Előadásai: Proceedings of the Engineering Symposium at Bánki* (ESB2021). Vol. 1., pp. 51-56, 2021.

[37] R. P. Arciniega-Rocha, A. Tick, V. C. Erazo-Chamorro, y G. Szabó, "Risk Perception and Mitigation in Hand Tool Use: A Comparative Study of Industrial Safety Perspectives from Ecuador and Hungary," *Safety*, vol. 11, no. 1, 2025, doi: 10.3390/safety11010014.

[38] S. M. Kyaw-Myint, L. Strazdins, M. Clements, P. Butterworth, y L. Gallagher, "A method of identifying health-based benchmarks for psychosocial risks at work: A tool for risk assessment," *Saf. Sci.*, vol. 93, pp. 143–151, 2017, doi: 10.1016/j.ssci.2016.11.016.

[39] F. Faragó y G. Szabó, "Qualitative Assessment of the Occupational Health and Safety Knowledge Management Practices of Hungarian Companies," in *Proceedings of the 9th International Ergonomics Conference. ERGONOMICS 2022. Lecture Notes in Networks and Systems*, vol 701., I. Salopek Čubrić, G. Čubrić, K. Jambrošić, T. Jurčević Lulić, and D. Sumpor, Eds. Springer, 2023, pp. 105–112.

[40] C. Markmann, A. Spickermann, H. A. von der Gracht, y A. Brem, "Improving the question formulation in Delphi-like surveys: Analysis of the effects of abstract language and amount of information on response behavior," *Futures and Foresight Science*, vol. 3, no. 1, p. e56, Mar. 2021, doi: 10.1002/FFO2.56;PAGE:STRING:ARTICLE/CHAPTER.

FACULTAD DE INGENIERÍA Y CIENCIAS APLICADAS
UNIVERSIDAD CENTRAL DEL ECUADOR

INGENIO
2025, VOL 8(2), JULIO - DICIEMBRE, PP. 115-126

REVISTA INGENIO

Evaluación de las Propiedades Mecánico-físicas del Mortero de Cemento Portland Adicionando Resina de Colofonia en Muros de Albañilería Confinada

Evaluation of the mechanical and physical properties of Portland cement mortar with the addition of rosin resin in confined masonry walls

Fabriccio Omar Puicon Rodriguez | Universidad Católica Santo Torribio de Mogrovejo - Perú

Recibido: 18/5/2025
Recibido tras revisión: 9/6/2025
Aceptado: 11/6/2025
Publicado: 10/7/2025

PALABRAS CLAVE
Resina de colofonia, mortero de cemento Portland, albañilería confinada, humedad

RESUMEN
El presente estudio se justifica por la necesidad de mejorar las propiedades del mortero de cemento portland frente a la humedad, uno de los principales problemas en edificaciones ubicadas en zonas húmedas, que afecta tanto la durabilidad como la habitabilidad de las viviendas. Se propuso evaluar el impacto de la adición de resina de colofonia sobre las propiedades mecánico-físicas del mortero utilizado en muros de albañilería confinada. El objetivo principal fue determinar si esta adición mejora la impermeabilidad y adherencia sin comprometer significativamente la resistencia estructural. Para ello, se llevaron a cabo ensayos conforme a normas técnicas peruanas y chilenas, que incluyeron pruebas de compresión en prismas, compresión diagonal en muretes, resistencia a la flexión, absorción de agua y adherencia a cizalle, utilizando morteros con porcentajes de colofonia de 0.2%, 0.4% y 0.5% en diferentes dosificaciones. Los resultados evidenciaron que la incorporación de colofonia reduce la resistencia a la compresión y flexión, así como la rigidez del mortero; sin embargo, mejora notablemente la impermeabilidad y la adherencia, especialmente en dosificaciones con 0.2% y 0.4% de resina. Se concluyó que, aunque el uso de colofonia disminuye ciertas propiedades mecánicas, sus beneficios físicos como la reducción de la absorción capilar y el aumento de la adherencia la convierten en una alternativa viable en viviendas de hasta dos pisos, en contextos donde el control de humedad es prioritario sobre la resistencia estructural.

KEY WORDS
Rosin, Portland cement mortar, confined masonry, humidity

ABSTRACT
This study is justified by the need to improve the moisture-resistant properties of Portland cement mortar, one of the main problems in buildings located in humid areas, affecting both the durability and habitability of homes. The objective was to evaluate the impact of adding rosin resin on the mechanical and physical properties of mortar used in confined masonry walls. The main objective was to determine whether this addition improves impermeability and adhesion without significantly compromising structural strength. To this end, tests were conducted in accordance with Peruvian and Chilean technical standards, including prism compression tests, diagonal compression tests on low walls, flexural strength, water absorption, and shear adhesion tests, using mortars with rosin percentages of 0.2%, 0.4%, and 0.5% at different dosages. The results showed that the addition of rosin reduces the mortar's compressive and flexural strength, as well as its stiffness. However, it significantly improves impermeability and adhesion, especially at dosages of 0.2% and 0.4% resin. It was concluded that although the use of rosin diminishes certain mechanical properties, its physical benefits, such as reduced capillary absorption and increased adhesion, make it a viable alternative in homes with up to two floors, in contexts where humidity control is a priority over structural strength.

1. Introducción

Es indiscutible que el cemento hoy en día es el material más utilizado a nivel mundial en la construcción, principalmente por la versatilidad, facilidad de aplicación y bajo costo de los materiales que se utilizan. Se usa como indicador para obtener el nivel de desarrollo de los países. Por lo mencionado, es esencial plantear nuevas investigaciones que busquen mejorar las propiedades de este material [1]. Para lograr las mejoras en sus propiedades, el cemento debe ser modificado con el uso de aditivos y/o adiciones que le aporten a mejoras y puedan ajustarse a las necesidades de todas las industrias [2].

En el uso de este se presentan problemas que perjudican su desempeño, como la humedad, la cual daña las construcciones de albañilería y de concreto armado, debido a las características de los materiales, los cuales absorben fluidos a través de los vacíos en el interior de los

https://doi.org/10.29166/ingenio.v8i2.8254

pISSN 2588-0829
eISSN 2697-3243
fing.revista.ingenio@uce.edu.ec

elementos constructivos. El motivo de la aparición de la humedad es debido a la ausencia de láminas impermeabilizantes y/o debido a que los métodos tradicionales no funcionan. Los morteros, albañilería y gravas son poros, hidrófilos y son muy permeables, por lo que se genera capilaridad [3]. Estas características permiten que la humedad proveniente de los cimientos, sobrecimientos o muros que mantengan contacto con suelos húmedos ascienda. El agua sube al muro por la capilaridad y una vez que el fluido se evapora dichas sales se cristalizan y se depositan en la superficie causando daños en los muros o en el concreto armado.

En la ciudad de Santiago de Chile, se presentan este tipo de problemas; los cales afectan 4 de 10 casas, debido a la falta de secado por el rápido desencofrado, los elementos retienen agua y por este motivo aparecen las manchas en los muros, desprendimiento de pintura, moho y eflorescencia. Además, perjudica la habitabilidad y estética de las viviendas [4]. Un parámetro importante es la presencia de agua dentro de los poros del material, el cual disminuye el rendimiento mecánico, afectando la resistencia a la compresión y corte [5]. En el caso de Perú, este tema representa uno de los grandes problemas que afectan a las viviendas en la costa y amazonia. Se presentó el caso en el colegio inicial Divino Niño Jesús en Lores, donde los daños que se presentaron en el concreto armando y en los muros de albañilería son la delaminación y la eflorescencia [6].

Esta investigación busca, mediante la adición de un nuevo material, evitar que el mortero absorba un exceso de humedad. Esto es crucial, ya que la absorción excesiva debilita la unión entre el ladrillo y el mortero. Si esta unión falla, la estructura puede debilitarse, lo que resultaría perjudicial para los habitantes de las viviendas.

Por esto surge la interrogante: ¿Cómo influye la incorporación de la resina de colofonia en las propiedades mecánicas y físicas en la elaboración del mortero? La investigación busca comprobar la hipótesis de que las propiedades mecánicas y físicas del mortero con resina de colofonia influye de manera positiva en su elaboración, aumentando la impermeabilidad y mejorar su adherencia. Para determinar si hay mejora en las propiedades, se realizarán los ensayos de resistencia a la compresión en pilas de albañilería, compresión diagonal en muretes de albañilería, determinar la absorción de morteros en albañilería, resistencia a la flexión del mortero y adherencia a cizalle.

En el aspecto técnico, el procedimiento y resultados se establecen de acuerdo con la norma NTP E070 con respecto a la calidad y requisitos mínimos del muro. En el aspecto social busca hacer llegar el conocimiento a las poblaciones que utilizan el mortero para el asentado de sus muros, pero sobre todo enfocándose en poblaciones en donde hay humedad y también para viviendas antiguas que busquen mejorar las zonas afectadas por la humedad y el tiempo.

De igual manera, el objetivo general de este estudio es evaluar las propiedades mecánico-físicas del mortero de cemento Portland con la adición de resina de colofonia en diferentes porcentajes, para su aplicación en muros de albañilería confinada. Para lograrlo, se establecieron los siguientes objetivos específicos:

Evaluar la resistencia a la compresión de prismas de albañilería y la compresión diagonal en muretes de mortero con resina de colofonia, utilizando porcentajes de 0.2%, 0.4% y 0.5%.

Obtener el módulo de elasticidad, módulo de corte y coeficiente de Poisson del mortero.

Evaluar la resistencia a la flexión del mortero.

Evaluar la cantidad de absorción del mortero.

Evaluar la adherencia del mortero.

Realizar un estudio comparativo de los resultados obtenidos en los ensayos de resistencia a la compresión (prismas y diagonal en muretes), flexión, absorción (según la NTP) y adherencia del mortero con los diferentes porcentajes de resina de colofonia, frente a los resultados de un mortero de cemento Portland tradicional.

2. Método

2.1 MUESTRA

El método de muestreo es por conveniencia, teniendo en cuenta un enfoque no probabilístico, donde no se emplearán formulas estadísticas para seleccionar las muestras.

El muestreo tomará en cuenta los parámetros de la norma E070 de albañilería y para cuantas muestras se harán, se tomará en cuenta las normas técnicas peruanas.

2.2 FORMA DE MUESTREO

Cantidad de muestras según las normas utilizadas

- Resistencia en compresión de prismas de albañilería: La norma NTP 399.605 menciona que como mínimo son 3 muestras o pilas de albañilería.
- Compresión diagonal en muretes de albañilería: La norma NTP 399.621 menciona que como mínimo son 3 muestras o muretes.
- Resistencia a la flexión de morteros de cemento: La norma NTP 334.120 dice que para tener resultados óptimos se debe realizar como mínimo 3 muestras por día en los que se analizará (3 días, 7 días y 28 días).
- Ensayo de absorción: La norma NTP 399.631 menciona que se deben de realizar por los menos 3 cubos

para poder sacar el promedio y obtener un resultado óptimo.

- Adherencia a cizalle: La norma chilena Nch 167 menciona que como mínimo se deben hacer 3 muestras.

La cantidad de muestras están establecidas en la tabla 1, 2 y 3.

Tabla 1

Cantidad de muestras a ensayar dividido en tipos de ensayo y tipos de mortero

TIPOS DE MORTEROS	ENSAYOS	MUESTRAS SEGÚN DOSIFICACIÓN		
		1:3	1:4	1:5
MORTERO PATRÓN	COMPRESIÓN DE PRISMAS DE ALBAÑILERÍA	3	3	3
	COMPRESIÓN DIAGONAL DE MURETES	3	3	3
	ADHERENCIA POR CIZALLE	3	3	3
	RESISTENCIA A LA FLEXIÓN DE MORTEROS DE CEMENTO HIDRÁULICO	9	9	9
	TASA DE ABSORCIÓN	3	3	3
TOTAL DE MUESTRAS		**63**		
ADICIÓN DE RESINA DE COLOFONIA 0.2%	COMPRESIÓN DE PRISMAS DE ALBAÑILERÍA	3	3	3
	COMPRESIÓN DIAGONAL DE MURETES	3	3	3
	ADHERENCIA POR CIZALLE	3	3	3
	RESISTENCIA A LA FLEXIÓN DE MORTEROS DE CEMENTO HIDRÁULICO	9	9	9
	TASA DE ABSORCIÓN	3	3	3
TOTAL DE MUESTRAS		63		
ADICIÓN DE RESINA DE COLOFONIA 0.4%	COMPRESIÓN DE PRISMAS DE ALBAÑILERÍA	3	3	3
	COMPRESIÓN DIAGONAL DE MURETES	3	3	3
	ADHERENCIA POR CIZALLE	3	3	3
	RESISTENCIA A LA FLEXIÓN DE MORTEROS DE CEMENTO HIDRÁULICO	9	9	9
	TASA DE ABSORCIÓN	3	3	3
TOTAL DE MUESTRAS		**63**		
ADICIÓN DE RESINA DE COLOFONIA 0.5%	COMPRESIÓN DE PRISMAS DE ALBAÑILERÍA	3	3	3
	COMPRESIÓN DIAGONAL DE MURETES	3	3	3
	ADHERENCIA POR CIZALLE	3	3	3
	RESISTENCIA A LA FLEXIÓN DE MORTEROS DE CEMENTO HIDRÁULICO	9	9	9
	TASA DE ABSORCIÓN	3	3	3
TOTAL DE MUESTRAS		**63**		
TOTAL		**252**		

Tabla 2

Cantidad de muestras por ensayos mecánicos

	ENSAYOS MECÁNICOS			
ENSAYOS	MUESTRA PATRÓN	ADICIÓN DE RESINA DE COLOFONIA 0.2%	ADICIÓN DE RESINA DE COLOFONIA 0.4%	ADICIÓN DE RESINA DE COLOFONIA 0.5%
COMPRESIÓN DE PRISMAS DE ALBAÑILERÍA	9	9	9	9
COMPRESIÓN DIAGONAL DE MURETES	9	9	9	9
ADHERENCIA POR CIZALLE	9	9	9	9
RESISTENCIA A LA FLEXIÓN DE MORTEROS DE CEMENTO HIDRÁULICO	27	27	27	27
TOTAL	216			

Tabla 3

Cantidad de muestras a ensayar por su propiedad física

	ENSAYOS FÍSICOS			
ENSAYOS	MUESTRA PATRÓN	ADICIÓN DE RESINA DE COLOFONIA 0.2%	ADICIÓN DE RESINA DE COLOFONIA 0.4%	ADICIÓN DE RESINA DE COLOFONIA 0.5%
TASA DE ABSORCIÓN	6	6	6	6
TOTAL	**24**			

2.3 ENSAYO PARA EL AGREGADO FINO

2.3.1 Análisis granulométrico del agregado fino, grueso y global

La normativa busca precisar la gradación de los agregados los cuales se están analizando. Los resultados nos dirán si está cumpliendo la distribución del tamaño de partícula, siguiendo los lineamientos [7]. Lo primero para realizar el ensayo es tomar una cantidad de muestra considerable para colocarla en un recipiente o mesa para poder dividirla en cuatro partes iguales, se elegirán dos partes opuestas para obtener la mejor muestra y así realizar el ensayo de granulometría. Luego se toma una muestra de 500g de agregado fino obtenido del cuarteo. El tamizado debe realizarse con movimientos circulares o de agitación, luego se pesa el material retenido en el tamiz para determinar la granulometría del agregado [7]. En la figura 1 se muestra la curva granulométrica. En Figura 1 muestra la curva granulométrica obtenida.

Figura 1

Curva granulométrica según la normativa E070

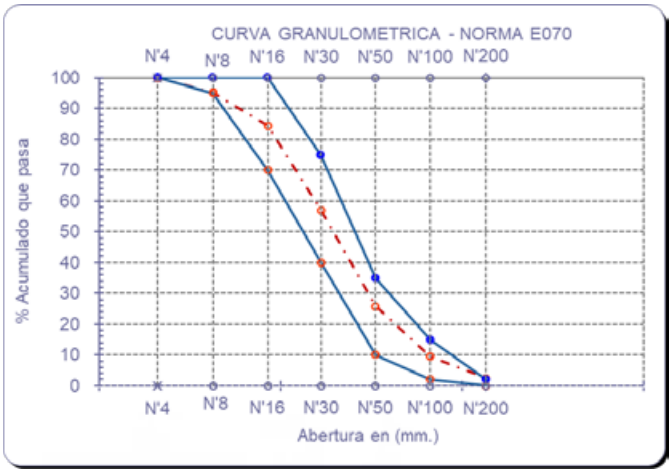

2.3.2 Densidad, densidad relativa y absorción del agregado fino

Se basa en establecer el peso específico seco, el peso específico saturado con superficie seca, el peso específico aparente y la absorción [8]. Se tomará una muestra de 500gr que ya se encuentre seca y que pasó por el tamiz 4 para colocarlo en una fiola previamente pesada. Una vez hecho esto, se colocará agua hasta tener unos 500cm3 para después agitarla para que salga el aire atrapado. Después se debe dejar 24 horas en reposo para pesar la fiola + muestra + agua. Por último, pasaremos a una tara

para luego colocarla en el horno y dejar 24 horas [8]. En la Tabla 4, se muestra el resultado de la absorción y el peso específico del agregado fino.

Tabla 4

Resultados del ensayo de densidad, densidad relativa y absorción del agregado fino

PESO ESPECÍFICO Y ABSORCIÓN			
DATOS DE LA ARENA			
Peso de la Muest. Sat. Sup. Seca.		500.00 g	500.00 g
Peso de la Muest. Sat. Sup. Seca + Peso de la fiola + Peso del agua.		939.40 g	944.10 g
Peso de la Muest. secada ahorno		497.50 g	497.10 g
Peso del Agua.		300.50 g	300.50 g
Peso de la fiola		138.90 g	144.60 g
Peso de la Muest. Sat. Sup. Seca + Peso de la fiola.		638.90 g	638.90 g
Peso de la Muest. secada ahorno + Peso de la fiola.		636.40 g	636. 40 g
Peso de la Muest. secada ahorno + Peso del frasco.		500.00 cm3	500.00 cm3
RESULTADOS			
Peso específico de la arena	2.494	2.492	**2.493**
Peso específico de la masa	2.506	2.506	2.506
Peso específico aparente	2.525	2.528	2.622
Porcentaje de absorción	0.50%	0.58%	0.54%

2.3.3 Contenido de humedad total evaporable de agregados por secado

Establece métodos para calcular el porcentaje total de humedad evaporable en una muestra de agregado mediante el proceso de secado [9]. Se tomará una muestra de 500 gr la cual sale del cuarteo ya hecho. Esta muestra será puesta en un horno por 24 horas y se dará en reposo por 1 hora para luego pesarla [9]. En la Tabla 5 se muestra el resultado del contenido de humedad.

Tabla 5

Resultados del ensayo de contenido de humedad total evaporable de agregados por secado

CONTENIDO DE HUMEDAD		
Peso de la muest. húmeda	500.00 g	500.00 g
Peso de la muestra seca	498.50 g	499.40 g
Cont. Humedad	0.30%	0.28%
Promedio		**0.29%**

2.3.4. Determinación de la masa por unidad de volumen o densidad y los vacíos en los agregados

Peso unitario suelto

Lo primero que se realiza es pesar el molde metálico para luego llenar el molde a una distancia de 5cm por encima del molde. Por último, se enraza con una varilla metálica [10].

Peso unitario compactado

El ensayo consiste en rellenar el molde en 3 capas iguales, aplicando 25 golpes con un avarilla metálica y 25 golpes con un mazo de goma en los lados por cada capa. Para finalizar se enraza y se pesa [10]. Los resultados del peso unitario suelto y compacto se muestran en Anexos, tabla 6.

2.4 Ensayo para obtener las propiedades mecánico-físicas

2.4.1 Determinación de la resistencia en compresión de prismas de albañilería

Determinar si cumple con la resistencia a la compresión fmt, utilizada para verificar el cumplimiento de la resistencia especificada para la albañilería f'm [11]. Se realizan prismas de como mínimo 2 unidades de albañilería o con una relación alto/espesor 1.3 y 5. Pasado los 28 días se ensayará el prisma, llevándolo a una máquina de compresión [11]. En Figura 2 se muestra el cómo se realiza el ensayo.

Figura 2

Procedimiento del ensayo de compresión en prismas de albañilería

2.4.2 Compresión diagonal en muretes de albañilería

Evalúa la resistencia a la compresión diagonal en muretes de albañilería a través de la aplicación de una carga diagonal de compresión [12]. Se deben realizar muretes de por lo menos 60x60 cm, teniendo 2 unidades enteras por hilada, se deben hacer 3 muertes por lo menos. El ensayo se realizará a los 28 días, colocando las muestras a 45° en la máquina de compresión [12]. En Figura 3 se muestra el cómo se realiza el ensayo.

Figura 3

Procedimiento del ensayo de compresión diagonal en muretes.

2.4.3 Módulo d elasticidad de la albañilería

Es la correlación que hay entre la carga normal y la distorsión unitaria para tensiones de tracción y compresión que están debajo del límite del material. Se le conoce como módulo de Young [13].

Ecuación para la determinación del Módulo de elasticidad, según [14].

$$E_m=500\times f'm$$

Donde:

Em = Módulo de elasticidad

f'm = Resistencia a la compresión axial

2.4.4 Módulo de corte de la albañilería

Es una constante elástica que describe el cambio en la forma de un material elástico cuando se le aplican fuerzas de corte [13].

La ecuación para determinar el Módulo de corte, según [14].

$$G_m=0.4\times E_m \quad (1)$$

Donde:

Gm = Módulo de corte

Em = Módulo de elasticidad

2.4.5 Módulo de Poisson

Es la correlación que hay entre las distorsiones transversales y las longitudinales, al estar sometida la albañilería a fuerzas de compresión [13].

La ecuación para determinar el Módulo de poisson, según [15].

$$G=\frac{E}{2*(1+v)} \quad (2)$$

Donde:

v = Módulo de poisson

G = Módulo de corte

E = Módulo de elasticidad

2.4.6 Resistencia a la flexión de morteros de cemento hidráulico

Evalúa la resistencia a la flexión de una pequeña muestra de mortero de cemento hidráulico utilizando una viga y aplicando una carga en el centro [16]. Para el ensayo se realizan 9 muestras las cuales se dividirán en 3 muestras para cada día de rotura como dice la norma (3, 7, y 28 días) para obtener la flexión del mortero [16]. En Figura 4 se muestra el cómo se realiza el ensayo.

Figura 4

Procedimiento del ensayo de resistencia a la flexión de morteros de cemento hidráulico

2.4.7 Tasa de absorción del agua de morteros de albañilería

Evalúa la absorción del agua en morteros que se utilizan en albañilería. Este método no se usa en campo debido a que los especímenes se preparan en condiciones controladas. Los resultados se pueden utilizar para evaluar la efectividad de aditivos y el impacto de otros componentes en la resistencia al agua del mortero [17]. Se realizaron 3 cubos de 5 cm y se dejó curar durante 28 días para que alcance su peso completo. Después se colocó en un recipiente de plástico; lo siguiente fue llenar el recipiente con agua hasta que el cubo se remoje 5mm. Luego se observó por 5 minutos hasta que el agua no baje su nivel [17]. En Figura 5 se muestra el cómo se realiza el ensayo.

Figura 5

Procedimiento del ensayo de tasa de absorción del agua de morteros de albañilería

2.4.8 Adherencia a cizalle

Consiste en someter a cizalle muestras formadas por 3 ladrillos adheridos con mortero [18]. Para obtener mejores resultados la norma chilena menciona que se deben hacer mínimo 3 muestras las cuales se ensayaron a los 28 días [18]. En (Anexo, Figura 6) se muestra el cómo se realiza el ensayo.

3. Resultados y discusión

3.1 RESULTADOS

Determinación de la resistencia en compresión de prismas de albañilería

(Ver Anexos Figura 7)

Método de ensayo de compresión diagonal en muretes de albañilería

(Ver Anexos Figura 8)

Obtención de módulo de elasticidad, módulo de corte y módulo de poisson

(Ver Anexos Tabla 7)

Resistencia a la flexión de morteros de cemento hidráulico

(Ver Anexos Figura 9)

Tasa de absorción del agua de morteros de albañilería

(Ver Anexos Figura 10)

Adherencia a cizalle

(Ver Anexos Figura 11)

3.2 DISCUSIONES

Según el objetivo general, evaluar las propiedades mecánico-físicas del mortero de cemento portland con la adición de los diferentes porcentajes de resina de colofonia en muros de albañilería confinada, para esto se realizaron los diferentes ensayos en el laboratorio, para lo cual se preparó la mezcla de mortero de manera tradicional y por otra parte una mezcla con resina de colofonia con sus diferentes porcentaje de adición propuesto en la tesis, mostrando una mejora en las características físicas y mecánicas del mortero pero disminuyendo las propiedades mecánicas de los muros.

Según el objetivo específico, evaluar la resistencia a la compresión de prismas de albañilería del mortero con resina de colofonia con los porcentajes de 0.2%,

0.4% y 0.5%, se observó que, al mezclar resina de colofonia, el mortero pierde resistencia conforme aumenta la cantidad de la colofonia. Esto se ve en la dosificación 1:3 patrón que alcanzó una resistencia a la compresión en prismas de 84.20 kg/cm2, pero cuando se le agregó el porcentaje de 0.2% de colofonia, la resistencia bajó a 59.67 kg/cm2 lo que en porcentaje quiere decir 29%; estos resultados se repitieron con los demás prismas. En el tema de los muretes que se ensayaron, se repitió el mismo comportamiento que las pilas. En la mezcla 1:3 patrón, logró llegar a una resistencia de 11.79 kg/cm2 y en cambio con 0.2% de colofonia bajó a 8.25 kg/cm2 lo que es porcentaje refleja un 30%. Al comparar la investigación de [19], se determina que al agregar más colofonia esta se vuelve menos porosa y absorbente; sin embargo, también se determinó que el mortero es menos resistente al momento de resistir cargas axiales. Lo mismo estableció G. Sosa [20], que al presentar diferentes dosificaciones de colofonia en el concreto, sobre todo cuando se agrega mayor cantidad de colofonia se obtenían menos resistencia a la compresión en el concreto. Con estos resultados se afirma que la colofonia no deja pasar fácilmente el agua, haciendo que no suba la humedad e impide que el cemento se hidrate, ocasionando que la mezcla se vuelva de baja resistencia.

Según el objetivo específico, obtener el módulo de elasticidad, módulo de corte y poisson de los ensayos de compresión de prismas y compresión diagonal en muretes, estas propiedades se calcularon a partir de los resultados obtenidos de las pruebas de resistencia a la compresión en prismas y compresión diagonal en muretes. Se determinó que al aumentar la cantidad de colofonia en el mortero los valores disminuyen, por esto lo que se asume que el mortero se vuelve más flexible, es decir, menos rígido ante las cargas. Todos los morteros en los que se añadió resina no lograron cumplir lo mínimo que menciona la norma E070. Esto da a entender que, si bien el mortero pierde rigidez, aun se puede considerar funcional en estructuras que no estén sometidas a grandes cargas. Estudios como el de G. Sosa [20], nos permite comparar cómo al incorporar colofonia en el concreto, este afecta la rigidez del material, ya que la resina actúa como agente incorporador de aire. Lo mismo plantea [19], quien demostró que la combinación de tanino y colofonia en morteros afecta las propiedades físicas y mecánicas, una de ellas es la rigidez, logrando afirmar que esta mezcla es más ligera y porosa, si bien logra mejorar su trabajabilidad, pero modifica su capacidad para soportar cargas severas.

Según el objetivo específico, evaluar la resistencia a la flexión del mortero con resina de colofonia con los porcentajes de 0.2%, 0.4% y 0.5%, se observó que al agregar colofonia en los diferentes porcentajes de 0.2%, 0.4% y 0.5%, tiende a reducir su resistencia a la flexión, especialmente cuando se usa más de 0.2% de colofonia. Las pruebas se realizaron a los 3, 7 y 28 días de curado, y en los primeros días se observó que el mortero con 0.2% de colofonia mantenía una resistencia parecida al patrón de las dosificaciones 1:3 y 1:4; sin embargo, cuando el porcentaje de colofonia subía a 0.4% o 0.5%, bajaba la resistencia, sobre todo en la dosificación 1:5, que es la que tiene menos cemento y por eso es más frágil a esfuerzos de tracción. Los resultados indican que si el porcentaje de colofonia se mantiene menor a 0.2%, el mortero se comporta de manera parecida al patrón, pero si se pasa pierde rigidez. Si se compara con estudios pasados como el de M. Fernández *et. al* [19], se establece que al usar colofonia y tanino en morteros puede ser beneficioso siempre y cuando se utilice en dosificaciones bajas; en sus ensayos notaron que estas mezclas mejoraban la durabilidad y algunas propiedades mecánicas, pero también concluyeron que pueden aparecer burbujas o vacíos internos que hacen más débil la mezcla. De manera similar G. Sosa [20], menciona que la colofonia al actuar como aditivo introduce aire y mejora la trabajabilidad, va a afectar la resistencia al usar proporciones de colofonia en grandes cantidades. Se puede concebir que la resistencia a la flexión del mortero depende de que se formen bien las uniones internas del cemento al fraguarse, ya que la colofonia al ser una resina que repele el agua forma una película interna que impide que el cemento se hidrate del todo; haciendo que la mezcla del mortero no se forme bien.

Según el objetivo específico, evaluar la cantidad de absorción del mortero con resina de colofonia con los porcentajes de 0.2%, 0.4% y 0.5%, se determinó que a medida que aumentaba el porcentaje de la colofonia, la absorción de agua disminuía y los resultados reflejaron que en todos los casos el mortero con colofonia era más impermeable que el patrón. Los ensayos realizados en tres etapas (0.25 horas, 1.5 horas y 24 horas), siguiendo el procedimiento que dice la norma. La mezcla con 0.2% de colofonia fue la que alcanzó el mejor comportamiento de impermeabilidad, ya que fue la que logró reducir de forma significativa la absorción tanto en las primeras horas como a lo largo del ensayo. Se identificó que se mantiene una porosidad más cerrada debido a la colofonia. Al comparar con el estudio de [19], donde menciona que la colofonia al adicionarse con el mortero genera una disminución importante en la porosidad y absorción de agua, mejorando la durabilidad del material ante ambientes agresivos. De la misma manera [20], concluyó que la colofonia al actuar como un agente impermeabilizante natural reduce la absorción capilar al formar una película hidrofóbica dentro de la mezcla, lo que protege al concreto frente al ingreso de humedad sin necesidad de aplicar aditivos sintéticos o revestimientos adicionales. Por esto, se afirma que esta propiedad es fundamental para prolongar la vida útil del mortero en contacto con los suelos húmedos, zonas costeras o edificaciones antiguas donde la humedad ascendente es una patología frecuente, la cual genera una barrera dentro del mortero impidiendo que el agua llegue

a la zona de acero, evitando la corrosión y reduciendo la aparición de manchas de humedad en la superficie.

Según el objetivo específico, evaluar la adherencia del mortero con resina de colofonia con los porcentajes de 0.2%, 0.4% y 0.5%, se observó que a diferencia de otras propiedades mecánicas que disminuyeron con el uso de la resina de colofonia, la adherencia mejorό con el aumento de la colofonia. En la dosificación 1:3, la adherencia fue menor que la alcanzada por el mortero con 0.2% de colofonia, y en los porcentajes 0.4% y 0.5% fue aún más notable. Los resultados obtenidos son bastantes útiles, ya que una buena adherencia garantiza que los muros trabajen como un solo conjunto y no se separen las piezas con el tiempo, sobre todo en la presencia de vibraciones de pequeños sismos o pequeñas cargas laterales. Lo que indican G. Sosa [20], y M. Fernández [19], establece que la colofonia actúa como repelente de agua, mejorando la unión entre componentes del mortero, esto debido a que genera una película adhesiva natural entre las superficies del cemento y el ladrillo. O. Hernández y R. Meli [21], determinaron que la adherencia del mortero y ladrillo no conlleva importancia en la resistencia y ductilidad del muro ante cargas laterales. Así se afirma que estos compuestos mejoran el contacto entre el mortero fresco y la superficie rugosa del ladrillo, reduciendo la formación de microburbujas de aire y aumentando el área efectiva de contacto entre ambos materiales. Además, como la resina disminuye la porosidad del mortero, también reduce la pérdida de agua durante el fraguado inicial, lo que permite un mejor asentado y pegado del ladrillo sin que se despegue por secado rápido o falta de humedad. Este tipo de comportamiento es especialmente útil en zonas donde se trabaja con ladrillo artesanal.

Según el objetivo específico, realizar un estudio comparativo de los resultados del ensayo de resistencia a la compresión de prismas de albañilería y diagonal en muretes, flexión, absorción (según la NTP), y adherencia del mortero con los diferentes porcentajes de resina de colofonia ante los resultados de un mortero de cemento portland tradicional. Los resultados indicaron que en general el uso de la colofonia afecta algunas propiedades mecánicas como la resistencia a la compresión en prismas y muretes, y flexión, pero mejora considerablemente la adherencia y disminuye la absorción de agua. En los prismas, el mortero patrón alcanzó resistencias más altas que las dosificaciones a las que se le añadieron colofonia, además ninguna dosificación con colofonia alcanzó las características mínimas que menciona la norma E070; sin embargo, el ensayo de compresión en muretes, la única dosificación 1:3 con 0.2% de colofonia si alcanzó las características mínimas de la norma. Por otro lado, los ensayos de flexión, la tendencia fue similar, manteniendo una disminución leve en la resistencia para los morteros con colofonia. Sin embargo, cuando se ensayó la tasa de absorción de agua y la adherencia a cizalle, los morteros con colofonia especialmente con 0.2% o 0.4% superaron al mortero patrón, mostrando una menor absorción y una mejor capacidad de agarre entre ladrillos y morteros. G. Sosa [20], determinó que la colofonia al actuar como biopolímero introduce aire en la mezcla, mejorando la trabajabilidad, pero reduciendo sus propiedades mecánicas, dependiendo del porcentaje adicionado.

Estos estudios previos coinciden que el uso de la colofonia debe manejarse con cuidado y en proporciones adecuadas para logar un equipo entre resistencia y durabilidad. Por esto M. Fernández [19], definió que, al añadir colofonia al mortero, mejora su impermeabilidad y disminuye la porosidad, aunque también indicó una disminución en ciertas propiedades estructurales, lo cual concuerda con los resultados de este estudio. Esto es crucial en zonas donde la humedad es un problema constante, ya que ayuda a prevenir la formación de hongos, eflorescencias y desprendimientos de revestimiento. Además, el hecho de que el mortero con colofonia tenga una mejor adherencia permite que los muros trabajen más unidos y con menos riesgo de separación o fisuras con el paso del tiempo.

4. Conclusiones

Se concluyó que la adición de colofonia genera una disminución en la resina a la compresión tanto en prismas como en muretes. Sin embargo, la dosificación 1:3 con 0.2% de colofonia lograron cumplir las características mínimas que pide la norma E070, permitiendo su uso en muros no portantes (tabiquería), viviendas de no más de 2 pisos sin comprometer la parte estructural.

Los valores que se obtuvieron de los módulos elásticos indicaron que se presentaron variaciones con respecto al mortero patrón, estos resultados fueron esperados por el comportamiento del material con un aditivo hidrofóbico. Estas propiedades si bien es cierto que disminuyeron, no quiere decir que no se puedan utilizar en proyectos que no requieran un comportamiento de mucha demanda estructural.

La resistencia a flexión presentó variaciones leves entre mezclas, sin tener disminuciones importantes que comprometan el desempeño del mortero. La mezcla con 0.2% de colofonia mantuvo una buena capacidad a flexión, lo cual sugiere que dicho porcentaje es el más adecuado para mantener un equilibrio entre las propiedades mecánicas y físicas.

La incorporación de colofonia redujo notablemente la tasa de absorción de agua en comparación con el patrón. Destacando con una mejora física significativa. Esta propiedad es clave para mitigar problemas de humedad ascendente, especialmente en construcciones con climas húmedos.

Los resultados mostraron un aumento en la adherencia a cizalle en las mezclas con colofonia, especialmente

en aquellas con mayor porcentaje del aditivo. Esta mejora en la cohesión del ladrillo y mortero es un aporte relevante para garantizar la integridad de los muros frente a esfuerzos de baja sismicidad o a bajos empujes laterales.

La comparación evidenció que, si bien hay una reducción parcial de las propiedades mecánicas, los beneficios físicos obtenidos con la adición de colofonia compensan esa perdida en contextos donde la resistencia no sea un parámetro necesario, sino donde la humedad es un factor primordial. Por tanto, se valida la hipótesis de que la resina mejora el desempeño físico del mortero sin comprometer su funcionalidad estructural en condiciones específicas.

Referencias

[1] D. Heras Murcia, "Morteros de cemento con nano-adiciones de hierro y sílice" Tesis de maestría, Universidad Politécnica de Madrid, España, 2015.

[2] J. Alcaide Romero, "Caracterización de morteros con adición o sustitución de diferentes materiales carbonosos" Tesis Doctoral, Universidad de Alicante, España, 2007.

[3] A. Adco Mamani y A. Apaza Mamani, "Influencia del Polietileno en la Humedad por Capilaridad en Muros de Mampostería en la Urbanización Clara Victoria-Juliaca", Tesis de Grado, Universidad Cesar Vallejo, Perú, 2022.

[4] J. P. Fernandez Curotto, "Humedad proveniente del suelo en edificaciones", Tesis de Grado, Universidad Nacional de Chile, Chile, 2008.

[5] N. Proietti, P. Calicchia, F. Colao, S. De Simone, V. Di Tullio, L. Luvidi, F. Prestileo, M. Romani y A. Tatì, «Moisture Damage in Ancient Masonry: A Multidisciplinary Approach for In Situ Diagnostics,» *Minerals,* vol. 11, nº 406, p. 23, 2021.

[6] L. B. Pusaclla Bernal, "Los suelos con alto contenido de sales influyen en los daños en viviendas autoconstruidas en la zona II de Tahuantinsuyo- Independencia 2017", Tesis de Grado, Universidad César Vallejo, Perú, 2017.

[7] INACAL, "Análisis granulométrico del agregado fino, grueso y global" Lima, 2001.

[8] INACAL, "Método de ensayo normalizado para la densidad, la densidad relativa (peso específico) y absorción del agregado fino" Lima, 2013.

[9] INACAL, "Método de ensayo normalizado para contenido de humedad total evaporable de agregados por secado" Lima, 2013.

[10] INACAL, "Método de ensayo normalizado para determinar la masa por unidad de volumen o densidad ("peso unitario") y los vacios en los agregados" Lima, 2011.

[11] INACAL, "Método de ensayo para la determinación de la resistencia en compresión de prismas de albailería" Lima, 2013.

[12] INACAL, "Método de ensayo de compresión diagonal en muretes de albañilería" Lima, 2004.

[13] R. Yaipen Trelles, "Determinación del módulo de elasticidad, coeficiente de poisson, módulo de corte, del concreto, utilizando materiales de la región de Piura" Tesis de Grado, Universidad Católica Santo Toribio de Mogrovejo, Perú, 2022.

[14] A. San Bartolomé, D. Quiun y W. Silva, *Diseño y construcción de estructuras sismoresistentes de albañilería*, Lima: Fondo Editorial Pontificia Universidad Católica del Perú, 2018.

[15] C. R. Catalán Oliva, "Algunas consideraciones sobre el modulo de poisson" Unidad de investigación y desarrollo vial, San salvador, 2008.

[16] INACAL, "Método de ensayo normalizado de resistencia a la flexión de morteros de cemento portland" Lima, 2002.

[17] INACAL, "Método de ensayo normalizado para la tasa de absorción del agua de morteros de albañileria" Lima, 2015.

[18] INN, "Construcción-Ladrillos cerámicos-Ensayos" Chile, 2001.

[19] M. Fernandez Cánovas, N. Hurtado y G. Kawiche, «Influencia que sobre las propiedades físico-mecánicas de los morteros de cemento portland tiene la adición de colofonia y tanino,» *Materiales de construcción,* vol. 39, nº 216, pp. 15-22, 1989.

[20] G. Sosa Davila, "Efecto del biopolímero extraido de pinus radiata como aditivo en las propiedades del concreto Huancayo - Junin 2018" Universidad Nacional de Centro del Perú, Perú, 2019.

[21] O. Hernández y R. Meli, "*Modalidades de refuerzo para mejorar el comportamiento sísmico de muros de mampostería*" UNAM, México, 1976.

Anexos

Figura 6

Procedimiento del ensayo de adherencia a cizalle

Figura 7

Resistencia a la compresión en prismas

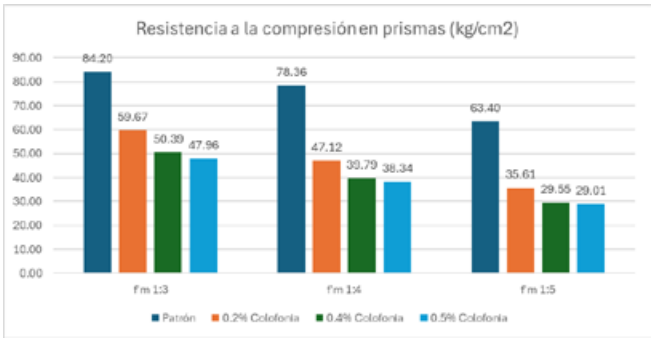

Figura 8

Resistencia a la compresión diagonal en muretes

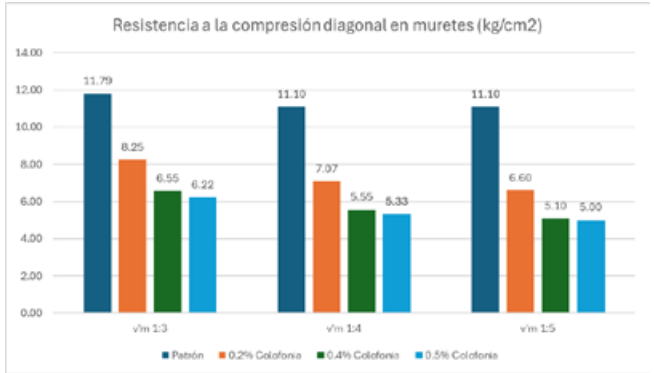

Figura 9

Resistencia a la flexión de morteros de cemento hidráulico

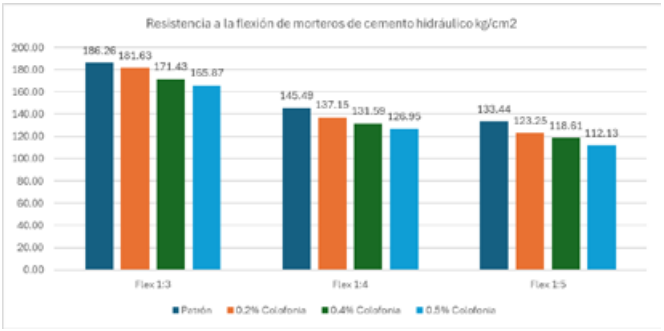

Figura 10

Tasa de absorción a las 24 horas

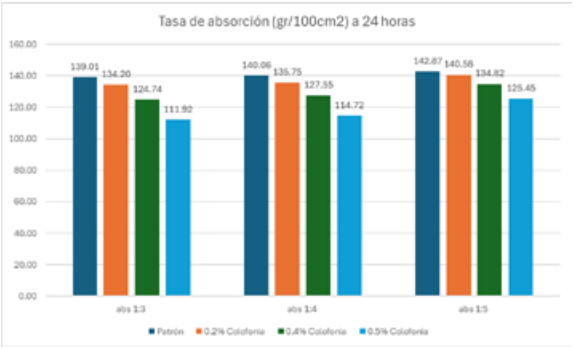

Figura 11

Adherencia a cizalle

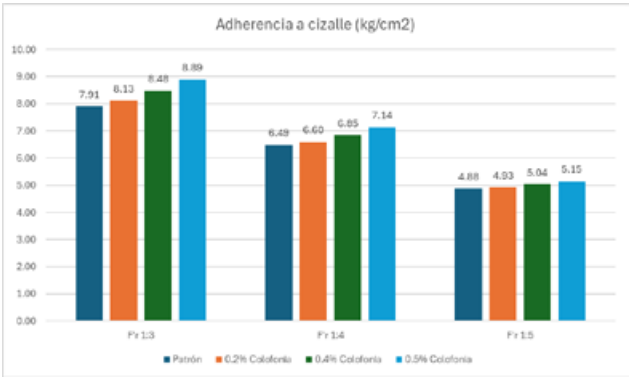

Tabla 6

Resultados del ensayo de determinación de la masa por unidad de volumen o densidad y los vacíos en los agregados

PESO UNITARIO		
PESO U. SUELTO	A	B
Peso de la muestra húmeda	8466	8473
Volumen de molde	0.00530	
Peso unitario suelto húmedo	1598	
PESO UNIT. SUELTO SECO	1602	
PESO U. COMPACTADO	A	B
Peso de la muestra húmeda	9207	9223
Volumen de molde	0.00530	
Peso unitario compactado húmedo	1738	
PESO UNIT. COMPACTADO SECO	1743	

Tabla 7

Módulo de elasticidad, módulo de corte y módulo de poisson

MUESTRAS	**Em (kg/cm2)**	**Gm (kg/cm2)**	**Módulo de Poisson**
PATRÓN 1-3	**42097.98**	**16839.19**	**0.25**
0.20% COLOFONIA	**29834.42**	**11933.77**	**0.25**
0.40% COLOFONIA	**25192.84**	**10077.14**	**0.25**
0.50% COLOFONIA	**23982.49**	**9593.00**	**0.25**
PATRÓN 1-4	**39177.98**	**15671.19**	**0.25**
0.20% COLOFONIA	**23559.58**	**9423.83**	**0.25**
0.40% COLOFONIA	**19894.02**	**7957.61**	**0.25**
0.50% COLOFONIA	**19170.43**	**7668.17**	**0.25**
PATRÓN 1-5	**31700.89**	**12680.36**	**0.25**
0.20% COLOFONIA	**17804.14**	**7121.66**	**0.25**
0.40% COLOFONIA	**14773.98**	**5909.59**	**0.25**
0.50% COLOFONIA	**14506.56**	**5802.62**	**0.25**

FACULTAD DE INGENIERÍA Y CIENCIAS APLICADAS
UNIVERSIDAD CENTRAL DEL ECUADOR

INGENIO
2025, VOL 8(2), JULIO - DICIEMBRE, PP. 127-142

REVISTA INGENIO

Development of Oat Husk-Derived Nano-Silica for High-Performance and Sustainable Mortar Applications

Desarrollo de Nanosílice Derivada de Cáscara de Avena para Aplicaciones de Mortero Sostenibles y de Alto Rendimiento

Mohammadfarid Alvansazyazdi | Universitat Politécnica de Valencia - Spain
Alvaro Yerandi Carlosama Carde | Universidad Central del Ecuador- Ecuador
Jorge David Rosillo Pilamunga | Universidad Central del Ecuador- Ecuador
Pablo Mauricio Bonilla Valladares | Universidad Central del Ecuador- Ecuador
Debut Alexis Patrice Martial | Universidad de las Fuerzas Armadas - Ecuador
Jorge Luis Santamaria Carrera | Universidad Central del Ecuador- Ecuador
Hugo Alexander Cadena Perugachi | Universidad Central del Ecuador- Ecuador
Andrea Estefania Logacho Morales | Universidad Central del Ecuador- Ecuador
Jhon Fabricio Tapia Vargas | Constructora COVEVIM T&T S.A. - Ecuador

Recibido: 29/4/2025
Recibido tras revisión: 19/5/2025
Aceptado: 6/6/2025
Publicado: 10/7/2025

KEY WORDS
Nano-silica, oat husk, sol-gel, mortar, mechanical properties, plastering.

ABSTRACT
This study investigates the incorporation of nano-silica synthesized from agro-industrial waste—specifically oat husks—into plastering mortars. Amorphous silica is extracted through chemical treatment and converted into nano-silica via a sol-gel process, yielding 2.79%. Characterization through EDS, SEM, TEM, and XRD confirms nanoscale silica formation. Mortars are formulated using Atena Máster type N cement and fine aggregates from the "Copeta" quarry, verified under NTE INEN 2 536 standards. Nano-silica is added at dosages of 0.25%, 0.50%, 0.75%, and 1.00% by cement weight. The mixtures are evaluated in both fresh and hardened states. Fresh-state tests assess workability and flow, while compressive strength is measured at 7, 14, and 28 days. Results show that 0.25% nano-silica provides optimal performance, achieving 12.6 MPa at 28 days. Higher dosages lead to strength reduction, indicating a performance threshold. A cost-benefit analysis highlights the economic and environmental viability of converting agro-waste into high-performance materials. The findings underline nano-silica's potential to enhance mechanical properties while promoting sustainability. This research demonstrates that controlled use of nano-silica from waste sources offers an eco-friendly, efficient solution for improving plaster mortar in the construction industry.

PALABRAS CLAVE
Nano-sílice, cáscara de avena, sol-gel, mortero, propiedades mecánicas, enlucido.

RESUMEN
Este estudio investiga la incorporación de nano-sílice sintetizada a partir de residuos agroindustriales—específicamente cáscaras de avena—en morteros para enlucido. La sílice amorfa se extrae mediante un tratamiento químico y se convierte en nano-sílice mediante un proceso sol-gel, obteniéndose un rendimiento del 2,79 %. La caracterización mediante EDS, SEM, TEM y DRX confirma la formación de sílice a escala nanométrica. Los morteros se formulan utilizando cemento Atena Máster Tipo N y agregados finos provenientes de la cantera "Copeta", verificados conforme a la norma NTE INEN 2536. La nano-sílice se incorpora en proporciones de 0,25 %, 0,50 %, 0,75 % y 1,00 % en peso respecto al cemento. Las mezclas se evalúan en estado fresco y endurecido. Las pruebas en estado fresco analizan la trabajabilidad y la fluidez, mientras que la resistencia a la compresión se mide a los 7, 14 y 28 días. Los resultados muestran que la adición del 0,25 % de nano-sílice proporciona el mejor desempeño, alcanzando 12,6 MPa a los 28 días. Dosificaciones superiores provocan una disminución en la resistencia, lo que indica un umbral de rendimiento. Un análisis costo-beneficio resalta la viabilidad económica y ambiental de convertir residuos agroindustriales en materiales de alto desempeño. Los hallazgos subrayan el potencial de la nano-sílice para mejorar las propiedades mecánicas de los morteros, al tiempo que promueven la sostenibilidad. Esta investigación demuestra que el uso controlado de nano-sílice proveniente de fuentes residuales constituye una solución ecológica y eficiente para mejorar el mortero de enlucido en la industria de la construcción.

https://doi.org/10.29166/ingenio.v8i2.8165

pISSN 2588-0829
eISSN 2697-3243
fing.revista.ingenio@uce.edu.ec

1. Introduction

Mortar has been a fundamental component in societal development for decades, playing a crucial role in the advancement of civilization. As noted by Salamanca Rodrigo [1], he first mortar was made from stones and mud, later evolving to clay-based mixtures. By the 19th century, lime and sand were commonly used. Mortar is considered a specialized concrete mixture due to its similar composition, albeit with fine aggregate.

Currently, structural mortar has high demand due to its diverse applications, such as masonry bonding and plastering. There are standards that outline specifications for mortar preparation in construction; however, they do not specify on-site tests to determine its strength [2].

The search for innovative materials in the construction sector not only depends on advances in nanomaterials but also on the efficient management of experimental data and systematic analysis, as demonstrated through the application of executive dashboards for project monitoring [3].

In recent years, construction has undergone significant changes due to the emergence of nanotechnology. Materials have evolved into "super materials," reducing environmental impact while enhancing their molecular structure to become lighter, stronger, self-adaptive, and intelligent [4]. These materials are modified at a scale of 1 to 100 nanometers, influencing physical, chemical, and biological reactions to reinforce the polymer matrix and regulate the controlled release of additives or active agents with antimicrobial properties [5].

The successful implementation of disruptive technologies, such as the incorporation of rice husk-based nano-silica, largely depends on organizational agility and the ability to rapidly adapt to emerging synthesis and characterization methodologies [6].

Just as the integration of information and communication technologies (ICTs) has transformed education methodologies, the incorporation of locally synthesized nano-silica into mortars represents a crucial step towards a more sustainable and innovative construction industry [7].

Among all nanomaterials, nano-silica has garnered significant attention from the construction industry. This is due to its superior pozzolanic activity, surpassing that of silica fume due to its larger specific surface area. This component reacts more efficiently with calcium hydroxide (portlandite), which is responsible for producing C-S-H gel, leading to enhanced early-age mechanical strength [8].

Given the high acceptance and interest shown by construction researchers, this study aims to analyze the characteristics that emerge when incorporating nano-silica into the mortar matrix. To achieve this, comparisons will be made with conventional mortar using standard materials such as cement, water, and fine aggregate. By the end of the study, the efficiency of nano-silica incorporation will be evaluated in terms of compressive strength and permeability improvements.

1.1. Silica Mortars and Nanoparticles

1.1.1.. MORTARS

Definition and types of mortars

Mortar in the construction sector is defined as the combination of three main materials: cement or any binder, fine aggregate, and water. Often, it is necessary to add an admixture to the mix in order to improve certain properties of the mortar. Upon setting, the mixture exhibits behavior similar to that of concrete.

The NTE INEN 2518 standard describes five types of mortar based on the classification presented by the ASTM C-270 standard, with each type of mortar exhibiting its own characteristics, as outlined below.

Type M Mortar: It is characterized by greater durability compared to other types of mortars. It is used in structures that support heavy loads or are in contact with the ground or water.

Type S Mortar: Its main characteristic is adhesion to construction materials, such as in tile coatings for floors and walls.

Type N Mortar: It has medium strength, making it very useful as a binder for masonry blocks and wall coatings.

Type O Mortar: It has excellent workability but low strength. It is recommended for use in non-load-bearing walls of buildings with a maximum of two stories and coatings that are not exposed to harsh weather conditions.

Importance of Mortar in Construction

Mortars have various applications in construction, both in structural elements, such as in masonry buildings where this binder serves to support loads, and in non-structural elements. The most common use in our context is for non-structural elements, such as adhesives or coatings [9].

Mortar contributes in various ways to the preservation of a structure, such as in the use of mortars for waterproofing, thereby preventing damage to structural elements that could compromise the safety of the building. Similarly, mortar ensures the bonding of elements like blocks used in walls that divide different spaces, acting as a thermal and acoustic insulator to provide comfort for building occupants.

The aesthetic aspect of a construction largely depends on the final finishes, which are achieved with mortars to

eliminate imperfections or provide a specific style both inside and outside the building.

Improving mortar can aid in the evaluation of the seismic behavior of special moment frames using nonlinear incremental dynamic analysis [10].

Composition and Properties of Conventional Mortar

Mortar, like any construction material, possesses chemical, physical, and mechanical properties that vary according to the specific needs of the construction project. These properties are considered from the design of the mix to its preparation process.

Composition mortar

To prepare mortar, a binder, fine aggregate, and water are required. In some cases, special additives or aggregates may be used to enhance certain properties.

Properties of Mortar in the Fresh State

In their plastic state, mortars display a range of key properties that are crucial for assessing their behavior and effectiveness during fabrication and application in construction. Among these properties, workability and consistency are essential to ensure ease of handling and uniform application, thereby guaranteeing the quality of the construction work. [11]

Flow

This property is measured in the laboratory. The procedure involves placing the mortar in the form of a truncated cone on a vibrating table, then measuring the percentage increase in diameter after allowing the mortar to fall 25 times within 15 seconds from a height of 12.7 mm. [9]

Masonry units absorb a certain percentage of water, so it is recommended to maintain a workability range between 130% and 150% to counteract this absorption. [12]

Water Retention

The water retention capacity of mortar is essential to ensure that workers have sufficient time to adjust masonry units before the mortar hardens. [13]

Water retention capacity can be increased through various techniques, such as increasing the binder content, adding fine sand, or using water-retaining materials. [2]

Workability

This property is crucial in the mortar application process, as good workability facilitates the worker's task and ensures proper positioning of the masonry, while also preventing potential voids at the joints. Additionally, in vertical plastering, the mortar provides good adhesion and uniform distribution for a better finish. [2]

Hardening

The hardening of mortar is directly related to workability. As the mortar loses water, its workability decreases, which could be detrimental. This hardening rate can be modified through the use of additives or techniques such as adjusting the temperature during the setting process.

1.1.2. Properties of Mortar in the Hardened State

Compressive Strength

One of the fundamental properties is compressive strength, which is influenced by three main factors. The first factor is the cement-to-sand ratio, where having a higher amount of cement relative to sand will exponentially increase the strength. The second factor indicates that mortars with a high fineness modulus exhibit greater strength. Lastly, it has been established that plastic mixtures perform better under compression than fluid mixtures. [14]

Absorption

The ability of mortars to absorb and retain liquids is a key factor in their strength and durability. High absorption can increase vulnerability to water infiltration, which could deteriorate structures and promote the appearance of cracks, corrosion of steel reinforcement. [15]

Permeability

Permeability in mortars refers to their ability to allow the passage of liquids or gases. A highly permeable mortar facilitates the infiltration of water and other substances, which can lead to moisture, structural corrosion, and the deterioration of building materials. Various factors influence this characteristic, such as poor mixing of components, application errors, or the use of inadequate or deteriorated materials. The presence of permeable mortars increases the risk of damage in areas where they have been used. [16]

1.2. NANOTECHNOLOGY AND NANOMATERIALS.

Nanotechnology emerged in the latter decades of the 20th century, driven by the development of new enabling technologies for imaging, manipulating, and simulating matter at the atomic scale [17]. This field involves controlling matter at the nanoscale and exploiting novel phenomena and properties, often by combining nanotechnology with other study areas like supramolecular chemistry [18]. By reducing material dimensions to the

nanometer scale, particularly below 100 nanometers, quantum effects become prominent, significantly altering their physical, chemical, and electronic properties [19]. The application of nanotechnology can modify certain properties of concrete [20]. Nanomaterials are unique as they provide a high surface-to-volume ratio, representing the engineering of useful and functional objects at the molecular or atomic scale [21]. Nanomaterials are classified into four main categories. Among these, 0-D materials, such as Au and Ag nanoparticles and fullerenes, exhibit all their dimensions at the nanoscale. Meanwhile, 1-D and 2-D materials, such as carbon nanotubes and graphene, respectively, have one or two dimensions smaller than 100 nm. These latter materials are widely used in industries such as pharmaceuticals and electrical adhesives [22].

1.3. SILICA NANOPARTICLES

Background

Silica nanoparticles have gained widespread acceptance and recognition worldwide due to their diverse physicochemical properties. Based on particle size, mesoporous silica, ranging from 2 to 50 nm, exhibits enhanced adsorption/absorption behavior for hydrocarbons and can adsorb large molecules such as proteins [23]. In contrast, nanoporous silica particles, which are smaller than 2 nm, have the ability to absorb gas molecules [24]. Additionally, this material emerges as an alternative to microsilica, which is produced through the reaction of silicon at high temperatures [25]. The incorporation of nano-silica enhances performance and durability, contributing to the reuse of alternative materials and by-products from industrial processes, thereby generating a direct environmental benefit [26]. It is important to note that when using this nano-addition, cement demand decreases, while water demand in the mix increases due to its high specific surface area [6].

The use of agro-industrial waste, such as oat husks, for the synthesis of nano-silica offers a sustainable alternative that reduces environmental impact and promotes circular economy practices in the construction sector [27].

The various investigations take into account different sustainability problems in materials used in construction which can be improved, having several materials from which to choose, taking into account that the most important thing is to preserve the environment in order to preserve our planet [28].

Characteristics

Silica nanoparticles are spherical and exhibit pozzolanic activity. In mortars, they enhance dispersion and workability while also filling voids within the mixture.

Their incorporation increases concrete strength due to the production of C-S-H with improved properties, as this compound results from the reaction with portlandite. Additionally, they enhance workability, as their high specific surface area demands a greater amount of water. Furthermore, their structure is more compact, as the pores are filled by the small particles, thereby preventing chemical attacks and material corrosion [29].

Methods of obtaining Silica

One of the first methods for obtaining nano-silica was proposed by Beck in 1992, known as the sol-gel process. This method primarily involves forming a colloidal suspension, which subsequently undergoes gelation. During this process, hydrolysis and condensation of salts occur with the addition of catalysts, while acids or bases are introduced at different stages.

The gas-phase method involves reducing quartz in a furnace at temperatures ranging from 1500 to 2000°C. This process produces spherical nano-silica, commonly obtained from the metal industry. Alternatively, nano-silica can be extracted from silicon tetrachloride using hydrogen or oxygen at high temperatures.

The precipitation method utilizes sodium silicate or rice husk. The ashes are heated and washed to remove acids, then further washed to reach a pH of 3. Subsequently, bases are added, and the ashes are washed again until a pH of 7 is achieved, resulting in the extraction of silica [30].

The optimization of synthesis methodologies, such as controlling the pH and sequential acid-base reflux processes, is essential to maximize yield and nanoparticle quality. Similar optimization strategies have been effectively applied in advanced material surface treatments using NSGA-II algorithms [31].

Ilustración 1

Process for nanosilica synthesis.

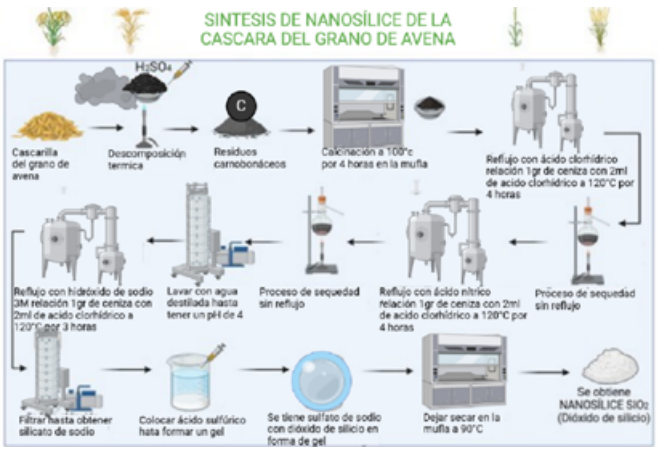

2. Materials and Methods

This study has characterized various resources intended for construction, based on national standards such as the NTE INEN and international standards like ASTM. The materials characterized include sand as fine aggregate, cement, and nano silica.

The process and dosing used for the analysis are presented, along with an in-depth interpretation of the results obtained from the tests conducted on mortar in both its fresh and hardened states. Among the tests performed are flowability, compressive strength at 24 hours, 3 days, 7 days, and 28 days.

The materials used for the characterization and analysis of the mortar behavior in construction are shown in Table 1 below.

Tabla 1

Materials Used

Material	Source/Specification
Fine Aggregate	Copeta Quarry
Cement	Master Atenas
Water	EPMAPS
Oat-based Nanosilica	Self-synthesis

2.1. NANOSILICA SYNTHESIS.

Separation of the husk and grain.

The methodology consisted of placing the grains in a blender, where the blades, applying mechanical force, separated the husk from the grain. Once this was done, a sieve and vertical movements were used to achieve the complete separation of both elements.

Sample weighing.

The initial weight of the oat husk is recorded in order to determine the yield of the ashes obtained after combustion, expressed as a percentage.

Sample Pyrolysis

The ground oat husks are placed in a heat-resistant container, such as a crucible, to undergo the heating process. A heating mesh is placed between the heat source and the crucible. This step is crucial to ensure the safety of the process and to guarantee an even heat distribution. To ensure the integrity of the container and prevent possible fractures due to direct exposure to the flame, a heating mesh is placed between the heat source and the crucible. This step is critical to maintain process safety and ensure uniform heat distribution.

Ash formation

The crucible with the ashes is placed in a muffle furnace, where the material undergoes a calcination process at a temperature of 1000 °C for a period of 4 hours. This thermal treatment allows the complete conversion of the carbonaceous residue into ashes.

Assembly of the reflux equipment.

First, the universal stand is fixed to the workbench, and the clamps are placed to secure the flask and condenser. Then, a round-bottom flask with an oil bath is mounted, securing the flask to the stand with a clamp. Next, the reflux condenser is connected to the neck of the flask using an adapter or ground joint, securing the connection with another clamp. Afterward, the water hoses are connected to the condenser: one for the inlet (lower part) and one for the outlet (upper part), ensuring proper water flow. The outlet hose is directed to a drain or container. The heating mantle is placed to facilitate the handling of reagents, and finally, the oil is evenly distributed in a pot to ensure proper heating of the flask.

Ash reflux with mineral acids

The ashes are placed in a round-bottom flask, filling at least half of its capacity, and are heated evenly using a pot with oil. The water flow in the condenser is turned on to prevent vapor loss during heating. For the hydrochloric acid treatment, 200 ml of acid are mixed with 100 g of ashes and subjected to reflux at 120 °C for 4 hours. Afterward, the excess acid is evaporated until dryness is achieved. In the nitric acid treatment, the dry ashes are mixed with nitric acid in the same proportion and refluxed again for 4 hours. The excess acid is then evaporated, leaving the ashes ready for the next step in the synthesis.

Washing of ash from acid reflux with distilled water.

After the reflux treatment, the ashes are filtered under vacuum. To completely remove the solid from the reactor, portions of distilled water are added, which are also filtered. The solid is then repeatedly washed with distilled water until the pH of the washing water is between 6 and 7, ensuring the neutralization of the acidic residues. At this point, the ashes contain a higher proportion of silicon dioxide.

Reflux with 3M concentration sodium hydroxide.

The washed ashes, rich in silicon dioxide, are mixed with a 3M NaOH solution (200 ml per 100 g of ashes) and subjected to reflux for 3 hours to ensure a complete reaction. The mixture is then cooled and filtered under vacuum,

separating the solids. The filtrate, which contains sodium silicate, is collected for storage or further processing.

Precipitation and formation of the nanosilica sol-gel system.

The sodium silicate filtrate is neutralized with sulfuric or hydrochloric acid until a pH of 7 is reached, generating a nano-silica gel. The gel is then dried in an oven at 100°C until a dry solid is obtained. Subsequently, it is washed with distilled water until the conductivity is between 17 and 40 µS/cm, removing impurities. Finally, the gel is dried in the oven, resulting in pure nano-silica powder ready for use.

2.2. NANOSILICA

For the use of these particles, the synthesis of nano-silica from oat husk was carried out using the sol-gel method. To obtain the required amount, 4 months were spent, resulting in 150 grams of nano-silica with good purity according to the characterization tests performed. The decision to conduct our own synthesis was due to the availability of the necessary resources and to obtain real properties along with their applications using products found in our country, Ecuador. The oat husk was obtained from San Gabriel, the capital of the Montúfar canton, in the Carchi province.

Validation of silica nanoparticles through laboratory tests.

To verify that the purity, quality, and properties of the nano-silica are adequate, Energy Dispersive Spectroscopy (EDS), Scanning Electron Microscopy (SEM), Transmission Electron Microscopy (TEM), and X-Ray Diffraction (XRD) tests were conducted. These tests will allow us to understand the internal structure, composition, and both physical and chemical properties.

Energy Dispersive Spectroscopy (EDS) Assay

This test allows us to perform a microanalysis and quantification of the elements present in the sample, enabling the mapping of different regions represented by different color scales.

Ilustración 2:

Identification and quantification of chemical elements.

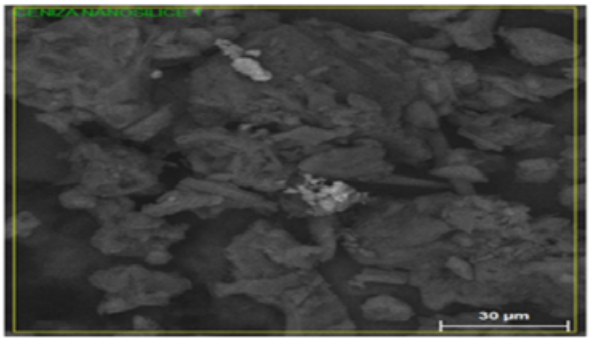

It works by measuring the energy and intensity of the X-rays when the sample is exposed to the electrons from an electron microscope, which interact with the atoms of the sample. The X-rays emitted by the microscope are specific to each element, allowing the images to be recognized by colors [32].

Barrido Microscopy (SEM)

This test allows us to analyze the crystalline structures present in the samples, as well as the topography on the surface, how they interact electrically, and their chemical composition approximately 1 µm from the top of the sample, reaching an analytical magnification of 1,000,000 times, enabling nanometric visualization [33].

Ilustración 3:

Morphology and surface topography of silica nanoparticles.

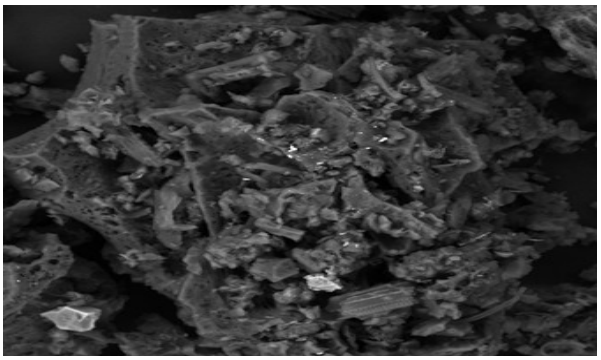

Transmission Electron Microscopy (TEM).

The analysis of TEM images of nano-silica particles allows us to gain a deep understanding of the morphology and structure of the nanoparticles.

The transmission electron microscope operates on the same principle as the optical microscope, except that it uses an electron beam to focus on the specimen and produce the image. It has a wavelength of approximately 0.005 nm, which is equivalent to 100,000 times shorter than the wavelength produced by light [34].

Ilustración 4

Morphology and structure of silica nanoparticles.

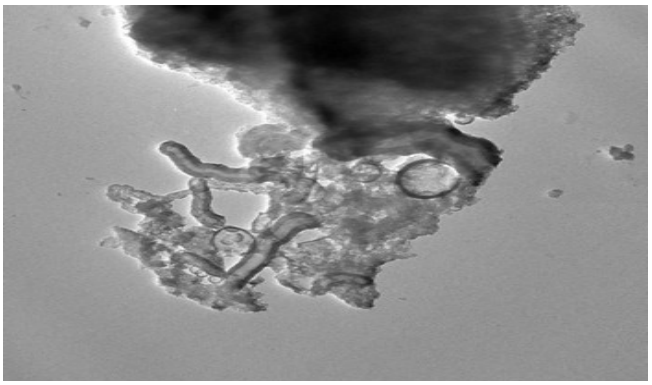

X-Ray Diffraction

The principle of this method is to irradiate a sample with a monochromatic X-ray beam so that the electrons around the atoms vibrate under the action of the X-rays, periodically altering the electric field, causing each electron to act as a secondary wave source that emits electromagnetic waves [35].

Ilustración 5

Spectrogram resulting from X-ray diffraction.

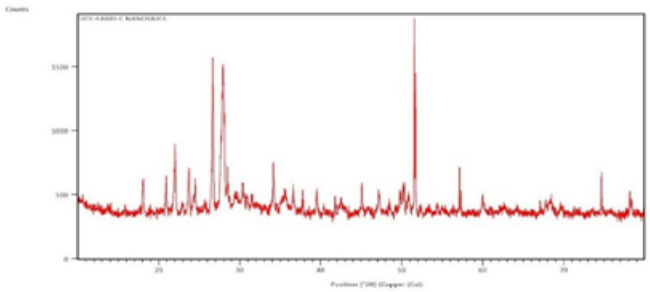

2.3. DESIGN METHODOLOGY.

Material Characterization

Initially, the characterization of the materials used in the production of mortar cubes is carried out to establish the mix proportions.

Granulometry

The suitability of the fine aggregate size for the mortar is evaluated following the procedure outlined in NTE INEN 696, determining the maximum aggregate size and the fineness modulus. Sieving is performed using the sieves specified by the standard, and the data on the mesh openings of each sieve are plotted alongside the percentage of material passing through each one, comparing them with the limits set by NTE INEN 2536. Three samples of sand are prepared, and granulometric tests are conducted to verify the consistency of the obtained results.

Gráfica 1

Granulometric Distribution

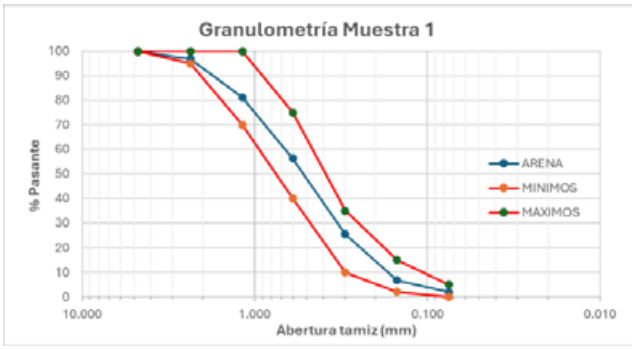

Material Finer than Sieve No. 200

A washing procedure is performed through Sieve No. 200 (75 µm) using a selected sample of fine aggregate, and the loss of material is determined as a percentage relative to the initial sample, following the procedure outlined in NTE INEN 697.

Tabla 2

Percentage of Finer Material

MUESTRA	Masa seca Inicial (g)	Masa seca Final (g)	Masa que pasa tamiz 200	% Material más fino de 75um
1	504.60	492.00	12.60	**2.5%**
2	503.50	491.40	12.10	**2.4%**
3	503.70	490.10	13.60	**2.7%**

Colorimetry

The content of organic impurities in the fine aggregate is determined by immersing a sand sample in sodium hydroxide for one day. After this period, the color of the resulting liquid is compared with a standardized color palette, following the procedure outlined in NTE INEN 855. This test helps assess the presence of organic materials that could negatively affect the setting and bonding properties of the mortar.

Fotografía 1:

Color Comparison for the Colorimetry Test

Crumbly Particles

NTE INEN 698 defines the method for determining the percentage of crumbly particles or clay lumps in the fine aggregate. To perform this test, the sample is immersed in distilled water for 24 hours, after which each particle is manually tested by attempting to break it apart with the fingers. The percentage of crumbly particles is then calculated by weighing the particles that break apart and comparing this mass to the total initial mass of the sample. This test helps assess the quality of the fine aggregate, as the presence of crumbly particles can negatively affect the strength and durability of the mortar.

Tabla 3

Presence of Crumbly Particles

MUESTRA	Masa Inicial (g)	Masa Retenida (g)	% Partículas desmenuzables
1	25.10	24.90	**0.8%**
2	25.70	25.50	**0.8%**
3	25.40	25.20	**0.8%**

Lightweight Particles

The percentage of lightweight particles is determined by immersing a sample of aggregate in a high-density liquid, allowing the lighter particles to remain suspended. The mass of these suspended particles is then measured according to the procedure outlined in NTE INEN 699. This test helps identify any lightweight materials within the aggregate, which can affect the strength and performance of the mortar.

Tabla 4

Presence of Lightweight Particles.

MUESTRA	Masa Seca (g)	Masa Seca partículas flotantes (g)	% Partículas livianas
1	216.02	0.55	**0.3%**
2	197.22	0.75	**0.4%**
2	229.70	0.90	**0.4%**

Sulfate Degradation

Following the procedure outlined in NTE INEN 863, the specified aggregate samples are subjected to a repetitive process of exposure and drying in a sulfate solution. After completing the test, each sample is weighed to determine the effect caused by the sulfate exposure. This test helps assess the aggregate's durability and resistance to sulfate-induced degradation, which can negatively affect the performance of the mortar.

Tabla 5

Percentage of Loss Due to Sulfate Degradation

FRACCIÓN		Masa inicial (g)	Masa final (g)	% de pérdida
Pasa tamiz	se retiene en tamiz			
600µm	300µm	100.00	99.20	**1%**
1,18mm	600µm	100.00	99.00	**1%**
3,36mm	1,18mm	100.00	98.70	**1%**

Specific Weight and Absorption Capacity

The specific weight and absorption capacity are determined following the procedure established in NTE INEN 856. This involves bringing the aggregate sample to the Saturation with Surface Dry (SSD) state and measuring its mass. Then, the volume of the sample is determined, and it is dried to measure its mass again. Finally, the required values are calculated using the formulas specified in the standard.

Loose and Compacted Density

Following the procedure outlined in NTE INEN 858, the samples are placed in a standardized container, both in loose and compacted states. The mass and volume of the fine aggregate sample are then determined.

Cement Density

According to NTE INEN 156, a Le Chatelier flask, diesel, and a cement sample are used. By measuring the mass and volume of the cement, its density can be determined. The test is repeated three times to validate the results, which are presented in the following table.

Mix Design

A mortar mix is prepared to produce 9 cubes for the compressive strength test, following the material dosage established in NTE INEN 488. For the mix, type N cement from Atenas is used, for which no exact quantity is specified. An initial water/cement ratio of 0.52 is used and adjusted until the flow required by the NTE INEN 488 standard is achieved.

Material Mixing

The procedure for preparing the mortar mix according to the NTE INEN 155 standard includes: drying the sand for 24 hours, sieving the cement to remove clumps, and controlling the water temperature. 740 g of cement and 2035 g of sand are weighed, and the water volume is measured based on the water/cement ratio. The mixing process consists of several stages: first, adding water and cement at low speed, then incorporating the sand, switching to medium speed to mix, homogenizing the

mixture, and finally mixing again at medium speed to achieve a uniform consistency.

Determination of the Mix Flow

According to NTE INEN 488, the flow of the mortar mix must be 110±5, measured in accordance with NTE INEN 2502. The procedure includes cleaning and preparing the flow table, filling and compacting the mold with mortar in two stages, smoothing the surface, and allowing it to rest for 1 minute. Then, the mold is removed, the table is dropped 25 times in 15 seconds, and the resulting diameter is measured at four points. Finally, the measurements are summed to calculate the total flow of the mix.

The mortar produced with Type N cement demonstrates adequate workability. However, when nanomaterials are incorporated as a partial cement replacement, a reduction in workability is observed, leading to deficiencies in its fresh-state properties. [36]

Specimen Preparation

The procedure for preparing mortar cubes, according to NTE INEN 488, includes cleaning the molds, applying release agent, and mixing the remaining mortar at medium speed for 15 seconds. Then, the molds are filled, compacted in two stages with uniform strikes, the surface is smoothed with a trowel, the molds are labeled, and they are transferred to the curing chamber under controlled conditions.

Addition of Nanosilica to the Mortar Mix

The influence of nanosilica on the compressive strength of the mortar will be evaluated at 1, 7, and 28 days, incorporating 0.25%, 0.50%, 0.75%, and 1.0% into different mixes. For this, the amount of nanosilica will be calculated based on the weight of the cement, partially replacing it. The dispersion will be prepared by mixing the nanosilica with the water before incorporating all the mortar components. Tests will be repeated for each dosage, and the results will be compared to determine the optimal proportion.

As this is a specialized concrete incorporating materials such as nano-silica, a specific mixing methodology is required to ensure proper adhesion of the nano-silica nanoparticles within the mixture. It is recommended to reserve a minimum amount of water to effectively dissolve the nano-silica, ensuring a homogeneous blend. [37]

Curing and Compressive Strength

The curing conditions for fresh mortar typically involve maintaining a constant temperature of approximately 23°C and a relative humidity of 50% during the initial setting phase. For hardened mortar, the samples are kept at a temperature of 23 ± 2°C and a relative humidity of at least 50% for periods of 4, 7, 14, and 28 days. [38]

The compressive strength test of mortar cubes according to NTE INEN 488 includes demolding the specimens without damaging them and placing them under controlled humidity and temperature conditions. Before the test, the dimensions of the cubes are measured and recorded in the compression machine. The specimen is placed in the machine, correctly centered, and the load is applied, recording the maximum force and stress in MPa at the moment of failure. The variation in permissible ages according to the standard is also considered.

When incorporated into the matrix of cement-based materials such as concrete, nanosilica has been demonstrated to significantly enhance performance. This study reveals that the addition of nanosilica can increase the strength and durability of concrete by up to four times. Both microsilica and nanosilica exhibit high pozzolanic activity, enabling them to regulate undesirable crystallization within the concrete matrix. [39]

Absorption Capacity

The absorption test in mortars determines the amount of water the material can absorb within a specified time, indicating its porosity. The specimens are cured for 28 days and then completely dried in an oven before recording their initial weight (W_1). Subsequently, they are submerged in water at room temperature for 24 hours, ensuring the absence of trapped air bubbles. Afterward, the specimens are removed and weighed again to obtain the final weight (W_2). he absorption is calculated using the equation: Absorption (%) = $((W_2 - W_1) / W_1) \times 100$, where W_1 is the dry weight and W_2 is the weight after immersion.

Permeability

To determine the permeability of the mortar, the contact angle test, also known as the drop test, will be used. This test allows us to measure the ability of a liquid to wet a solid surface [40]. It involves placing a drop on the surface and measuring the angle formed between the tangent of the drop and the surface of the material at the contact point. The materials and procedure are as follows.

3. Results and Discussion

3.1. YIELD.

Based on the results obtained from nano-silica, it is considered that the yield is low; however, the presence of silica in the oat husk is a significant advantage. The advantage lies in the fact that being an

abundant agro-industrial byproduct with very low cost, it makes it an economical and sustainable alternative. This allows for the reuse of these wastes to promote the circular economy and reduce environmental impact.

3.2. ENERGY DISPERSIVE SPECTROSCOPY (EDS)

Gráfica 2:

On the left is the composition of the nanosilica and on the right the ash residue of synthesis síntesis.

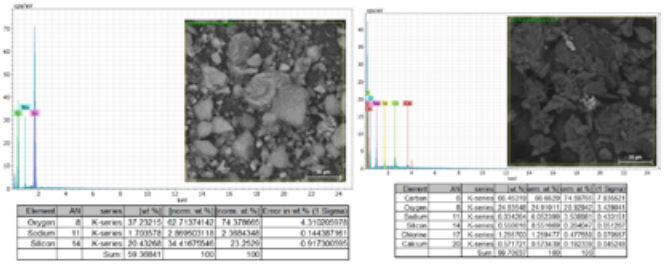

In the graph on the left, we can discuss a high relative purity, despite the presence of sodium residues, as it shows a high content of oxygen and silicon, both in weight and atoms, suggesting that the material is predominantly silica. The graph on the right shows that the silica content in the sample is low, indicating that the synthesis process has not been fully efficient in producing nano-silica. Therefore, these ashes could not be treated as they would not contain a significant amount of silica, considering the time it takes.

3.3. SCANNING ELECTRON MICROSCOPY (SEM)

Image 1

On the left is the SEM image of the nanosilica and on the right the ash residue of the synthesis.

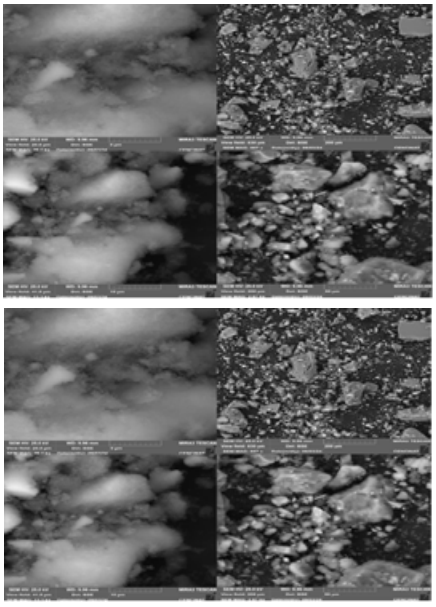

The left side, we can observe that the aggregates are spherical or nearly spherical, which is characteristic of nano-silica synthesized by methods such as sol-gel. Additionally, the agglomeration indicates that the particles are interacting with each other due to electrostatic or van der Waals attraction. On the right side, the particles appear to have very irregular and rough surfaces. This is typical of residues that have been subjected to high temperatures but have not been fully calcined. The roughness may indicate the presence of pores and gaps left as a result of burning the organic material. Some of the observed structures appear to be fibrous or laminar. These could be remnants of the original biomass, such as traces of plant fibers.

3.4. TRANSMISSION ELECTRON MICROSCOPY (TEM)

Image 2

On the left is the TEM image of the nanosilica and on the right the ash residue of the synthesis.

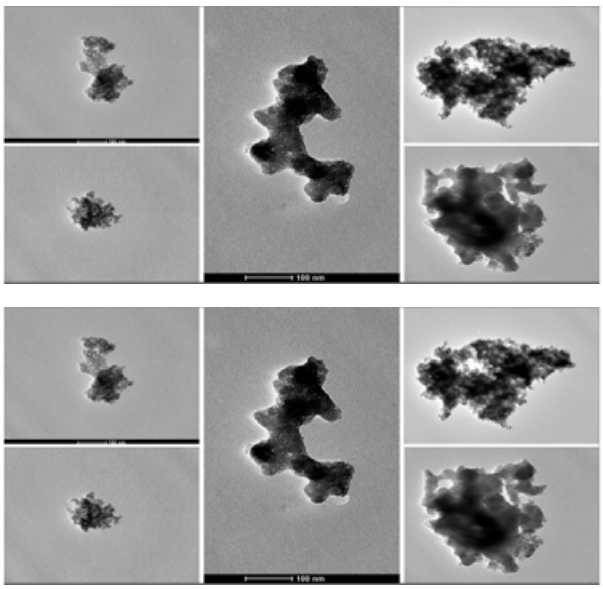

The tests show that for the nano-silica, by performing the following analysis, we can observe that the particle size obtained by this methodology is 8.04 nm, which is close to the range typically considered for nano-silica particles, which usually fall between 1 and 100 nm. On the other hand, for the ashes, the particle size obtained by this methodology is 143.816 nm, which is outside the range considered for nano particles.

3.5. X-RAY DIFFRACTION (XRD)

Gráfica 3

Nanosilica diffractogram shown.

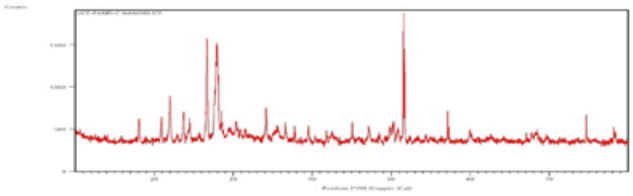

One of the most representative peaks is found at 26.6°, indicating the presence of quartz (crystalline SiO2), as this position is characteristic of this material. Quartz is one of the most common forms of silicon dioxide, which is consistent with the fact that the sample is nano-silica. The presence of smaller peaks could be related to the presence of other silica phases or impurities in the sample.

The incorporation of nano-silica into cementitious matrices has been shown to significantly enhance mechanical properties by reducing porosity and improving microstructural densification, aligning with recent findings in high-performance mortar development [41].

3.6. PERMEABILITY

Gráfica 4

Contact angle of conventional mortar and with the addition of nanosilica.

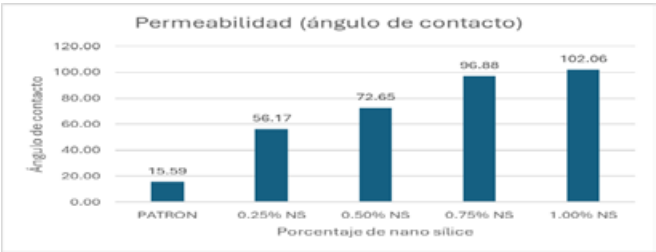

The contact angle values obtained from the conventional mortar samples and mortar with the addition of nano-silica at 28 days of curing are presented. These values are key to evaluate the wettability of the surface, which is correlated with the permeability of the material. The angle increases with the increase in the nano-silica content, ranging from the lowest value of 15.59° for the control mixture, indicating a high affinity of water with the surface, to the maximum value of 102.06° with the addition of 1.00% nano-silica, showing a hydrophobic trend.

3.7. ABSORPTION

Gráfica 5

Absorption percentage depending on the nanosilica percentage.

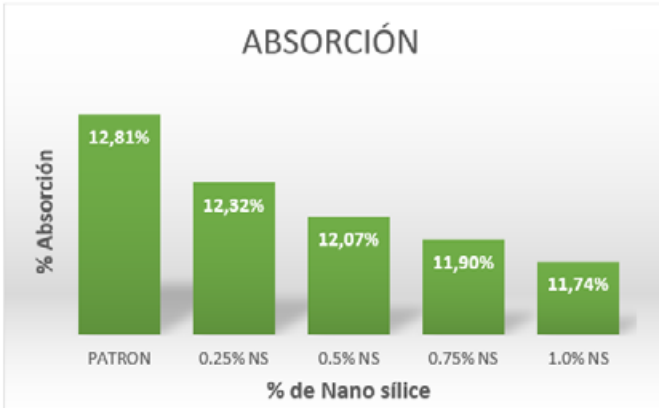

The graph shows the relationship between the absorption percentage and the nanosilica content (% NS). It is observed that as the concentration of nanosilica increases, the absorption percentage progressively decreases. The highest absorption value (12.81%) is found in the reference sample (PATRÓN), while the lowest value (11.74%) corresponds to the sample with 1.0% nanosilica. This indicates that the incorporation of nanosilica reduces the absorption of the material.

3.8. COMPRESSIVE STRENGTH

Gráfica 6:

Compressive strength with different nanosilica percentages at different ages.

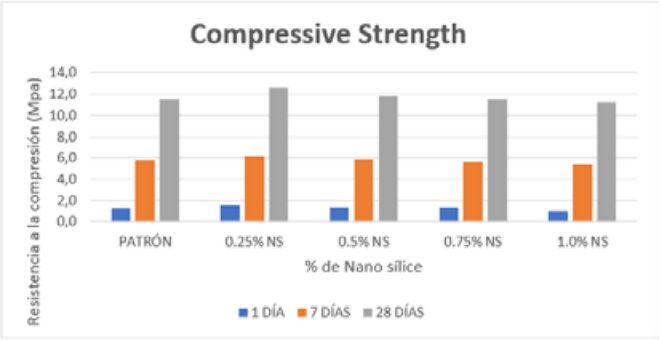

The graph shows the evolution of compressive strength (in MPa) as a function of nanosilica content and curing time (1, 7, and 28 days). The samples with 0.25% and 0.5% nanosilica show a slight improvement in strength compared to the reference, especially at 28 days. However, at higher concentrations (0.75% and 1.0% NS), the strength tends to stabilize or even slightly decrease. This suggests that there is an optimal point in the addition of nanosilica to improve compressive strength without compromising the material's structure.

3.9. X-RAY DIFFRACTION (XRD) MORTAR CUBES.

Gráfica 7

The diffractogram is shown on the left of the conventional mortar and on the right with the addition of 0.25% nanosilica.

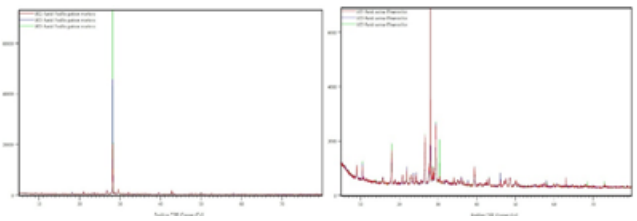

In the control sample, the high peak near 30° suggests the predominance of residual alite or belite, indicating incomplete hydration (less than 100%). Additionally, the small peaks between 18° and 34° suggest typical hydration without substantial chemical modifications. On the other hand, with the addition of nano-silica, a reduction in the relative intensity of the portlandite peak, typically located around 18°, 34°, and 47° in 2θ, is observed. This reduction implies that nano-silica has reacted with portlandite to form more C-S-H gel (calcium silicate hydrate), which results in a denser cement matrix, thereby improving mechanical properties. The reduction of free portlandite means there is less material available to react with CO2 or sulfates, thus enhancing the material's durability in aggressive environments. This occurs because the reaction of nano-silica generates products that fill the capillary pores, reducing total porosity and improving mechanical strength, which in turn leads to long-term durability.

3.10. ANALYSIS OF THE COST OF PRODUCTION OF NANOSILICA.

According to the calculation, it is observed that producing 100 grams of nano-silica costs $368.97. When compared to the commercial prices of Aerosil 200, which is around $161.95 for 4.5 kg in the United States, the laboratory production cost is significantly higher than the market value. This indicates that at an industrial level, the methods are more efficient and cost-effective.

4. Conclusión

- The synthesis of nano-silica from oat husks using the sol-gel method proved to be a viable process, achieving a yield of 2.79%, showing a significantly higher efficiency compared to the study conducted by the pharmaceutical laboratory of the Faculty of Chemical Sciences at the Central University of Ecuador, which achieved a yield of 0.98% using the extraction and gravimetry method. This difference suggests that the sol-gel method optimizes the recovery of silica from agro-industrial waste, thus improving its viability for applications in cementitious materials. Furthermore, the ability to adjust synthesis parameters to control particle morphology and size opens new opportunities for its incorporation into high-performance materials.
- The characterization analysis conducted through the EDS, SEM, TEM, and XRD tests allowed the evaluation of both the chemical composition and morphology of the nano-silica and oat husk ash. The EDS spectra confirmed the high purity of the synthesized nano-silica, with an approximate concentration of SiO2 (90%), while the remaining content consisted of trace impurities. In contrast, the oat husk ashes showed approximately 1% silica. Regarding the images obtained by SEM and TEM, it was revealed that the synthesized nano-silica exhibited spherical particles with an approximate size of 8-15 nm and a homogeneous distribution. On the other hand, the oat husk ashes presented larger aggregates with dimensions greater than 100 nm. This finding suggests that controlling the synthesis process plays a crucial role in obtaining nanoparticles with optimized properties. The X-ray test of the nano-silica revealed the presence of amorphous phases characteristic of SiO2, with a broad peak at 2θ = 22°, which is favorable for its reactivity in cementitious applications. This suggests that the sol-gel synthesis method enables the production of a material with high potential reactivity in cement matrices.
- The study on the influence of nanosilica addition in mortars reveals that compressive strength varies depending on the addition percentage and curing time, showing better results at lower doses. At 1 and 7 days, the mix with 0.25% nanosilica exhibited the highest strength compared to mixes with 0.5%, 0.75%, and 1%, while higher doses did not provide consistent improvements. At 28 days, the trend remains, with 0.25% reaching the highest strength (12.6 MPa). This suggests that small amounts of nanosilica optimize strength, but higher doses may not be beneficial.
- This study evaluated the economic feasibility of producing nano-silica from oat husks, with an approximate cost of $368.97 per 100 grams of product under laboratory conditions, using agro-industrial waste, promoting the circular economy and environmental sustainability. By utilizing an abundant, low-cost waste material and the ability to customize the properties of the material according to its specific application, its production in laboratories could be justified due to particular technical requirements. Under current conditions, however, the production is not competitive.

References

[1] R. Salamanca, "La Tecnología de los Morteros," Diciembre 2001. [En línea]. Disponible en: https://www.redalyc.org/pdf/911/91101107.pdf. [Último acceso: 6 Agosto 2024].

[2] INEN, "Morteros para unidades de mamposteria,"» Enero 2010. [En línea]. Disponible en: https://drive.google.com/file/d/1iazTpPDp6H0oNMoryoeKryG4FaNmgHrl/view. [Último acceso: 7 Agosto 2024].

[3] M. Alvansazyazdi, N. Salgado, A. Borghei, S. Camino y M. Guzmán, "Web-Based Executive Dashboard Reports for Public Works Clients in Construction Industry.," en *[Nombre de la Conferencia o Libro si se conoce]* pp. 285-294, 2019.

[4] A. Global, "Nanotecnología en la construcción," 6 Noviembre 2023. [En línea]. Disponible en: https://www.arcus-global.com/wp/nanotecnologia-en-la-construccion/. [Último acceso: 7 Agosto 2024].

[5] BricKaffix, "Nanotecnología en la construcción, Innovación y Eficiencia," 25 Mayo 2023. [En línea]. Disponible en: https://brickaffix.mx/nanotecnologia-construccion/. [Último acceso: 7 Agosto 2024].

[6] M. Alvansazyazdi, H. Alvansaz, M. Hakakian, N. Salgado y A. Camino Solórzano, "An Investigation and Presentation of a Model for Factors Influencing the Agility of Human Resources: A Case Study of Yazd Electricity Distribution Company," In Á. Rocha *et al.* (Eds.), pp. 823-834, 2019.

[7] N. Salgado, J. Guaña, C. Escobar y M. Alvansazyazdi, "Result of the Methodology for Learning English Distance with the Use of TICs. Case Study: Central University of Ecuador.," *In Á. Rocha et al. (Eds.),* WorldCIST', nº 19, pp. 227-233, 2019.

[8] L. Moragues y M. Sanchez, "Influencia de la adición de nano sílice en algunos aspectos de la durabilidad, en hormigones autocompactantes de alta resistencia.," 2013. [En línea]. Disponible en: https://oa.upm.es/29970/1/INVE_MEM_2013_165946.pdf. [Último acceso: 7 Agosto 2024].

[9] Instituto Ecuatoriano de Normalización (INEN), *Morteros para unidades de Mampostería*. Quito, Ecuador, 2010

[10] M. Khorami, M. Khorami, H. Motahar, M. Alvansazyazdi, M. Shariati, A. Jalali y M. Tahir, "Evaluation of the seismic performance of special moment frames using incremental nonlinear dynamic analysis," *Structural Engineering and Mechanics,* vol. 63, nº 2, pp. 259-268, 2017.

[11] M. Alvansazyazdi, A. Villalba, S. Saltos, J. Santamaria, A. Cadena, M. Leon, L. Leon, P. Bonilla, B. Heredia, J. Bucheli, A. Debut, y M. Feizbahrh, "Enhancing Sustainable Construction: An Evaluation of NanoGraphene's Effectiveness in Mortar Composition," *Int. J. Eng. Technol. Sci.*, 2023.

[12] M. Şişman, E. Teomete, J. Yanik, y U. Malayoglu, "The effect of nano-biochar produced from various raw materials on flow and mechanical properties of mortar," *Constr. Build. Mater.*, 2025.

[13] H. Du, S. Du, y X. Liu, "Durability performances of concrete with nano-silica," *Constr. Build. Mater.*, 2014.

[14] M. M. Badalyan, N. G. Muradyan, R. S. Shainova, y A. A. Arzumanyan, "Effect of Silica Fume Concentration and Water–Cement Ratio on the Compressive Strength of Cement-Based Mortars," *Constr. Build. Mater.*, 2024.

[15] M. Usman *et al.*, "Study on Relationship Between Mechanical Properties and Water Absorption Characteristics of Mortars by Using Digital Image Correlation Method (DICM)," *Materials*, 2025.

[16] C. M. Stolz, A. Rysdyk, M. Amario, M. Najjar, E. G. Vazquez, y A. N. Haddad, "Evaluation of Water Vapor Permeability in Mortars Produced with Crystallizing Additive," *NanoWorld J.*, 2023.

[17] A. Rityparna y S. Mozumdar, "Nanotecnología," *SpringerNAture,* pp. 35-36, 12 Mayo 2013.

[18] G. Williams, C. Haynes, M. Tarifas, C. Caltagirone, J. Rugallo y F. Vendaval, "Advances in applied supramolecular technologies," *Chemical Society Reviews,* vol. 50, pp. 2737-2763, 22 Septiembre 2021.

[19] R. Checkers, P. MarshallJosh, P. DvorakLiam, K. B. TwightLan ChenKentaro, E. AndreevaAlexandra, E. F. OverlandThomas, K. CozzolinoCarl y Brozek, "Size-Dependent Properties of Solution-Processable Conductive MOF Nanocrystals," *J. Am. Chem. Soc.*, pp. 5784-5794, 30 Enero 2022.

[20] M. Alvansazyazdi y J. Rosero, "The pathway of concrete improvement via nano-technology.," *INGENIO,* vol. 2, nº 1, p. 1, 2019.

[21] S. Sim y N. Wong, "Nanotechnology and its use in imaging and drug delivery.," 5 Marzo 2021. [En línea]. Disponible en: https://www.spandidos-publications.com/10.3892/br.2021.1418. [Último acceso: 24 Septiembre 2024].

[22] A. Barhoum, M. García, J. Jeevanandam y E. Hussien, "Review on Natural, Incidental, Bioinspired, and Engineered Nanomaterials: History, Definitions, Classifications, Synthesis, Properties, Market, Toxicities, Risks, and Regulations," 6 Enero 2022. [En línea]. Disponibel en: https://www.mdpi.com/2079-4991/12/2/177. [Último acceso: 24 Septiembre 2024].

[23] A. Sosa, G. Romanelli y L. Pizzio, "Nanoestructuras de sílice, con diámetro y distribución de mesoporos variable, modificadas con ácido tungstofosfórico como catalizadores en la síntesis de quinoxalinas," 18 Abril 2020. [En línea]. Disponible en: https://www.redalyc.org/journal/3090/309063462006/html/. [Último acceso: 7 Agosto 2024].

[24] J. Manazo, M. Lozano, y M. Vallet-Regí, "Nanopartículas mesoporosas de sílice y la osteoporosis," Diciembre 2022. [En línea]. Disponible en: https://scielo.isciii.es/scielo.php?script=sci_arttext&pid=S1889-836X2022000400001 [Accedido el 25 de Septiembre de 2024].

[25] M. Alvansazyasdi, C. Bombon y B. Rosero, "Estudio de la incorporación de nanosílice en concreto de alto desempeño (hpc)," *INGENIO,* vol. 5, nº 1, pp. 12-21, 2022.

[26] M. Alvansaz, B. Arévalo y A. Julio, "Adoquines de hormigón ecoamigables fabricados con la incorporación de una Mezcla de Micro-Nano Sílice" *INGENIO,* vol. 5, nº 1, pp. 34-42, 2022.

[27] L. W. Morales, M. Alvansazyazdi, *et al.*, "Prevención de la contaminación por la fabricación de hormigones con nanopartículas," ResearchGate, 2020.

[28] M. AlvansazYazdi, R. Zakaria, M. Mustaffar, M. Majid, R. MohamadZin, M. Ismail y K. Yahya, "Bio-composite materials potential in enhancing sustainable construction," *Desalination and Water Treatment,* vol. 52, pp. 3631-3636, 2014.

[29] P. Damodaran, M. Nagarajan, and L. Thangasamy, "Assessing the Durability, Mechanical, and Microstructural Properties of Nanosilica-enhanced Coconut Shell Concrete: A Sustainable Approach," *J. Environ. Nanotechnol.*, 2024.

[30] A. Moreno, "Optimización en la incoporación de nanoadiciones al cemetno para la mejora de sus prestaciones y durabilidad.," 2018. [En línea]. Disponible en: https://1library.co/document/zw5073lz-optimizacion-incorporacion-nanoadiciones-cemento-mejora-prestaciones-durabilidad.html. [Último acceso: 8 Agosto 2024].

[31] A. Golsha, M. Rezazadeh Shirdar, S. Gohery y M. Alvansazyazdi, "Optimization of Pre-Treatment Parameters before Diamond Coating using Non-Dominated Sorting Genetic Algorithm (NSGA-II)," *Advanced Materials Research*, nº 463-464, 399-405, 2012.

[32] BRUKER, "What is EDS/EDX? introducing Energy Dispersive X-Ray Spectroscopy," 2024. [En línea]. Disponible en: https://www.bruker.com/en/landingpages/bna/technology/what-is-eds.html. [Último acceso: 15 Septiembre 2024].

[33] A. Erol, "High-Magnification SEM Micrograph of siloxanes," 17 Diciembre 2018. [En línea]. Disponible en: https://www.intechopen.com/chapters/64959. [Último acceso: 15 Septiembre 2024].

[34] F. Morkobi, "Transmission Electron Microscope (TEM)," 19 MAyo 2022. [En línea]. Disponible en: https://microbenotes.com/transmission-electron-microscope-tem/. [Último acceso: 15 Septiembre 2024].

[35] DRAWELL, "The ultimateguide to XRD-From theory to practice," 18 Noviembre 2022. [En línea]. Disponible en: https://www.drawellanalytical.com/the-ultimate-guide-to-xrd-from-theory-to-practice/. [Último acceso: 15 Septiembre 2024].

[36] M. Alvansazyazdi, J. Fraga, E. Torres, G. Bravo, J. Santamaria, M. Leon, A. Cadena, L. Leon, P. Bonilla, B. Heredia, A. Debut, M. Feizbahr, y R. Yuri, "Comparative Analysis of a mortar for plastering with hydraulic cement type HS incorporating nano-iron vs cement-based mortar for masonry type N," *Int. J. Eng. Technol. Sci.*, 2024.

[37] M. Alvansazyazdi, D. Farinango, J. Yaucan, A. Cadena, J. Santamaria, P. M. Bonilla-Valladares, M. Leon, A. Debut, M. Feizbahr, L. Leon, y B. Ayala, "Exploring Crack Reduction in High-Performance Concrete: The Impact of Nano-Silica, Polypropylene, and 4D Metallic Fibers," *Int. J. Eng. Technol. Sci.*, 2023.

[38] M. Alvansazyazdi, J. Figueroa, A. Paucar, G. Robles, M. Khorami, P. M. Bonilla-Valladares, A. Debut, y M. Feizbahr, "Nano-silica in Holcim general use cement mortars: A comparative study with traditional and prefabricated mortars," *Adv. Concr. Constr.*, 2024.

[39] M. Alvansazyazdi, J. Tapia, y A. Barrionuevo, "Study of an Environmentally Friendly High-Performance Concrete (HPC) Manufactured with the Incorporation of a Blend of Micro-Nano Silica," *Rev. Científica Arq. Urbanismo*, 2024.

[40] M. Alvansazyazdi, F. Alvarez, J. Pinto, M. Khorami, P. Bonilla, A. Debut, y M. Feizbahr, "Evaluating the Influence of Hydrophobic Nano-Silica on," *Sustainability*, pp. 3–4, 2023.

[41] M. Alvansazyazdi, J. Figueroa, A. Paucar, G. Robles, M. Khorami, P. M. Bonilla-Valladares, A. Debut y M. Feizbahr, "Nano-silica in Holcim General Use Cement Mortars: A Comparative Study with Traditional and Prefabricated Mortars.," *Advances in Concrete Construction,* vol. 17, nº 3, pp. 135-150, 2024.

[42] J. Gonzalez, "ESTUDIO DEL MORTERO DE PEGA USADO EN EL CANTÓN CUENCA PROPUESTA DE MEJORA UTILIZANDO ADICIONES DE CAL," 2016. [En línea]. Disponible en: https://dspace.ucuenca.edu.ec/bitstream/123456789/23664/1/TESIS%20final%20.pdf.. [Último acceso: 7 Agosto 2024].

[43] A. Romero, "DISEÑO EXPERIMENTAL DE UN MORTERO DE CEMENTO REFORZADO CON FIBRAS NATURALES DE ORIGEN ANIMAL "PLUMAS DE AVES"," 2022. [En línea]. Disponible en: https://www.studocu.com/ec/document/universidad-laica-vicente-rocafuerte-de-guayaquil/arquitectura/t-uide-0328-material/46344469.. [Último acceso: 7 Agosto 2024].

[44] S. Correa, "Dosificación morteros," de *Dosificación morteros*, 1985, pp. 17-23.

[45] F. Gottschalk, B. Debray, F. Klaessing y P. Barry, "Predicting accidental release of engineered nanomaterials to the environment," 2 Febrero 2023. [En línea]. Disponible en: https://www.nature.com/articles/s41565-022-01290-2. [Último acceso: 24 Septiembre 2024].

[46] D. Heras, "Morteros de cemento con nano-adiciones de hierro y sílice,"

[47] R. Chudley y R. Greeno, "Building Construction Handbook," 2008. [En línea]. Disponible en: http://students.aiu.edu/submissions/profiles/resources/onlineBook/s6C5h7_construction-handbook-chudley.pdf.

[48] G. Rivera, *Concreto Simple*. Cauca, Colombia, 2009.

[49] V. Cervantes, "Aplicaciones Generales de la nanotecnología en el campo de la Construcción," *PITRA,* 2011.

[50] L. Molina y M. Garzón, "Propiedades de concretos y morteros modificados con nanomateriales: Estado del Arte," *Arquetipo,* vol. 14, pp. 81-98, 2017.

[51] Graphenemex, "Nanotecnología y protección contra la corrosión: La era del Óxido de grafeno," 2018. [En línea]. Disponible en: https://www.graphenemex.com/tag/esmalte-alquidalico/.

[52] D. Sanchez de Guzman, *Tecnología del concreto y del mortero*. Santafé de Bogotá: Bahandar Editores Ltda, 2001.

[53] A. Cardona, "la versatilidad del mortero, su importancia y sus posibilidades en la construcción," universidad militar nueva granada, Bogotá, 2021.

[54] BRUKER, "What is EDS/EDX? Introducing Energy Dispersive X-Ray Spectroscopy," 2024. [En línea]. Disponible en: https://www.bruker.com/en/landingpages/bna/technology/what-is-eds.html. [Último acceso: 15 Septiembre 2024].

[55] A. Erol, "High-Magnification SEM Micrograph of Siloxanes," 17 Diciembre 2018. [En línea]. Disponible en: https://www.intechopen.com/chapters/64959. [Último acceso: 15 Septiembre 2024].

[56] F. Mokobi, "Transmission Electron Microscope (TEM)-Definition, Principle, Images," 19 Mayo 2022. [En línea]. Disponible en: https://microbenotes.com/transmission-electron-microscope-tem/. [Último acceso: 15 Septiembre 2024].

[57] S. K. S. S. M. Ranjana*, "NANOSILICA'S INFLUENCE ON CONCRETE HYDRATION, MICROSTRUCTURE, AND DURABILITY," *JOURNAL OF APPLIED ENGINEERING SCIENCES ,* 2024.

[58] T. Ji, "Preliminary study on the water permeability and microstructure of concrete incorporating nano-SiO2," *Cement and Concrete Research,* 2015.

[59] R. Salamanca Correa, "Dosificaciónde morteros," vol. 3, nº 2, pp. 17-23, 1985.

[60] X. Chen, E. Gruyaert, Ö. Cizer y J. Li, "Materconstrucc," 2023. [En línea]. Disponible en: https://materconstrucc.revistas.csic.es/index.php/materconstrucc/article/download/3501/4271?inline=1.

[61] G. O. S. R. Caiza C, "Permeabilidad de diferentes dosificaciones de morteroutilizados en la industria de la construcción en el Ecuador," *UNIVERSIDAD CENTRAL DEL ECUADOR,* 2020.

[62] M. Alvansazyazdi, F. Alvarez-Rea, J. Pinto-Montoya, M. Khorami, P. M. Bonilla-Valladares, A. Debut, y M. Feizbahr, "Evaluating the Influence of Hydrophobic Nano-Silica on Cement Mixtures for Corrosion-Resistant Concrete in Green Building and Sustainable Urban Development," *Sustainability*, 2023.

Annexes

Table 6

Percentage of Absorption of Fine Aggregate.

MUESTRA 1	
Masa picnómetro vacío (g):	188.7
Masa picnómetro + Arena SSS (g):	684.2
Masa picnómetro + agua + Arena S	996.1
Masa del picnómetro con agua (g):	686.23
Densidad del agua (g/cm3):	1.0
Masa de agua desalojada (g):	309.9
Masa de la muestra SSS (g):	495.5
Volumen de agua desalojado (cm3)	185.67
Masa de la muestra SSS (g):	490.25
Masa de la muestra seca (g):	483.2
RESULTADOS:	
Peso específico (g/cm3):	**2.7**
Peso específico (kg/m3):	**2670**
Absorción %	**1.5**

Table 7

Loose and Compacted Density of Sand.

Densidad Suelta Arena			
Masa molde (g):	628.9		
Volumen molde (cm3):	1000		
MUESTRA	1	2	3
Masa del arido+ molde 1 (g):	2244.2	2257.1	2243.2
Masa del arido+ molde 2 (g):	2245.3	2262.5	2245.7
Masa del arido+ molde 3 (g):	2245.1	2259.4	2247.7
Promedio (g):	2244.9	2259.7	2245.5
Densidad del agua (kg/m3):	998.0		
RESULTADOS:			
Masa unitaria (g/cm3):	1.62	1.63	1.62
Masa unitaria (kg/m3):	1620	1630	1620

Densidad Suelta Arena			
Masa molde (g):	628.9		
Volumen molde (cm3):	1000		
MUESTRA	1	2	3
Masa del arido+ molde 1 (g):	2244.2	2257.1	2243.2
Masa del arido+ molde 2 (g):	2245.3	2262.5	2245.7
Masa del arido+ molde 3 (g):	2245.1	2259.4	2247.7
Promedio (g):	2244.9	2259.7	2245.5
Densidad del agua (kg/m3):	998.0		
RESULTADOS:			
Masa unitaria (g/cm3):	1.62	1.63	1.62
Masa unitaria (kg/m3):	1620	1630	1620

Table 8

Average Cement Density.

Densidad del cemento			
MUESTRA #	1	2	3
Masa cemento inicial:	64.02	64	64.02
Lectura Inicial (vol. Gasolina en frasco):	0.1	0.1	0.1
Lectura Final (vol. Gasolina en frasco):	23.6	23.4	23.4
Volumen desplazado:	23.5	23.3	23.3
Peso diesel + muestra:	390.26	390.29	390.88
RESULTADOS:			
Densidad del cemento:	**2.72**	**2.75**	**2.75**
Promedio	**2.74**		

Table 9

Material Dosage According to NTE INEN 488.

MATERIAL	NÚMERO DE ESPECÍMENES 6	9
Cemento, g	500	740
Arena, g	1.375	2.035
Agua, cm^3		
- Portland (a/c = 0,485)	242	359
- Portland con incorporador de aire (a/c = 0,460)	230	340
- Otros (para un flujo de 110 ± 5)	-----	-----

Table 10

Results of nanosilica synthesis.

UNIVERSIDAD CENTRAL DEL ECUADOR
FACULTAD DE INGENIERÍA Y CIENCIAS APLICADAS
CARRERA DE INGENIERÍA CIVIL

Realizado p: Carlosama A. & Rosillo J.

Proyecto: Síntesis de nano sílice a partir de la cáscara de avena para modificar las propiedades físicas y mecánicas del mortero con un enfoque eco amigable.

RENDIMIENTO DE LA SINTESIS DE NANOSÍLICE

PROCESO	CANTIDADES
Materia prima incial: Cascara de	5371 g
Peso de las cenizas despues de	567 g
Rendimiento de las cenizas	10.56%
Cantidad de sílice obtenida	100 g
Rendimiento de nanosílice	2.79%

Table 11

Nanosilica Production Cost.

UNIVERSIDAD CENTRAL DEL ECUADOR
FACULTAD DE INGENIERÍA Y CIENCIAS APLICADAS
CARRERA DE INGENIERÍA CIVIL

Realizado por: Carlosama A. & Rosillo J.
Proyecto: Síntesis de nano sílice a partir de la cáscara de avena para modificar las propiedades físicas y mecánicas del mortero con un enfoque eco amigable.

ANÁLISIS DE PRECIOS UNITARIOS DE LAS MEZCLAS DE MORTERO

Rubro: Síntesis de nanosílice de 100 gr
Unidad: gr

A. MATERIAL

DESCRIPCIÓN	UNIDAD	CANTIDAD	PRECIO UNITARIO	COSTO
Cáscara de avena	kg	5.37	0.50	2.69
Ácido Sulfúrico	L	1.13	4.00	4.54
Hidróxido de sodio	kg	1.13	3.00	3.40
Agua destilada	L	80.00	0.50	40.00
Energía eléctrica	kW/h	20.50	0.10	2.05
SUBTOTAL				52.67

B. MANO DE OBRA

DESCRIPCIÓN	UNIDAD	Cantidad	Jornal (USD/hora)	COSTO
Técnico de laboratorio	hora	20.50	3.00	61.50
Ayudante de laboratorio	hora	20.50	2.50	51.25
SUBTOTAL				112.75

C. MATERIALES

DESCRIPCIÓN	UNIDAD	CANTIDAD	PRECIO UNITARIO (USD/h)	COSTO C=A*B
Horno de calcinación	hora	20.000	1.00	20.000
Bomba de succión al vacío	hora	150.000	1.00	150.000
SUBTOTAL				170.00

D. COSTO INDIRECTO

DESCRIPCIÓN	CANTIDAD A	COSTO HORA
	10%	33.542
SUBTOTAL		33.54

NOTA: ESTOS PRECIOS NO INCLUYEN EL IVA		
	TOTAL COSTO DIRECTO (A+B+C+D)	368.97
	COSTO INDIRECTO	0
	COSTO TOTAL DEL RUBRO: (USD)	368.97

INGENIO
2025, VOL 8(2), JULIO - DICIEMBRE, PP. 143-156

REVISTA INGENIO

Evaluación del Impacto de Servicios Auxiliares de V2G en una Red de Distribución: Caso de Estudio Alimentador Centro Babahoyo

Impact Assessment of V2G Ancillary Services on a Distribution Network: A Case Study of the Centro Babahoyo Feeder

Martin Junior Mainato Baren | Universidad Técnica Estatal de Quevedo, UTEQ - Ecuador
Frixon Samuel Macias Salazar | Universidad Técnica Estatal de Quevedo, UTEQ - Ecuador
Cristian Samuel Laverde Albarracín | Universidad Técnica Estatal de Quevedo, UTEQ - Ecuador

Recibido: 25/1/2025
Recibido tras revisión: 14/4/2025
Aceptado: 30/5/2025
Publicado: 10/7/2025

PALABRAS CLAVE
V2G, Red de distribución, servicios auxiliares, vehículo eléctrico.

RESUMEN
El artículo aborda la implementación de la tecnología Vehicle-to-Grid (V2G) en la red eléctrica de Babahoyo, Ecuador, para evaluar su influencia en la eficiencia energética. A pesar del crecimiento tecnológico en las redes eléctricas, con la integración de energías renovables y dispositivos de control, como vehículos eléctricos (VEs), existe una carencia de investigaciones previas en Babahoyo y de estudios sobre V2G. Ecuador consume una parte significativa de su energía en combustibles fósiles para el transporte, y se considera a los VEs como una solución eficiente y ecológica. La tecnología V2G permite que los VEs inyecten energía en la red durante picos de demanda, mejorando la eficiencia y regulando la potencia. El estudio incluye simulaciones que revelan que la incorporación de Estaciones de Carga de Vehículos Eléctricos (EVSEs) en la red de Babahoyo suaviza la demanda en días laborables, reduce la sobrecarga en transformadores y mejora la calidad del suministro eléctrico.

KEY WORDS
V2G, Distribution network, ancillary services, electric vehicle.

ABSTRACT
The article addresses the implementation of Vehicle-to-Grid (V2G) technology in the electrical grid of Babahoyo, Ecuador, to evaluate its influence on energy efficiency. Despite the technological growth in electrical networks, with the integration of renewable energies and control devices, such as electric vehicles (EVs), there is a lack of previous research in Babahoyo and studies on V2G. Ecuador consumes a significant portion of its energy in fossil fuels for transportation, and EVs are considered an efficient and ecological solution. V2G technology allows EVs to inject energy into the grid during peak demand, improving efficiency and regulating power. The study includes simulations that reveal that the incorporation of Electric Vehicle Charging Stations (EVSE) in the Babahoyo network smoothes demand on weekdays, reduces overload in transformers and improves the quality of the electrical supply.

I. INTRODUCCIÓN

En la actualidad las redes de distribución de energía eléctrica están en auge tecnológico, las redes eléctricas están incorporando tecnologías que permiten la generación a partir de fuentes renovables, como la energía fotovoltaica y eólica, así como la implementación de dispositivos de medición y control para optimizar su funcionamiento ante la incorporación de nuevas cargas, una de estas nuevas cargas son los vehículos eléctricos. [1]. En el Ecuador hay pocos estudios como [2] y [3], que evalúan el impacto del parque de VEs sobre las redes de distribución y por ende no existe un estudio que considere la implementación de V2G en la ciudad de Babahoyo.

Ecuador destina gran parte de su energía al transporte, principalmente a través de combustibles fósiles contaminantes con un 98% del consumo de energía proveniente de diésel y gasolinas. Específicamente, el 78% del diésel y el 95,6% de las gasolinas fueron consumidos en actividades de transporte. Esta alta dependencia de combustibles fósiles genera serias implicaciones ambientales, incluyendo emisiones significativas de gases de efecto invernadero, contaminación del aire y contribución al cambio climático. Para abordar esta problemática, se considera que los vehículos eléctricos (VEs) son una opción eficiente y efectiva [2]. La tecnología V2G permite que los

https://doi.org/10.29166/ingenio.v8i2.8150

pISSN 2588-0829
eISSN 2697-3243
fing.revista.ingenio@uce.edu.ec

VEs inyecten energía almacenada en sus baterías a la red durante momentos de alta demanda, aliviando la carga y mejorando la eficiencia. Además, esta tecnología ayuda a regular la potencia activa, equilibrar las cargas y filtrar armónicos de corriente y tensiones en la red [5].

La implementación de la tecnología V2G a la ciudad de Babahoyo representa un avance tecnológico representativo, además representa un aporte importante al medio ambiente. También hay que considerar que, al tener la opción de aportar energía a la red, podremos realizar el neteo de energía de los kWh suministrados y reducir los rubros de energía eléctrica consumidas en la localidad, haciendo uso de las regulaciones creadas en los últimos años por la Agencia de Regulación y Control de Energías y Recursos Naturales No Renovables ARCERNNR No. 001/2021 y 002/2022.

En resumen, el presente estudio analiza el impacto de la tecnología V2G en la red eléctrica de Babahoyo, Ecuador. Destaca los beneficios de los VEs para optimizar el uso de energía y reducir la contaminación, este último se medirá mediante el uso del factor de emisión de equivalencias de gases efecto invernadero. Además, se investiga cómo la tecnología V2G afecta los parámetros eléctricos y aporta servicios auxiliares de la red, para lo cual se realiza diferentes simulaciones con el uso del software Cymdist, en el cual se emplearán 3 escenarios con diferentes casos de estudios, para conocer el comportamiento de la curva de la demanda cuando existe la hora pico y como los vehículos aportan con diferentes servicios auxiliares a la red de distribución.

1.1. CARACTERÍSTICAS DE LA TECNOLOGÍA V2G

1.1.1. Tecnología Vehicle-2-Grid

Los VEs han experimentado una revolución en la industria automotriz en las últimas décadas, impulsando un cambio significativo hacia una movilidad más limpia y sostenible. Estos innovadores automóviles utilizan motores eléctricos y baterías recargables en lugar de motores de combustión interna, lo que les permite producir cero emisiones en el punto de uso y reducir drásticamente el impacto ambiental en comparación con sus contrapartes de gasolina y diésel [6].

Los propietarios de VE también disfrutan de un menor costo operativo, ya que los vehículos eléctricos requieren menos mantenimiento y el precio de la electricidad suele ser más bajo que el de la gasolina o el diésel. Además, su eficiencia energética es notable, ya que los motores eléctricos son más eficientes en la conversión de energía en movimiento que los motores de combustión interna [6].

En la actualidad, existen cuatro tipos principales de vehículos eléctricos, a saber, Vehículos Eléctricos de Batería (BEVs), Vehículos Eléctricos Híbridos Enchufables (PHEVs), Vehículos Eléctricos Híbridos (HEVs) y Vehículos Eléctricos de Celda de Combustible (FCEVs) [6].

Esta tecnología permite que un VE no solo reciba energía de la red eléctrica (Grid-to-Vehicle), sino que también pueda devolver energía en sentido contrario, desde las baterías del vehículo hacia la red (Vehicle- to-Grid). Gracias a esta capacidad de flujo bidireccional de energía, el VE puede funcionar como un sistema de almacenamiento de energía cuando está conectado a la red [6].

Sin embargo, en este último caso, se debe tener en cuenta las diversas necesidades de autonomía de cada usuario, que pueden variar ampliamente entre diferentes vehículos y propietarios [6].

1.1.2. Modelo de red eléctrica para la implementación de Vehicle to grid

Los componentes esenciales de un sistema V2G incluyen: 1) una conexión eléctrica de doble vía con la red,

2) la capacidad de comunicación con las estaciones de carga para gestionar los procesos de carga y descarga,

3) un sistema de auditoría de los servicios prestados a la red (como un medidor bidireccional), y 4) estaciones de carga junto con vehículos habilitados para V2G [7].

Figura 1.

Dibujo esquemático que muestra las conexiones propuestas de la línea eléctrica y el control inalámbrico entre los vehículos y la red

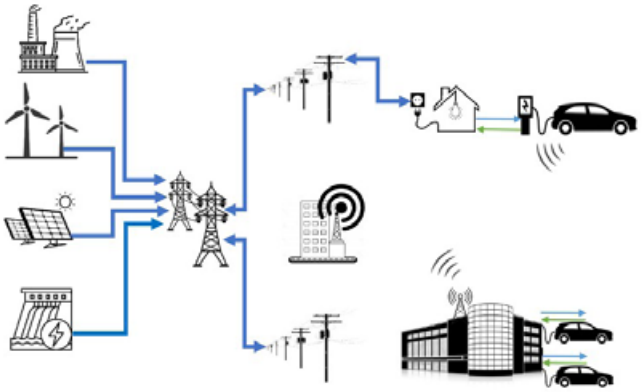

La comunicación entre el operador y los VEs posibilita una coordinación eficiente entre ambas partes, permitiendo la gestión óptima de la potencia de carga. Esto garantiza que se cumplan tanto los requisitos de carga del VE como la entrega de energía a la red, según lo requerido [7].

Los sistemas de comunicación para la bidireccionalidad de la energía en V2G, utilizan los siguientes protocolos y tecnologías:

Figura 2.

Diagrama representativo de los protocolos de comunicación en la movilidad eléctrica

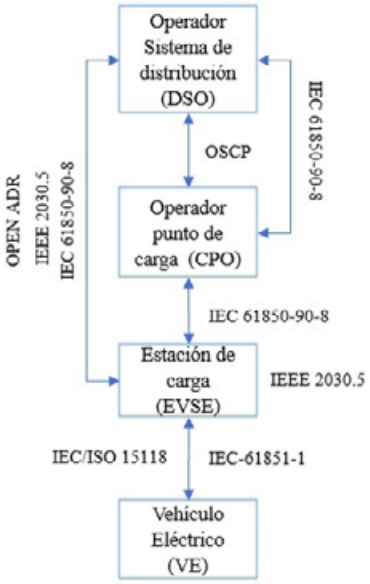

Estándares para la comunicación entre los Vehículos eléctricos y las estaciones de carga

1.1.2.1 ISO IEC 15118

El propósito de esta regulación es optimizar las comunicaciones entre las estaciones de carga, vehículos eléctricos y la red eléctrica [8]. Hasta ahora, la única normativa existente en este ámbito era la IEC 61851, que se encargaba de regular la comunicación entre las estaciones de carga y los vehículos eléctricos [8].

Esta normativa incorpora diversas características, tales como la regulación del 'plug and charge', que implica un conector capaz de identificar el modelo del vehículo sin requerir que el propietario introduzca manualmente los detalles de carga para el pago. Asimismo, facilita la comunicación y regulación de dispositivos V2G y vehicle to home (V2H). Además, permite que los operadores de la red tengan la capacidad de intervenir en el proceso de recarga, ajustando la intensidad de carga, ya sea para aumentarla o reducirla según sea necesario [9].

1.1.2.2 IEC-61851-1

Este estándar tiene como objetivo su aplicación en sistemas de suministro de energía para la carga de vehículos en carretera, abarcando un rango de tensiones de entrada de hasta 1000V en corriente alterna o hasta 1500V en corriente continua, y un rango de tensiones de salida de hasta 1000V en corriente alterna o hasta 1500V en corriente continua. Esto incluye a vehículos eléctricos de carretera, así como a vehículos híbridos enchufables (PHEV) que obtienen toda o parte de su energía de un sistema de almacenamiento [10].

La norma internacional IEC 61851-1 ha definido cuatro modos de carga para los VEs, este estudio se centrará el modo 4, ya que este permite la bidireccionalidad del flujo de energía entre el VE y el EVSE [10].

El modo cuatro de carga habilita la recarga en corriente continua (CC). Dado que este modo opera con altas potencias, el convertidor debe estar ubicado fuera del vehículo y en la propia estación de carga. En este modo de carga, existen dos estándares para los conectores, uno de origen japonés y otro europeo, conocidos como CHAdeMO y CCS respectivamente [9].

- **CHAdeMO**

CHAdeMO representa una norma de carga en corriente continua (CC) destinada a vehículos eléctricos, permitiendo una comunicación sin interrupciones entre el automóvil y el dispositivo de carga [11]. Es una norma de origen japones, publicada por organismos de normalización como la IEC, IEEE, EN y JIS; dichos enchufes son idénticos en todo el mundo y por lo general son usados por los fabricantes de vehículos japoneses, coreanos y algunos europeos [9].

En la actualidad, CHAdeMO es el único protocolo de carga en el mundo con la funcionalidad de carga bidireccional (V2G) habilitada, con producción a gran escala y un sistema de certificación implementado para garantizar la interoperabilidad entre vehículos eléctricos y dispositivos V2G. Hasta la fecha, existen más de 20 modelos de cargadores bidireccionales disponibles y se han instalado más de 10,000 unidades de este tipo en Japón y en todo el mundo [11].

Los proyectos que utilizan las capacidades V2G del protocolo CHAdeMO se han estado llevando a cabo en todo el mundo desde 2012. Recientemente, su escala y número han estado creciendo, con cada vez más iniciativas en Europa y Estados Unidos. Estos proyectos de demostración proporcionan hallazgos y datos valiosos para la implementación a gran escala de la tecnología V2H (Vehicle-to-Home) / V2G en el mercado [11]

- **CCS1/2**

El sistema CCS1/2 es el estándar de carga rápida que se ha implementado en la Unión Europea para la carga de vehículos eléctricos [12]. Permite que se carguen absolutamente todos los vehículos, incluso los que antes venían con otros conectores. La Unión Europea establece que todas las recargas de VEs que se realicen en el modo de carga 4 deben implementar al menos un conector CCS [12].

La ventaja de este tipo de conector CCS2 hembra es que permite la carga rápida, pero también permite recibir la carga de un conector de carga lenta tipo 2 llamado Mennekes [12]. Con lo cual, con el CCS2, los vehículos se pueden cargar en casa con la corriente alterna durante la noche. Y luego, cargar a toda potencia en cualquier electrolinera [12]. Está compuesto por un total de 9 pines que permiten la carga en corriente alterna (AC) y en corriente continua (CC) [12]. Estos pines del conector CCS2 se organizan en dos grupos:

- Los pines de carga en corriente continua (CC), que se usan para la carga rápida de la batería del vehículo
- Los pines de carga en corriente alternan (AC), encargados de la carga normal o lenta.

En el sistema CCS2, los conectores incluyen un pin de control y un pin de proximidad, con funciones idénticas a las del tipo 2 (Menekkes). Además, se encuentran dos conectores de potencia, uno para el polo negativo (CC-) y otro para el polo positivo (CC+), dado que se trata de corriente continua, y un pin de protección o conexión a tierra, que es compartido con el tipo 2 [12].

El protocolo europeo de carga rápida conocido como CSS Combo, es promovido por la asociación CharIN, que incluye a miembros como BMW, Ford, Honda y fabricantes de equipos [8]. En contraste con CHAdeMO, este protocolo es de acceso abierto, lo que significa que cualquiera puede acceder a las últimas versiones o actualizaciones sin necesidad de ser miembro de una organización [8]. Inicialmente, se reguló bajo la norma DIN SPEC 70121, pero actualmente, el estándar de comunicación para carga rápida conforme a este protocolo está definido en la norma IEC 15118 [8].

1.1.2.3 SAE J3072

La norma SAE J3072 establece los requisitos para una función de sistema de inversor de soporte de red que está integrada en un vehículo eléctrico enchufable (PEV) que se conecta en paralelo con un sistema de energía eléctrica (EPS) a través de equipos de suministro de vehículos eléctricos (EVSE) acoplados conductivamente [13]. Esta norma también define la comunicación entre el PEV y el EVSE requerida para configurar y autorizar la función de inversor a bordo del PEV para la descarga en un sitio. Los requisitos aquí establecidos están destinados a ser utilizados en conjunto con IEEE 1547 y IEEE 1547.1. Esta norma también respaldará inversores interactivos que cumplan con los requisitos de IEEE 1547-2003 y IEEE 1547.1-2005, reconociendo que muchas jurisdicciones de servicios públicos pueden no autorizar la interconexión [13].

1.1.2.4 IEEE 2030.5

El protocolo de comunicación IEEE 2030.5 aporta un valor significativo a los operadores de la red eléctrica al ayudarles a conectarse y aprovechar el mundo de los recursos energéticos distribuidos [14].

Tiene como objetivo ayudar a los fabricantes, operadores e integradores de sistemas de EVSE y PEV a implementar los requisitos de SAE J3072 utilizando el protocolo IEEE 2030.5 [15]. El EVSE es un servidor IEEE 2030.5 que aloja todos los recursos necesarios de SAE J3072 para interactuar con un PEV compatible con J3072 [15]. Cuando un PEV se conecta al EVSE, comienza la secuencia de autorización de SAE J3072. El PEV establece una sesión TLS para comunicarse con el servidor EVSE [15]. El PEV realiza la Búsqueda de Recursos para encontrar las ubicaciones de los recursos relevantes en el servidor EVSE, luego el PEV lleva a cabo el Intercambio de Información de J3072 necesario para obtener la autorización para la descarga, el EVSE evalúa el intercambio de información para determinar si el PEV cumple con todas las condiciones necesarias para la autorización de la descarga. El EVSE otorga o niega la autorización [15].

Esta secuencia de operaciones, desencadenada por la conexión inicial del PEV al EVSE, ocurre una sola vez. Si el EVSE niega la autorización al PEV, este último no intenta nuevamente la secuencia de autorización. En su lugar, el PEV opera en su modo de operación "No SAE J3072", continuando, monitoreando la señal de autorización de la descarga en caso de cambios en su estado de autorización [15].

Luego, el PEV ingresa a operaciones periódicas donde monitorea continuamente su autorización para la descarga. Si el PEV está autorizado para la descarga, envía información de metrología y estado al servidor EVSE. Si el PEV no está autorizado para la descarga, envía el estado de "no autorizado" al EVSE y puede enviar información de metrología y otro estado, pero no está obligado a hacerlo. Las operaciones periódicas continúan durante la duración de la sesión de carga [15].

1.1.3. Servicios Auxiliares de V2G

El V2G tiene la capacidad de proporcionar servicios complementarios, tales como una regulación rápida de la frecuencia y la tensión, la gestión del equilibrio de carga, una eficiente reserva de energía y respaldo de energía para la integración con fuentes de energía renovable. En este contexto, la función del agregador u operador de red es de suma importancia, ya que actúa como un intermediario entre los vehículos eléctricos y el sistema eléctrico, permitiendo la optimización del flujo de energía de manera que se logre una regulación efectiva de la red [16].

Cabe mencionar que un agregador en la tecnología de *Smart grid*, es un intermediario entre los propietarios de los vehículos eléctricos y la red de energía eléctrica, esto con la finalidad coordinar y gestionar la participación de los VEs conectados a la red en respuesta a la demanda [16].

Los principales servicios auxiliares que se evaluaran en el presente artículo son: la amortización de la curva de demanda del alimentador y las variaciones de tensiones que ocurren a lo largo del alimentador.

1.1.3.1 Regulación de tensión

La regulación de tensión desempeña un papel fundamental en el suministro de potencia reactiva a la red eléctrica. La implementación de sistemas de compensación reactiva en las cercanías de las cargas resulta más efectiva, ya que minimiza la necesidad de transportar potencia reactiva a través de las redes de distribución. Esta estrategia no solo contribuye a la reducción de pérdidas eléctricas en las líneas, sino que también optimiza la eficiencia operativa de la red, favoreciendo una mayor estabilidad y calidad del servicio eléctrico [17].

La regulación de la tensión mediante V2G se lleva a cabo mediante un cargador bidireccional de cuatro cuadrantes que, según las necesidades del sistema, posibilitará la inyección de potencia reactiva desde el vehículo eléctrico hacia la red [17].

El cargador bidireccional permite una mayor versatilidad en la participación de la gestión de energía hacia la red, ya que este permite que el vehículo no solo consuma energía de la red para cargar su batería, sino que también pueda devolver energía hacia la red cuando sea necesario. El término denominado "4 cuadrantes" se refiere a la capacidad del cargador opere bajo 4 configuraciones distintas: el primer cuadrante el cargador actúa entregando energía eléctrica al VE desde la red y el segundo cuadrante el VE libera la energía almacenada en la batería y la devuelve a la red para contribuir al suministro de energía cuando se lo requiera [17].

2. MÉTODO

2.1 CARACTERÍSTICAS DE LA RED DE DISTRIBUCIÓN

El alimentador Centro Babahoyo es de tipo radial, está conectado a la subestación Terminal Terrestre que tiene una capacidad de 20/25MVA está ubicada en la parte céntrica de la ciudad en las coordenadas -1.80365,-79.52168; el alimentador constituye la red de distribución primaria de la ciudad de Babahoyo, esta operando a un nivel de tensión de 13.8 kV en el lado de alta tensión y mediante transformadores de distribución se reduce a tensiones de 240/120 V, el alimentador cuenta con un total de 2705 usuarios regulados.

La longitud de alimentador es de 2427.4m, la mayor parte del alimentador abastece a la demanda energética urbana, a pesar de que existe una mayor cantidad de usuarios residenciales, la carga de los clientes industriales es mayor.

Tabla 1.

Consumo de energía por tipo de usuario

Tipo de usuario	Cantidad de usuarios	Consumo de energía %	kVA
Residenciales	1804	33%	521.75
Comerciales	783	32%	496.55
Industriales	118	35%	478.75

2.2 MODELAMIENTO DE LA RED DE DISTRIBUCIÓN

Para el modelamiento del alimentador de distribución, fue necesario obtener los datos de la empresa Distribuidora como: Longitud de cada tramo del alimentador, dispositivos de maniobra y protección (reconectadores, seccionadores y fusibles), tipo de estructuras, transformadores y conductores. El modelamiento con los datos reales presenta la ventaja de conocer la participación de los servicios auxiliares de V2G antes y después de la incorporación en la red de distribución, todo el modelamiento de la red se lo realizo en el software CYME 9.0 debido a su alta especialización en el análisis de redes de distribución eléctrica, especialmente en sistemas que integran recursos energéticos distribuidos, como la generación fotovoltaica, almacenamiento de energía y tecnologías de EVSE. En la figura 3 se muestra la red de distribución del alimentador Centro Babahoyo, en el cual con la ayuda del mapa de colores permite identificar la densidad de carga a lo largo del alimentador, donde el color amarillo indica que existe una densidad de carga elevada, mientras que el color azul denota una densidad de carga menor.

Figura 3.

Recorrido del alimentador Centro Babahoyo en el Software CYME

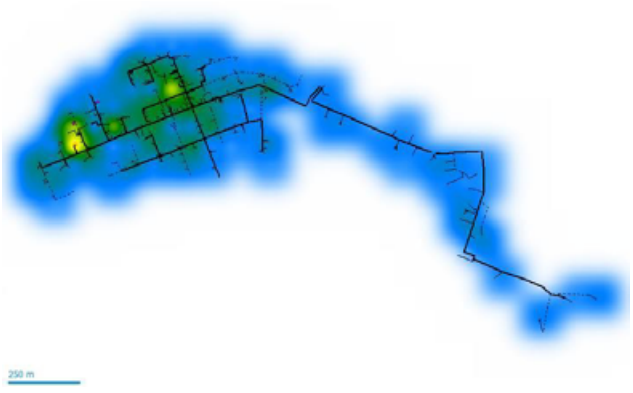

2.3 DESCRIPCIÓN DE LOS CASOS DE ESTUDIO

Para realizar el análisis de la incorporación de V2G en la red de distribución, se tomó a consideración escenarios diferentes para conocer el comportamiento de la red de distribución mediante la penetración de servicios auxiliares. El primer escenario consiste en modelar el sistema con curvas de carga de los usuarios en la red en días laborables comprendidos de lunes a viernes, el segundo escenario se realizará en los días comprendidos el fin de semana y el último escenario será evaluado en días festivos, el objetivo de considerar los escenarios mencionados es para conocer el comportamiento de la red mediante la inserción de servicios auxiliares mediante el V2G, en diferentes eventualidades del año.

Para cada escenario se realizarán los respectivos casos de estudio, el primer caso de estudio consiste en modelar el sistema de distribución en condiciones normales; es decir cómo está operando la red actualmente, el segundo caso consiste en modelar la red con inserción de los VEs y conocer cómo éstos ayudan a suavizar la curva de la demanda del alimentador y finalmente el siguiente caso se analizará las tensiones a lo largo del alimentador para ver donde se están produciendo estas condiciones anormales y dar posibles soluciones con la inserción de los EVSEs.

2.4 MODELO DE ESTACIONES DE CARGA DE VEHÍCULOS ELÉCTRICOS

Para realizar los casos de estudio con el software CYME, se utilizó un sistema de almacenamiento por baterías (BESS), el cual consta con diferentes componentes como el módulo de batería que almacena la potencia activa proveniente de la red y la transfiere cuando esta es solicitada por medio de los convertidores DC/DC, como la energía debe ser enviada hacia la red eléctrica utiliza un inversor CA/CC. Por otro lado, usando la capacidad del inversor, la potencia reactiva puede ser transferida en distintas direcciones. Dado que todos los componentes mencionados no cuentan con capacidades de operación inteligente, el BESS incorpora un controlador especializado. Este controlador gestiona el suministro bidireccional de potencia activa y reactiva (carga/descarga), basado en un esquema de control avanzado que utiliza mediciones en tiempo real de variables eléctricas en puntos estratégicos de la red. De esta manera, el BESS contribuye a la regulación dinámica del sistema, optimizando el perfil de tensión y mejorando la calidad y confiabilidad del servicio eléctrico. Este módulo BESS será el modelo del equipo bidireccional de carga de vehículos eléctricos

(EVSE – Electrical Vehicle Supply Equipment) para las respectivas simulaciones.

3. RESULTADOS Y DISCUSIÓN

Para la implementación de las EVSEs, se consideraron ciertos aspectos técnicos, como la potencia de los cargadores y su ubicación, debido a que éstos juegan un papel fundamental en la configuración de la red. Los EVSEs fueron ubicados en lugares y establecimientos de acceso públicos, entre los cuales se tiene al garaje del malecón de la ciudad y al parqueadero del GAD municipal, así mismo se colocó en una gasolinera la cual está conectada al alimentador a estudio y finalmente en una avenida principal, donde existe un mayor flujo vehicular debido a que en esta avenida están ubicadas la mayoría de entidades públicas, todos estos criterios se aplicaron a las EVSEs con potencias de 50kW y 20kW. Las EVSEs con potencias de 7kW fueron ubicadas cerca de conjuntos residenciales. En la tabla 2 se indica la cantidad de EVSEs instaladas a lo largo del alimentador. Cabe recalcar en estaciones de 7.4kW hasta la actualidad no se cuenta con opciones comerciales que permitan la bidireccionalidad de la energía, sin embargo, se consideran estas estaciones debido a que a nivel mundial son las potencias más utilizadas en el mercado residencial.

Tabla 2.

Cantidad de cargadores habilitados para v2g instalados en el alimentador

Potencia de los cargadores	Unidades	Ubicación de los EVSEs en los nodos
50 kW	6	1068234, OID891, OID50772, OID900, OID898, OID866
		1068158-I, OID831-I, OID856-I, OID862-I, OID874-I, OID878-I
20kW	12	OID882-I, OID888-I
		OID893-I, OID896-I
		OID900-I, 1068147-I

		1067489-R, 1068138-R, 1068139-R
		1068156-R, 1068181-R
		1068182-R, 1068183-R
		1068195-R, 1068197-R
		1068198-R, 1068207-R
		1068208-R, 1068209-R
		1068214-R, 1068222-R
7.4kW	30	
		1068223-R, OID50778-R, OID50770-R, OID9125-R, OID7311-R, OID7302-R, OID7268-R, OID7267-R, OID6103-R, OID5992-R, OID5975-R, OID3994-R, OID2321-R, 1068281-R, OID908-R,

Las potencias utilizadas de los cargadores son de valores comerciales**

Una vez que se efectuó la ubicación de los EVSEs, se configuraron, para realicen el proceso de carga y descarga, para lo cual los EVSEs responderán en función a la cargabilidad de la línea en el tramo al cual están conectados, si la cargabilidad está por debajo del 65% los cargadores empezaran a suministrar energía a las baterías de los vehículos y si está por encima del valor referenciado estos empezaran a descargarse para

aliviar la demanda de la red.

Figura 4:

Carga-descarga del conjunto de los EVSEs conectados al alimentador.

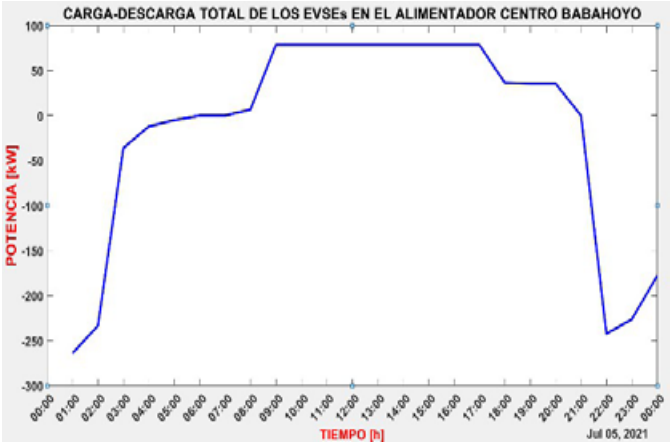

La funcionalidad de carga de los vehículos se da en horas comprendidas entre las 8 de la mañana hasta las 17:00 horas de la tarde, que corresponden a los vehículos que se conectaran a los cargadores de 50kW y 20kW. Según [18], en un estudio realizado en Canadá se logró determinar que las estaciones públicas son más propensas a ser utilizadas desde las 8:00 a.m. hasta las 16:30 p.m., por lo cual dichas horas se denotan debido a que en ese horario se efectúa la carga de los vehículos en espacios públicos como parqueos y garajes de ciertos establecimientos que comprenden el horario laboral de los propietarios de los vehículos, una vez pasado este horario la energía almacenada de los VEs pueden tener la capacidad de ser enviada hacia la red por medio de las EVSEs, para abastecer una parte de la demanda dando como resultado un aplanamiento en la curva de la demanda en cabecera del alimentador. Así mismo los vehículos que se conectaran a cargadores de 7.4kW realizarán su carga en horas de la madrugada, el comportamiento de la carga de estos VEs permite que en las horas durante se produce el valle de la curva de la demanda, incremente la misma [18]. En la figura 4 se muestra la potencia tanto de carga y descarga del grupo de EVSEs conectados en el alimentador.

3.1 Caso de estudio: Incorporación de EVSE en el alimentador

Para el caso de estudio analizado se tomó como referencias la gestión de inicio y finalización de la carga tanto en cargadores de espacios públicos como los tipos residenciales según [18]. En el cual se denotan que existe una mayor densidad de inicio en carga en espacios públicos en horas comprendidas entre las 7:30 a

8:30 a.m. y un segundo pico entre las 12:00 y 1:30 p.m., mientras que para los cargadores de los usuarios residenciales suele iniciarse entre las 5 p.m. y 6 p.m., dicho comportamiento se lo puede apreciar mediante la figura 5.

Figura 5.

Curvas de inicio de sesión para los cargadores públicos y residenciales.

En la figura 6 se muestra la distribución de finalización de cargas, para los usuarios residenciales la gestión de carga termina entre las 7:30 a.m. y las 8:00 a.m. Mientras que las estaciones de carga públicas se dan en horas comprendidas entre las 4:00 p.m. y 5:00 p.m. Este estudio fue tomado como referencia para la evaluación del comportamiento de la curva a lo largo del día, si bien los horarios de inicio y finalización de las sesiones de carga no coinciden exactamente entre los usuarios residenciales y las estaciones públicas, se observa una cierta similitud en las tendencias generales. Esta diferencia se debe a las variaciones en los perfiles de demanda de cada tipo de infraestructura, lo que provoca que, los horarios específicos de inicio y término no se alinean completamente.

En el caso inicial el comportamiento de la curva de carga diaria del alimentador comprendido en un día, indica que, en periodos del día, a partir desde las 7:00 am, empieza a aumentar la demanda producida por los consumidores, donde se empieza a producir el valor pico a partir de las 16:00, mientras que las horas valles del alimentador se dan en horas comprendidas desde las 2:00 am hasta las 6:00 am.

Se realizó una comparación del comportamiento de la curva de la demanda de energía de la red cuando se conectaron los EVSEs, para aquello se observó que las curvas de la demanda de las 3 fases en el periodo comprendido desde las 5:00 a.m. hasta las 07:00 a.m. no existe un cambio en la curva de demanda debido a que en este horario, por lo general las estaciones de carga de los usuarios residenciales culmina, ya que en ese horario los propietarios de los vehículos los utilizan para la transportación hacia su destino y conectarlos nuevamente a una estación de carga por lo general tipo pública, como se denota en la grafica 7, a partir de las 7:00 a.m. nuevamente existe variación en la demanda. Así mismo, se evidenció que la curva de la demanda cuando existe inyección de potencia hacia la red eléctrica disminuye en horas pico correspondiendo a la 6:00 pm, pasando de 418kVA a 410kVA para la fase A, 487kVA a 469kVA para la fase B y 555kVA a 549kVA para la fase C respectivamente. En horas comprendidas del valle de la curva esta empieza a incrementar en las horas comprendidas entre la 1:00 am hasta las 5:00 am, dicha eventualidad se da debido a que los cargadores conectados a los usuarios residenciales gestionan su carga en estos horarios, dando como resultado el suavizado de la curva de la demanda en cabecera del alimentador.

En la figura 7 se muestra las curvas de la demanda por cada fase, correspondiendo la curva de color roja a la fase A, la curva azul a la fase B y a la curva negra a la fase C respectivamente, el comportamiento de las curvas denota que incorporando EVSEs en la red de distribución esta disminuye en horas del día, lo que ayuda a que la red en este horario pueda tener la capacidad de satisfacer una mayor demanda, así mismo ayuda a disminuir la cargabilidad en los equipos de la red como lo son las líneas y los transformadores de la red de distribución.

3.2 CASO DE ESTUDIO: CONDICIONES ANORMALES PRESENTADAS EN EL ALIMENTADOR.

Tabla 3.

Subtensiones efectuadas en el alimentador

Nodos con subtensiones en el alimentador

Nombre del nodo	Subtensión con EVSEs %	Subtensión sin EVSE %	Hora de la subtensión
1056	94,54	94,49	7/5/2021 10:00
210	93,98	93,97	7/5/2021 17:00
216	92,00	91,98	7/5/2021 9:00
217	94,94	94,92	7/5/2021 18:00
237	92,00	92,01	7/5/2021 8:00
268	94,86	94,84	7/5/2021 17:00
346	88,44	88,45	7/5/2021 1:00
361	92,93	92,88	7/5/2021 9:00
365	93,91	93,91	7/5/2021 1:00
856	92,49	92,48	7/5/2021 8:00

Tabla comparativa del caso base y el caso 1**

Al realizar los respectivos flujos de carga mediante los perfiles de los usuarios se obtuvo los nodos que presentan problemas de tensión como lo es la subtensión, para el flujo de carga efectuado en el alimentador Centro Babahoyo se eligió límites de trabajo en función a la condición que se presente; mayor al 105% se presentara una sobretensión y menor a un 95% se presentara una subtensión, esto con respecto a los límites de tensión, mientras que para los límites de sobrecarga para líneas o transformadores, se tomó un valor del

100%, lo cual se evidencia que incorporando potencia mediante los cargadores de los vehículos se logra corre-

gir en pequeñas proporciones el porcentaje de la subtensión como se le puede apreciar en la tabla 3.

3.3 CASO DE ESTUDIO: INCORPORACIÓN DE EVSES EN NODOS CON SUBTENSIONES.

En los nodos que se producían subtensiones se implementó los EVSEs para que estos permitan que las tensiones estén dentro del rango establecido (0.95 y 1.05 pu), a pesar de que se conectaron los EVSEs en los nodos con subtensiones no todos los nodos presentaron mejoras en las tensiones, para el nodo 1056 en un inicio presentaba una subtensión del 94.54% con un tiempo de 7 horas, al implementar el EVSE en el nodo, este si corrigió sus valores pasando a un 97% dejando de presentar la subtensión como se muestra en la figura 8, sin embargo, para el nodo 346 el valor de tensión no entró en los rangos establecidos, la curva de la figura 9 muestra el comportamiento de la curva de la tensión a lo largo del día, se observa que en las horas desde la 1:00 hasta las 14:00 el EVSE suministra suficiente potencia reactiva para que los valores de la tensión se mantengan en 240V, pero a las 16:00 ya no es capaz de mantener el valor de tensión debido a que este se descarga al límite configurado, es por ello que el EVSE con esa potencia no es capaz de solucionar del todo el problema de subtensión, una solución factible es un incrementar la potencia del EVSE o implementar otro mecanismo que inyecte reactivos a dicho nodo que mejore el perfil de tensión.

La potencia de los EVSEs es de gran importancia ya que, dependiendo de la capacidad de estos, tendrán la capacidad de suministrar servicios auxiliares a la red de distribución, como la energía reactiva para ayudar a corregir las caídas de tensión producidas a lo largo del día.

Caso de estudio: Incorporación de EVSEs en equipos con sobrecargas.

Se realizó un análisis en función a la cargabilidad de los equipos, en el cual se determinó que el transformador 1068270 presentaba una cargabilidad de 103.5% de manera global, como se observa en la figura 10 el transformador en las 24 horas del día presenta cargabilidad elevada, debido a que abastece a 67 usuarios que están ubicados donde existe alto consumo de energía de la red, correspondiendo 28 a usuarios comerciales, 35 residenciales y 4 industriales; dicho transformador está ubicado en el centro de la ciudad de Babahoyo.

Al implementar la EVSE el comportamiento de la tensión del nodo, como se muestra en la figura 11, presentó una mejora, es decir una disminución en la cargabilidad del transformador, en horas desde las 07:00 p.m. hasta 03:00 a.m. la cargabilidad paso de un 103.5% a un 94.6% disminuyendo la cargabilidad del transformador, sin embargo en horas desde las 3:00 a.m. hasta las 7:00 a.m. el transformador se sobrecargó pasando de un 103.5% a 112.6%, dicho comportamiento se refleja debido a que los vehículos eléctricos se conectan a la red, mientras que en horas del día desde las 7:00 a.m. hasta las 18:00 p.m. el comportamiento de la curva se mantiene igual debido a que no existe ni carga ni recarga de los vehículos eléctricos mediante los EVSEs, dicho comportamiento de la curva durante las 24 horas se da debido a que los EVSEs se los configuró a que trabajen con el comportamiento de los cargadores residenciales. En las horas donde se producían las descargas de energía hacia la red se observa como la tecnología V2G por medio del controlador de carga puede ayudar a la red de distribución.

3.4 Caso de estudio: Incorporación de EVSEs en el alimentador en fines de semana y días festivos.

La curva de carga de demanda en general varía entre días laborables y días festivos/fines de semana debido a cambios en los patrones de consumo. En días laborables, la demanda tiende a ser más alta durante las horas de trabajo, impulsada por la actividad industrial y comercial, así como por las rutinas diarias de las personas. Durante los días festivos y fines de semana, la demanda se redistribuye, con una disminución en la actividad industrial y comercial, y un aumento en el consumo residencial, especialmente en actividades de entretenimiento y hogareñas.

Al verificar las curvas de carga del alimentador sin EVSE del caso de estudio "Incorporación de EVSE en el alimentador", figura 5 y las curvas de carga del alimentador de este caso, las cuales se encuentran graficadas en la figura 12 se puede evidenciar la redistribución de la demanda en las horas del día en el alimentador, en días de fines de semana y días festivos.

El comportamiento de la curva de carga del alimentador al incorporar los EVSEs se puede visualizar en la figura 12, donde la mayoría de los EVSEs empiezan a cargarse a la 1:00 am y terminan de cargarse a las 5:00 am aproximadamente. La descarga de ciertos vehículos que todavía se encuentran conectados a la red, empieza desde las 7:00 am hasta las 19:00 pm y por último vuelven a conectarse los EVSEs a la 21:00 pm.

Se realizó una comparación del comportamiento de la curva de la demanda de energía de la red cuando se conectaron los EVSEs, para lo cual se evidenció que la curva de la demanda cuando existe inyección de potencia hacia la red eléctrica disminuye, en horas pico correspondiendo a las 14:00 pm, pasando de 537kVA a 531kVA para la fase C, 486kVA a 468kVA para la fase B y 376kVA a 369kVA para la fase A respectivamente.

Durante las horas de menor demanda eléctrica, la curva de carga comienza a mostrar un aumento en su valor, específicamente en el intervalo de tiempo que abarca desde la 1:00 de la madrugada hasta las 5:00 de la mañana. Este fenómeno se produce debido a que los cargadores

conectados en los hogares de los usuarios empiezan a gestionar su carga durante este período.

En la Figura 12, se presentan las curvas de demanda correspondientes a cada fase de manera diferenciada. La curva de color rojo representa la fase A, la curva azul corresponde a la fase B, y la curva de color negro se refiere a la fase C. La observación clave en el comportamiento de estas curvas indica que, al incorporar los EVSEs en la red de distribución, se produce una disminución en la demanda durante ciertas horas del día. Este efecto contribuye a que la capacidad de la red eléctrica en ese período sea suficiente para satisfacer una demanda mayor, al mismo tiempo que reduce la carga en los componentes de la red, como las líneas de distribución.

3.5 CASO DE ESTUDIO: INCORPORACIÓN DE EVSES EN NODOS CON SUBTENSIONES ANÁLISIS EN FINES DE SEMANA Y DÍAS FESTIVOS.

Luego de realizar el análisis de subtensiones con la implementación de EVSEs de manera general, los perfiles de tensión en varios nodos no presentaron mejoras considerables comparando con el perfil de tensión del caso sin EVSEs, ya que no superaron el valor mínimo de subtensión permitido (0.95).

Para solucionar los problema de subtensión se incorporó nuevos EVSEs de 50 kW en los nodos que presentaron subtensiones en la red, con la finalidad de mejorar el perfil de tensión en los nodos críticos, para el nodo 1056 en un inicio presentaba una subtensión del 93.98% con un tiempo de 12 horas, al implementar el EVSE en el nodo, este si corrigió sus valores pasando a un 98% dejando de presentar la subtensión como se muestra en la figura 11, donde la curva de color rojo representa al perfil de tensión en el nodo 1056 cuando no se ha incorporado ningún EVSE a la red, la curva de color azul representa al perfil de tensión del nodo cuando se incorporó EVSEs de manera general a la red y el color negro representa la curva del perfil de tensión en el nodo cuando se incorporó EVSEs en los nodos que presentaban subtensión.

El nodo 346 el valor de subtensión era uno de los más críticos, la curva de la figura 7 muestra el comportamiento de la curva de la tensión a lo largo del día, se observa que presenta una subtensión de 88.48% en todo el día sin EVSE en el nodo, con la incorporación del nodo el perfil sube a 98 %, dejando el nivel de tensión en el rango permitido.

3.6 CASO DE ESTUDIO: INCORPORACIÓN DE EVSES EN EQUIPOS CON SOBRECARGAS.

Se llevó a cabo un análisis centrado en la carga de los equipos, y como resultado, se determinó que el transformador 1068270 presentaba una carga global del 103.5%, este valor se refleja en la Figura 10, donde se observa, que, a lo largo de las 24 horas del día, el transformador opera a un nivel de carga del 103.5%.

Sin embargo, tras la implementación de las EVSE, se observó una mejora en su carga. Durante las horas comprendidas entre la 1:00 a.m. y las 3:00 a.m., la carga del transformador disminuyó del 103.5% al 96.3%, aliviando la carga del transformador en ese período. No obstante, entre las 3:00 a.m. y las 7:00 a.m., se registró un aumento en la carga, llegando al 112.6%. A las 7:00 a.m., el EVSE se desconecta de la red, simulando la partida de los usuarios para realizar otras actividades. Durante este período, la carga se mantuvo en 103.5% debido a la inactividad del EVSE. Finalmente, desde las 6:00 p.m. hasta la medianoche, el EVSE vuelve a inyectar energía en la red, reduciendo la carga del transformador al 96.3% para finalizar el día, como se observa en la figura 16, donde la curva de color roja continua representa a la cargabilidad del transformador sin la incorporación de los EVSEs, y la curva de color azul discontinua representa a la cargabilidad del transformador con la incorporación de los EVSEs.

3.7 Discusión

El estudio llevado a cabo por [2] destacó las ventajas de los VEs en la red de distribución, con un enfoque en el nivel de carga de los alimentadores y los transformadores de distribución, así como los niveles de tensión y la demanda en los alimentadores. A través de varios escenarios planteados, se pudo determinar la influencia de la incorporación de VEs de distintos modelos. Se observó que una penetración del 10% de vehículos de tipo Kia logró reducir la carga del transformador durante las horas pico, lo que representó un resultado positivo para la red de distribución. A diferencia del estudio realizado se tomó a consideración un modelo de cargador para vehículos eléctricos donde se evaluó la curva de la demanda en días laborables y no laborables, donde se evalúo la tensión a lo largo del alimentador, en el cual se tomó a consideración cargadores de tipo residenciales y de uso público, para conocer cómo se comporta la curva en todo instante de tiempo. En la investigación [18], describen el comportamiento de la gestión de carga en el inicio y finalización de los cargadores de uso público y residenciales, lo que ayudó a describir el comportamiento de la curva de los EVSEs en el alimentador Centro Babahoyo, en el estudio desarrollado hubo resultados favorables para el alimentador estudiado, dentro de los resultados más relevantes se tiene una disminución en la curva de carga en los días laborables mediante la implementación de los EVSE, ya que éstos fueron ubicados en lugares idóneos para la carga de los EVs, así mismo ciertos transformadores que estaban operando en estado de sobrecarga mediante la inyección de energía mediante los VEs se logró reducir la cargabilidad de los transformadores pasando a valores por debajo del 100%.

4. CONCLUSIONES

La implementación de la tecnología V2G (Vehicle-to-Grid) en la red eléctrica de la ciudad de Babahoyo, Ecuador, ofrece beneficios significativos tanto para la optimización del uso de la energía como para la reducción de la contaminación ambiental. Esta tecnología permite que los vehículos eléctricos inyecten energía almacenada en sus baterías en la red durante momentos de alta demanda, lo que alivia la carga y mejora la eficiencia. Además, contribuye a regular la potencia activa y equilibrar las cargas en la red. Al incorporar puntos de carga de vehículos eléctricos en lugares estratégicos, se logra suavizar la curva de la demanda durante el día laborable, reduciendo la carga en los transformadores y líneas de distribución. Esto también conduce a una disminución de la sobrecarga en ciertos equipos de la red, mejorando la calidad del suministro eléctrico.

En los resultados obtenidos tras la implementación de estaciones de carga de vehículos eléctricos (EVSEs) en la red de distribución de Babahoyo, se evidenció una reducción significativa en la carga de los transformadores. Por ejemplo, el transformador 1068270, que inicialmente operaba al 103.5% de su capacidad, experimentó una disminución al 96.3% durante ciertas horas, aliviando así la sobrecarga. Además, se logró una reducción en la carga pico de la red, disminuyendo la demanda de 537kVA a 531kVA en horas de alta demanda. Estos datos numéricos respaldan las ventajas de la tecnología V2G en la optimización de la red eléctrica y la mejora de la confiabilidad del suministro, destacando su potencial para la gestión inteligente de la energía.

El análisis detallado de la incorporación de EVSEs (Estaciones de Carga de Vehículos Eléctricos) en la red eléctrica de Babahoyo revela la importancia de esta tecnología para mejorar la eficiencia del sistema eléctrico. Los EVSEs, ubicados estratégicamente en lugares públicos y residenciales, juegan un papel crucial en la gestión de la carga y descarga de vehículos eléctricos. Durante los días laborables, contribuyen a aplanar la curva de la demanda, reduciendo la carga en horas pico y mejorando la capacidad de la red. En días festivos y fines de semana, redistribuyen la demanda de energía, adaptándose a los patrones de consumo cambiantes. Además, se observa que los EVSEs pueden ayudar a corregir problemas de subtensión y sobrecarga en ciertos nodos y equipos de la red. Esta investigación destaca el potencial de la tecnología V2G para mejorar la infraestructura eléctrica y promover la adopción de vehículos eléctricos como una alternativa más sostenible y eficiente en el transporte.

REFERENCIAS

[1] F. Samuel et al., "Análisis de la incorporación de sistemas fotovoltaicos tipo red en el alimentadorcentro Babahoyo 13.8kv de CNEL EP unidad de negocios Los Ríos," Universidad Tecnica Estatal de Quevedo, Quevedo, 2022. Accedido: 20 de Agosto de 2023. Disponible en: https://repositorio.uteq.edu.ec/server/api/core/bitstreams/58785567-4aed-4380-8cb6- a6848bf-22db7/content

[2] E. Delgado y J. Medina, "Análisis del impacto de la implementación de la tecnología V2G en redes de distribución eléctrica," 2021, pp. 1–128, Accessed: Aug. 02, 2023. [Online]. Available: http://dspace.ucuenca.edu.ec/handle/123456789/36033

[3] G. Camino, "Análisis técnico y económico de la integración de flotas de vehículos eléctricos a nivel residencial en sistemas modernos de distribución de energía eléctrica," 2022. Accessed: Aug. 20, 2023. [Online]. Available: https://bibdigital.epn.edu.ec/bitstream/15000/22793/1/CD%2012277.pdf

[4] C. Perez, "Transporte lidera estadísticas de consumo energético en Ecuador," Quito, 2022.

[5] G. K. R. Nikhil, "Impact of EV on Integration with Grid System A Review," en 8th International Conference on Power Systems (ICPS), Apr. 2020, doi: 10.1109/ICPS48983.2019.9067587.

[6] Carrera, "Estimacion de costos de energia electrica para la recarga de vehiculos electricos basado en la optima respuesta de la demanda" 2020.

[7] W. Kempton and J. Tomić, "Vehicle-to-grid power fundamentals: Calculating capacity and netrevenue," J Power Sources, vol. 144, no. 1, pp. 268–279, Jun. 2005, doi:10.1016/j.jpowsour.2004.12.025.

[8] LugEnergy, "¿Qué es la ISO 15118?," 2023.

[9] A. Internacional de Energías Renovables, Perspectivas de innovación: Carga inteligente para vehículos eléctricos. 2019. [Online]. Disponible en: www.irena.org

[10] CTN 203, "UNE-EN IEC 61851-1 Sistema conductivo de carga para vehículos eléctricos," 2022, Accessed: Sep. 09, 2023. [Online]. Available: file:///D:/DESCARGAS%20NAVEGADOR/(EX)UNE-EN_IEC_61851-1=2020-2.pdf

[11] CHAdeMO, "A decade of in-market experience with V2G/VGI," 2022. https://www.chademo.com/technology/v2g (accessed Aug. 22, 2023).

[12] Floox, "¿Qué es el sistema CCS2 en la carga de un vehículo eléctrico?," 2023.

[13] H. Asgeirsson, "Electric Vehicle V2G AC Standards SAE, IEEE, UL," 2021.

[14] F. Wauquiez, "IEEE 2030.5 – Connect to the Wide World of Distributed Energy Resources." https://www.ge.com/digital/tech/ieee-20305-connect-wide-world-distributed-energy-resources (accessed Sep. 09, 2023).

[15] SunSpec Alliance, "IEEE-2030.5-V2G-AC-Profile Implementation Guide for SAE J3072," 2022, Accessed: Sep. 08, 2023. [Online]. Available: https://sunspec.org/wp-content/uploads/2022/06/SunSpec-IEEE-2030.5-V2G-AC-Profile-TEST-1.0.pdf

[16] B. Dumnić et al., IEEE EUROCON 2019: 18th International Conference on Smart Technologies: 1st - 4th July 2019, Novi Sad, Serbia.

[17] J. Wang, G. R. Bharati, S. Paudyal, O. Ceylan, B. P. Bhattarai, and K. S. Myers, "Coordinated Electric Vehicle Charging with Reactive Power Support to Distribution Grids," IEEE Trans Industr Inform, vol. 15, no. 1, pp. 54–63, Jan. 2019, doi: 10.1109/TII.2018.2829710.

[18] T. Jonas, N. Daniels, and G. Macht, "Electric Vehicle User Behavior: An Analysis of Charging Station Utilization in Canada," Energies (Basel), vol. 16, no. 4, Feb. 2023, doi:10.3390/en16041592.

ANEXOS

Figura 6.

Curvas de finalización del comportamiento de los cargadores públicos y residenciales.

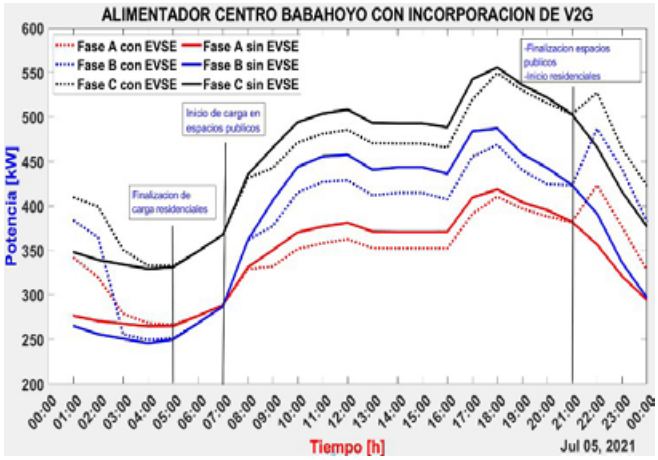

Figura 7.

Curvas de la demanda en cabecera del alimentador de las 3 fases, con y sin implementación de EVSEs.

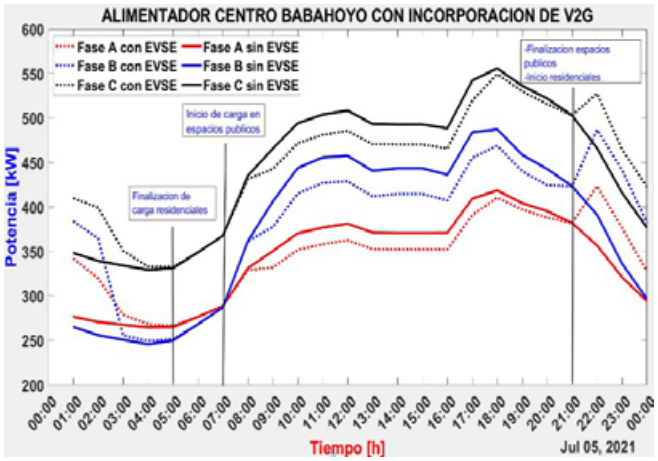

Figura 8.

Comportamiento de la tensión en el nodo 1056 cuando se implementó EVSE.

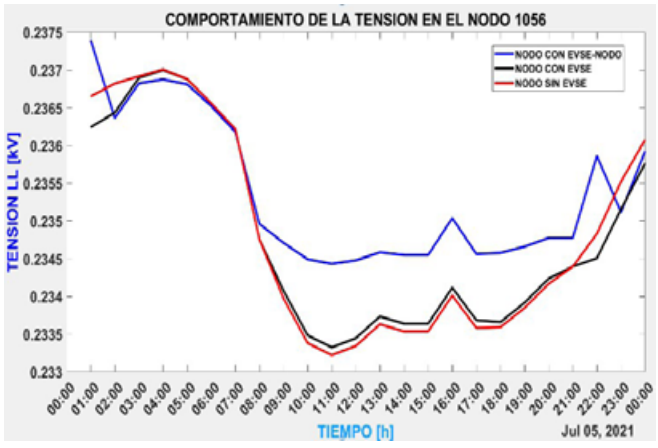

Figura 9.

Comportamiento del perfil de tensión a lo largo del día en el nodo 346

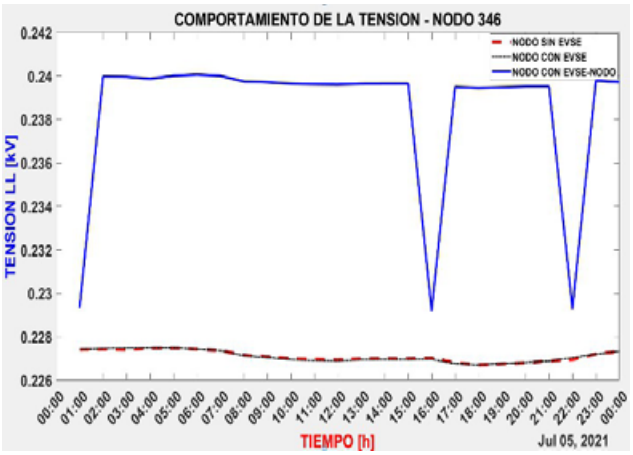

Figura 10.

Porcentaje de cargabilidad del transformador cuando no existe inyección de energía mediante los EVSEs durante un día laborable.

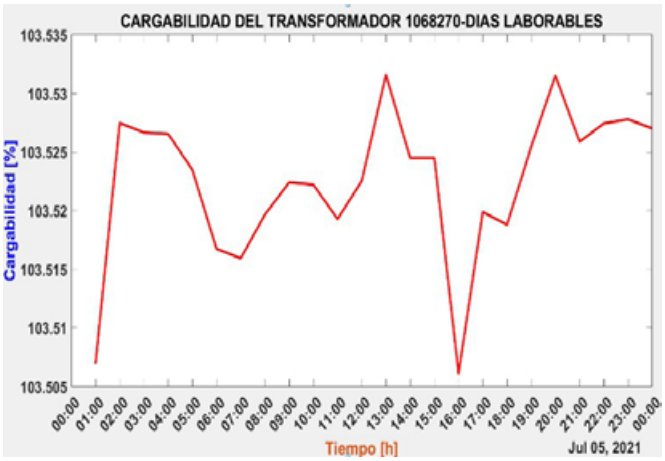

Figura 11.

Porcentaje de cargabilidad del transformador durante el periodo de un día con y sin EVSE

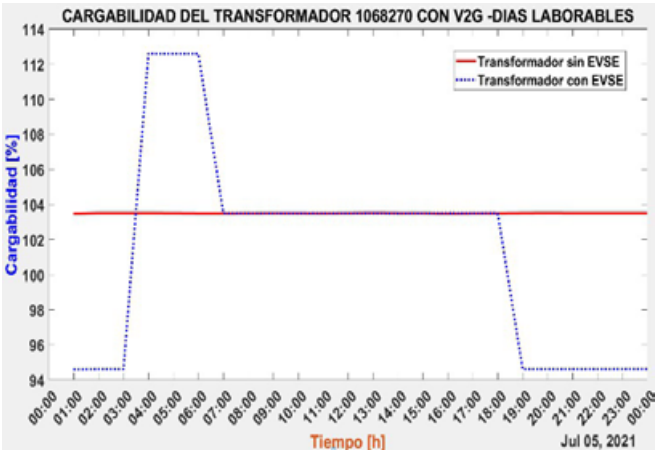

Figura 12.

Porcentaje de cargabilidad del transformador durante el periodo de un día

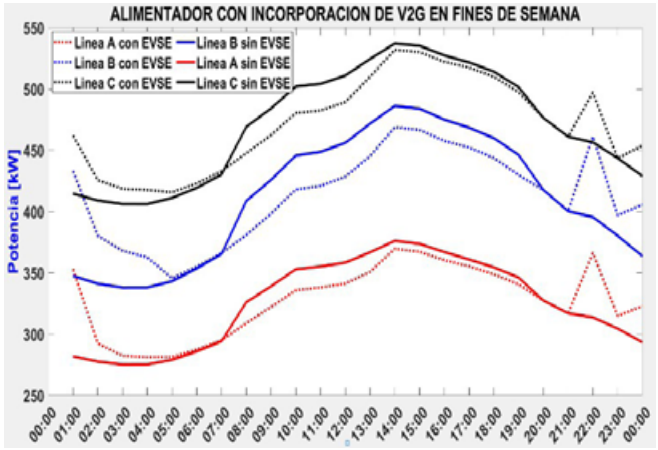

Figura 13.

Tensión en el nodo 1056 durante el fin de semana, mediante diferentes escenarios.

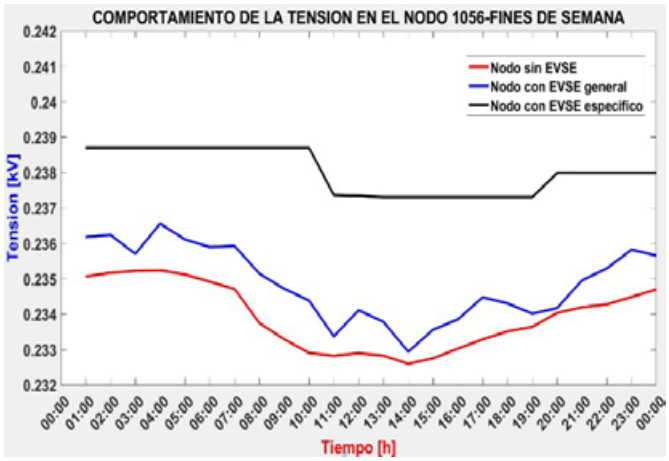

Figura 14.

Tensión en el nodo 1056 en condiciones diferentes en días de fines de semana

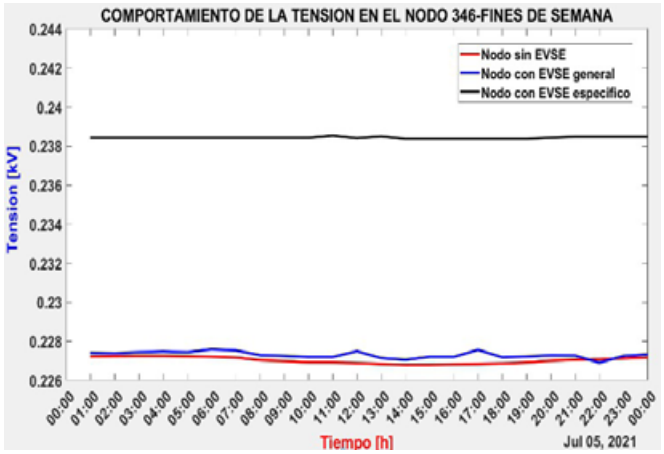

Figura 15.

Porcentaje de cargabilidad del transformador durante el periodo de un día de fin de semana

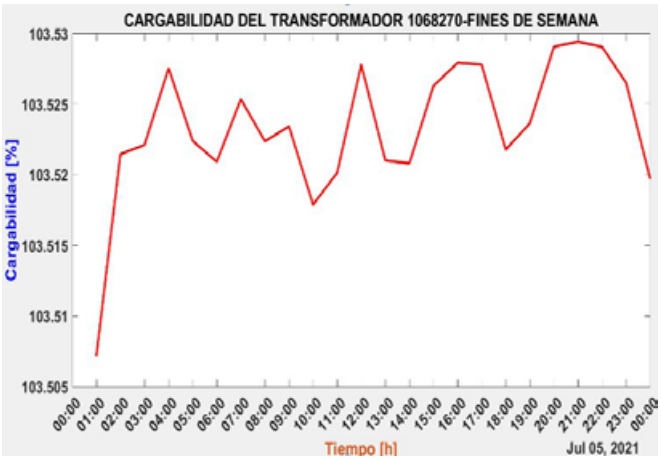

Figura 16.

Porcentaje de cargabilidad del transformador con carga y descarga del EVSE durante el periodo de un día.

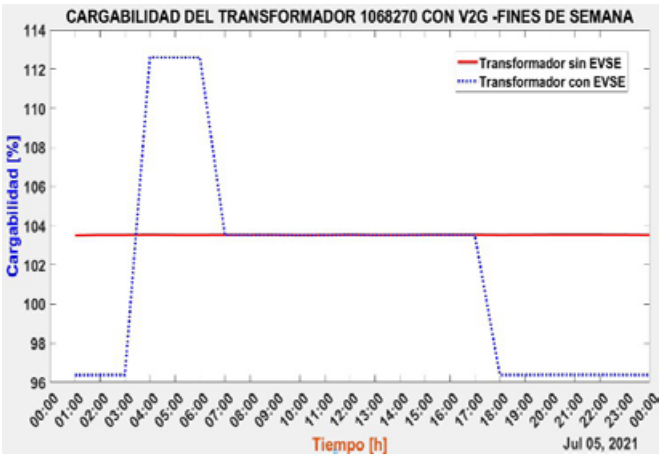

FACULTAD DE INGENIERÍA Y CIENCIAS APLICADAS
UNIVERSIDAD CENTRAL DEL ECUADOR

INGENIO
2025, VOL 8(2), JULIO - AGOSTO, PP. 157-166

REVISTA INGENIO

Data Loss Study in Zonal Systems and Servers in a Shopping Center Parking Lot

Estudio de Pérdida de Datos en Sistemas Zonal y Servidores de un Parqueadero en un Centro Comercial

Holger Santillán | Universidad Politécnica Salesiana - Ecuador
Carlos Feijoo | Universidad Politécnica Salesiana - Ecuador
Anthony Alcívar | Universidad Politécnica Salesiana - Ecuador
David Cárdenas | Universidad Politécnica Salesiana - Ecuador
Peregrina Wong | Universidad Politécnica Salesiana - Ecuador

Recibido: 8/10/2024
Recibido tras revisión: 28/4/2025
Aceptado: 14/5/2025
Publicado: 10/7/2025

KEY WORDS
Packet loss, Radio link, PowerBeam 5AC Gen2, Wireshark, IT Infrastructure.

ABSTRACT
This study analyzes the packet loss in the radio link of PowerBeam 5AC Gen2 antennas connected to various Meypar equipment in the "red dot" area of the Guayaquil shopping center. The objective is to optimize communication and ensure a stable network environment for the equipment. A tester was used to measure the continuity of the cabling, and oxidation was observed in all eight strands. In addition, Wireshark software was used to analyze packet traffic on 14 devices, including 1 transmitter, 1 ticket validator, 6 perimeter cameras, 2 license plate cameras, 2 IP intercoms and 2 antennas. Four critical scenarios were identified: the license plate cameras (1600 packets), the transmitter (293 packets) and the ticket validator (280 packets), registering a total of 2173 packets lost in these devices. To solve this problem, an exhaustive analysis of the IT infrastructure was carried out, identifying critical failures and implementing backup solutions, data recovery and system security improvements, thus minimizing the risk of data loss and ensuring the operational continuity of the parking lot.

PALABRAS CLAVE
Pérdida de paquetes, Radioenlace, PowerBeam 5AC Gen2, Wireshark, Infraestructura de TI.

RESUMEN
El presente estudio analiza la pérdida de paquetes del radio enlace con las antenas PowerBeam 5AC Gen2 a diferentes equipos Meypar de la zona punto rojo del centro comercial de la ciudad de Guayaquil, se busca determinar la comunicación óptima para un entorno estable de la red en los equipos. Se utilizó un tester para medir la continuidad del cableado y se observa físicamente que las 8 hebras de todo el cableado esta con óxido. También se utilizó el software de Wireshark para examinar el comportamiento de los paquetes hacia los equipos Meypar que son 1 emisor, 1 validador de tickets, 6 cámaras de perimetrales, 2 cámaras de matrícula, 2 interfonias ip y 2 antenas, en total 14 escenarios, siendo 4 los más críticos, que son las 2 cámaras de matrículas 1600 paquetes, 1 emisor 293 paquetes y 1 validador de ticket 280 paquetes, en estos 4 equipos se registra niveles de pérdida totales de 2173 paquetes. Para abordar el problema, se llevó a cabo un análisis exhaustivo del sistema zonal, identificando fallos críticos en la infraestructura de TI. Se implementaron soluciones de respaldo y recuperación de datos, junto con mejoras en la seguridad del sistema, logrando así minimizar el riesgo de pérdida de datos y asegurando la continuidad operativa del parqueadero.

1. Introduction

Shopping malls [1], highly crowded and active places, have prioritized safety and efficient management of their operations. Improvements in zonal systems and servers have optimized parking monitoring and management [2]. Automation, vehicle control and real-time surveillance have significantly increased efficiency and safety. However, this technological dependence has introduced new vulnerabilities, such as data loss [3].

Beyond operational disruptions, the misuse of technology can compromise security and infrastructure [4]. Causes of data loss include hardware failures, human error, cyberattacks, and adverse weather conditions. Previous incidents have demonstrated the serious consequences of this loss, including chaos, financial losses.

In order to tackle this issue effectively, it becomes necessary to explore both the root causes and the possible impacts of data loss in zonal systems and parking servers [5]. Gaining insight into these factors will help identify practical solutions aimed at reducing such incidents and improving the overall reliability of the systems involved.

https://doi.org/10.29166/ingenio.v8i2.7301

pISSN 2588-0829
eISSN 2697-3243
fing.revista.ingenio@uce.edu.ec

The main objective is to assess the internal and external factors that contribute to data loss and analyze their impacts on daily operations [4], customer security, and corporate reputation.

Once the problems have been identified, the study proposes practical recommendations to reduce the frequency and severity of these incidents. The aim was to identify the enigma of the network [6], in the current parking system, evaluate the data recovery protocols and propose technological improvements. A framework was developed to implement backup and recovery strategies applicable to various operational situations of the shopping center.

The approach not only mitigated the challenges associated with data mitigation [7], but also improved the system's resilience to future incidents. To achieve these objectives, a quantitative methodology was used, which combines technical analysis and procedure reviews. The first phase consisted of an audit of the zonal systems and servers, identifying points of vulnerability [8], and evaluating their performance under normal and stressful conditions.

Hardware and software tests [9] were performed on the network to identify critical issues and analyze the probability of attenuation in the data. Historical failures will be monitored and data from past incidents will be collected to identify patterns. In addition, failure and crisis simulations were carried out to evaluate the resilience of the parking system.

The analysis of data loss in zonal systems and servers is a field of study that has become increasingly relevant, especially in the context of managing complex infrastructures such as parking lots in shopping malls [10]. These systems rely heavily on the integrity and continuous availability of data to ensure smooth and efficient operation.

The ability to prevent and mitigate data loss [11], not only improves operational efficiency, but also ensures user security and satisfaction. To address this problem, it is essential to delve into the underlying technical concepts, review the related work, and apply mathematical equations that allow modeling the risks associated with data loss and developing strategies to counteract them.

One of the key concepts in this study is clearance attenuation, which refers to the amount of power of a signal [12], which is lost when it is transmitted through the air without physical obstacles in between. This attenuation clearance is primarily due to the dispersion of signal energy as it expands through space, with the final application being a drop in signal strength as it reaches the receiver. To calculate the percentage loss, the attenuation free space equation is applied, as shown in equation 1:

$$FSPL=20\log10(d)+20\log10(f)+20\log10(c4\pi) \quad (1)$$

Where:

d: is the distance between the transmitter and receiver in meters (m).

f: is the frequency of the signal in Hertz (Hz).

c: is the speed of light in a vacuum (m/s).

Simplifying the constant, the formula can also be written as equation 2:

$$FSPL=20\log10(d)+20\log10(f)-147.55 \quad (2)$$

If the distance d is in kilometers (km) and the frequency f is in Megahertz (MHz), the adapted formula would be equation 3:

$$FSPL=20\log10(d)+20\log10(f)+32.44 \quad (3)$$

In equation 1, it is the distance in meters between the transmitter and receiver, it is the frequency of the signal in Hertz, and it is the speed of light in a vacuum. The importance of understanding and calculating attenuation in free space lies in its direct impact on the planning of communication networks in open environments, such as parking lots, where distances can be significant and signals must be transmitted without interruptions to ensure proper operation of the system.

Another critical concept to consider is the Fresnel zone, an ellipsoidal region that details around the line directly between a transmitter and a receiver. The concept is fundamental as it can serve as a basis for understanding how obstructions in the Fresnel zone can lead to signal diffraction, resulting in signal loss, from there, data loss. The Fresnel zone is crucial when it comes to environments such as obstacle areas such as vehicles and buildings, which could hinder signal propagation, as shown in equation 4:

$$F_n = \sqrt{\frac{n\lambda d_1 d_2}{d_1 + d_2}} \quad (4)$$

Where:

F_n: is the radius of the Fresnel zone at the point under consideration (meters).

n: is the number of the Fresnel zone (for the first zone, n=1).

λ: is the wavelength of the signal (meters).

d_1: is the distance from the transmitter to the point under consideration (meters).

d_2: is the distance from the point under consideration to the receiver (meters).

The wavelength (λ) can be calculated from the frequency (f) of the signal using equation 5.

$$\lambda = \frac{c}{f} \quad (5)$$

Where:

c: is the speed of light, meters/second.

f: is the frequency of the signal (Hertz).

Effective communication system design requires careful planning, particularly with respect to the Fresnel zone [13]. This region, which surrounds the direct line-of-sight between a transmitter and a receiver, has an elliptical shape and plays a crucial role in signal propagation. When objects intrude into this space, they can cause diffraction and weaken the signal. By accounting for the Fresnel zone during installation, engineers can better position antennas and related equipment to reduce interference and maintain consistent data transmission quality.

Network security and analytics are critical areas in data loss prevention [14], and tools such as Wireshark and Cisco Packet Tracer are indispensable for these purposes. Wireshark is a network protocol analysis tool that allows administrators to capture and analyze data packets in real-time [15]. Their ability to identify vulnerabilities in network infrastructure is crucial to prevent data loss and ensure the safe operation of systems [16].

Wireshark allows network traffic to be analyzed [17], at a very detailed level, which can help identify specific issues such as attacks or bad behavior and address them before they cause significant damage to the system. Cisco Packet Tracer also offers a simulation environment that can be used to model and analyze the operating behavior of complex networks under different operating conditions [18]. In this way, the software can be used as a tool to analyze the potential fallibility of the existing network and investigate its resilience with respect to different combinations of operating circumstances.

Simulations conducted using Cisco Packet Tracer help identify vulnerabilities in the network infrastructure [19], allowing engineers to develop strategies that reduce the risk of data loss. Additionally, the ability to test different network configurations enables the optimization of network designs, ultimately enhancing both performance and reliability.

A review of related studies shows that substantial research has been carried out on network management in similar environments [20]. These studies have explored various methods to tackle data loss, including simulations, empirical analysis, and the application of advanced technologies.

For example, some studies have used the simulation of the Fresnel zone and the configuration of equipment through tools such as the AirOS applications (shown in Figure 1) and UISP Design Center of Ubiquiti Networks, which has allowed the optimization of network infrastructure in high-density environments [21], such as shopping malls [16]. These approaches have proven to be effective in improving network coverage and reducing the incidence of data loss.

Figure 1

Monitoring via the AirOS web app.

Another key aspect in the management of parking in shopping centers is the implementation of advanced systems [22], such as Meypar equipment. This system is essential for the automation and optimization of access control and use of parking spaces. Meypar integrates with real-time monitoring and management systems, enabling more efficient and safer parking lot operation [23].

In addition, its configurability through applications such as the User Terminal allows administrators to fine-tune and control the system, minimizing the risks of operational failures and data loss [24]. The use of mathematical equations is another essential component in modeling data loss scenarios.

In addition to equation (1) of Loss of Clearance (FSPL), other equations related to information theory and the capacity of communication channels are used to calculate the maximum amount of data that can be reliably transmitted over a channel [25]. These calculations are critical for designing network systems that can withstand the required data load without significant loss.

Mathematical modeling is also applied to analyze how different environmental and operational conditions affect signal propagation and overall network performance [26]. These models provide valuable information for decision-making in the design and operation of parking lot communication systems, allowing engineers to anticipate potential problems and develop strategies to mitigate them before they occur.

The use of advanced tools such as Cisco Packet Tracer and Wireshark, along with the application of robust technical concepts and the integration of cutting-edge technologies, has enabled researchers to develop effective solutions to mitigate the risks of data loss in critical environments [27]. The strategies developed from these studies not only improve operational efficiency, but also strengthen the security and resilience of systems in the face of possible contingencies.

The evolution of technology in the management of networks and communication systems continues to offer new opportunities to improve the management of complex infrastructures such as shopping mall parking lots.

The integration of new tools and techniques allows for more accurate and efficient management, reducing the risk of data loss and improving the overall experience for users [28].

Research in this field is essential to further advance in the protection and optimization of these systems, ensuring their robustness and reliability in the future [29]. It encompasses a wide range of key concepts, analytical tools, related works, and mathematical equations, providing a solid foundation for understanding and addressing the challenges associated with data loss in zonal systems and servers.

The combination of advanced techniques, careful planning, and the use of simulation tools allows network administrators to develop safer and more efficient systems, ensuring operational continuity in critical environments such as shopping mall parking lots [30], [31].

2. Method

The methodology used in this research is structured in a mixed approach that integrates quantitative and experimental methods, with the aim of achieving an exhaustive and detailed analysis of the zonal system and the parking servers in a shopping center. Quantitative methodology is critical as it allows for accurate and objective numerical data to be collected that is critical for evaluating network infrastructure performance.

Key variables measured include packet loss rate, cabling stability and quality, latency, network node performance, and data transmission rate across different segments of the system. Obtaining this data allows for early identification of any anomalies or inefficiencies that may be contributing to data loss, which is crucial for corrective interventions before problems are amplified.

In parallel, the experimental methodology focuses on the simulation of the system using advanced tools such as Cisco Packet Tracer, Wireshark, and other web applications specialized in network analysis. The simulation is a critical stage of the methodology, since it allows to virtually model the parking environment and test various network configurations in a controlled environment.

This phase is essential to predict how the network will behave under different operational scenarios, such as variation in data traffic density, interference in the radio frequency signal, and possible failure of key equipment such as routers and switches. Through simulation, it is possible to experiment with different network configuration and optimization strategies, making it easier to identify the most robust and efficient solution to minimize data loss and ensure optimal system performance.

The development of the prototype is based on a detailed model of the existing infrastructure of the shopping center's parking lot, which is used as a basis for simulation and analysis. This prototype includes all the critical components of the system, such as ticket dispensers, ticket validators, license plate cameras, perimeter cameras, and the main server, which are interconnected through a radio link.

This part of the system, often marked as the "red dot," is labeled a critical zone because it plays a central role in maintaining wireless communication between key components. Its functionality depends heavily on uninterrupted data exchange to keep operations synchronized. Any disruption in this area can compromise system performance, potentially causing data loss or service interruptions. For this reason, a detailed assessment is essential, along with preventive actions to strengthen the reliability of the communication link.

Figure 2.

Network diagram of the parking lot equipment.

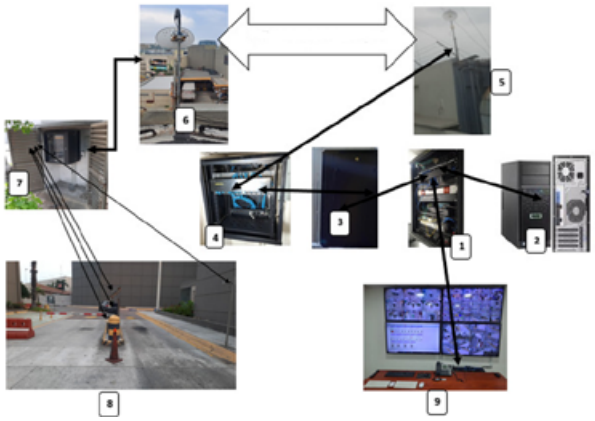

As can be seen in Figure 2, the detail of the intercommunication of the local network of the parking lot is found.

1. Main node.
2. Server.
3. Warehouse node.
4. Iron node.
5. PowerBeam 5 AC Gen 2 transmitter antenna.
6. PowerBeam 5 AC Gen 2 Receptor Antenna.
7. Red dot node.
8. Meypar Equipment.
9. Monitoring center.

Also, as these equipment, they communicate to the server, specifically the red dot area, because they have communication through a radio link. Before detailing the specific phases of the methodology, it is critical to understand that this comprehensive approach is designed to address both the identification and resolution of problems in the parking network infrastructure.

The methodology not only focuses on data collection and simulation, but also includes practical implementation and continuous monitoring to ensure the

sustainability of the improvements made. This structured process allows for a thorough evaluation of the system, making it easier to identify critical points and implement effective solutions to minimize data loss and optimize overall performance. Below, we can see Figure 3 with the 6 main phases in this methodology:

Figure 3.

Phases to follow in this methodology

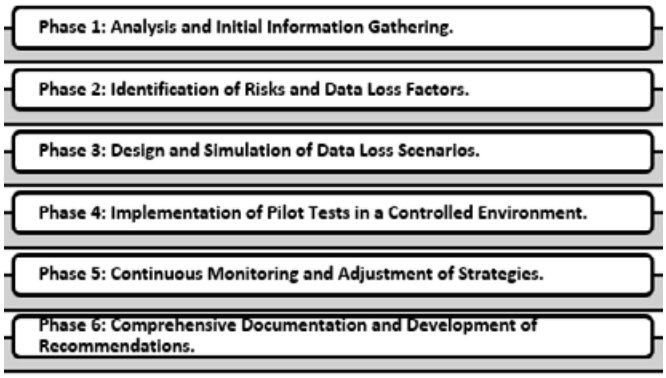

The main steps to be followed in this mixed methodology that integrates quantitative and experimental methods begin with phase 1 initial data collection. This process involves an exhaustive and meticulous evaluation of the existing system, where detailed measurements were made on the Meypar equipment of the parking lot of the shopping center in the red dot area.

These measurements include phase 2, verification of the condition of structured cabling, inspection of network equipment, and real-time monitoring of data traffic, this phase is crucial to establish a baseline against which the results of simulations and subsequent implementations can be compared. The data collected is used to build phase 3, a virtual model of the system in Cisco Packet Tracer, which simulates both normal operating conditions and failure scenarios.

Once the virtual model is complete, it moves on to simulation. During this phase, various configurations and optimization strategies are tested to determine which ones offer the best combination of performance and resiliency. This includes simulating situations such as network congestion, critical node drops, and radio link signal interference.

The simulation allows not only to identify possible points of failure, but also to evaluate the effectiveness of different mitigation measures, such as optimizing the network topology, improving packet routing, and implementing redundancies at critical points in the system. Each configuration is evaluated in terms of its impact on data loss, latency, and overall system availability.

The most promising configurations are then selected for phase 4 deployment in the controlled environment. During this phase, pilot tests are carried out in a section of the parking lot, which implements the selected configurations to verify the system that works in real conditions. During this period of time, various real-time monitoring tools are used to monitor and collect data about the system.

This allows configurations to be adjusted and refined as needed, ensuring that the system implemented throughout the facility performs optimally and meets the expected quality and efficiency standards. The process does not end with implementation, but extends to phase 5 of continuous monitoring and adjustment, where the system is monitored on a regular basis to ensure that the implemented configurations continue to work efficiently over time.

This phase includes post-implementation data collection and comparison with the initially established baseline, allowing the actual impact of improvements to be assessed and further adjustments made if new optimization opportunities are identified. This monitoring is critical to ensure the sustainability of the improvements implemented and to ensure that the system continues to operate without significant disruption or data loss.

Finally, phase 6 is carried out, the process of exhaustive documentation where all the steps followed, the configurations tested, the results obtained, and the lessons learned are recorded. This documentation is crucial not only to support decisions made during the project, but also to provide a valuable reference for future research and similar projects.

By documenting in detail each aspect of the process, a resource is created that can be used by other engineers and professionals in the area to replicate or adapt the solutions developed to different contexts, thus contributing to the advancement of knowledge in the management of zonal systems and servers in critical environments such as shopping centers.

3. Results and discussion

3.1. RESULTS

The results obtained in the study of data loss in the zonal system and servers of a parking lot in a shopping center are presented in detail through various tables and analyses that reflect the performance of the system and the problems detected. To quantify the signal attenuation in the wireless link, the equations of Loss of Free Space and Fresnel Zone were applied.

Equations (3), (4), and (5) were used to evaluate signal attenuation levels based on transmission distance and signal frequency, as well as to assess the influence of potential environmental obstructions on propagation performance. Once the corresponding data from the AirOS web application have been acquired, which are detailed

in Figure 1, the calculation of the attenuation of the free space will be carried out using equation 3.

$$FSPL=20\log_{10}(2.4\ km)+20\log_{10}(5225\ MHz)+32.44$$

$$FSPL=114.406\ dB$$

The result of FSPL=114.406 dB represents the clearance between the PowerBean 5AC antennas. To obtain the Fresnel zone between the antennas, the values obtained from Figure 1 must be considered, for this I use equations 4 and 5.

$$\lambda - \frac{3 * 10^8}{5225 * 10^9}$$

$$\lambda = 0.057\ m$$

The result of λ=0.057 m represents the wavelength that was used to solve equation 4, which resulted in F_n=5.86 m of the Fresnel zone.

$$F_n = \sqrt{\frac{1 * 0.057 * 1200m_1 * 1200m_2}{1200_1 + 1200_2}}$$

$$F_n = \sqrt{\frac{1 * 0.057 * 1200m_1 * 1200m_2}{2400}}$$

$$F_n = \sqrt{\frac{1 * 0.057 * 1200m_1 * 1200m_2}{2400}}$$

$$F_n = \sqrt{\frac{34.449}{2400}}$$

$$F_n = 5.86\ m$$

Therefore, as shown in Figure 4, a simulation was performed in the Cisco Packet Tracer software, where we were able to perform several tests such as; disconnection and connection of the wireless link, of the pc's, server and switches, sending and receivingpackets through ping between the pc's and server. Based on this simulation, it was possible to have a more referential idea of the possible problems in the attenuation of the network in the red dot sector in the parking lot of the shopping center.

Figure 4.

Point-to-Point Wireless Link Simulation.

Next, he performed an exhaustive analysis of the data collected through the WireShark application, where the source and destination IPs were filtered to identify the equipment with significant packet loss which we observe in Figure 5. This analysis is summarized in Table 1, where it is observed that equipment such as license plate cameras and ticket vending machines presented the highest losses of packages.

Figure 5.

Packet filtering.

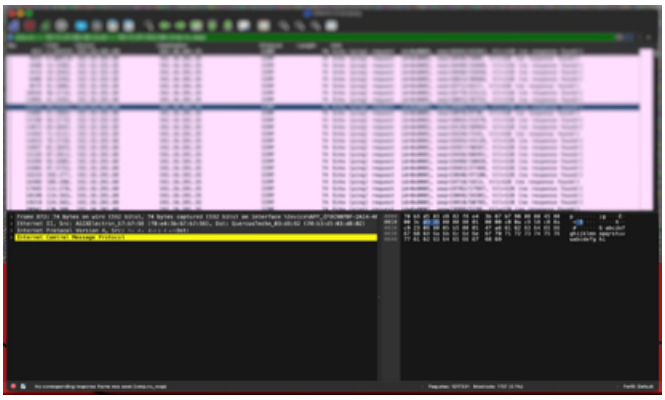

Table 1

Result of the analysis on each team

RED DOT ANALYSIS	20/2/24	12:43-15:26	02:43
TOTAL PACKETS ANALYZED		1217331	
EQUIPMENT	IP	PACKAGES	LOST
Ticket Dispenser	15	19078	220
Interphony	25	19076	220
Registration Chamber	35	3971	1507
Rear Perimeter Acts	145	19280	2
Acti Front Perimeter	185	19296	0
Acti Perimetral Facial	215	19296	0
Ticket validator	55	19262	4
Interphony	75	19296	0
Registration Chamber	95	15540	440
Rear Perimeter Acts	135	19296	0
Acti Front Perimeter	165	19296	0
Acti Perimetral Facial	225	19298	0
Antenna Transmitter	103	9648	0
Antenna Receptor	104	9648	0
Total Lost Packages			2393
Bytes per packet	74		
Bits per packet	592		

The results show that these devices are essential for parking access control, pointing to the need for enhancements in the existing infrastructure. Table 1 provides a summary of the outcomes from the different scenarios analyzed, detailing the total number of captured packets, lost packets, and the packet loss rate.

Once the problem areas were identified, corrective maintenance was performed, which involved replacing the damaged UTP cabling with new cables that meet the IEEE 802.3an standards. Post-replacement results show a significant improvement in data transmission, as shown in Table 2.

Table 2.

Result of the analysis in each team.

RED DOT ANALYSIS	27/6/24	02:59-10:59	08:00
TOTAL PACKETS ANALYZED		927215	
EQUIPMENT	IP	PACKAGES	LOST
Ticket Dispenser	15	24405	2
Interphony	25	24404	2
Registration Chamber	35	24413	0
Rear Perimeter Acts	145	24416	0
Acti Front Perimeter	185	24419	0
Acti Perimetral Facial	215	24417	0
Ticket validator	55	24425	0
Interphony	75		0
Registration Chamber	95	24424	1
Rear Perimeter Acts	135	24423	0
Acti Front Perimeter	165	24426	0
Acti Perimetral Facial	225	24427	0
Antenna Transmitter	103	24424	0
Antenna Receptor	104	24423	0
Total Packages Lost			5
Bytes per packet	74		
Bits per packet	592		

In Table 2, the number of lost packages was drastically reduced, especially in license plate camera and ticket dispensing devices. This loss reduction suggests that the wiring change was effective in mitigating previously detected data transmission issues.

Comparing the data from before and after maintenance showed a significant drop in the number of lost packets. In particular, the camera of the IP 35 recorded a reduction from 1507 to 0, which means a 100% improvement. Therefore, the initial hypothesis that worn wiring was one of the key factors influencing data loss was proven.

The results obtained allow us to conclude that the maintenance actions carried out were effective in improving the quality of the network and the efficiency in the transmission of data in the parking lot. Early identification of critical points and the implementation of appropriate corrective solutions have proven to be essential to ensure the proper functioning of the zonal system and servers.

In addition, as visualized in Figure 6, the reduction in packet attenuation ensures greater reliability in access control and monitoring systems, which is crucial for the operability of the shopping center. In summary, the analysis of the results reveals that, with proper maintenance and the updating of critical components, it is possible to significantly reduce failures in data transmission, thus guaranteeing a more efficient and reliable service for parking lot users.

Figure 6

Result bar diagram referring to table 2.

3.2. DISCUSSION

One of the main issues identified is the significant variability in packet loss across different devices. Specifically, the license plate cameras showed a high rate of data loss, with one camera (IP 35) losing 1,727 packets and another (IP 95) losing 440 packets. This packet loss can be attributed to various factors, such as network congestion, equipment malfunctions, or signal interference.

In an urban and commercial environment, radio signals are frequently affected by interference from other electronic devices, such as Wi-Fi routers, mobile phones, and other wireless systems; because of this, Rattle's reflected packet numbers are common to both systems, with consequent packet collisions and data loss. Radio frequency interference is one of the main forms of packet loss in a high-density environment [7].

The presence of physical structures, such as walls, vehicles, and other obstacles in the parking lot, can attenuate radio signals, resulting in packet loss. The effectiveness of radio links depends on direct line of sight. According to studies, physical barriers can significantly decrease signal quality on wireless links [8].

Incorrect configuration of antenna parameters, such as alignment, tilt angle, and transmit power, can significantly affect link quality. It highlights the importance of proper configuration to minimize packet loss [9]. Equipment performance can be affected by improper maintenance or lack of maintenance.

Dust, moisture, and general wear and tear can damage antennas and other components. The reliability of wireless systems depends on regular maintenance [11]. Detailed network infrastructure planning is critical to ensuring optimal performance. The antennas should be high and free of obstacles, ensuring a direct line of sight between the attachment points. Using RF planning tools can help identify optimal locations.

They emphasize the importance of strategic location in wireless network planning. Conduct field studies prior to implementation to identify potential sources of interference and physical obstacles. These studies allow antenna configuration to be adjusted and network planning more effectively. Field studies are essential for successful wireless network planning [12].

To reduce interference and maximize link quality, adjust technical parameters such as frequency, transmit power, and receiver sensitivity. They have shown that optimal equipment configuration can significantly reduce packet loss. Implement mitigation techniques, such as the use of band filters and the selection of less congested channels [13].

In addition, the use of antenna technology with dynamic tuning capabilities can help avoid interference. Interference mitigation is crucial to improving the stability of wireless networks. Create continuous monitoring to detect and resolve issues instantly. The use of network management software can provide early warnings about link degradation and allow for immediate corrective actions.

He notes that continuous monitoring can improve the operational efficiency of wireless networks [8]. To ensure that improvements to the network have had the desired effect, it is essential to reevaluate performance after making changes to the network. Field testing and performance data analysis are included in this. Post-implementation re-evaluation this is important for quality control.

Consider installing a fiber optic link as the primary connection, keeping radio links as a backup solution. This would ensure that the service would not be interrupted in the event of radio link failures. They suggest that a backup infrastructure can improve the resilience of networks. Implement a regular maintenance schedule for all network components, including cleaning, inspection, and replacement of worn parts.

Studies have shown that preventive maintenance can significantly reduce the incidence of failures and improve overall system performance [11]. Interference, physical obstacles, suboptimal configurations, and lack of maintenance are significant challenges that affect network stability and reliability.

However, by implementing mitigation strategies, continuous monitoring, periodic re-evaluation, and regular maintenance, it is possible to significantly improve network performance by 99.8%. These improvements will not only increase the efficiency and reliability of the network, but will also contribute to a better experience for parking users and the overall safety of the environment.

4. Conclusions

The operation of the radio links, which use PowerBeam 5AC Gen2 antennas, made it possible to determine that the data loss exceeded what is allowed by the IEEE 802.3an and 802.3af/at standards. Under critical conditions, the number of lost packets reached 2393, which meant a significant degradation of the transmitted packets and negatively affected the continuity of transmission to and from the most sensitive areas of the parking lot.

After the implementation of corrective measures, such as the replacement of the rusty UTP cabling with new one in accordance with IEEE standards and the optimization of the radio link configuration, a significant improvement in the quality of data transmission was achieved. Specifically, the number of lost packages was reduced by 99.8%, going from 2393 to only 5 packages in the areas assessed. This percentage improvement confirms that the degradation of the service was directly related to the conditions of the cabling and the suboptimal configuration of the links.

Another key factor contributing to the high failure rate in the network was the absence of a preventive and corrective maintenance program. Implementing regular equipment inspections and preventive maintenance every six months has been shown to reduce the likelihood of failure by 30% before maintenance is even required. This approach has proven to be a crucial strategy, significantly reducing data loss and improving the overall performance and reliability of the parking lot facility.

4.1. RECOMMENDATIONS

Perform a full audit of existing radio links, with a focus on optimizing configuration and replacing equipment that exhibits an unacceptable packet loss rate. Implement real-time monitoring tools to proactively detect and correct data loss.

Install equipment that operates on less congested frequencies and use technologies such as MIMO (Multiple Input Multiple Output) to improve resilience to interference. Additionally, replace UTP cabling with more

rust-resistant versions, such as high-quality coated or outdoor-certified cables.

Establish and implement a preventive maintenance plan that includes periodic inspections of all network components, regular cleaning of connections, and performance testing of equipment. This plan must be documented and executed by trained personnel, with status reports after each intervention.

Design and execute an appropriate electric landing plan, ensuring that all critical equipment is connected to surge protection systems. In addition, review and restructure the physical distribution of equipment to minimize exposure to electromagnetic interference and electrical hazards.

Implementing a hybrid connectivity infrastructure that uses fiber optic links as the primary means of data transmission, complemented by radio links as a backup, will enhance stability and provide redundancy. This approach ensures service continuity, even in the event of a failure in one of the systems.

References

[1] E. Soacha, T. De Grado, R. Ruiz, Y. Alejandro, A. Sandoval, y D. Stefany, "Software to manage and manage the resources available in parking lots of small shopping centers – system parking," Nov. 2017. [En línea]. Disponible en: https://repositorio.ucundinamarca.edu.co/handle/20.500.12558/1207 [Accedido el 29 de mayo de 2024].

[2] J. Santiago y C. Pullopaxi, "Implementation of a system that guides the circulation of vehicles and the occupation of available spaces in the parking lots of the Medical Towers and Metropolitan Hospital," Enero 2014. [En línea]. Disponible en: http://bibdigital.epn.edu.ec/handle/15000/7122 [Accedido el 29 de mayo de 2024].

[3] Y. C. Lin y Z. S. Shih, "Design and simulation of a radio spectrum monitoring system with a software-defined network," *Computers & Electrical Engineering*, vol. 68, pp. 271–285, May 2018, https://doi.org/10.1016/J.COMPELECENG.2018.03.043

[4] W. Rehan, S. Fischer, O. Chughtai, M. Rehan, M. Hail, y S. Saleem, "A novel dynamic confidence interval based secure channel prediction approach for stream-based multichannel wireless sensor networks," *Ad Hoc Networks*, vol. 108, p. 102212, Nov. 2020, https://doi.org/10.1016/J.ADHOC.2020.102212

[5] W. Rehan, S. Fischer, M. Rehan, y M. H. Rehmani, "A comprehensive survey on multichannel routing in wireless sensor networks," *Journal of Network and Computer Applications*, vol. 95, pp. 1–25, Oct. 2017, https://doi.org/10.1016/J.JNCA.2017.07.006

[6] J. Mulder *et al.*, "26.3 An 800MS/S 10b/13b receiver for 10GBASE-T Ethernet in 28nm CMOS," in *2015 IEEE International Solid-State Circuits Conference - (ISSCC) Digest of Technical Papers*, 2015, pp. 1–3. doi: 10.1109/ISSCC.2015.7063126.

[7] M. Peng y F. Qin, "Clarification of basic concepts for electromagnetic interference shielding effectiveness," *J Appl Phys*, vol. 130, no. 22, p. 225108, Dec. 2021, https://doi.org/10.1063/5.0075019

[8] A. Colliander *et al.,* "Spatial Downscaling of SMAP Soil Moisture Using MODIS Land Surface Temperature and NDVI During SMAPVEX15," *IEEE Geoscience and Remote Sensing Letters*, vol. 14, no. 11, pp. 2107–2111, 2017, https://doi.org/10.1109/LGRS.2017.2753203

[9] B. Ojaghi, F. Adelantado, E. Kartsakli, A. Antonopoulos, y C. Verikoukis, "Sliced-RAN: Joint Slicing and Functional Split in Future 5G Radio Access Networks," in *ICC 2019 - 2019 IEEE International Conference on Communications (ICC),* 2019, pp. 1–6. https://doi.org/10.1109/ICC.2019.8761081

[10] D. H. Cuzco Torres y S. J. Pinos Carangui, "Design of a Smart Parking System for the Historic Center of the City of Cuenca, Applying an LPWAN Network," 2022. [En línea]. Disponible en: http://dspace.ups.edu.ec/handle/123456789/22405 [Accedido el 29 de mayo de 2024].

[11] S. ZOUGA, M. Benchagra, and A. Abdallah, "Backstepping Control Based on the PSO Algorithm for a Three-Phase PV System Connected to the Grid under Load Variation," in 2020 International Conference on Electrical and Information Technologies (ICEIT), 2020, pp. 1–6. https://doi.org/10.1109/ICEIT48248.2020.9113235

[12] F. Guo, H. Zhang, H. Ji, X. Li, y V. C. M. Leung, "An Efficient Computation Offloading Management Scheme in the Densely Deployed Small Cell Networks With Mobile Edge Computing," *IEEE/ACM Transactions on Networking*, vol. 26, no. 6, pp. 2651–2664, 2018, https://doi.org/10.1109/TNET.2018.2873002

[13] Z. Qian, Y. Zhao, X. Liu, L. Ge, y J. Mao, "A Novel Filter in Antenna (FiA) With Compact Size and High Performance," *IEEE Trans Antennas Propag*, vol. 72, no. 7, pp. 5550–5559, 2024, https://doi.org/10.1109/TAP.2024.3401477

[14] M. N. Al Rafi, M. A. J. Mojumder, S. S. Newaz, y R. Khan, "Study of Radio Link Losses in Different Mediums and Receiving Stations," in *2021 IEEE 19th Student Conference on Research and Development (SCOReD),* 2021, pp. 192–196. https://doi.org/10.1109/SCOReD53546.2021.9652725

[15] J. Allison, "Simulation-Based Learning via Cisco Packet Tracer to Enhance the Teaching of Computer Networks," in *Proceedings of the 27th ACM Conference on on Innovation and Technology in Computer Science Education* Vol. 1, in ITiCSE '22. New York, NY, USA: Association for Computing Machinery, 2022, pp. 68–74. https://doi.org/10.1145/3502718.3524739

[16] S. Unni, D. Raj, K. Sasidhar, y S. Rao, "Performance measurement and analysis of long range Wi-Fi network for

over-the-sea communication," in *2015 13th International Symposium on Modeling and Optimization in Mobile, Ad Hoc, and Wireless Networks (WiOpt),* 2015, pp. 36–41. https://doi.org/10.1109/WIOPT.2015.7151030

[17] S. N. R. Shah, N. H. Ramli Sulong, R. Khan, M. Z. Jumaat, y M. Shariati, "Behavior of Industrial Steel Rack Connections," *Mech Syst Signal Process*, vol. 70–71, pp. 725–740, 2016, doi: https://doi.org/10.1016/j.ymssp.2015.08.026

[18] L. Khichadi y K. Nagamani, "Performance Evaluation of Power over Ethernet in an Ethernet Switch," in *2019 International Conference on Communication and Electronics Systems (ICCES),* 2019, pp. 1091–1095. https://doi.org/10.1109/ICCES45898.2019.9002072

[19] M. A. Islam, R. Irishika, K. Iokibe, y Y. Toyota, "Suppression of Mode Conversion by Improved Shielding Effect of Ethernet Cable Connector Based on Imbalance Factor Matching," in *2019 International Conference on Computer, Communication, Chemical, Materials and Electronic Engineering (IC4ME2),* 2019, pp. 1–4. https://doi.org/10.1109/IC4ME247184.2019.9036533

[20] H. J. Santillan Carranza, J. O. Enriquez Sandoval, y J. F. Bonilla Castro, "Development of a Raspberry Pi-based Wireless Educational Tool," Rev. Ingenio, vol. 7, no. 7, pp. 12–22, 2024. doi: 10.29166/ingenio.v7i1.5630.

[21] S. Caniggia y F. Maradei, "Filter and Grounding Solutions for Limiting Radiated Emission of a PCB with an Attached UTP Cable," IEEE Electromagn. Compat. Mag., vol. 10, no. 1, pp. 33–40, 2021. doi: 10.1109/MEMC.2021.9400990.

[22] J. B. Eom, D. S. Moon, U. C. Paek, B. H. Lee, y G. H. Yang, "Fabrication and transmission characteristics of couplers using photonic crystal fibers," en Optical Fiber Communication Conference and Exhibit, 2002, 2002, pp. 465–466. doi: 10.1109/OFC.2002.1036488.

[23] A. E. Ibhaze, A. O. Gbadebo, A. A. Amusan, y S. N. John, "Performance Analysis of Fiber Attenuation in Passive Optical Networks," Indones. J. Electr. Eng. Informatics, vol. 11, no. 3, pp. 700–712, 2023. doi: 10.52549/ijeei.v11i3.4919.

[24] S. Buhr, X. Xu, M. Kreißig, y F. Ellinger, "A Low Power Fast Ethernet Physical Layer Transceiver," in *2019 26th IEEE International Conference on Electronics, Circuits and Systems (ICECS),* 2019, pp. 478–481. https://doi.org/10.1109/ICECS46596.2019.8964920

[25] M. A. Ebrahimzadeh, M. Dabbaqi, y N. Nakhaie, "Investigating the reduction of the error caused by the counting of vehicle traffic in city license plate reader cameras by mathematical models (case study: Mashhad city)," *Road*, p., 2024, https://doi.org/10.22034/road.2024.416435.2199

[26] A. U. Jibia y N. D. Robinson, "A PC-Based Multifunctional Virtual Oscilloscope," in *2019 2nd International Conference of the IEEE Nigeria Computer Chapter (NigeriaComputConf),* 2019, pp. 1–9. https://doi.org/10.1109/NigeriaComputConf45974.2019.8949640

[27] S. Kakuru, "Behavior based network traffic analysis tool," in *2011 IEEE 3rd International Conference on Communication Software and Networks,* 2011, pp. 649–652. https://doi.org/10.1109/ICCSN.2011.6014810

[28] R. Gooty, G. Modi, S. Williams, K. Kruckmeyer, V. Salomon, y D. Boldrin, "Radiation Evaluation of the DP83561-SP Radiation Hardened 10/100/1000 Ethernet PHY Transceiver with SEFI Handling Sub-System.," in *IEEE Radiation Effects Data Workshop,* 2022. https://doi.org/10.1109/REDW56037.2022.9921702

[29] M. Elhamdadi y E. K. M. Moutuou, "Finitely stable racks and rack representations," *Commun Algebra*, vol. 46, no. 11, pp. 4787–4802, 2018, https://doi.org/10.1080/00927872.2018.1455102

[30] F. Ullah *et al.,* "Barrier Access Control Using Sensors Platform and Vehicle License Plate Characters Recognition," *Sensors*, vol. 19, no. 13, 2019, https://doi.org/10.3390/s19133015

[31] H. J. Santillan Carranza, M. A. Suarez Carvajal, y D. H. Cardenas Villacres, "Development of an IoT Tool for Optimizing Humidity Control in Cocoa Cultivation," Memoria Investigaciones en Ingeniería, vol. 2023, no. 2023, pp. 246–265, 2023. doi: 10.36561/ING.25.14.